Secondary Metabolites from Fungi: Natural Product Diversity, Structure Elucidation and Bioactivity

Inaugural dissertation

for the attainment of the title of doctor
in the Faculty of Mathematics and Natural Sciences
at the Heinrich Heine University Düsseldorf

presented by

Huiqin Chen
from Zhejiang, P. R. China

Düsseldorf, 03. 2016

from the institute for Pharmaceutical Biology and Biotechnology
at the Heinrich Heine University Düsseldorf

Published by permission of the
Faculty of Mathematics and Natural Sciences at
Heinrich Heine University Düsseldorf

Supervisor: Prof. Dr. Peter Proksch
Co-supervisor: Prof. Dr. Rainer Kalscheuer

Date of the oral examination: 22. 04. 2016

Erklärung

Hiermit erkläre ich ehrenwörtlich, dass ich die vorliegende Dissertation mit dem Titel „Sekundärstoffe aus Pilzen - Vielfalt, Strukturaufklärung und Bioaktivität von Naturstoffen“ selbst angefertigt habe. Außer den angegebenen Quellen und Hilfsmitteln wurden keine weiteren verwendet. Diese Dissertation wurde weder in gleicher noch in abgewandelter Form in einem anderen Prüfungsverfahren vorgelegt.

Düsseldorf, den 01. 03. 2016

Huiqin Chen

Acknowledgements

First of all, I would like to express my heartfelt appreciation to Prof. Dr. Peter Proksch for giving me this cherish opportunity and excellent working conditions and facilities to purse my doctoral study in the Institute of Pharmaceutical Biology and Biotechnology, Heinrich-Heine University, Düsseldorf, as well as for his patient guidance, helpful suggestion, genial discussion, and comprehensive support for my study and life in Düsseldorf.

I am deeply indebted to Prof. Dr. Haofu Dai (Key Laboratory of Biology and Genetic Resources of Tropical Crops, Ministry of Agriculture, Institute of Tropical Bioscience and Biotechnology, Chinese Academy of Tropical Agricultural Sciences) for his unforgettable support and help to study in Germany.

My special thanks to Dr. Georgios Daletos for all of his precious help, scientific advices, preparations of manuscripts for publications, guidance since I started my research here, as well as sharing his expertise in NMR interpretations on NMR seminar.

I would like to express my sincerely appreciation to Prof. Dr. Wenhan Lin (National Research Laboratories of Natural and Biomimetic Drugs, Peking University, Health Science Center) for his constructive suggestion on structure elucidation and continuous encouragement. I am grateful to Prof. Dr. Heike Brötz-Oesterhelt (Interfakultäres Institut für Mikrobiologie und Infektionsmedizin, Mikrobielle Wirkstoffe, Tübingen, Germany) for her support of co-cultivation research projects and antibiotic assays; Prof. Dr. Tibor Kurtán (Department of Organic Chemistry, University of Debrecen, Debrecen, Hungary) for his professional CD calculation. And special thanks for their help to the publications.

My deep thanks to Prof. Dr. Rainer Kalscheuer (Institute of Pharmaceutical Biology and Biotechnology, Heinrich-Heine University, Düsseldorf) for his support for co-cultivation research projects, antibiotic assays, and for estimating my PhD study as the second referee.

I would like to express my appreciation to Prof. W. E. G. Müller (University of Mainz) and Prof. Dr. Matthias U. Kassack (Institut für Pharmazeutische und Medizinische Chemie, Heinrich-Heine University, Düsseldorf) for conducting cytotoxicity assays; Prof. Dr. Horst Weber and Prof. Dr. Bingui Wang (Laboratory of Experimental Marine Biology, Institute of

Oceanology, Chinese Acedemy of Science, Qindao, China) for their professional discussion and suggestion; Dr. Tommes, Mr. Bürgel, Ms. Karkoschke and Ms. Beuer for their NMR and MS measurements, and Prof. Dr. Claus Passreiter for his safety matters during study.

I am indebted to Mrs. Claudia Eckelskemper for her kind and generous help of administration, and the technicians Mrs. Waltraud Schlag, Mrs. Simone Miljanovic, Mrs. Katja Friedrich, Mrs. Heike Goldbach-Gecke, Mr. Dieter Jansen and Mrs Eva Müller for their hospitality help and support.

During my PhD study, I received help, support, and happiness from time to time, so I would like to take this opportunity to express my profound gratitude to all of these group members:

- The postdoctors Dr. Daowan Lai for his helping me to start my study here. Not only shared his scientific knowledges, but also instructed living in the new environment. Dr. Amal Hassan and Dr. Abdessamad Debbab for their sharing techniques and knowledge.
- The present postdoctors Dr. Zhen Liu for his valuable suggestion, pleased conversations and sharing his knowledge in NMR interpretations on NMR seminar. Dr Yanbo Zeng for his kind taking care during stay in Germany. Dr. Weaam Ebrahim for the advice and improvement on biology part. Dr. Elena Ancheeva, Dr. Ramsay Kamdern, and Dr. Sherif Elsayed for the nice time enjoyed together.
- Dr. Andreas Marmann for his patient guidance in the early time of working on fungi. Dr. Antonius R B Ola for his introduction on co-cultivation experiments. Dr. Cong-Dat Pham, Dr. Lena Hammerschmidt and Dr. Hendrik Niemann for their technic help.
- Mr. Amin Mokhlesi for having a nice working time in the same lab, and sharing happiness and bitterness throughout the studying time. Ms. Yang Liu, Mrs. Rini Muharini, Mr. Herve Sergi Akone for the accompany time, and discussion for working and living experience. Ms. Mi-Young Chung (thanks for translation of abstract part in the thesis, and enjoying the writing time together), Ms. Imke Form, Ms. Arta Kuci and Ms. Catalina Perez Hemphill for their language and technics help, as well as nice conversations during the time together. Mr. Marian Frank for sharing his biological knowledge. Thank all of you of studying together during Coffee Time.
- Ms. Mariam Moussa, Mr. Mohamed Elnaggar, Mrs. Catherine Bogner, Dr. Mousa Al

Tarabeen, Ms. Lisa Kuppers and Mr. Ferhat Oezkaya for all the help.

- I have enjoyed the time here with my brothers Shuai Liu, Hao Wang (thanks for the help on structure determination), and Haiqian Yu.
- Ms. Dhana Tommy and Ms. Nidja Rehberg for preparing bacterial strains during the co-cultivation project and antibiotic assays. Ms. Nihal Aktas and Dr. Festus Okoye for their cooperation on the experiment.
- Special thanks to visiting professors Mohamed S. Abdel-Aziz (Microbial Chemistry Department, Genetic Engineering and Biotechnology Division, National Research Center, Egypt) and Belma Konuklugil (Department of Pharmacognosy, Faculty of Pharmacy, Ankara University, Ankara, Turkey) for collecting interesting samples for fungi isolation
- Nice time spent with all of you Fang Lv, Linghong Meng, Xin Li, Blessing Umeokoli, Peter Eze, Dr. Odontuya, Pamela Nangmo Kemda, Rudiyansyah.

I am grateful to China Scholarship Council, Ministry of Education of China for the financial support during my study in Germany.

In the end, I would like to deepest gratitude and appreciation to my family for their encouraging and supporting me to finish this study.

To all of you, thank you very much!

Abstract

This dissertation describes secondary metabolites isolated from different fungi, including *Trichoderma harzianum*, *Aspergillus terreus*, *Penicillium* sp. (strains IO1 and IO2), *Alternaria alternata*, *Penicillium paxilli* and *Penicillium sclerotiorum*. The structures of isolated compounds were elucidated by analysis of MS and NMR data. The absolute configuration of chiral compounds was determined by comparison of the optical rotation with the literatures and by ECD spectroscopy.

In order to exploit the maximal chemical diversity of fungi, several cultivation methods were applied. The most common ways included the alteration of the medium type, salinity or pH to elicit the biosynthesis of specific metabolites, so that the corresponding metabolites were produced. Microbial interaction was considered to be the most important factor for triggering the production of bioactive secondary metabolites, and thus co-cultivation approaches were pursued to mimic the natural environment with the aim to activate silent gene clusters of axenic cultures. In addition, epigenetic modifiers were used to attempt the induction of new secondary metabolites by inhibition of histone deacetylases **(**HDACs) and DNA methyltransferases (DMATs).

This dissertation consists of the following parts:

1. *Trichoderma harzianum*

The endophytic fungus *T. harzianum* was isolated from leaves of *Cola nitida*. One new natural product 4'-hydroxy-deacetyl-18-deoxycytochalasin H (**1**), together with the known deacetyl-18-deoxycytochalasin H (**2**), 18-deoxycytochalasin H (**3**) and alternariol (**4**) were obtained from the first fermentation on rice medium. The secondary fermentation gave the known compounds waol A (**5**) and aspyridone A (**6**). The structure of the new compound was unambiguously determined by 1D and 2D NMR spectroscopy, and by HRESIMS measurements, as well as by comparison of the data with the literature. Compounds **1-3** showed potent cytotoxicity against the murine lymphoma cell line L5178Y and the human ovarian cancer cell lines A2780 sens and A2780 CisR (IC_{50} 0.19 - 6.97 μM). The A2780 cell lines included cisplatin-sensitive (sens) and -resistant (R) cells.

2. *Aspergillus terreus*

The soil-dwelling fungus *A. terreus* was isolated from a sediment sample collected from the lake of Wadi EI Natrun in Egypt. Co-cultivation of *A. terreus* with the bacteria *Bacillus subtilis* or with *Bacillus cereus* on solid rice medium resulted in an up to 34-fold increased accumulation of constitutively present fungal natural products (**10 ─ 21**) compared to axenic cultures of *A. terreus*. The fungal products included two new butyrolactone derivatives, isobutyrolactone II (**7**) and 4-O-demethylisobutyrolactone II (**8**), together with the known N-(carboxymethyl)anthranilic acid (**9**) that were not present in axenic fungal controls and were only detected during co-cultivation with *B. subtilis* or with *B. cereus*. In a second set of co-cultivation experiments, *A. terreus* was co-cultured with *Streptomyces lividans* or with *Streptomyces coelicolor*. These co-cultivation experiments failed to induce the fungal natural product accumulation in contrast to co-cultures with *Bacillus* sp..

Cultivation of *A. terreus* on rice, in liquid Wickerham medium or on white beans, respectively, resulted in specific HPLC chromatograms. Nine compounds different from the rice culture were isolated, in addition to the pair of dihydroisoflavipucine stereoisomers **22** and **23** from liquid Wickerham medium, and asterrelenin (**29**) and acetylaszonalenin (**30**) from the bean culture.

Butyrolactone II (**11**) and aspulvinone E (**20**) showed weak inhibition of *B. cereus* with minimal inhibitory concentrations (MICs) of 64 μg/ mL, respectively, while asterrelenin (**29**) showed weak inhibition of *Mycobacterium tuberculosis* with MIC 100 μg/ mL. For the results from cytotoxicity assays, terrein (**14**) showed moderate cytotoxicity with 80% inhibition of the murine lymphoma cell line L5178Y at a dose of 10 μg/ ml, while **29** and **30** showed weak cytotoxicity against human ovarian cancer A2780 sens cell line at the concentration of 10^2 μM.

3. *Penicillium* sp. strains IO1 and IO2

The marine-derived fungus *Penicillium* sp. strain IO1 isolated from the Mediterranean sponge *Ircinia oros* yielded a new fusarielin analogue (**31**), together with the known compounds griseofulvin (**32**) and dechlorogriseofulvin (**33**). The absolute configuration of **31** was determined on the basis of TDDFT ECD calculations. A further *Penicillium* sp. strain IO2 that

was isolated from the same sponge *I. oros* yielded the known compounds dehydrocurvularin (**34**), curvularin (**35**), and trichodimerol (**36**). Co-cultivation of both *Penicillium* strains IO1 and IO2 was found to induce the accumulation of the known norlichexanthone (**37**) and monocerin (**38**) that were not detected in either of the two axenic fungal controls. Griseophenone B (**39**) and echinulin (**40**) were isolated incidentally from the co-culture, however, these two compounds were not observed in the HPLC chromatograms due to their small amounts. Compounds **34** and **38** showed pronounced cytotoxicity against the murine lymphoma cell line L5178Y with IC_{50} values of 4.7 and 8.4 μM, respectively.

4. *Alternaria alternata*

A. alternata was isolated from leaves of the rainforest plant *Antiaris africana* collected in Cameroon. From the ethyl acetate extract of fermentations on rice, six compounds were isolated, with a pair of altersetin tautomers **41** and **42**. The new compound methyl 2-carboxy-3-hydroxy-(*E*)-cinnamate (**46**) gradually cyclized to **47** in MeOH.

5. *Penicillium paxilli*

P. paxilli had the same origin as *A. terreus*, isolated from a sediment sample collected from the lake of Wadi EI Natrun in Egypt. Ten known compounds, including eight paxillines and two pyrenocines, were isolated from rice cultures. Interestingly, the production of two pyrones was induced when cultured in an over-autoclaved plant mixed rice medium. Bioactivity tests showed cytotoxic activities of dehydroxy paxilline (**49**), pyrenocine B (**56**) and pyrenocine A (**57**) against L5178Y with IC_{50} values of 6.7, 4.9 and 1.1 μM, respectively. When assayed against A2780 sens, dehydroxy paxilline (**49**) and paspaline (**52**) caused pronounced inhibition with IC_{50} values of 6.4 and 3.2 μM, respectively, 10β-hydroxy-13-desoxy paxilline (**51**), pyrenocine B (**56**) and pyrenocine A (**57**) had moderate inhibitory effect with IC_{50} 24.5, 73.4 and 22.0 μM, while 21-isopentenylpaxilline (**50**) showed a weak inhibition with IC_{50} 105.6 μM. In addition, **49** was the only compound that showed inhibition against A2780 CisR cells with IC_{50} 1.1 μM.

The co-cultivation experiments of *P. paxilli* with bacteria (*B. subtilis*, *B. cereus*, *S. coelicolor* or *S. lividans*) failed to induce any changes in fungal natural product accumulation.

6. *Penicillium sclerotiorum*

P. sclerotiorum was isolated from the mangrove plant *Aegialitis annulata*. Five known compounds were isolated from this fungus, including (+)-isorotiorin (**60**), (+)-sclerotiorin (**61**), (+)-isochromophilone VI (**62**), isoharzianic acid (**63**) and harzianic acid (**64**).

Zusammenfassung

Diese Dissertation beschreibt Sekundärstoffe, die aus verschiedenen Pilzstämmen, wie beispielsweise *Trichoderma harzianum*, *Aspergillus terreus, Penicillium* sp. (Stämme IO1 und IO2), *Alternaria alternata, Penicillium paxilli* und *Penicillium sclerotiorum* isoliert wurden. Die Strukturaufklärung erfolgte mit Hilfe spektroskopischer Methoden, wie der Massenspektrometrie (MS) und der Kernspinmagnetresonanzspektroskopie (NMR). Die absolute Konfiguration chiraler Substanzen wurde durch Vergleich der optischen Rotation mit Literaturwerten oder durch ECD Spektroskopie bestimmt. Um die maximale chemische Diversität an sekundären Metaboliten aus den Pilzen zu erhalten, wurden verschiedene Kultivierungsmethoden durchgeführt. Die bekanntesten Methoden beinhalten die Änderung des Mediumtyps oder des pH-Werts, um die Biosynthese bestimmter Metabolite zu aktivieren, so dass diese entsprechend produziert werden.

Es wird davon ausgegangen, dass mikrobielle Interaktionen der wichtigste Faktor sind, um die Produktion von bioaktiven Sekundärmetaboliten anzuregen. Deshalb wurden Co-Kultivierungsversuche durchgeführt, um die natürliche Umgebung in der Natur nachzuahmen und mit dem Ziel, stille Biosynthese-Gencluster zu aktivieren. Zudem wurden epigenetische Modifikationen durchgeführt, um die Induktion von neuen sekundären Metaboliten zu fördern, indem Histon-Deacetylasen (HDAC) oder DNA-Methyltranferasen (DMAT) inhibiert wurden.

Diese Dissertation enthält folgende Kapitel:

1. *Trichoderma harzianum*

Der endophytische Pilz *T. harzianum* wurde aus den Blättern von *Cola nitida* isoliert. Aus der ersten Fermentation auf Reismedium wurde der neue Naturstoff 4‘-Hydroxy-deacetyl-18-deoxycytochalasin H (**1**) und die bekannten Verbindungen Deacetyl-18-deoxycytochalasin H (**2**), 18-Deoxycytochalasin (**3**) und Alternariol (**4**) erhalten. Die zweite Fermentation ergab die bekannten Substanzen Waol (**5**) und Aspyridon A (**6**). Die Struktur des neuen Naturstoffs **1** wurde mit Hilfe von 1D- und 2D-NMR-Spektroskopie, HRESIMS Messungen und Literaturvergleichen bestimmt. Die Substanzen **1-3** zeigten starke zytotoxische Aktivitäten gegenüber der Mauslymphomzelllinie L5178Y und der menschlichen Ovarialkrebszelllinie A2780 sens und A2780 CisR (IC_{50} 0,19-6,97 μM). Die A2780 Zelllinie beinhaltet sowohl die Cisplatin sensitiven (sens) als auch resistenten (CisR) Zellen.

2. *Aspergillus terreus*

Der in der Erde lebende Pilz *A. terreus* wurde aus einer Sedimentprobe des Wadi El Natrun Sees in Ägypten isoliert. Die Co-Kultivierung von *A. terreus* mit den Bakterienstämmen *Bacillus subtilis* und *Bacillus cereus* auf Reismedium resultierte in einer bis zu 34-fachen Erhöhung der Naturstoffproduktion der Pilze (**10**-**21**) im Vergleich zur axenischen Kultivierung des Pilzes. So wurden zwei neue Butyrolacton-Derivate Isobutyrolacton II (**7**) und 4-O-Demethylisobutyrolacton II (**8**) und die bekannte Verbindung N-(Carboxymethyl)anthranilsäure (**9**) gewonnen. Substanz **9** konnte nur in der Co-Kultivierung mit *B. subtilis* oder mit *B. cereus* isoliert werden. In der axenischen Kultur des Pilzes wurde sie nicht nachgewiesen.

Die Kulturen von *A. terreus* auf Reis-, flüssigem Wickerham- und Bohnenmedium wurden mittels HPLC untersucht. Neben neun verschiedenen Substanzen, die aus der Reiskultur isoliert wurden, wurden das Stereoisomerenpaar Dihydroisoflavipucin (**22**) und (**23**) aus der Wickerham-Flüssigkultur und Asterrelenin (**29**) und Acetylaszonalenin (**30**) aus der Bohnenkultur erhalten.

Substanzen **11** und **20** bewirkten eine schwache Inhibition gegenüber *B. cereus* mit einer minimalen Hemmkonzentration (MHK) von 150,9 und 216,2 μM, während **14** eine moderate Zytotoxizität gegenüber der Mauslymphomzelllinie L5178Y zeigte. Bei einer Dosis von 10 μg/mL wurde die Wachstumsrate um 80 % inhibiert.

3. *Penicillium* sp. Stämme IO1 und IO2

Der aus dem mediterranen marinen Schwamm *Ircinia oros* isolierte Pilz *Penicillium* sp. (Stamm IO1) brachte ein neues Fusarielin Analogon (**31**) und die bekannten Substanzen Griseofulvin (**32**) und Dechlorogriseofulvin (**33**) hervor. Die absolute Konfiguration von **31** wurde auf der Basis von TDDFT ECD Berechnungen ermittelt. Aus einer weiteren *Penicillium*-Art (Stamm IO2), ebenfalls aus dem Schwamm *I. oros* isoliert, wurden die bekannten Substanzen Dehydrocurvularin (**34**), Curvularin (**35**) und Trichodimerol (**36**) erhalten. Bei der Co-Kultivierung von beiden *Penicillium*-Stämmen IO1 und IO2 wurde die Bildung der bekannten Naturstoffe Norlichexanthon (**37**) und Monocerin (**38**) induziert, die unter axensischen Bedingungen in den Kontrollkulturen nicht produziert wurden. Griseophenon B (**39**) und Echinulin (**40**) wurden ebenfalls nach Co-Kultivierung isoliert, wobei sie aufgrund der geringen Menge nicht im HPLC detektierbar waren. Die Naturstoffe

39 und **40** zeigten eine deutliche Zytotoxizität gegenüber der Mauslymphom-Zelllinie L5178Y mit IC_{50}-Werten von 8,4 bzw. 4,7 μM.

4. *Alternaria alternata*

Alternaria alternata wurde aus Blättern der Regenwaldpflanze *Antiaris africana*, die in Kamerun gesammelt wurden, isoliert. Aus dem Ethylacetat-Extrakt der Fermentation auf Reis wurden die fünf bekannten Substanzen (5*S*)-Altersetin (**41**), Altersetin-2 (**42**), Altertoxin II (**43**), Altertoxin I (**44**) und Tenuazonsäure (**45**) isoliert, wobei **41** und **42** ein Stereoisomerenpaar sind. Zusätzlich wurde die neue Substanz Methyl-2-carboxy-3-hydroxy-(*E*)-cinnamat (**46**) isoliert, welche allerdings in Methanol graduell zu **47** zyklisiert.

5. *Penicillium paxilli*

Penicillium paxilli wurde aus der gleichen Bodenprobe isoliert wie *A. terreus*. Es wurden zehn bekannte Naturstoffe, darunter acht Paxilline und zwei Pyrenocine, aus Reiskulturen isoliert. Interessanterweise wurde die Produktion von zwei Pyronen induziert, indem Pflanzenmaterial der Wirtspflanze dem Reismedium beigemischt wurde. Bioaktivitätstests zeigten zytotoxische Aktivitäten von Dehydroxypaxillin (**49**), Pyrenocin B (**56**) und Pyrenocin A (**57**) gegenüber der Mauslymphomzelllinie L5178Y mit IC_{50}-Werten von 6,7, 4,9, bzw. 1,1 μM. Gegenüber der humanen Zelllinie A2780 sens zeigten Dehydroxypaxillin (**49**) und Paspain (**52**) eine Inhibition mit IC_{50}-Werten von 6,4 bzw. 3,2 μM, während 10β-Hydroxy-13-desoxypaxillin (**51**), Pyrenocin B (**56**) und Pyrenocin A (**57**) einen moderaten inhibitorischen Effekt mit IC_{50}-Werten von 24,5, 73,4 bzw. 22,0 μM aufwiesen. 21-Isopentenylpaxallin (**50**) zeigte eine schwache Inhibition mit einem IC_{50}-Wert von 105,6 μM. Zudem war Paxillin (**49**) die einzige Substanz, die mit einem IC_{50}-Wert von 1.1 μM gegenüber der Zelllinie A2780 CisR eine gute zytotoxische Aktivität besaß.

Co-Kultivierungsversuche von *P. paxilli* mit Bakterien (*B. subtilis, B. cereus, S. coelicolor oder S. lividans*) führten nicht zur Induktion von pilzlichen Naturstoffen.

6. *Penicillium sclerotiorum*

P. sclerotiorum wurde aus der Mangrove *Aegialitis annulata* isoliert. Es wurden fünf Substanzen aus diesem Pilz gewonnen. Dazu gehörten (+)-Isorotiorin (**60**), (+)-Sclerotioin (**61**), (+)-Isochromophilon VI (**62**), Isoharziansäure (**63**) und Harziansäure (**64**).

List of publications:

Result 3.1 Compounds isolated from endophytic fungus *T. harzianum*

Current status: published in *Natural Product Communications*, 2015, 10, 585-587.

Title: A new cytotoxic cytochalasin from the endophytic fungus *Trichoderma harzianum*

Authors: Huiqin Chen, Georgios Daletos, Festus Okoye, Daowan Lai, Haofu Dai and Peter Proksch

The overall contribution to the paper: 70% for the first author. The first author was involved in fungus identification, compound isolation, structure elucidation, as well as manuscript preparation.

Result 3.2.1 Inducing secondary metabolite production by co-cultivation of *A. terreus* with bacteria

Current status: published in *Phytochemistry Letters*, 2015, 12, 35-41.

Title: Inducing secondary metabolite production by the soil-dwelling fungus *Aspergillus terreus* through bacterial co-culture

Authors: Huiqin Chen, Georgios Daletos, Mohamed S. Abdel-Aziz, Dhana Thomy, Haofu Dai, Heike Brötz-Oesterhelt, Wenhan Lin, Peter Proksch

The overall contribution to the paper: 80% for the first author. The first author was involved in all laboratory work as well as manuscript preparation.

Result 3.3 Compounds isolated from two sponge-derived fungi *Penicillium* sp. (strains IO1 and IO2)

Current status: published in *Tetrahedron Letters*, 2015, 56, 5317-5320.

Title: A new fusarielin analogue from *Penicillium* sp. isolated from the Mediterranean sponge *Ircinia oros*

Authors: Huiqin Chen, Nihal Aktas, Belma Konuklugil, Attila Mándi, Georgios Daletos, Wenhan Lin, Haofu Dai, Tibor Kurtán and Peter Proksch

The overall contribution to the paper: 50% for the first author. The first author was involved in fungi identification, fungi fermentation, compound isolation and structure elucidation, as well as manuscript preparation.

Table of Contents

1. Introduction

1.1 History of natural products in drug discovery

Nature provides materials to human beings for basic necessities like food, clothing and residence, as well as the source of medicines for the treatment of diseases. The eastern culture has a long time documented history for humans to use substances directly collected from nature, which could date back to 2600 BC in Mesopotamia. Moreover, a serials of pharmaceutical records, such as Egyptian pharmaceutical recorded “Ebers Papyrus”, the Chinese Materia medica and Indian Tibetan medicine have been found to describe the medical functions of plants, animals and minerals, and were extensively employed in traditional clinic (Borchardt, 2002). Apart from East, the ancient Western scientists contributed substantially to the rational development of drugs from natural products. Instead of the entire material, active ingredients were involved in clinical treatment by the advance of chemistry, medicine and pharmacy. Gradually, compounds became the targets to administer. With those small molecules, the mysterious veil of the drug effect on diseases was unraveled. Foxglove extract was used to treat heart disease by William Withering in 1785, and led to the drugs digitoxin and digoxin, used for treating various causes of heart failure. Over decades, this small molecule “led to an understanding of the biochemistry and the biology of the sodium-potassium adenosine triphosphates pump” (Skou, 1988; Rishton, 2008). Later, morphine isolated from poppies led to “the development of a defined and dose-controlled medicine for pain”; salicylic acid from willow bark inspired to synthesize aspirin, which has the same function with salicylic acid while avoids the side effect; and penicillin found from mold plate led to the discovery of β-lactam antibiotics, sequentially (Rishton, 2008). Each of these discoveries was a milestone on the way to natural products development. Until now, bioactive natural products are used in three classes: natural products with biological activities are used directly as drugs, semi-synthetic natural products are derived from natural products templates, whereas synthetically derived compounds are inspired from natural products. (Cragg, Newman and Snader, 1997; Newman, Cragg and Snader, 2003)

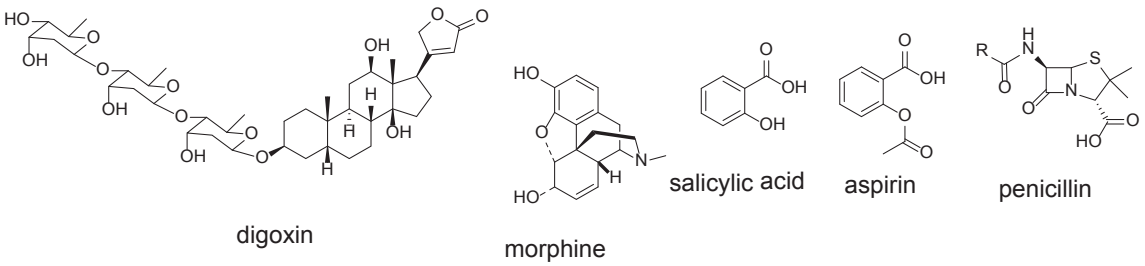

Figure 1.1 Compounds used as drugs from natural products.

1.2 Fungi as the important source of natural products

Since the discovery of penicillin from *Penicillium notatum* by Fleming in 1929, and its broad therapeutic use in 1940s, intensive investigation of bioactive metabolites from microorganisms was promoted. A series of structural diverse bioactive metabolites have played a vital role in the pharmaceutical industry.

1.2.1 Anti-infective agents

Penicillins are the first group of antibiotics discovered from fungi. In 1945, the structure of penicillin was elucidate using X-ray crystallography by Dorothy Crowfoot Hodgkin, and then synthesized by the chemist John C. Sheehan in 1957 (Sheehan and Henery-Logan, 1959). The family of penicillins includes penicillin G, penicillin V, and benzathine penicillin, and all of them are *β*-lactams. Penicillin G shows activity mainly against Gram-positive bacteria, and only a few Gram-negative bacteria such as *Neisseria gonorrhoeae* and *N*. *meningitidis* have been found to be susceptible to it. The four-membered *β*-lactam is the activity center in the structure of penicillin, and acts by binding to the penicillin-binding proteins, which catalyze the transglycosylase, transpeptidase, and carboxypeptidase activities. This reaction leads to an inhibition of the peptidoglycan cross-link formation and an imbalance between the cell wall production and degradation. Finally, the cell cytolysis is caused by the increasingly uncompensated of the osmotic pressure between inside and outside of the cells due to the weakened cell wall. (Shi *et al*., 2011; Spratt and Cromie, 1988; Sauvage *et al*., 2008) The biosynthesis of penicillin involves the condensation of *δ*-(L-*α*-aminoadipyl)-L-cysteine-D-valine (ACV) from L-*α*-aminoadipic acid, L-cysteine and L-valine epimerized from D-valine first, followed by oxidative conversion of the linear ACV

into the bicyclic intermediate isopenicillin N (Brakhage *et al*., 2004; Brakhage, 1998). Then penicillin G is produced by removing the *α*-aminoadipyl side-chain and replaced by a phenylacetyl side-chain (Brakhage *et al*., 2004; Brakhage, 1998). In 1948, another *β*-lactam antibiotic group, cephalesporins, came into the sight of scientist since cephalosporin C was isolated by Brotzu from *Cephalosporium acremonium* (Brotzu, 1948). This ring-expanded molecule compared to penicillins led to serials of semi-synthetic structures, such as cephalexin, and they were originally used to treat infections resistant to penicillins. (Newman, Cragg and Snader, 2000)

Griseofulvin is an antifungal drug used to treat fungal infections in skin, hair and nails, originally isolated from *Penicillium griseofulvum* (Grove *et al*., 1952). Its mode of fungistatic action is by interfering with microtubule function and mitosis inhibition through binding to tubulin (Huber and Gottlieb, 1968). The biosynthesis of griseofulvin is mediated by a polyketide synthase to form a 14-carbon poly-*β*-keto chain, which then undergoes cyclization, condensation, methylation, halogenation and oxidation reactions. Another antifungal drug group echinocandins was approved at the beginning of the 20th century, for caspofungin and anidulafungin as examples. Both of these two compounds were semisynthesis from echinocandin B, which was isolated from *Aspergillus* sp.. (Debona *et al*., 1995; Mishra and Tiwari, 2011) Echinocandins inhibit fungi by interfering with (1,3)-*β*-D-glucan synthase, which is a major fungal, but not human target. These drugs show significant activity against invasive infections by *Candida* and *Aspergillus* species. (Denning, 1997; Pfaller *et al*., 2005b; Pfaller *et al*., 2005a)

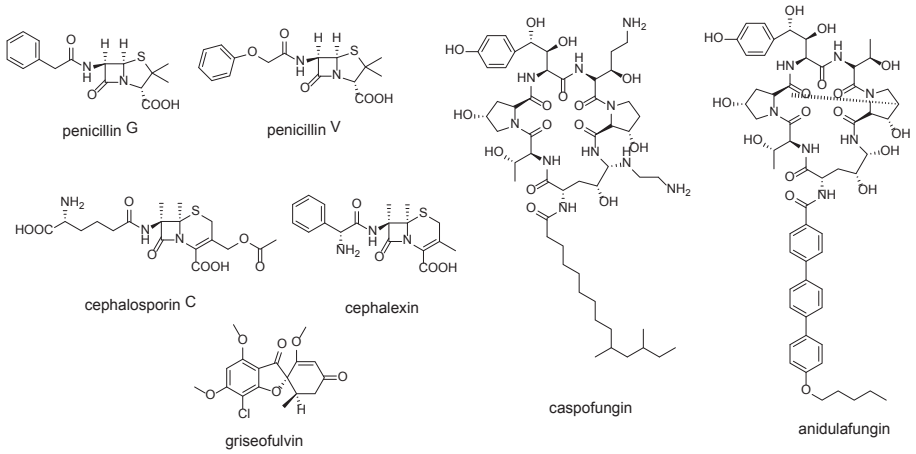

Figure 1.2 Compounds with anti-infection derived from fungi.

1.2.2 Anticancer agents

Pacilitaxel is an important anticancer drug that is used for the treatment of ovarian cancer, breast cancer, and lung cancer (Wood, Rowinsky and Donehower, 1995). It was initially isolated from the Pacific yew, *Taxus brevifolia*, and later Venilla R. and Muthumary J. gained this compound from an endophytic fungal culture of *Pestalotiopsis* sp. isolated from the tropical tree bark named *Tabebuia pentaphylla* (Vennila and Muthumary, 2011). The mechanism of action for pacilitaxel and its derivative docetaxel, is through the blockage of cell mitosis by stabilization of the microtubule polymer and consequently cell death (Zwawiak and Zaprutko, 2014). More anticancer agents include vinblastine and vincristine, which were originated from the plant *Catharanthus roseus* and later found from the culture of *Alternaria* sp. (Lingqi, 1998) and *Fusarium oxysporum* (Kumar *et al*., 2013), and both endophytic fungi isolated from the same plant host; topotecan and irinotecan, derivatives of camptothecin isolated from the stem and bark of the plant *Camptotheca acuminate*, presenting cytotoxicity against several cell lines including lung cancer, liver cancer, and ovarian cancer, are found from the culture of endophytic fungi such as *Entrophospora infrequens*, *Neuropsora* sp. and *Fusarium solani* (Kharwar *et al*., 2011).

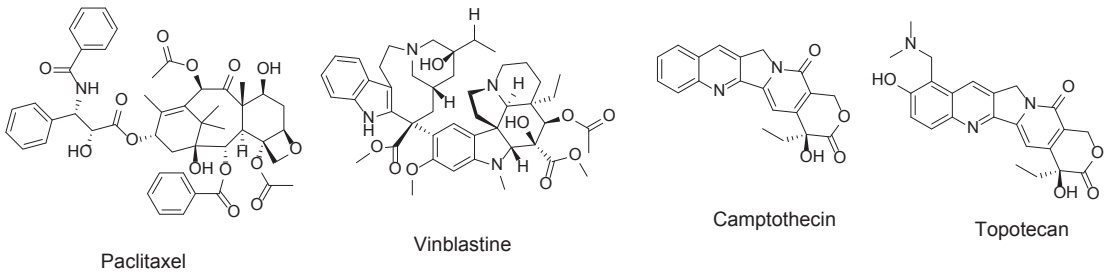

Figure 1.3 Anticancer agents.

1.2.3 Immunosuppressive agents

Cyclosporine A, initially found as a secondary metabolite produced by *Tolypocladium inflatum*, played an important role as immunosuppressant drug used to prevent rejection of organ or tissue transplantation. As the member of ciclosporins, it acts via binding to the cytosolic protein cyclophilin of T cells, and inhibits calcineurin, then lower the activity of T cells. (Cantrell and Smith, 1984) Further immunosuppressive agents, mizoribine was

originated from fungus *Eupenicillium brefeldianum*, and mycophenolic acid, whose prodrug of mycophenolate mofetil, firstly discovered from *Penicillium* sp., inhibits the proliferation of lymphocytes selectively via inhibition of inosinmonophosphat-dehydrogenase (IMPDH) (Ishikawa, 1999). Mycophenolic acid is "a selective, noncompetitive, reversible inhibitor of IMPDH, the rate-limiting enzyme in the de novo pathway of guanosine nucleotide synthesis" (Chin *et al*., 2006).

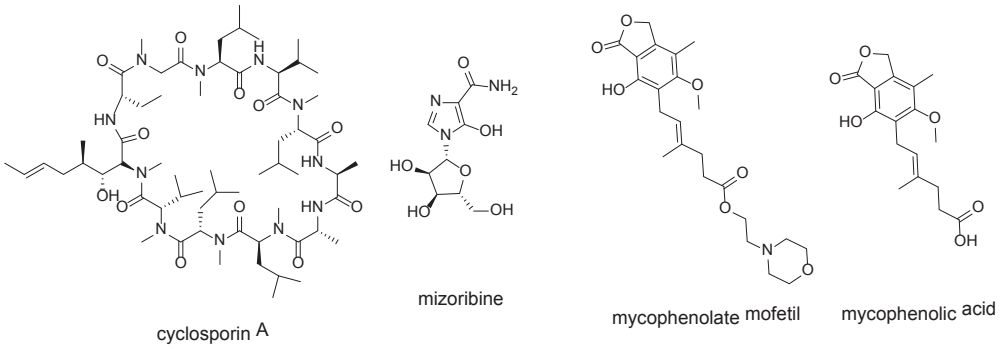

Figure 1.4 Immunosuppressive agents.

1.2.4 Cholesterol lowering agents

Lovastatin (mevinolin) was the first commercialized hydroxymethylglutaryl coenzyme A reductase inhibitor among cholesterol lowering agents, and was approved in 1987 (Alberts *et al*., 1989; Newman, Cragg and Snader, 2000). This compound was isolated from bacteria *Meiothermus ruber* and fungus *A*. *terreus* in 1979 and 1980, respectively, and led to the synthesis of three ring-opened lactones: fluvastatin, cerivastatin and atorvastatin (Newman, Cragg and Snader, 2000; Endo, 1979; Alberts *et al*., 1980). Another fungal derived statin, mevastatin, was isolated earlier than lovastatin from *Penicillium brevicompactum*, while it was not developed further (Endo, 1985). However, its derivatives rosuvastatin calcium and pitavastatin were approved at the beginning of 20th century as lipid-lowering agents and treatment of dyslipidemia, respectively (Chin *et al*., 2006).

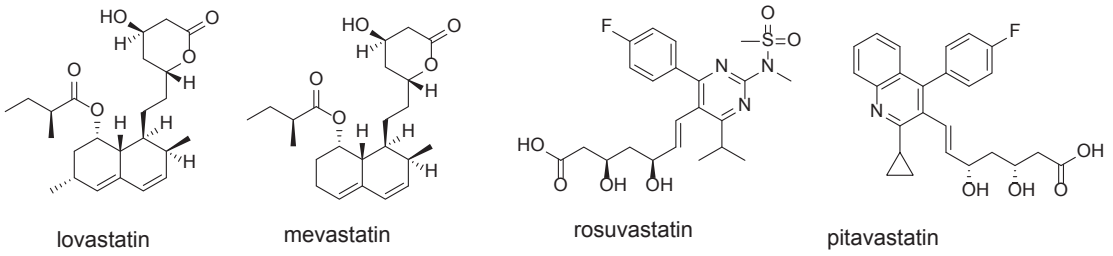

Figure 1.5 Cholesterol lowering agents.

1.3 Distribution of fungi

Fungi is a large group of eukaryotic organisms, and seem to occupy virtually every niche living and non-living on earth, including extreme environments, such as thermal vents, deep rock sediments, hot and dry deserts, high salinity marine environments, as well as polar regions (Doolittle *et al*., 1996; Strobel, 2003).

1.3.1 Endophytic fungi

Plants used in folk medicine have been widely studied as a source of bioactive secondary metabolites; however, the limited natural resources and low yield of target products become the bottleneck of commercial exploitation. Fortunately, endophytic fungi started to attract attention, and new avenues to natural products were explored in the past few decades. Endophytic fungi are a group of fungi "living in the internal tissues of plants for at least a part of their life cycle without causing any noticeable symptoms of infection". (Bacon and White, 2000; Porras-Alfaro and Bayman, 2011) Until now, none of literature has reported a plant living without endophytes. Therefore, it is not difficult to imagine that there are some kinds of communication exist between these different species to maintain this symbiotic association. (Gunatilaka, 2006; Aly, Debbab and Proksch, 2013) Several studies on secondary metabolites from the host-plant and their endophytic fungi have indicated that these small molecules played a crucial role during this communications at least in some aspects. Pacilitaxel, as aforementioned, was the first example isolated from both, plant and its endophytic fungi, and set the stage for scientists to put sight on the related endophytic fungi on searching for the pharmacologically important natural products produced by the host-plant. Further examples include the anticancer lead drug camptothecin and its analogues from the plants *Nothapodytes foetida* and *Camptotheca acuminata*, as well as their associated endophytes (Puri *et al*., 2005;

Shweta *et al*., 2010; Kusari, Zuhlke and Spiteller, 2011); the antidepressant agents hypericin and emodin produced by *Hypericum perforatum* and its endophytic fungus *Thielavia subthermophila* (Kusari *et al*., 2008); as well as natural insecticides azadirachtin A and B (Kusari *et al*., 2012).

1.3.2 Marine fungi

The ocean covers around three quarters of the earth's surface, and their environment is unique to terrestrial habitats due to special factors, such as high salinity, low water potential, and especially different nutrient conditions and high hydrostatic pressure (Raghukumar, 2008). This distinctive ecological system may build up diverse patterns of secondary metabolites in marine organisms different from terrestrial sources, and offer a high potential for new bioactive natural products for pharmaceutical and agrochemical purposes (Donia and Hamann, 2003; Saleem *et al*., 2007). "Marine fungi are an ecological rather than a taxonomic group", and their habitats are various ranging from floating wood to sediments, and from mangrove plants to animals (Hyde *et al*., 1998).

Marine invertebrates such as sponges, ascidians and soft corals are well known for harboring microbial symbionts and benefit from each other with regard to nutrients and defense. For example, up to 40% of sponge's volume was comprised by dense and diverse microbial communities. (Webster and Taylor, 2012) Due to the special physical sessile soft bodies scarcity of ability to move and in addition to lack of outer protection, sponges rely more on chemical than on physical defense, as well as nutrition acquisition to maintenance of life (Burns *et al*., 2003). The fungal symbionts may play a potential role in this chemical matter dependent survive, such as hydrolytic enzymes are involved to convert organic matter into easily accessible sources for filter feeding by sponge-host (Selvin *et al*., 2010), and bioactive secondary metabolites for defense produced directly or by supplying precursors for further biosynthesis (Debbab, Aly and Proksch, 2012; Taylor *et al*., 2007). In the last few years, comprehensive investigation of secondary metabolites from invertebrate-associated fungi led to the isolation of a number of active substances with unique structural skeletons. *Aspergillus ustus*, isolated from the marine sponge *Suberites domuncula* collected from the Adriatic Sea, afforded seven new drimane sesquiterpenoids together with three known compounds. Among

these compounds, two new compounds as well as known compound exhibited cytotoxicity against the murine lymphoma cell line L5178Y. (Liu *et al*., 2009) Two new aspyrone derivatives, chlorohydroaspyrones A and B were produced by the marine fungal strain *Exophiala* sp., that originated from the sponge *Halichondria panacea*, collected from Bogil Island. These compounds displayed moderate antibacterial activity against *Staphylococcus aureus*, methicillin-resistant *S. aureus* and multidrug-resistant *S. aureus*. (Zhang *et al*., 2008) In addition, soft coral *Sarcophyton* sp. associated fungus *Alternaria* sp. ZJ-2008003 studied by Zheng *et al.* (2012) yielded considerable new secondary metabolites including five new hydroanthraquinne derivatives, namely, tetrahydroaltersolanols C - F and dihydroaltersolanol A, five new alterporriol-type anthranoid dimers, alterporriols N - R, and seven known analogues. The known compound altersolanol C showed the strongest inhibitory activity against human colon carcinoma (HCT-116), human breast cancer (MCF-7/ADR), human prostatic cancer (PC-3), and human hepatoma (HepG2 and Hep3B) cells, with IC_{50} values between 2.2 - 8.9 *u*M. (Zheng *et al*., 2012)

1.3.3 Mangrove derived fungi

The mangrove ecosystem is confined to a dynamic zone between terrestrial and marine habitats, and distribute in tropical and subtropical latitudes. Thanks to the tidal activities of this area, which lead to the daily changes in sea water level, mangrove endophytes undergo both terrestrial and marine environments, which contribute to great diversity of fungi. (Bandaranayake, 2002; Shearer *et al*., 2007) These endophytes not only help the host to adapt to the harsh living conditions, but also improve the ability to confront with a plethora of microbial pathogens under this warm and moist climate (Latha and Mitra, 2004). Examination of mangrove-fungi may provide important data for the discovery of novel chemical scaffolds for drugs and drug leads. In recent years, a considerable number of secondary metabolites with various biological activities have been isolated from mangrove fungi. Li *et al*. (2011) reported four new norsesquiterpene peroxides, talaperoxides A-D, together with one known steperoxide B, isolated from the fungi *Talaromyces flavus* derived from leaves of the mangrove plant *Sonneratia apetala* (Lythraceae). Talaperoxides B and D exhibited cytotoxicity against human cancer cell lines MCF-7, MDA-MA-435, hepatocellular

carcinoma HepG2, cervical epithelial carcinoma HeLa, and prostatic carcinoma PC-3 cells with IC_{50} values between 2.8 and 9.4 *u*M. (Li *et al*., 2011) Shang *et al*. (2012) investigated secondary metabolites from semi-mangrove plant *Pongamia pinnata* (Fabaceae) derived endophytic fungal strain *Nigrospora* sp. MA75, and afforded three new compounds 2,3-didehydro-19-hydroxy-14-epicochlioquinone B, 6-O-desmethyl dechlorogriseofulvin and 6'-hydroxygriseofulvin, together with seven known compounds from a different sodium salt contained culture medium. 2,3-Didehydro-19°-hydroxy-14-epicochlioquinone B exhibited even stronger inhibition to *Escherichia coli*, *P*. *fluorescens*, and *S*. *epidermidis* than the positive control ampicillin with MIC 8.2, 1.0 and 1.0 *u*M, respectively. (Shang *et al*., 2012) Further chemical investigation on mangrove-derived fungi like fungus XG8D from leaves of *Xylocarpus granatum* (Meliaceae) isolated by Chokpaiboon *et al*., afforded a new chamigrane endoperoxide merulin D and four known analogues. The known compound merulin C caused complete inhibition of microvessel sprouting on rats at a concentration of 2.5 *u*M. (Chokpaiboon *et al*., 2011)

1.3.4 Fungi from sediment

Sediment in the marine ecosystem is characterized as detritus consisting of debris and carcasses of dead animals and plant. Hence, the different biological types in a specific region develop the special ingredients of the sediment, providing unique nutrients for fungal communities. In addition, other factors such as the level, temperature and upstream likewise influence the fungal community and its metabolites. Undoubtedly, sediment derived fungi are developing into another interesting fungal source for scientists. Examples include *Aspergillus carbonarius*, isolated from the marine sediment, afforded two new cytotoxic secondary metabolites, carbonarones A and B (Zhang *et al*., 2007); whereas *A*. *glaucus* obtained from mangrove roots sediment, yielded the novel anthraquinone derivative aspergiolide A, which inhibited the proliferation of several cancer cell lines. (Du *et al*., 2007)

1.4 Activation of silent gene clusters in fungi

Fungi comprise a large reservoir of bioactive natural products, however, the high rediscovery rate of known natural products frustrate the traditional methods involved in research (Scherlach and Hertweck, 2009). In nature, fungi live in a multi-organism co-existing environment, so that multispecies crosstalk with their host and other surrounding microorganisms, is considered as the factor to trigger the production of secondary metabolites with functional traits. Nevertheless, these corresponding biosynthetic gene clusters may fail to express under standard culture conditions in the laboratory due to the lack of activation signals. (Kusari, Singh and Jayabaskaran, 2014; Debbab, Aly and Proksch, 2012) The growing knowledge of microbial genomics provide better understanding of the biosynthesis of secondary metabolites and thus offers effective approaches to induce new metabolites from fungal cultures (Scherlach and Hertweck, 2009).

1.4.1 Inducing secondary metabolites through optimization of culture conditions

Cultivation parameters are known as critical factors for the amount and type of metabolite production by fungi. Therefore, “OSMAC (One Strain-MAny Compounds) approach” is applied by modification of easily accessible cultivation parameters, including media type and composition, pH value, oxygen supply, temperature, aeration, agitation, shape of culturing flask, or harvest points to achieve the production of novel natural products. (Bode *et al*., 2002; Kusari, Singh and Jayabaskaran, 2014; Debbab, Aly and Proksch, 2012) For instance, *Paraphaeosphaeria quadriseptata* induced six new secondary metabolites when cultivated in media containing distilled water instead of tap water (Paranagama, Wijeratne and Gunatilaka, 2007). In addition, Bode *et al*. (2002) showed that variation of the culture conditions of *A. ochraceus* yielded 15 additional compounds compared to the culture grown at standard conditions (Bode *et al*., 2002).

1.4.2 Stimulation of metabolite production by interspecies co-cultivation

Axenic culture of microorganisms in laboratory avoids the function occurred by symbiosis and competition between micro- and macro- organisms species compared to nature growing microorganisms (Kusari, Singh and Jayabaskaran, 2014). However, bioactive secondary

metabolites are thought to be induced in complex situations to enhance the competitiveness for limited space and nutrients (Scherlach and Hertweck, 2009). Therefore, the approach of co-cultivation is applied to microbial culture in laboratory based on this theory. That is cultivation of two different microbial strains instead of single strain in one culture vessel, so that the opportunity of direct interaction between these microbes was produced, then may lead to new secondary metabolites previously not observed in the respective axenic cultures (Pettit, 2009; Schroeckh *et al*., 2009).

Several publications have recently reported the induction of new or known metabolites by the co-cultivation approach. Co-cultivation of two marine derived microbes, surface-associated fungus *Emericella* sp. and actinomycete *Salinispora arenicola* in liquid culture, led to the isolation of two cyclic depsipeptides emericellamides A and B, which were not detected in axenic cultures (Oh *et al*., 2007). Another study on the isolation of secondary metabolites from the endophytic fungus *Fusarium tricinctum*, not only triggered three new natural products macrocarpon C, 2-(carboxymethylamino)benzoic acid, and (-)-citreoisocoumarinol by mixed fermentation with *B. subtilis* 168 trp C2 on solid rice medium, but also considerable accumulation of the constitutively present secondary metabolites. In addition, antibacterial activity against several Gram-positive bacteria including MRSA was observed on these induced fungal products. (Ola *et al*., 2013)

1.4.3 Epigenetic modifiers

Chromatin is consisted of DNA and associated histone proteins, whereas the latter control gene expression and DNA replication. Epigenetic modifications of chromatin including covalent modifications of bases in the DNA and of amino acid residues in the histones regulate the expression of genetic information, which is related to secondary metabolites production in fungi. DNA methylation of cytosine by DNA methyltransferases (DNMTs) and reactions of lysine and arginine residues in histone (especially acetylation of the lysine ε-amino group) have been shown to play crucial functions in biosynthesis secondary metabolites. (Scherlach and Hertweck, 2009; Lyko and Brown, 2005; Cichewicz, 2010)

The reported chemical small-molecules used to manipulate epigenetic modification include

5-azacytidine, 5-aza-2'-deoxcytidine, methylthioadenosine and S-adenosylhomocysteine as DNA methyltransferase (DNMT) inhibitors, as well as trichostatin A, suberoylanilide hydroxamic acid (SAHA), trapoxin B, apicidin, HC-toxin, sodium butyrate and valproic acid as histone deacetylase (HDAC) inhibitors (Cichewicz, 2010). Several laboratories have successfully triggered silent biosynthetic pathways to induce new secondary metabolites by applying some of these inhibitors. The marine-derived fungus *Microascus* sp. was introduced to produce a new cyclodepsipeptide by histone deacetylase inhibitor SAHA cultured in Dzapek-Dox/artificial seawater media, that was believed to activate the silent Hybrid PKS/NRPS biosynthetic pathway (Vervoort, Drašković and Crews, 2010). Another experiment like *Beauveria felina* using SAHA led to the accumulation of three new cyclodepsipeptides and five known ones (Chung *et al*., 2013).

1.4.4 Genetic engineering

Recently, some effective approaches have been applied to exploit new secondary metabolites from fungi "based on molecular biology like the generation of gene 'knock outs', promoter exchange, overexpression of transcription factors or other pleiotropic regulators" (Brakhage and Schroeckh, 2011). The successful examples like deletion of genes (hdaA) encoding an *Aspergillus nidulans* HDAC caused transcriptional activation of two secondary metabolite gene clusters (Scherlach and Hertweck, 2009).

1.5 Aims and significance of the study

As aforementioned, fungi are believed to be a treasure chest of bioactive natural products, and are expected to provide novel chemical structures for drug discovery for combating emerging diseases.

The aim of this study was investigation on secondary metabolites from promising fungal strains. In order to improve the less productive of laboratory fungi, several approaches were applied to activate silent biosynthetic gene clusters based on an ecological perspective. The soil-derived fungus *A. terreus* was successfully triggered to produce new metabolites together with an increased accumulation of constitutively present secondary metabolites by co-cultivation with bacteria such as *Bacillus* sp. on solid rice medium. Furthermore,

additional metabolites accumulated when fungus was grown on rice, in liquid Wickerham medium or on white beans medium. It is also interesting that co-cultivation of two sponge-associated fungi *Penicillium* sp. strains IO1 and IO2 resulted in the accumulation of two known compounds that were not present in either of the fungal axenic controls.

In addition, the investigation of biologically active and structural diverse secondary metabolites from fungi led to the identification of one new cytotoxic cytochalasin from the endophytic fungus *Trichoderma harzianum*; two new butyrolactones and one stereoisomers of dihydroisoflavipucine from *A. terreus*; one new fusarielin analogue whose absolute configuration was determined by ECD calculation, isolated from *Penicillium* sp. strain IO1; as well as one new aromatic compound and its derivative together with a stereoisomer of altersetin obtained from the endophytic fungus *Alternaria alternata*.

Pure compounds were subjected to various bioassays such as antimicrobial assays against *Staphylococcus aureus*, *B. subtilis*, *B. cereus* and *Mycobacterium tuberculosis*, as well as cytotoxicity against the mouse lymphoma cell line L5178Y and human ovarian cancer cell lines A2780 sens and A2780 CisR.

2. Materials and Methods

2.1 Instrument and chemicals

2.1.1 Instrument

Chemical instruments	
Analytical balance	MC-1/TE150 2S, Sartorius
Rotary evaporator	Rotavapor R-215, Buchi
Drying oven	Heraeus
Vacuum pump	CVC 2II, Vacuubrand
Hot plate and magnetic stirrer	IKA® RCT classic
Fractions collector	Retriever II, ISCO
Desiccator	Glaswerk wertheim
UV lamp (254 and 365 nm)	Camag
Ultra sonnicator	RK510H, Bandelin
Centrifuge	Pico 17, Thermo
Nitrogen generator	JUN-AIR 2000-40BS
Speedvac	Cooling trap RVT400, Savant
Freeze dryer	Alpha 1-2LD, Christ
UV/Vis spectrometer	Lambda 25, Perkin Elmer
Polarimeter	P-2000, JASCO
Dishwasher	G7883, Miele
High resolution ESI-MS	UHR-QTOF maXis 4G (Bruker Daltonics)
Analytic HPLC	
Pump	Ultimate 3000 pump, Dionex
Detector	Ultimate 3000 RS Diode Array Detector, Dionex
Column oven	STH585, Dionex
Column	Eurospher100-C18, [5um; 125×4mm], Knauer
Software	Chromeleon

Semi preparative HPLC	
Pump	L-7100, Merck
Detector	UV-L7400
Column	Eurospher 100-10C18, [10um; 300×8mm], Knauer
Precolumn	Eurospher 100-10C18, Knauer
Printer	Chromato-Intergartor D-2000, Merck
LC-MS	
Analytical HPLC	PH1100 series (photodiode array detector), Agilent
MS	Finigan LCQ-DECA, Thermoquest
Ionizer	ESI and APCI, Thermoquest
Vacuum pump	Edwards
Column	Eurospher 100-3C18, [5um; 100×2mm], Knauer
NMR	
Avance III 300	Bruker
Avance DRX 500	Bruker
Avance III 600	Bruker
Biological instrument	
Laminar air flow	Heraeus
Ultra Turrax	T25 basic, IKA-WERKE
pH meter	pH Level1, Inolab
Shaker	Certomat R/SII
Autoclave	Steritechnik AG
PCR machine	iCycler, Bio-Rad
Mixer mill	VF2, IKA Labortechnik

2.1.2 Chemicals

General laboratory chemicals

Methanol

n-Hexan

Dichloromethane

These solvents were purchased as technical solvents from ZCL (the central chemical storage), University of Duesseldorf, and were distilled before using.

Ethyl acetate p.a.	Fisher Scientific
Acetone p.a.	VWR
n-Butanol p.a.	PanReac AppliChem
Solvents for HPLC and LC-MS	
Methanol	HPLC grade, Fisher Scientific
Acetonitrile	HPLC grade, VWR
Formic acid	AppliChem
Trifluoroacetic acid	PanReac AppliChem
Nanopure water	produced by passing distilled water through nano- and ion- exchange filter cells (Barnstead)
Solvents for optical rotation	
Methanol	Spectral grade, Sigma
Dichloromethane	Spectral grade, Sigma
Acetone	Spectral grade, Sigma
Solvents for NMR	
Methanol-d_4	Euriso-top
DMSO-d_6	Euriso-top
Chloroform-d_4	Euriso-top
Acetone-d_6	Euriso-top
Pyridine-d_5	Euriso-top
Reagent for fungal identification	Zymoclean^{TM} Gel DNA Recovery Kit

2.2 Fungi isolation and cultivation

2.2.1 Fungi isolation

2.2.1.1 Isolation of plant endophytic fungi

The plant materials were washed with sterilized water to remove dust, then immersed in 70% ethanol for 1-2 min to sterilize microorganisms on the surface. After drying, the surface was overturned on the first petri dish containing isolation medium with the aid of a sterilized tweezer, as a control to ensure that no alive microbes remained on the surface. Then several segments (ca.1.5 × 1.5 mm) were cleaved from different parts of the plant materials with a sterilized razor blade and put into the second agar plate, with the fresh cut edge on contact with the agar. The plates were kept in the fungi room at room temperature (22°C).

Composition of medium for fungal strains isolation:

Bacto agar (BD)	15.0 g
Malt extract (PanReac AppliChem)	15.0 g
Chloramphenicol (Sigma)	0.2 g
Artificial sea salt	10.0 g (for marine fungal strain)
pH	7.4 - 7.8 (adjusted with NaOH/ HCl)
Distilled water	ad 1000 ml

2.2.1.2 Isolation of sponge-derived fungi

The sponge was surface sterilized by immersing in 70% ethanol for 30 sec., followed by rinsing three times in sterilized artificial sea water. Subsequently, the sponge was cleaved aseptically into small segments (ca. 1.5 × 1.5 mm). The material was placed on isolation medium contained plates and incubated at room temperature (22°C). (Chen *et al*., 2015a)

2.2.1.3 Isolation of soil-derived fungi

Sediment sample (1.0 g) was placed into a sterile falcon tube, and then 20.0 mL sterile demineralised water was added, followed by vigorous shaking of the suspension. Next, 100.0 μL of the suspension was transferred into a sterile Eppendorf tube, followed by addition of 900.0 μL sterile demineralised water and mixing. This step was repeated 4 times to generate a total of 5 stepwise dilutions. With the aid of a sterile pipette, one drop of the last dilution was

transferred onto an agar plate, then a sterile inoculation loop was used to spread out the dilution; thereby generating 2 agar plates per dilution.

2.2.2 Fungi purification

After several days, hyphae grew from the material on the agar plates, and different hyphae were transferred into different fresh agar plates with a sterilized loop, containing short term storage medium. This purification step was repeated until the hyphae in the whole agar plate were consistent.

Composition of medium for purification and short term storage of fungal strains:

Bacto agar (BD)	15.0 g
Malt extract (PanReac AppliChem)	15.0 g
Artificial sea salt	10.0 g (for marine fungal strain)
pH	7.4-7.8 (adjusted with NaOH/HCl)
Distilled water	ad 1000 ml

2.2.3 Long term storage for pure fungal strains

The pure fungal strains were transferred into petri dish containing long term storage medium, and cultivated in the fungi room. For long term storage, fungi grown on malt agar were transferred into low temperature freezer vials, and the strains were kept in -80°C fridge.

Composition of medium for long term storage of fungal strains:

Malt extract (PanReac AppliChem)	20.0 g
Yeast extract (BD)	0.1 g
Glycerin (VWR)	50.0 g
Artificial sea salt	10.0 g (for marine fungal strain)
Bacto agar (BD)	13.0 g
Distilled water	ad 1000 ml

2.2.4 Small scale cultivation of pure fungal strains for HPLC chromatogram analysis and bioassay screening

After the fungal strains covered almost the whole agar plates, small pieces of 1/4 plate of agar were sliced and delivered into 1 L Erlenmeyer flask containing 100.0 mg autoclaved rice

medium. The cultivation was performed at room temperature (22°C).

The strains were likewise cultivated on different media, including liquid Wickerham medium and white bean medium.

Composition of rice medium:

Rice	100.0 g
Artificial sea salt	3.0 g (for marine fungal strain)
Distilled water	110.0 ml

Composition of liquid Wickerham medium:

Yeast extract (BD)	3.0 g
Malt extract (PanReac AppliChem)	3.0 g
Peptone (BD)	5.0 g
Glucose (Caelo)	10.0 g
Artificial sea salt	3.0 g (for marine fungal strain)
pH	7.4-7.8 (adjusted with NaOH/HCl)
Distilled water	ad 1000ml

Composition of bean medium:

Bean	100.0 g
Artificial sea salt	3.0 g (for marine fungal strain)
Distilled water	110.0 ml

Bean medium was kept for overnight before autoclaved.

2.3 Identification of pure fungal strains

DNA was extracted from fungal cells with Lysis solution in ZR Bashing™ Lysis tube and purified with fungal/ Bacterial DNA Buffer, DNA Pre-wash Buffer, and Fungal/ Bacterial DNA Wash Buffer in Zymo-Spin™ IV Spin Filter and Zymo-Spin™ IIC Column, then kept in a 1.5 mL sterilized microcentrifuge tube with DNA Elution Buffer.

DNA amplification by PCR was performed in an iCycler thermocycler.

In 0.2 ml PCR tubes:

Add 25 μL Hot StarTaq Master Mix

1.5 μL primer mix (10 pmol/μL each) (primer mix: ITS1 and ITS4)

10-100 ng template DNA (usually 1 μL is enough)

Water ad 50 μL.

ITS1: 5'-TCCGTAGGTGAACCTGCGG-3'

ITS4: 5'-TCCTCCGCTTATTGATATGC-3'

PCR program:

1. Initial denaturation 95.0 °C for 15.0 min,
2. Denaturation 95.0 °C for 1.0 min,
3. Annealing 56.0 °C for 1.0 min,
4. Extension 72.0 °C for 1.0 min
5. Final extension 72.0 °C for 10.0 min.

Steps 2-4 were repeated 35 times, then kept under conditions at -4 °C when all cycles were finished.

PCR products were purified by gel electrophoresis:

1% agarose gel was used: 1.2 g agarose + 120 mL TBE buffer + 12 μL SYBR Safe DNA gel stain. 50 μL of PCR products mixed with 10 μL 6X gel loading dye were loaded in the gel wells and 10 μL Ladder Quidk-load^{TM} 100 bp DNA Ladder were loaded in two edge wells. Then, the electrophoretic gel was run at 75 eV for 45 min. After electrophoresis, the bands were detected at about 550 bp by comparing with the DNA ladder under UV. Finally, 7.5 μL of the PCR product and 2.5 μL of the ITS1 primer were submitted for sequencing.

2.4 Taxonomy

Trichoderma harzianum

The strain of *T. harzianum* was isolated from leaves of *Cola nitida*, collected from Awo-idemili in Imo State, Nigeria, in February 2012. The voucher specimen is deposited at the International Center for Ethnomedicine and Drug Development with the number INTERCEDD/802. (Chen *et al*., 2015c)

Phylum	Ascomycota
Subphylum	Pezizomycotina
Class	Sordariomycetes
Order	Hypocreales
Family	Hypocreaceae
Genus	*Trichoderma*
Species	*T. harzianum*

Figure 2.1 *T. harzianum*

Aspergillus terreus

The fungus *A. terreus* was isolated from sediment collected in November 2012 from the Lake Wadi EI Natrun in Egypt.

Phylum	Ascomycota
Class	Eurotiomycetes
Order	Eurotiales
Family	Trichocomaceae
Genus	*Aspergillus*
Species	*A. terreus*

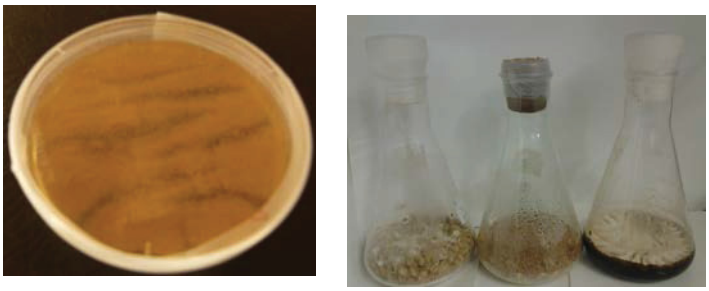

Figure 2.2 *A. terreus*

***Penicillium* sp. strains IO1 and IO2**

The *Penicillium* sp. strains IO1 and IO2 were isolated from the sponge *Ircinia oros*, collected at Kemer of Antalya, Turkey, in March 2012. A voucher specimen is deposited at Ankara University, Faculty of Pharmacy, Ankara, Turkey. (Chen *et al*., 2015a)

Phylum	Ascomycota
Class	Eurotiomycetes
Order	Eurotiales
Family	Trichocomaceae
Genus	*Penicillium*

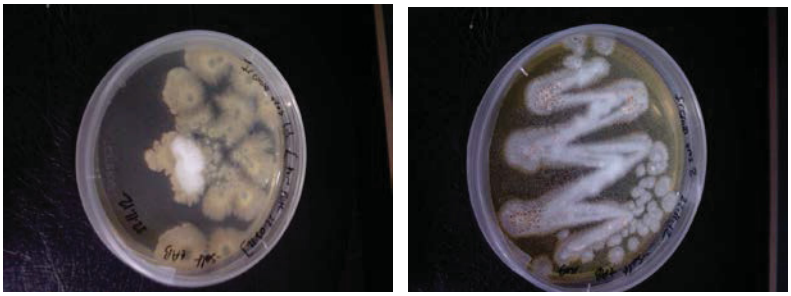

Figure 2.3 *Penicillium* sp. strains IO1 and IO2

Alternaria alternata

The fungus *A. alternata* was isolated from the rainforest plant *Antiaris africana* in Cameroon in October, 2013.

Phylum	Ascomycota
Class	Dothideomycetes
Order	Pleosporales
Family	Pleosporaceae
Genus	*Alternaria*
Species	*A. alternata*

Penicillium paxilli

The fungus *P. paxilli* was isolated from sediment collected in November 2012 from the Lake Wadi EI Natrun in Egypt.

Phylum	Ascomycota
Class	Eurotiomycetes
Order	Eurotiales
Family	Trichocomaceae
Genus	*Penicillium*
Species	*P. paxilli*

Penicillium sclerotiorum

The fungus *P. sclerotiorum* was isolated from the mangrove plant *Aegialitis annulata* in Hainan, China in 2012.

Phylum	Ascomycota
Class	Eurotiomycetes
Order	Eurotiales
Family	Trichocomaceae
Genus	*Penicillium*
Species	*P. sclerotiorum*

2.5 Large scale cultivation of interesting fungal strains

Depending on the results of the HPLC chromatogram analysis and bioactivity assays, large scale cultivations of interesting fungal strains were carried out.

2.6 Extract of fungal cultures

2.6.1 Extract of fungal cultures on rice medium

Depending on the fungal growth, the fermentation took 2-4 weeks to complete. Ethyl acetate was used to stop the fermentation, and the rice medium was sliced into small pieces, followed by placing the flasks on the shaker for 8 h. After that, liquid-liquid separation with *n*-hexane and 90% methanol was performed. The 90% methanol part was evaporated by a rotary

evaporator, afterwards partitioned by ethyl acetate and water. The ethyl acetate part was used for secondary metabolites isolation.

2.6.2 Extract of fungal cultures in liquid Wickerham medium

The mycelium was submerged in ethyl acetate and mixed using an Ultraturrax at 4000 u/min for 10 min, next filtered under vacuum with a Büchner funnel. The liquid part was partitioned successively by *n*-hexane, EtOAc and *n*-BuOH. The extracts were concentrated under vacuum.

2.6.3 Extract of fungal cultures on bean medium

The procedure for extraction on bean medium was the same as for rice medium culture.

2.7 Co-cultivation of fungus and fungus

Both co-culture and axenic cultures of the two strains of *Penicillium* sp. (stains IO1 and IO2) were performed on solid rice medium. Fungi were kept under static conditions at 22 °C until they reached their stationary phase of growth. (Chen *et al*., 2015a)

2.8 Co-cultivation of fungus and bacterium

2.8.1 Co-cultivation of *A*. *terreus* with *B*. *subtilis* 168 trpC2 and *B*. *cereus*T

Co-cultivation of the fungus with the different bacteria was carried out in Erlenmeyer flasks (1L) employing solid rice medium. Twenty-eight Erlenmeyer flasks (four flasks for axenic *A*. *terreus*, four for *A*. *terreus* and *B*. *subtilis*, four for *A*. *terreus* and autoclaved *B*. *subtilis*, four for *A*. *terreus* and *B*. *cereus*, four for axenic *B*. *subtilis*, four for autoclaved *B*. *subtilis*, and four for axenic *B*. *cereus*) containing 60.0 mL of distilled water and 50.0 g of commercially available milk rice (Milch-Reis, ORYZA) each were autoclaved before inoculating the fungus and the bacterium.

B. *subtilis* and *B*. *cereus* were grown in lysogeny broth (LB). An overnight culture of *Bacillus* sp. was used to inoculate prewarmed (LB medium (1:20), which was then incubated at 37 °C by shaking at 200 rpm to mid exponential growth phase (optical density at 600 nm (OD_{600}) of 0.2–0.4). A 10 mL volume of the bacterial culture was added to the rice medium, which was further incubated for 4 days at 37 °C (Chen *et al*., 2015b).

Composition of LB medium:

Tryptone	10.0 g
Yeast extract	5.0 g
NaCl	10.0 g
pH	7.0
Distilled water	ad 1000 mL

Next *A. terreus* grown on malt agar (5 pieces, 1 cm × 1 cm) was added to the rice medium containing bacteria (after 4 days incubation, ten flasks cultured with *B. subtilis* were autoclaved) under sterile conditions. Fungal and bacterial controls were grown on rice medium. Co-cultures and axenic cultures of *A. terreus*, *B. subtilis* and *B. cereus* were kept under static conditions at 22 °C until they reached their stationary phase of growth (2 weeks for controls of *A. terreus* and bacteria; 4 weeks for co-cultures). Then 300 mL of EtOAc was added to the cultures to stop the growth of cells followed by shaking at 140 rpm for 8 h. The cultures were then left overnight and filtered on the following day using a Büchner funnel. The EtOAc was removed under vacuum. Each extract was then dissolved in 50 mL of MeOH, and 100 μL of this solution was dissolved in 400 μL MeOH, then 20 μL of solution was injected into the analytical HPLC column. (Chen *et al*., 2015b)

2.8.2 Co-cultivation of *A. terreus* with *S. coelicolor* A2(3) and *S. lividans* TK24

Twenty Erlenmeyer flasks (four flasks for axenic *A. terreus*, four for *A. terreus* and *S. coelicolor*, four for *A. terreus* and *S. lividans*, four for axenic *S. coelicolor*, four for axenic *S. lividans*) containing 60.0 mL of Yeast Malt (YM) medium and 50.0 g of commercially available milk rice (Milch-Reis, ORYZA), each was autoclaved before inoculating the fungus and the bacterium. An overnight culture of *Streptomyces* sp. was used to inoculate prewarmed YM medium (1:20), which was then incubated at 30 °C by shaking at 200 rpm to mid exponential growth phase. This preculture was then incubated in fresh YM medium overnight to reach mid exponential growth phase. A 10 mL volume of the bacterial culture was added to the rice medium, which was further incubated for 4 days at 30 °C. After this pre-incubation, the same process as described in co-cultivation experiments of *A. terreus* with *B. subtilis* 168 and *B. cereus* T was carried out. (Chen *et al*., 2015b)

Composition of YM medium:

Agar	20.0 g
Glucose	10.0 g
Yeast extract	3.0 g
Peptone	5.0 g
Malt extract	3.0 g
pH	7.4-7.6
Distilled Water	ad 1000 mL

2.9 Isolation of secondary metabolites

2.9.1 Methods for isolation

Several techniques were used for the isolation of secondary metabolites.

2.9.1.1 Vacuum liquid chromatography (VLC)

Vacuum liquid chromatography is used for the first steps separation for samples with large amounts. The column is packed tightly with silica gel or reversed phase silica gel. The sample mixed with the material is loaded onto the top of the column after evaporating the solvent completely. The column is ready when sand and cotton are packed into the column as well. The systems of *n*-hexane/ ethyl acetate and DCM/ MeOH are used to step gradient elution of the silica gel column from non-polar to polar, while water/ MeOH system is used for reversed phase silica gel column eluted from polar to non-polar. Each fraction is evaporated respectively.

2.9.1.2 Column chromatography (CC)

Column chromatography is used for further separation and purification. There are several options of materials according to different characteristic of the samples.

- Normal-phase chromatography: polar stationary phase materials are used to pack the column, such as silica gel (Si) or diol, and non-polar solvent system is used for mobile phase, such as *n*-hexane/ ethyl acetate or DCM/ MeOH. The column is eluted with a gradually increasing amount of polar solvent. The samples are separated according to the polarity. The non-polar compounds are eluted earlier than the polar compounds.

- Reversed-phase chromatography: non-polar stationary phase materials such as C-18 or C-8 are used, and polar solvent, usually water with increasing amount of methanol or acetonitrile is employed for mobile phase. The hydrophilic compounds are eluted earlier than the hydrophobic compounds.

For normal-phase or reversed-phase chromatography, TLC is used to select suitable mobile system with R_f value.

- Size-exclusion chromatography: sephadex LH20 is used as stationary phase, and most of the solvents can be used as mobile phase (e.g. methanol, dichloromethane, acetone, or water). It is worth mentioning that different material has specific swell size in particular solvents, whereas material is not able to sit down in some solvents like chloroform due to the density. In this case, instead of a single solvent, a mixture of solvents is preferred. Samples are separated according to the size. Big molecules are eluted first followed by the smaller ones. (Ebada *et al*., 2008)

2.9.1.3 High performance liquid chromatography (HPLC)

HPLC is a highly improved form of column chromatography. Pumps instead of gravity provide higher pressure and speed; material is replaced by smaller size particles for better separation; and a UV detector is employed to detect traces of components.

- Analytic HPLC: methanol and 0.1% formic acid/ H_2O are used as the mobile phase with 1.0 mL/ min flow rate. The following gradient: 0 min (10% MeOH); 5 min (10% MeOH); 35 min (100% MeOH); 45 min (100% MeOH) is performed as a regularly program. Routine detection of UV wavelengths are 235, 254, 280, and 340 nm. The obtained UV-spectra of detected peaks are compared with those in UV-spectra database.
- Semi-preparative HPLC: Methanol and 0.1% trifluoroacetate/ water or water are used as the mobile phase with a flow rate of 5.0 mL/ min. According to the retention time from the analytic HPLC, the mobile system program and the UV wavelength for the target compounds are set. The target peaks are collected during the program is performed.

2.9.1.4 Thin layer chromatography (TLC)

Thin layer chromatography is one of the most common isolation techniques for analysis. TLC is performed on a sheet of glass or aluminum foil coated with the materials such as silica gel or C-18. The samples are applied to the TLC plates with a capillary. The mobile phase system is kept in the cylinder under saturated conditions. Detection of the compounds is performed by observing the absorption at 254 and 366 nm under a UV-lamp or after spraying with anisaldehyde reagent.

Anisaldehyde spray reagent

Methanol	85.0 mL
Glacial acetic acid	10.0 mL
Conc. H_2SO_4	5.0 mL (added slowly)
Anisaldehyde	0.5 mL

- Analytic TLC: is used to check the similarity of collections from the column, in order to combine different fractions for further separation; optimize the solvent system for column chromatography separation; as well as to check the purity of obtained compounds.
- Preparative TLC: is used for isolation. Cut the bands of target compounds under UV, and afterwards obtain the compounds by eluting these independent materials with suitable solvent.

2.9.2 Isolation of secondary metabolites from fungal strains

2.9.2.1 Process of secondary metabolites isolation from *T. harzianum*

The crude extract from the first small scale cultivation was subjected to vacuum liquid chromatography (VLC) using a step gradient of *n*-hexane/ EtOAc, followed by DCM/ MeOH, to yield 10 fractions (F1-F10). Fraction 5 (F5), eluted with *n*-hexane/ EtOAc (70 : 30), was purified by semi-preparative HPLC using MeOH/ H_2O as the mobile phase to yield **1** (1.52 mg). Following the same procedure, fraction 4 (F4), eluted with *n*-hexane/ EtOAc (50 : 50), afforded **2** (1.39 mg) and **3** (3.31 mg). (Chen *et al*., 2015c) Fraction 3 (F3), eluted with *n*-hexane/ EtOAc (80 : 20), was submitted to Sephadex LH-20 to obtain **4** (1.0 mg).

Following the same way, from the crude extract (0.56 g) of the second fermentation of *T. harzianum*, compouds **5** (1.34 mg) and **6** (5.0 mg) were obtained.

2.9.2.2 Isolation of secondary metabolite from co-cultivation of *A. terreus* with bacteria

The crude extract of the co-cultures of *A. terreus* with *B. subtilis* and *B. cereus* (8.0 g) was submitted to VLC with silica gel using a step gradient of *n*-hexane/ EtOAc followed by DCM/ MeOH, to yield 10 fractions (F1-F10). Fraction 2 (F2), eluted with *n*-hexane/ EtOAc (90 : 10), was further purified using Sephadex LH-20 with methanol as the mobile phase to give 5 subfractions (F2.1-F2.5). F2.2 was recrystallized to afford **18** (0.78 mg). F2.5 was separated by semipreparative HPLC with MeOH/ H_2O (62 : 38) to yield **11** (2.0 g). Fraction 4 (F4), eluted with *n*-hexane/ EtOAc (50 : 50), was further purified using Sephadex LH-20 (MeOH) followed by semipreparative HPLC with MeOH/ H_2O (70 : 30) as the mobile phase to afford **17** (2.0 mg). Fraction 5 (F5), eluted with *n*-hexane/EtOAc (30 : 70), was submitted to Sephadex LH-20 (MeOH) to yield 10 subfractions (F5.1 - F5.10). F5.2 was recrystallized to afford **19** (24.9 mg). F5.5 was chromatographed two times over Sephadex LH-20 (MeOH) to afford **12** (40.6 mg), **13** (2.3 mg), **15** (1.3 mg). F5.8 was submitted to Sephadex LH-20 column chromatography with methanol as the mobile phase to obtain 5 subfractions. F5.8.1 was separated by semipreparative HPLC with MeOH/ H_2O (70 : 30) to yield **7** (1.2 mg), **8** (4.2 mg), **10** (14.5 mg), **16** (2.1 mg), **21** (1.6 mg), respectively. F5.8.3 was purified by Sephadex-LH 20 column chromatography (MeOH) to afford **20** (1.9 mg). Fraction 6 (F6), eluted with *n*-hexane/EtOAc (10 : 90), yielded **14** (7.3 mg) by recrystallization. Fraction 10 (F10), eluted with 100% MeOH, was further purified by Sephadex LH-20 column chromatography (MeOH) followed by semipreparative HPLC with MeOH/ H_2O (82 : 18) to yield **9** (1.0 mg). Compounds **9 - 21** were identified by comparing their ^{1}H NMR, LC-MS and UV data with the literature. (Chen *et al*., 2015b)

The similar procedure was conducted to the EtOAc extract from the broth of liquid Wickerham medium culture (0.75 g) and bean culture (1.2 g), respectively. **22** (5.4 mg), **23** (2.7 mg), **24** (1.4 mg), **25** (0.79 mg), **26** (1.25 mg), **27** (1.0 mg), **28** (5.4 mg), **29** (9.1 mg) and **30** (1.2 mg) were isolated.

2.9.2.3 Process of secondary metabolites isolation from *Penicillium* sp. strains and their co-cultivation

The crude extract of *Penicillium* sp. strain IO1 0.99 g was subjected to VLC using a step gradient of *n*-hexane/ EtOAc followed by DCM/ MeOH, to yield 13 fractions (F1 - F13). Fraction 4, eluted with *n*-hexane/ EtOAc (40 : 60), was submitted to Sephadex LH-20 (MeOH) to yield 7 subfractions (F4.1 - F4.7). F4.5 was separated by Sephadex LH-20 (MeOH) followed by semipreparative HPLC with MeOH/ H_2O to yield **33** (5.32 mg). F4.6 was submitted to Sephadex LH-20 (MeOH) followed by semipreparative HPLC with MeOH/ H_2O to yield **31** (5.20 mg). Fraction 6 (F6), eluted with 100% EtOAc, was purified using Sephadex LH-20 (MeOH) to afford **32** (136.74 mg).

The crude extracts of *Penicillium* sp. strain IO2 0.99 g and co-culture 1.88 g were subjected to VLC, respectively, then followed by Sephadex LH-20 (MeOH) and semipreparative HPLC (MeOH/ H_2O) to yield **35** (7.1 mg), **36** (8.7 mg), **37** (19.8 mg), **38** (14.5 mg), **39** (0.2 mg) and **40** (0.6 mg). (Chen *et al*., 2015a)

2.9.2.4 Scheme of process of secondary metabolites isolation from *A. alternate*

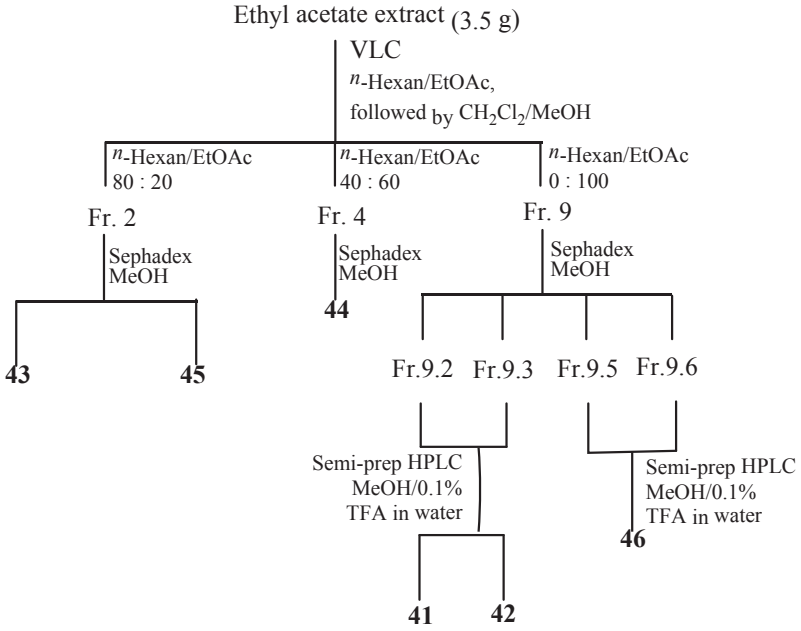

Figure 2.4 Isolation scheme of the EtOAc crude extract from *A. alternate*

2.9.2.5 Scheme of process of secondary metabolites isolation from *P. paxilli*

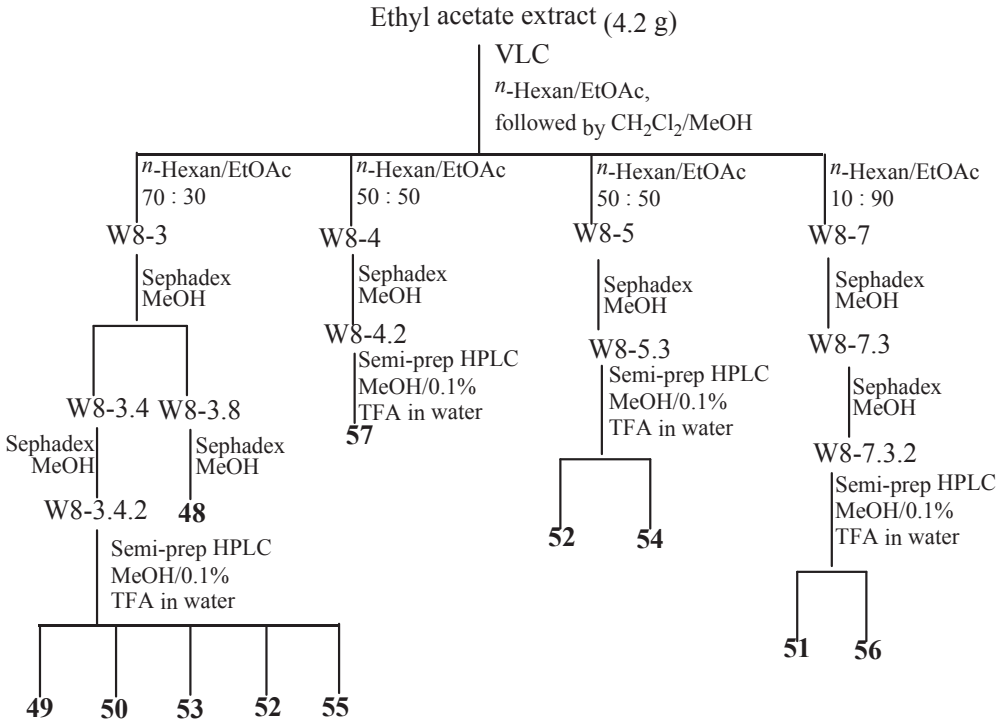

Figure 2.5 Isolation scheme of the EtOAc crude extract from *P. paxilli*

2.9.2.6 Scheme of process of secondary metabolites isolation from *P. sclerotiorum*

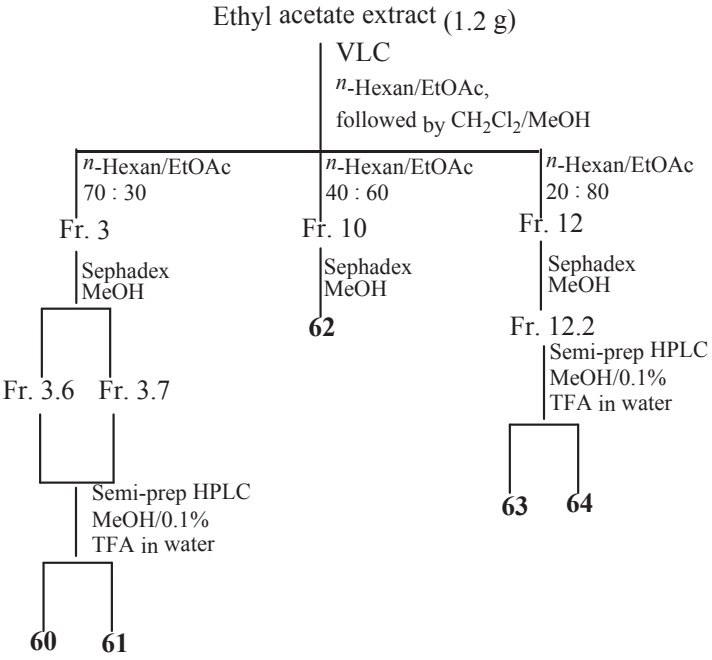

Figure 2.6 Isolation scheme of the EtOAc crude extract from *P. sclerotiorum*

2.10 Structure elucidation of isolated compounds

2.10.1 Nuclear magnetic resonance spectroscopy (NMR)

For nuclei with I = 1/2, when placed in a magnetic field, two spin states exist, +1/2 and -1/2, with the magnetic moment of the lower energy aligned with the external field and the higher energy spin state opposed to the external field. The diverge between the two spin states is responded to the external magnetic field. The low state of nuclei will be excited to upper state by absorbing energy from radiation, whereas the upper state nuclei will return to low state by releasing the energy. If the population of the upper and lower energy spin states is not the same, there is a Boltzmann distribution of the nuclei with a slight excess in the lower state, hence, the slight excess of nuclei is observed. (Atta-Ur-Rahman, 2012; Bovey, Mirau and Gutowsky, 1988)

1D NMR (^{1}H NMR, ^{13}C NMR, DEPT) and 2D NMR (^{1}H–^{1}H COSY, HMBC, HSQC, ROESY, *et al.*) spectroscopy are frequently used to elucidate structures. ^{1}H NMR spectroscopy is a well-established and important application during isolation: chemical shifts give the information about the chemical environment of the protons; integrations show the number of protons; and *J*-coupling constants provide detailed connectivity of adjacent protons. ^{13}C NMR and DEPT display the information of carbons involved in the structures including C, CH, CH_2 or CH_3. ^{1}H–^{1}H COSY (Correlation Spectroscopy) and ROESY (Rotating-Frame Overhauser Spectroscopy) give the different relationship of neighboring protons (adjacent connection for ^{1}H–^{1}H COSY and adjacent in space for ROESY), while HMBC (Heteronuclear Multiple-Bond Correlation Spectroscopy) and HSQC (Heteronuclear Single-Quantum Correlation Spectroscopy) provide the different relationship between protons and carbons (HMBC detects ^{1}H and ^{13}C correlations over longer ranges of about 2 – 4 bonds, while HSQC detects direct correlations between ^{1}H and ^{13}C nuclei). The samples for NMR are dissolved in deuterated solvents, while tetramethylsilane (TMS) is the internal standard.

2.10.2 Mass spectrometry (MS)

The MS principle consists of ionizing chemical compounds to generate charged molecules or molecule fragments followed by measurement of their mass-to-charge ratios by using a variety of techniques.

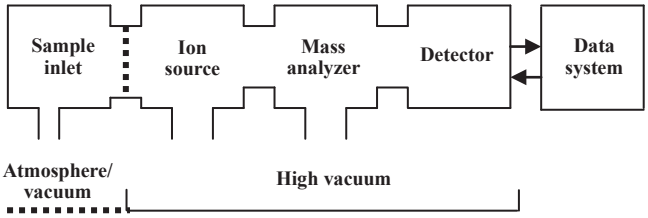

Figure 2.7 General scheme of a mass spectrometer (Gross, 2004).

A variety of approaches are employed to conduct each part of the MS instrument in accordance to specific characteristics of the samples or intent. Following list some of the typical MS methods: (Gross, 2004; Galen, 2005; Jimenez, 2006)

- Sample introduction system:

1. Direct insertion probe (DIP): Sample in heated/ cooled glass/ metal vial as particles or film of analyte
2. Direct exposure probe (DEP): Sample particles or film of analyte on resistively heated metal filament
3. Reservoir/reference inlet: Heated reservoir with sample vapor
4. Gas chromatography (GC): Elutes directly into ion source
5. Liquid chromatography (LC): Connected with ion source via particle beam interface

- Ionization methods:

1. EI: electron ionization
2. ESI: electrospray ionization
3. APCI: atmospheric-pressure chemical ionization
4. CI: chemical ionization
5. MALDI: Matrix assisted laser desorption
6. FAB: fast atom bombardment

- Separation of ions:

1. Quadrupoles (Q): continuous ion beam in linear radio frequency quadrupole field; separation due to stability of trajectories.
2. Time-of-flight (TOF): time dispersion of a pulsed ion beam; separation by time-of-flight
3. Magnetic sectors (B): deflection of a continuous ion beam; separation by momentum in magnetic field due to Lorentz force

4. Quadrupole ion trap (QIT): trapped ions; separation in three-dimensional radio frequency quadrupole field due to stability of trajectories

During natural products isolation and structure elucidation, some wide-used MS approaches are employed:

- LC-MS: HPLC column connected with MS detector is commonly used for mixtures of substances.
- High resolution mass spectrometry: accurate mass measurement is used to calculate the molecular formula of the compound.
- ESI-MS: molecular weight is available, and little fragments can be observed.
- EI-MS: good quantity of fragments provides structural information, and the "fingerprint" is usually available in spectra libraries.

Some special chemical elements, such as Cl or Br, are induced by isotopic peaks in the mass spectrum.

2.10.3 Stereochemistry

Compounds with chiral centers give stereoisomers, which play an important role on their physical and biological properties. Several techniques used to determine the stereochemistry.

2.10.3.1 Optical rotation

The stereochemistry of the structures with only one chiral center could be determined by comparing their optical rotation with those reference compounds. Pure compounds were dissolved in spectral grade solvent with certain concentrations and measured three times under adjusted temperature, followed by comparison of their $[a]_D$ value with the literature.

2.10.3.2 Mosher reaction

Mosher reaction is an empirical method based on NMR spectroscopy to deduce the configuration of secondary alcohol centers or analogs, such as amines where the hydroxy group is replaced by an amine. (*R*)-(+)-*α*-Methoxy-*α*-trifluoromethylphenylacetic acid (*R*-(+)-MTPA-OH) or *R*-(+)-MTPA-Cl together with (*S*)-(-)-*α*-Methoxy-*α*-trifluoromethylphenylacetic acid (*S*-(-)-MTPA-OH) or *S*-(-)-MTPA-Cl are used as mosher reagents. *R*-MTPA ester and *S*-MTPA ester are obtained after reaction of mosher reagent with the compound. The anisotropic, magnetic shielding effect on protons

residing above (or below) the plane of the aryl ring on the MTPA esters results in a more upfield chemical shift for the affected (spatially proximal) protons in the NMR spectrum. The conversion of $\Delta\delta^{SR}$ (δ_S — δ_R) values are signed to determine the absolute structures of the secondary alcohol stereocenters. Those protons that have positive $\Delta\delta^{SR}$ values reside within R^1, whereas those with negative values "belong to" R^2. (Hoye, Jeffrey and Shao, 2007)

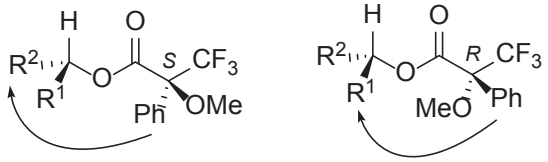

2.10.3.3 Circular dichroism spectroscopy (CD)

"When the molecular contains one or more chiral chromophores, the absorption of left-handed circularly polarized light and right-handed circularly polarized light would be different, thus, circular dichroism (CD) occurs." CD signal present positive or negative "depending on whether L-CPL is absorbed to a greater extent than R-CPL (CD signal positive) or to a less extent (CD signal negative)" under the same wavelength. (http://www.chem.uci.edu/~dmitryf/manuals/Fundamentals/CD%20spectroscopy.pdf)

According to different wavelength used in the experiments, ECD (electronic circular dichroism) and VCD (vibrational circular dichroism) have been studied. For ECD, a chromophore is necessary in the structure, which is responsible for UV or Vis range absorption bands rely on electronic transitions, whereas, the absorption band of VCD used is in IR range, therefore, most of chiral moieties are possible to produce VCD spectra. (Berova *et al*., 2007; Taniguchi *et al*., 2008)

In this study, during determination of the absolute configuration of the new compound fusarielin I (**30)**, isolated from *Penicillium* sp., ECD calculation was carried out. Mixed torsional/ low mode conformational searches were carried out by means of the Macromodel 9.9.223 software using the Merck Molecular Force Field (MMFF) with implicit solvent model for chloroform applying a 21 kJ/mol energy window. Geometry reoptimizations [B3LYP/6-31G(d) level in gas phase and B97D/TZVP level with PCM solvent model for MeCN] such as TDDFT calculations were performed with Gaussian 09 using various functional (B3LYP, BH&HLYP, PBE0) and TZVP basis sets. ECD spectra were generated as the sum of Gaussians with 3600 cm^{-1} half-height width (corresponding to ca. 25 at 265 nm),

using dipole-velocity computed rotational strengths. Boltzmann distributions were estimated from the ZPVE corrected B3LYP/6-31G(d) energies in the gas-phase calculations and from the B97D/TZVP energies in the PCM model calculations. The MOLEKEL software package was used for visualization of the results. (Chen *et al*., 2015a)

2.11 Biological assays of isolated compounds

2.11.1 Toxicity assay

Cytotoxicity was tested using the MTT assay. Briefly, cells were plated on 96-well plates with 10^4 cells per well. The cells were allowed to attach for 24 h and then treated with different concentrations of the compounds for 24 h. For the MTT assay, culture medium was replaced by medium containing 0.7 mg/ mL {3-(4,5-dimethylthiazol-2-yl)-2,5-diphenyltetrazolium bromide} (MTT) and cells were incubated for 2 h at 37 °C to allow the viable cells to reduce MTT to purple formazan. Cells were lysed with a solution of 95% isopropanol and 5% formic acid. The concentration of reduced MTT as a marker for cell viability was measured using a Wallac Victor^2 multilabel counter at 560 nm. Cells incubated only with vehicle control (DMSO) were considered 100% viable.

In this study, cytotoxicity was tested against the murine lymphoma (L5178Y) cell line, and human ovarian cancer (A2780 sens and A2780 CisR) cell lines, with kahalalide F and cisplatin as positive controls, respectively. (Chen *et al*., 2015a)

2.11.2 Antibacterial assays

MIC values were determined by the broth microdilution method according to CLSI guidelines. For preparation of the inoculum, the direct colony suspension method was used with an inoculum of 5×10^5 colony forming units/ mL after the last dilution step. Compounds were added from stock solution (10 mg/ mL in DMSO), resulting in a final DMSO amount 0.64 % at the highest antibiotic concentration tested (64 μg/ mL). Serial 2-fold dilutions of antibiotics were prepared with DMSO being diluted along with the compounds. (Chen *et al*., 2015b)

2.11.3 Antifungal assays

The antifungal assay was performed using the agar diffusion method (Kirby-Bauer) and nystatin was used as a positive control. A 100 μL of fungal *Cladosporium cladosporioides*

spore suspension was spread out onto the surface of potato dextrose agar medium (PDA). Immediately, 10-20 mL of tested samples were loaded onto the sterilized disc paper (5mm diameter, Oxoid Ltd) to give final disc loading concentrations of 250-500 μg for crude extracts as well as 50-100 μg for pure compounds. The impregnated discs were transferred onto the surface of the PDA medium. The fungal cultures were then incubated at room temperature for 5-7 days and the growth inhibition was measured around the disc. The result was then compared to positive control (nystatin), which has a concentration of 5, 10, 20, 50 μg (Bauer, 1966).

3 Results

3.1 Compounds isolated from endophytic fungus *Trichoderma harzianum*

Trichoderma sp. are widely used in plant agriculture for their ability as fungicides for disease controls (Harman, 2006), as they are known for their extensive secondary metabolism (Reino *et al*., 2008). Serials of secondary metabolites have been reported from *Trichoderma* sp., including acorane sesquiterpenes, peptaibols, terpenoids, and steroids (Ren *et al*., 2009; Citron *et al*., 2011; Stack *et al*., 1986; Bartmańska and Dmochowska-Gladysz, 2007).

Cytochalasins are a group of fungal cell permeable mycotoxins that have the ability to bind to the actin filaments and block their polymerization and elongation, causing inhibition of cell division and apoptosis (Haidle and Myers, 2004). Cytochalasins were discovered in 1966 (Rothweiler and Tamm, 1966), and were later obtained from *Pestalatia* sp., *Phomopsis* sp., and *Hypoxylon fragiforme* (Li *et al*., 2010; Burres *et al*., 1992; Lingham *et al*., 1992).

The crude extract of the endophytic fungus *T. harzianum* grown on solid rice medium exhibited strong cytotoxicity against the murine lymphoma cell line L5178Y. Bioassay-guided isolation yielded a novel cytochalasin (**1**), together with three known compounds (**2-4**). In a second set of experiments, fermentation led to two known compounds (**5** and **6**).

3.1.1 4'-Hydroxyl-deacetyl-18-deoxycytochalasin H (1, new compound)

4'-Hydroxyl-deacetyl-18-deoxycytochalasin H	
Biological Source	*Trichoderma harzianum*
Sample Code	CL-V5P2
Sample Amount	1.52 mg
Molecular Formula	$C_{28}H_{37}NO_4$
Molecular Weight	451 g/mol
Solubility	MeOH
Physical Description	White amorphous powder
Optical Rotation	$[\alpha]^{20}_D$ +39.6 (c 0.288, MeOH)
HPLC Retention Time	21.33 min (standard gradient)

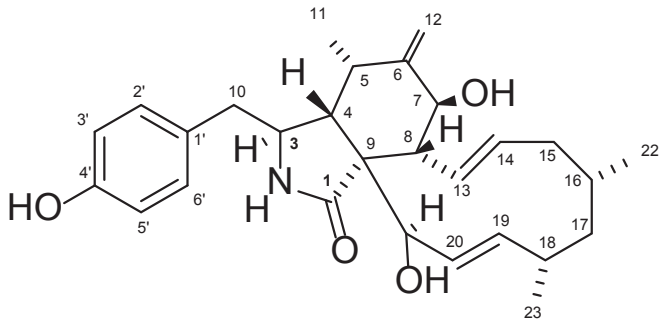

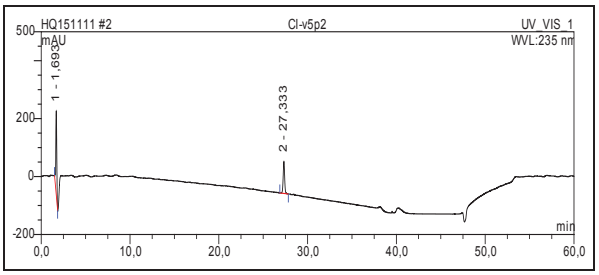

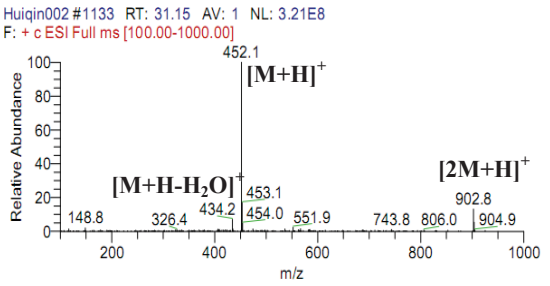

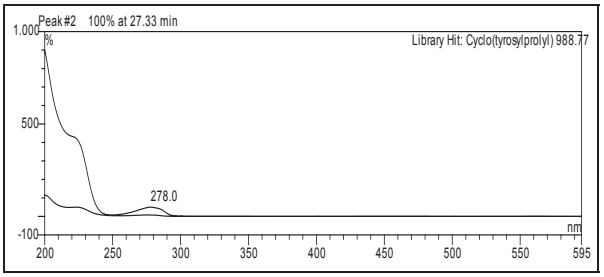

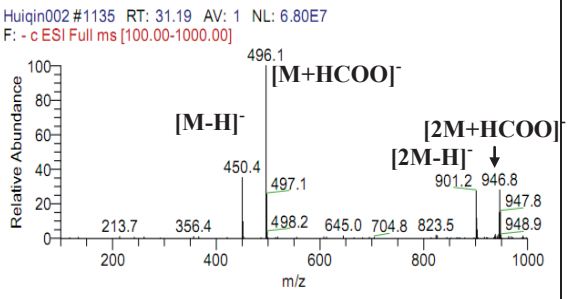

Compound **1** was obtained as a white amorphous powder. The molecular formula was determined as $C_{28}H_{37}NO_4$ on the basis of the pseudomolecular ion peak at *m/z* 452.2795 $[M + H]^+$ observed in the HRESIMS spectrum. The ^1H NMR spectrum of **1** indicated the presence of three secondary methyl groups at δ_H 0.88 (3H, d, J = 6.7 Hz, H_3-11), 0.99 (3H, d, J = 7.0 Hz, H_3-22) and 0.99 (3H, d, J = 7.0 Hz, H_3-23), as well as two symmetrical doublets at δ_H 6.74 (2H, d, J = 8.4 Hz, H-3'/5') and 7.03 (2H, d, J = 8.4 Hz, H-2'/6'), typical of a *para*-hydroxy-substituted phenyl group (Table 3.1.1). The ^{13}C NMR spectrum of **1** showed the corresponding carbon signals [δ_C 14.2 (C-11), 23.0 (C-22), 25.6 (C-23), 129.4 (C-1'), 116.3 (C-3'/5'), 132.1 (C-2'/6'), 157.3 (C-4')] and revealed in addition one carbonyl group at δ_C 178.9 (C-1), six sp^2 carbons (including four methines, one methylene at δ_C 112.8, and one quaternary carbon at δ_C 152.1), two oxygenated sp^3 carbons (including two methines at δ_C 72.3 and 77.5), and ten aliphatic sp^3 carbons (including six methines, three methylenes and one quaternary carbon at δ_C 55.3), as supported by DEPT and HSQC spectra. (Chen *et al*., 2015c)

Detailed analysis of the COSY spectrum disclosed the presence of a continuous spin system starting from H-13 and sequentially extending until H-21. In addition, HMBC correlations (Figure 3.1.1) of H_3-11 to C-4 (δ_C 49.8), C-5 (δ_C 34.1) and C-6 (δ_C 152.1); H_3-22 to C-15 (δ_C 44.1) and C-17 (δ_C 49.7); as well as of H_3-23 to C-17 (δ_C 49.7), C-18 (δ_C 35.3) and C-19 (δ_C 134.3), established their connectivity to C-5, C-16 and C-18, respectively. The attachment of the aromatic unit to the methylene group (H_2-10) at C-1', was deduced from HMBC correlations of H_2-10 [δ_H 2.74 (1H, dd, J = 13.7, 6.0 Hz) and 2.65 (1H, dd, J = 13.7, 6.0 Hz)] to C-2'/6' (δ_C 132.1). These data were in agreement with those observed for **2**, except for the presence of an additional hydroxy group located at C-4' in compound **1**, which accounts for the molecular weight difference of 16 amu observed between both compounds. (Chen *et al*., 2015c)

The relative configuration of **1** was determined by analysis of the coupling constants and the ROESY spectrum. The geometry of the double bonds in the macrocyclic ring was in accordance with the observed ROESY correlations between H-7/H-13 and H-8/H-14 (Figure 3.1.2). The ROESY spectrum further suggested the α-orientations of H-3, H_3-11, and H-21, based on the observed correlations between H-3/H_3-11 and H-20/H-21, while the

β-orientations of H-4, H-5, H-16 and H-18 were apparent from the NOE cross-peaks between H-4/H-21, H-16/H-18 and H-18/H-19 (Figure 3.1.2), as well as the small coupling constant between H-4 and H-5 ($^3J_{4,5}$ = 4.8 Hz), indicating their *cis* relationship. Thus, the relative stereochemistry of **1** was established to be identical as that observed for the crystal structure of **2** (Ondeyka *et al*. 1992). In addition, based on the $[\alpha]_D$ value of **1**: $[\alpha]^{20}_D$ +39.6 (c 0.288, MeOH), which is on the positive side, as observed for **2** and **3**, as well as based on their close biogenetic relationship, it is assumed that compounds **1** – **3** share the 3*S*, 4*R*, 5*S*, 7*S*, 8*R*, 16*S*, 18*S*, 21*R* configuration. Hence, the structure of **1** was assigned as a new natural product named 4'-hydroxy-deacetyl-18-deoxycytochalasin H. (Chen *et al*., 2015c)

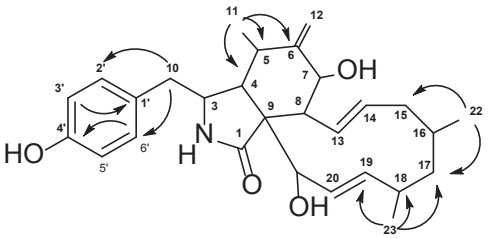

Figure 3.1.1 Key HMBC correlations of **1**.

(Chen *et al*. 2015c)

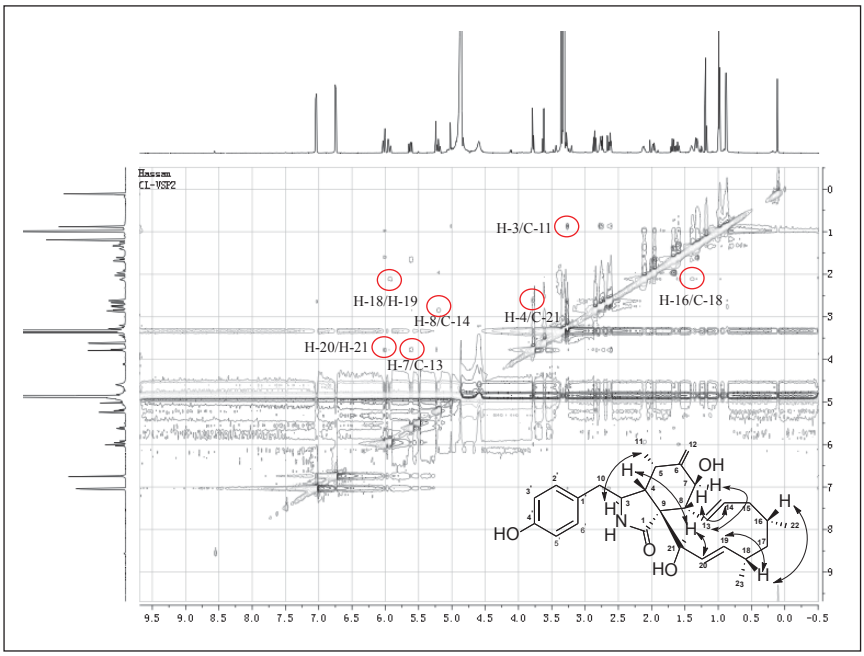

Figure 3.1.2 Key ROESY correlations of **1**.

Table 3.1.1 ^{1}H NMR and ^{13}C NMR spectral data of **1** (δ in ppm). (Chen *et al*., 2015c)

Position	δ_C[a]	δ_H (J in Hz)[b]
1	178.9 (s)	
3	55.2 (d)	3.28 (1H, td, 6.0, 3.9)
4	49.8 (d)	2.62 (1H, dd, 4.8, 3.9)
5	34.1 (d)	2.77 (1H, m)
6	152.1 (s)	
7	72.3 (d)	3.78 (1H, d, 10.5)
8	46.7 (d)	2.86 (1H, t, 10.5)
9	55.3 (s)	
10a	44.1 (t)	2.74 (1H, dd, 13.7, 6.0)
10b		2.65 (1H, dd, 13.7, 6.0)
11	14.2 (q)	0.88 (3H, d, 6.7)
12a	112.8 (t)	5.24 (1H, br.s)
12b		5.02 (1H, br.s)
13	129.7 (d)	5.62 (1H, dd, 15.7, 10.5)
14	137.1 (d)	5.20 (1H, ddd, 15.7, 10.5 4.6)
15a	44.1 (t)	1.97 (1H, dd, 12.6, 4.6)
15b		1.68 (1H, dt, 12.6, 11.0)
16	34.5 (d)	1.40 (1H, m)
17a	49.7 (t)	1.61 (1H, td, 13.4, 3.0)
17b		1.32 (1H, dt, 13.4, 3.0)
18	35.3 (d)	2.13 (1H, m)
19	134.3 (d)	5.94 (1H, ddd, 16.5, 7.0, 2.4)
20	132.5 (d)	6.02 (1H, dd, 16.5, 2.4)
21	77.5 (d)	3.79 (1H, br.s)
22	23.0 (q)	0.99 (3H, d, 7.0)
23	25.6 (q)	0.99 (3H, d, 7.0)
1'	129.4 (s)	
2'	132.1 (d)	7.03 (1H, d, 8.4)
3'	116.3 (d)	6.74 (1H, d, 8.4)
4'	157.3 (s)	
5'	116.3 (d)	6.74 (1H, d, 8.4)
6'	132.1 (d)	7.03 (1H, d, 8.4)

[a] in CD_3OD, 150 MHz

[b] in CD_3OD, 600 MHz

3.1.2 Deacetyl-18-deoxycytochalasin H (2, known compound)

Deacetyl-18-deoxycytochalasin H	
Biological Source	*Trichoderma harzianum*
Sample Code	CL-V4.2P2
Sample Amount	1.39 mg
Molecular Formula	$C_{28}H_{37}NO_3$
Molecular Weight	435 g/mol
Solubility	MeOH
Physical Description	White amorphous powder
Optical rotation	$[\alpha]^{20}_{D}$ +51.2 (c 0.288, MeOH)
HPLC Retention Time	28.78 min (standard gradient)

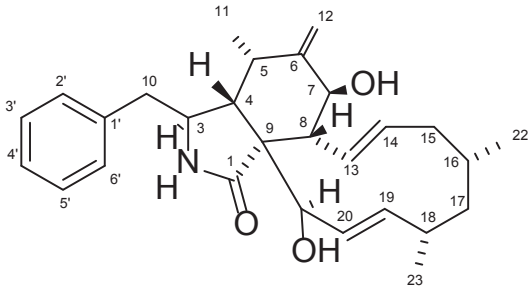

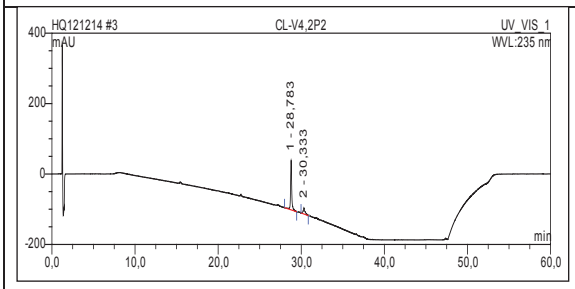

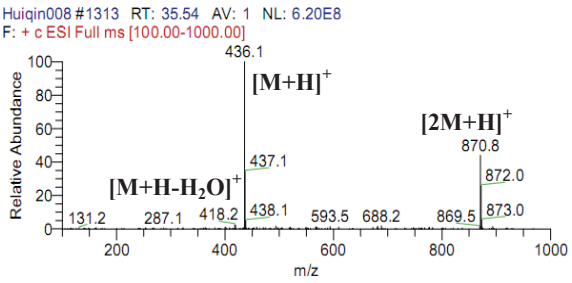

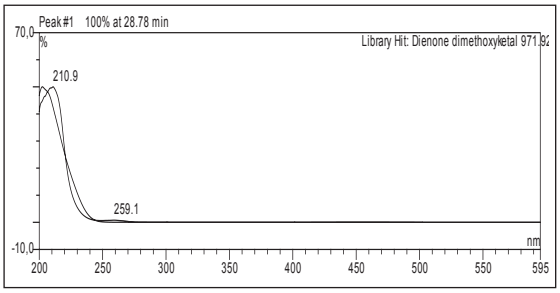

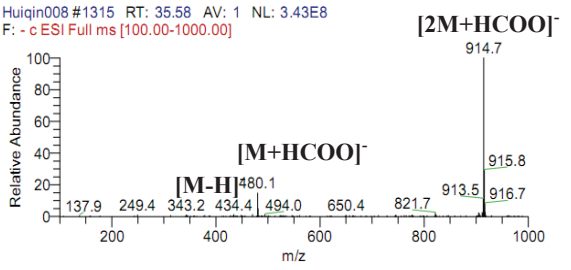

Deacetyl-18-deoxycytochalasin (**2**) was obtained as a white amorphous powder. It exhibited UV absorption at λ_{max} (MeOH) 210 nm, showing high similarity to the UV spectrum of **1**. The molecular weight was deduced as 435 g/mol from the positive and negative ion peaks at *m/z* 436.1 $[M + H]^+$, 418.2 $[M + H - H_2O]^+$, 870.8 $[2M + H]^+$, 434 $[M - H]^-$, 480 $[M + HCOO]^-$ and 914.7 $[2M + HCOO]^-$ measured by ESI-MS, thus revealing a 16 amu decrease in the molecular weight compared to **1**. The ^1H and ^1H–^1H COSY NMR spectra displayed characteristic protons of a mono-substituted aromatic ring at δ 7.32 (2H, t, J = 7.5Hz, H-3'/5'), 7.23 (1H, m, H-4') and 7.22 (2H, m, H-2'/6'); a terminal double bond [δ 5.23 (1H, br. s, H-12a) and 5.01 (1H, br. s, H-12b)]; three methyl groups at δ_H 0.84 (3H, d, J = 6.7 Hz, H-11), 0.98 (3H, d, J = 7.0 Hz, H-22) and 0.96 (3H, d, J = 7.0 Hz, H-23); as well as the same continuous spin system as in **1** (H-13 to H-21), including two double bonds at δ 5.61 (1H, dd, J = 15.5, 10.0 Hz, H-13), 5.19 (1H, ddd, J = 15.5, 10.0, 4.6 Hz, H-14), 5.92 (1H, ddd, J = 16.5, 6.8, 2.4 Hz, H-19) and 6.00 (1H, dd, J = 16.5, 2.4 Hz, H-20) and two methyl groups H_3-22 and H_3-23. Based on the data mentioned above, as well as by comparison with the literature, **2** was found to be identical to deacetyl-18-deoxycytochalasin H, which was previously isolated from the endophytic fungus *Phomopsis* sp. (Elsässer *et al*., 2005).

3.1.3 18-Deoxycytochalasin H (3, known compound)

18-Deoxycytochalasin H	
Biological Source	*Trichoderma harzianum*
Sample Code	CL-V4.2P3
Sample Amount	3.31 mg
Molecular Formula	$C_{30}H_{39}NO_4$
Molecular Weight	477 g/mol
Solubility	MeOH
Physical Description	White amorphous powder
Optical rotation	$[\alpha]^{20}_{D}$ +58.2 (c 0.288, MeOH)
HPLC Retention Time	30.73 min (standard gradient)

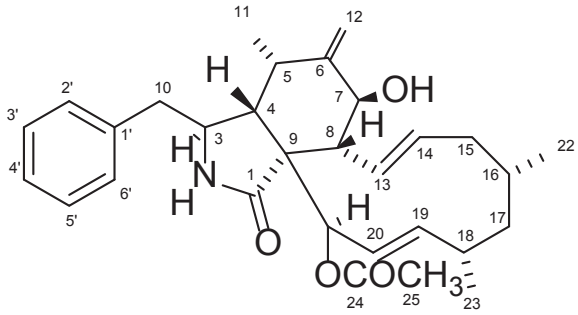

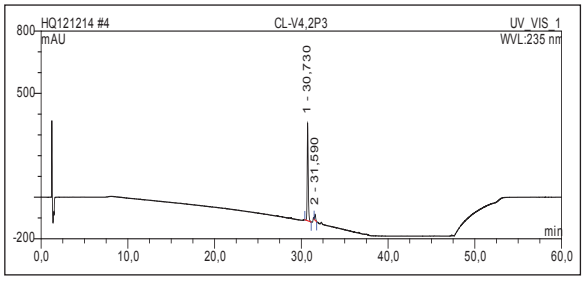

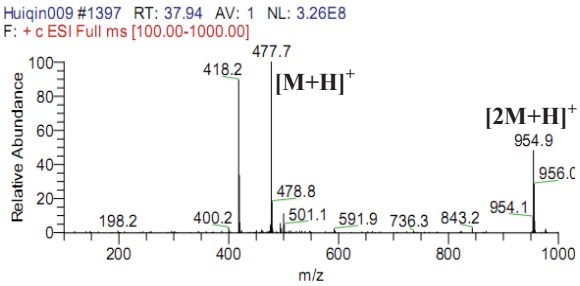

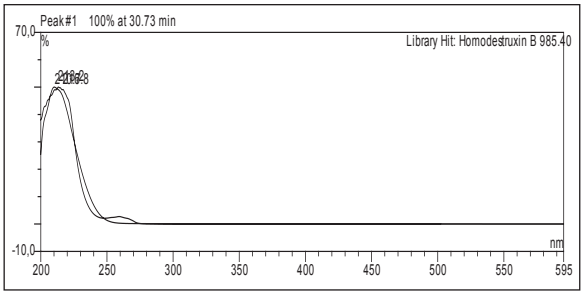

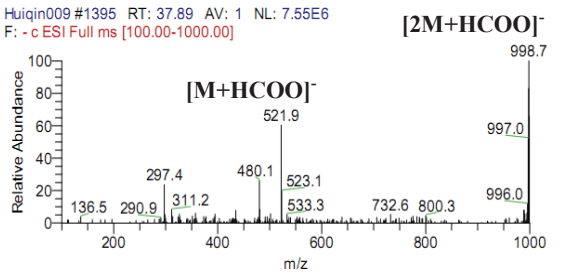

18-Deoxycytochalasin H (**3**) was obtained as a white amorphous powder. The UV spectrum showed the same pattern as for compounds **1** and **2**. Positive and negative ESI-MS showed pseudomolecular ion peaks at *m/z* 477.7 $[M + H]^+$, 954.9 $[2M + H]^+$, 521.9 $[M + HCOO]^-$ and 998.7 $[M + HCOO]^-$ indicating a molecule weight of 477 g/mol. The ^1H NMR and ^1H–^1H COSY spectra revealed one mono-substituted aromatic ring [δ_H 7.19 (2H, dd, J = 7.5, 1.3 Hz, H-3', 5'), 7.23 (1H, t, J = 7.5 Hz, H-4'), and 7.30 (2H, t, J= 7.5 Hz, H-2', 6')], three double bonds [δ_H 5.65 (1H, dd, J = 15.5, 10.0 Hz, H-13), 5.24 (1H, ddd, J = 15.5, 10.0, 4.8 Hz, H-14), 5.72 (1H, ddd, J = 16.5, 7.0, 2.5 Hz, H-19) and 5.86 (1H, dd, J = 16.5, 2.5 Hz, H-20)] including one terminal double bond [δ_H 5.21 (1H, br. s, H-12a) and 4.99 (1H, br. s, H-12b)], as well as four methyl groups [δ_H 2.24 (3H, s, H-25), 0.98 (3H, d, J = 6.9 Hz, H-23), 0.99 (3H, d, J = 6.9 Hz, H-22) and 0.59 (3H, d, J = 6.8 Hz, H-11)]. These data were in agreement with those of **2**, apart from the presence of an additional acetyl group at C-21, which accounts for 42 amu difference in molecular weight observed between both compounds. This was further corroborated by the fragment ion peak formed by the loss of 60 mass units in the ESI-MS spectrum. Thus, compound **3** was identified as 18-deoxycytochalasin H (Ondeyka *et al*., 1992; Elsässer *et al*., 2005), which was reported as a HIV-1 protease inhibitor from the bark-inhabiting ascomycete *Hypoxylon fragiforme* (Dombrowski *et al*., 1992; Ondeyka *et al*., 1992).

Table 3.1.2 ^{1}H NMR spectral data of **2** and **3** (in CD_3OD, 500 MHz, δ in ppm, J in Hz).

position	**2**	**3**
3	3.24 (1H, m)	3.26 (1H, m)
4	2.63 (1H, dd, 5.0, 3.8)	2.17 (1H, dd, 5.2, 3.0)
5	2.75 (1H, m)	2.65 (1H, m)
7	3.78 (1H, d, 11.0)	3.80 (1H, d, 10.5)
8	2.84 (1H, t, 11.0)	2.90 (1H, t, 10.5)
10a	2.83 (1H, dd, 13.4, 6.0)	2.85 (1H, dd, 13.2, 5.1)
10b	2.74 (1H, dd, 13.4, 6.0)	2.73 (1H, dd, 13.2, 7.9)
11	0.84 (3H, d, 6.7)	0.59 (3H, d, 6.8)
12a	5.23 (1H, br.s)	5.21 (1H, br.s)
12b	5.01(1H, br.s)	4.99 (1H, br.s)
13	5.61 (1H, dd, 15.5, 10.0)	5.65 (1H, dd, 15.5, 10.0)
14	5.19 (1H, ddd, 15.5, 10.0, 4.6)	5.24 (1H, ddd, 15.5, 10.0, 4.8)
15a	1.96 (1H, dd, 12.7, 4.6)	2.00 (1H, dd, 12.6, 4.8)
15b	1.67 (1H, dt, 12.7, 10.8)	1.71 (1H, dt, 12.6, 10.9)
16	1.38 (1H, m)	1.43 (1H, m)
17a	1.59 (1H, td, 12.2, 3.2)	1.57 (1H, td, 13.0, 3.1)
17b	1.31 (1H, m)	1.37 (1H, m)
18	2.13 (1H, m)	2.13 (1H, m)
19	5.92 (1H, ddd, 16.5, 6.8, 2.4)	5.72 (1H, ddd, 16.5, 7.0, 2.5)
20	6.00 (1H, dd, 16.5, 2.4)	5.86 (1H, dd, 16.5, 2.5)
21	3.75 (1H, br.s)	5.39 (1H, t, 2.2)
22	0.98 (3H, d, 7.0)	0.99 (3H, d, 6.9)
23	0.96 (3H, d, 7.0)	0.98 (3H, d, 6.9)
25		2.24 (3H, s)
2'	7.22 (1H, m)	7.30 (1H, t, 7.5)
3'	7.32 (1H, t, 7.5)	7.19 (1H, dd, 7.5, 1.3)
4'	7.23 (1H, m)	7.23 (1H, t, 7.5)
5'	7.32 (1H, t, 7.5)	7.19 (1H, dd, 7.5, 1.3)
6'	7.22 (1H, m)	7.30 (1H, t, 7.5)

3.1.4 Alternariol (4, known compound)

Alternariol	
Biological Source	*Trichoderma harzianum*
Sample Code	CL-V3.6
Sample Amount	1.0 mg
Molecular Formula	$C_{14}H_{10}O_5$
Molecular Weight	258 g/mol
Solubility	MeOH
Physical Description	White amorphous powder
HPLC Retention Time	26.13 min (standard gradient)

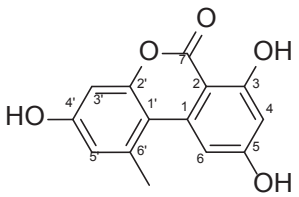

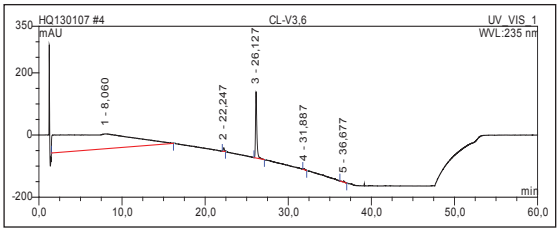

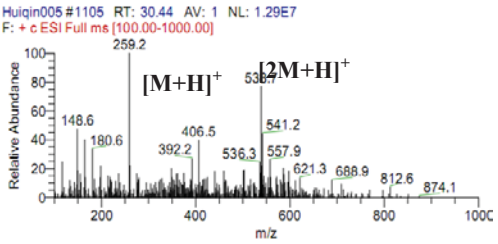

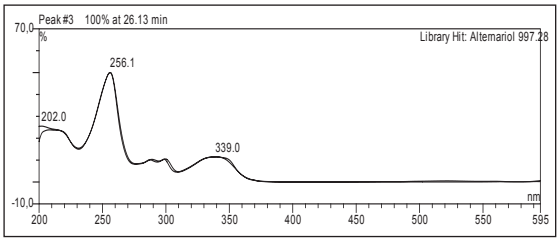

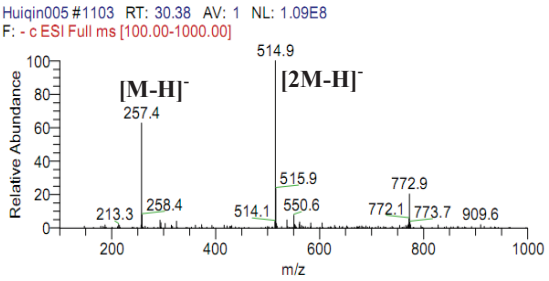

Alternariol (**4**) was isolated as a white amorphous powder. It displayed UV absorptions at λ_{max} (MeOH) 202, 256 and 339 nm, identical to those of alternariol. In addition, positive and negative ESI-MS displayed pseudomolecular ion peaks at *m/z* 259.2 $[M + H]^+$, 538.7 $[2M + H]^+$, 257.4 $[M - H]^-$ and 514.9 $[2M - H]^-$ indicating a molecular weight of 258 g/mol. HPLC co-chromatography analysis of **4** with alternariol as standard was carried out, and resulted in the same retention time and UV spectra for both compounds. Thus, **4** was identified as alternariol.

3.1.5 Waol A (5, known compound)

Waol A	
Biological Source	*Trichoderma harzianum*
Sample Code	FL-E-2.2.2p
Sample Amount	1.34 mg
Molecular Formula	$C_{13}H_{16}O_4$
Molecular Weight	236 g/mol
Solubility	MeOH
Physical Description	colorless oil
HPLC Retention Time	20.24 min (standard gradient)

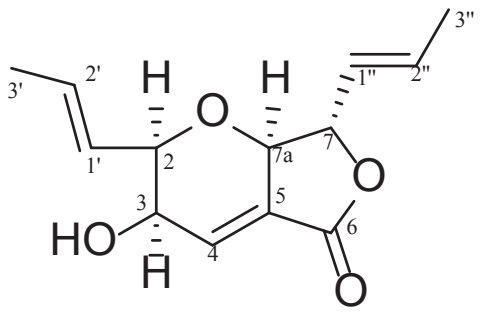

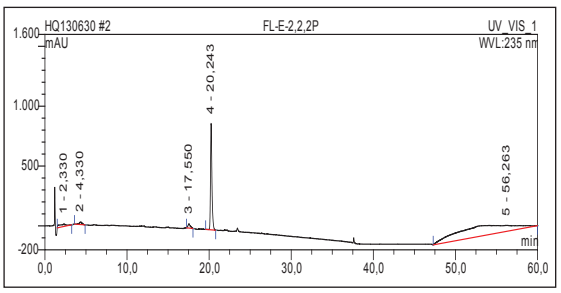

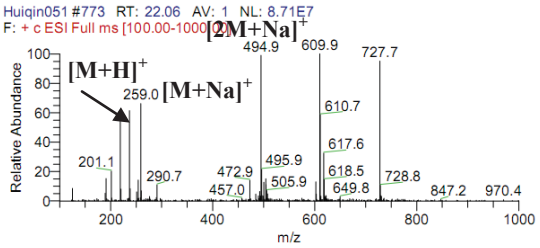

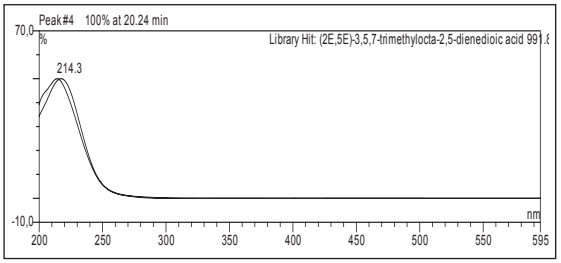

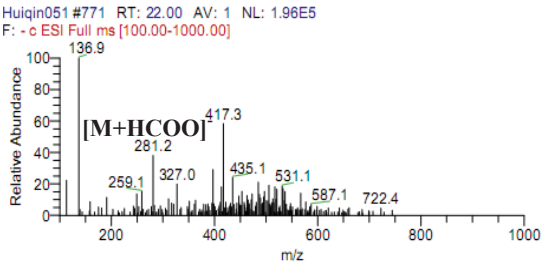

Waol A (**5**) was isolated as a colorless oil (1.34 mg) from the EtOAc extract of solid rice cultures of *T. harzianum*. It displayed UV absorption at λ_{max} (MeOH) 214 nm. The molecular weight of 236 g/mol was indicated by the positive and negative ESI-MS pseudomolecular ion peaks at *m/z* 237 $[M + H]^+$, 259.0 $[M + Na]^+$, 494.9 $[2M + Na]^+$ and 281.2 $[M + HCOO]^-$. The ^{1}H NMR revealed five olefinic protons at δ_H 6.78 (1H, dd, *J* = 2.6, 2.4 Hz, H-4), 6.02 (1H, dq, *J* = 13.1, 6.6 Hz, H-2"), 5.86 (1H, dq, *J* = 15.8, 5.8 Hz, H-2') and 5.69 (2H, m, H-1'/1"); four protons at oxygenated carbons at δ_H 4.58 (1H, dd, *J* = 7.8, 7.8 Hz, H-7), 4.43 (1H, dt, *J* = 7.8, 2.2 Hz, H-7a) and 4.04 (2H, m, H-2/3); as well as two methyl groups at δ_H1.81 (3H, dd, *J* = 6.5, 1.4 Hz, H-3"), and 1.77 (3H, dd, *J* = 6.5, 1.0 Hz, H-3'). The geometry of both double bonds was assigned to be *E* according to large coupling constants $^3J_{1', 2'}$ = 15.8 Hz and $^3J_{1", 2"}$ = 13.1 Hz, respectively. The spectral data mentioned above were found to be identical to those of Waol A (Gao and Snider, 2004). Waol A was first isolated from *Myceliophthora lutea*, and shows a broad spectrum of activities against cultured tumor cell lines (Gao and Snider, 2004; Nozawa *et al*., 1995).

Table 3.1.3 ^{1}H NMR spectral data of **5** and waol A (δ in ppm, *J* in Hz).

Position	**5** (CD_3OD, 500 MHz)	Waol A (Acetone-d_6)[b]
2	4.04 (m)	4.04-4.08 (m)
3	4.04 (m)	4.04-4.08 (m)
4	6.78 (dd, 2.6, 2.4)	6.89 (dd, 3.7, 2.4)
7	4.58 (dd, 7.8, 7.8)	4.60 (dd, 7.9, 7.9)
7a	4.43 (dt, 7.8, 2.2)	4.38 (ddd, 7.9, 2.4, 1.8)
1'	5.69 (m)	5.71 (ddq, 15.3, 6.7, 1.2)[a]
2'	5.86 (dq, 15.8, 5.8)	6.01 (dq, 15.3, 6.7)
3'	1.77 (dd, 6.5, 1.0)	1.79 (dd, 6.7, 1.2)
1"	5.69 (m)	5.61 (ddq, 15.3, 7.9, 1.2)[a]
2"	6.02 (dq, 13.1, 6.6)	5.92 (dq, 15.3, 6.7)
3"	1.81 (dd, 6.5, 1.4)	1.79 (dd, 6.7, 1.2)

[a] exchanged

[b] Gao and Snider, 2004

3.1.6 Aspyridone A (6, known compound)

Aspyridone A	
Biological Source	*Trichoderma harzianum*
Sample Code	FL-E-2.3p
Sample Amount	5.0 mg
Molecular Formula	$C_{19}H_{23}NO_4$
Molecular Weight	329 g/mol
Solubility	MeOH
Physical Description	White amorphous solid
HPLC Retention Time	31.21 min (standard gradient)

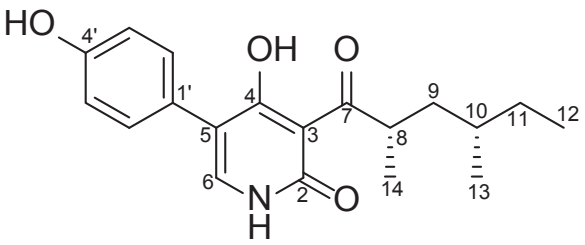

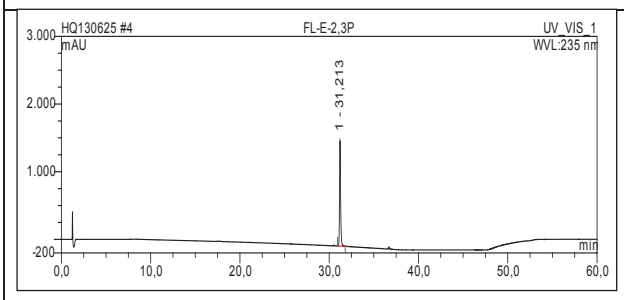

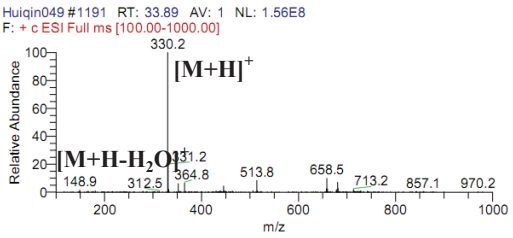

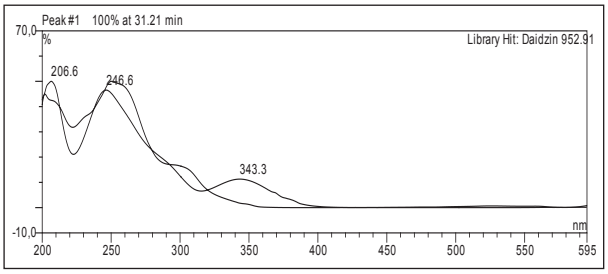

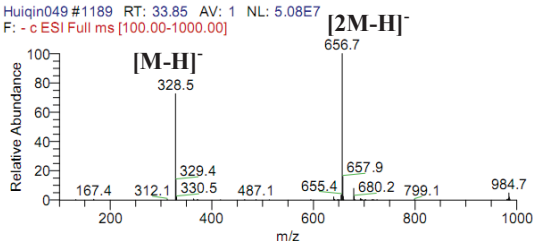

Aspyridone A (**6**) was obtained as a white amorphous solid (5.0 mg) from the EtOAc extract of the solid rice culture of *T. harzianum*. It displayed UV absorptions at λ_{max} (MeOH) 206,

246, and 343 nm. The ESI-MS spectrum showed positive and negative pseudomolecular ion peaks at *m/z* 330.2 $[M + H]^+$, 312.5 $[M + H - H_2O]$, 328.5 $[M - H]^-$ and 656.7 $[2M - H]^-$, suggesting a molecular weight of 329 g/mol. The ^1H NMR spectrum indicated a *para*-hydroxy-substituted phenyl group with two symmetrical doublets at δ_H 7.29 (2H, d, J = 8.6 Hz, H-2'/6') and 6.83 (2H, d, J = 8.6 Hz, H-3'/5') and three methyl groups at δ_H 1.15 (3H, d, J = 6.8 Hz, H_3-14), 0.92 (3H, d, J = 6.5 Hz, H_3-13) and 0.92 (t, J = 7.3 Hz, H_3-12). The ^{13}C NMR and DEPT spectra of **6** showed the corresponding carbon signals [δ_C 158.3 (C-4'), 131.4 (C-2'/6'), 125.2 (C-1'), 116.1 (C-3'/5'), 19.4 (C-13), 17.5 (C-14) and 11.7 (C-12)]. Furthermore, the spectrum displayed six sp^2 carbons, including one methine at δ_C 140.6 (C-6) and five quaternary carbons [containing one carbonyl group at δ_C 214.5 (C-7), one amide carbonyl at δ_C 163.9 (C-2) and one oxygenated carbon at δ_C 177.6 (C-4)], as well as four sp^3 carbons (including two methines and two methylenes).

The ^1H–^1H COSY correlations starting from H_3-12 and sequentially extending until H-8 [δ_H 4.40 (1H, m)] together with the correlations from H_3-14 to H-8 and from H_3-13 to H-10 [δ_H 1.42 (1H, m)] revealed an alkyl chain from H-12 to H-18 with CH_3-13 and CH_3-14 connected to C-8 and C-10, respectively. In addition, HMBC correlations from H-12 to C-11 (δ_C 30.9), C-10 (δ_C 33.6) and C-9 (δ_C 41.9); from H_3-13 to C-11, C-10 and C-8 (δ_C 41.2); from H_3-14 to C-8 and C-7; and from H_2-9 to C-13, C-11, C-10, C-8 and C-7 supported the attachment of the side chain at C-8. In addition, the phenolic group was connected to C-5, as deduced by the HMBC correlations from H-6 to C-5 (δ_C 115.9) and C-1'. The above spectroscopic data were consistent with those reported in the literature for aspyridone A, firstly reported from *Aspergillus nidulans* (Bergmann *et al*., 2007).

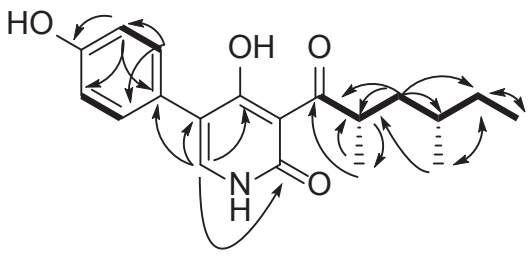

Figure 3.1.3 ^1H–^1H COSY (bold lines) and key HMBC (arrows) correlations of **6**.

Table 3.1.4 ^{1}H NMR spectral data of **6** and aspyridone A (δ in ppm, J in Hz).

Position	**6**		Aspyridone A[a]	
	δ_H (CD_3OD, 600 MHz)	δ_C (CD_3OD, 150 MHz)	δ_H (DMSO-d_6, 500 MHz)	δ_C (DMSO-d_6, 125 MHz)
2		163.9		161.3
3		107.0		105.3
4		177.6		176.0
5		115.9		112.4
6	7.49 (s)	140.6	7.54 (s)	140.7
7		214.5		212.3
8	4.40 (m)	41.2	4.35 (m)	39.5
9	1.66 (m) 1.36 (m)	41.9	1.53 (m) 1.31-1.21 (m)	39.7
10	1.42 (m)	33.6	1.36 (m)	31.8
11	1.38 (m) 1.20 (m)	30.9	1.31-1.21 (m) 1.11 (m)	29.4
12	0.92 (t, 7.3)	11.7	0.80 (m)	11.2
13	0.92 (d, 6.5)	19.4	0.84 (d, 6.5)	18.8
14	1.15 (d, 6.8)	17.5	1.04 (d, 6.7)	16.9
1'		125.2		123.4
2'/6'	7.29 (d, 8.6)	131.4	7.23 (d, 8.6)	130.1
4'		158.3		156.7
3'/5'	6.83 (d, 8.6)	116.1	6.76 (d, 8.6)	115.0

[a] Bergmann *et al*., 2007

All isolated compounds, except compound **4**, were assayed for their cytotoxicity toward L5178Y, A2780 sens, and A2780 CisR cancer cell lines (Table 3.1.5). Compound **3** showed the strongest activity against the aforementioned cell lines with IC_{50} values of 0.19, 0.42, and 6.55 μM, respectively. (Chen *et al*., 2015c)

Table 3.1.5 Cytotoxic activities of **1**-**3**.

Compound	IC_{50} (μM)		
	L5178Y	A2780 sens	A2780 CisR
1	2.55	6.97	> 10.0[b]
2	2.30	4.36	> 10.0[b]
3	0.19	0.42	6.55
Positive[a]	4.30	1.00	10.0

[a] Kahalalide F for L5178Y, and cisplatin for A2780 sens and A2780 CisR

[b] only IC_{50} values < 10.0 μM are reported

3.2 Inducing secondary metabolite production by the soil-dwelling fungus *Aspergillus terreus* through different techniques

A. terreus was isolated from sediment collected from the lake in Wadi EI Natrun in Egypt. The inland saline lake produces progressively concentrated brine, because of the specific climate conditions that remove water by evaporation. The changes in evaporation and precipitation affect the physical and chemical conditions of the lake, which control the distribution and abundance of aquatic life. (Taher, 1999) *A. terreus* is a fungus worldwide distributed in soil, and has been found to produce a variety of secondary metabolites and mycotoxins, such as butyrolactones, lovastatin, and terrein.

Interestingly, several methods have been reported to induce new secondary metabolites from fungi, including co-cultivation with bacteria, medium engineering, and treatment with epigenetic modifiers. Herein, different methods were employed to induce the secondary metabolite production from *A. terreus*.

3.2.1 Inducing secondary metabolite production by co-cultivation of *A. terreus* with bacteria.

Fungi and bacteria co-exist in complex ecosystems such as soil, water or living tissues of plants, where they compete and communicate with each other as well as with other organisms such as algae, protozoans and even their metazoan hosts (in the case of endophytes) (Strobel *et al*., 2004; Aly *et al*., 2011; Brakhage and Schroeckh, 2011). It is generally accepted that one of the roles of secondary metabolites is to provide biological advantage for the producer in response to its environment, which implies the presence of sensing mechanisms to control production of metabolites (Chiang *et al*., 2011). In mimicking the natural microbial environment, co-cultivation of different microbes in one culture vessel (also called mixed cultivation) may lead to an enhancement of the accumulation of constitutively present natural products (Oh *et al*., 2007; Schroeckh *et al*., 2009; Nuetzmann *et al*., 2011) or may trigger the expression of silent biosynthetic pathways yielding new compounds (Oh *et al*., 2005; Cueto *et al*., 2001), due to microbial crosstalk and chemical defense (Pettit, 2011).

3.2.1.1 Isobutyrolactone II (7, new compound)

Isobutyrolactone II	
Biological Source	Co-cultivation of *Aspergillus terreus* and *Bacillus* sp.
Sample Code	BvW-5.8.1P5
Sample Amount	1.2 mg
Molecular Formula	$C_{18}H_{16}O_6$
Molecular Weight	328 g/mol
Solubility	MeOH
Physical Description	yellow gum
Optical rotation	$[\alpha]^{20}_D$ +8.7 (*c* 0.2, MeOH)
HPLC Retention Time	22.75 min (standard gradient)

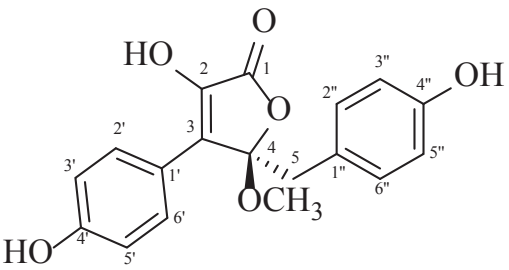

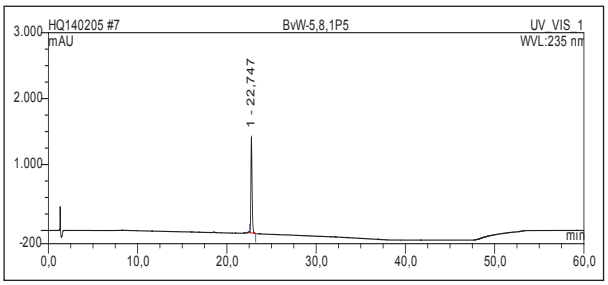

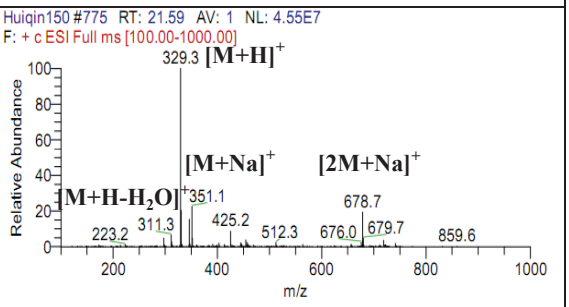

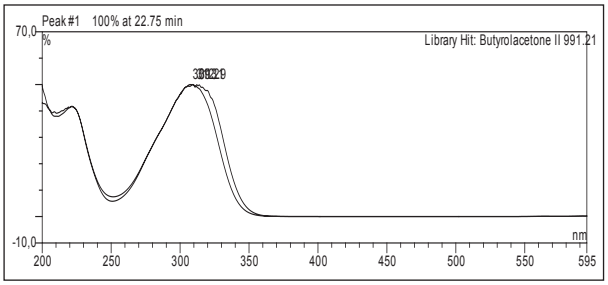

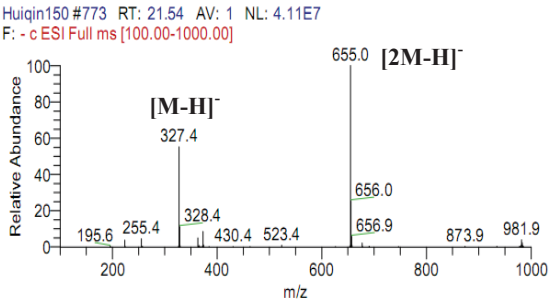

Isobutyrolactone II (**7**) was obtained as a yellow gum. The molecular formula was determined as $C_{18}H_{16}O_6$ on the basis of the prominent ion peak at *m/z* 329.1018 $[M + H]^+$ observed in the HRESIMS spectrum, requiring eleven degrees of unsaturation. It displayed UV absorptions at λ_{max} (MeOH) 201, 224, and 313 nm, characteristic for butyrolactone derivatives. Inspection of the ^{1}H NMR spectrum of **7** indicated the presence of four symmetrical doublets at δ_H 7.72 (2H, d, *J* = 8.8 Hz, H-2'/6'), 6.90 (2H, d, *J* = 8.8 Hz, H-3'/5'), 6.62 (2H, d, *J* = 8.5 Hz, H-2"/6") and 6.51 (2H, d, *J* = 8.5 Hz, H-3"/5"), typical of two *para*-hydroxy phenyl substituents, one methoxy group at δ_H 3.10 (3H, s, 4-OCH_3), a methylene group at δ_H 3.18 (1H, d, *J* = 14.0 Hz, H-5) and 3.13 (1H, d, *J* = 14.0 Hz, H-5), and three hydroxy protons at δ_H 10.59, 9.90, and 9.20 (2-OH, 4'-OH, and 4"-OH, respectively) (Table 3.2.1). The ^{13}C NMR and HSQC spectra of **7** confirmed the corresponding carbon signals, including eight sp^2 methines [δ_C 128.9 (C-2'/6'), 115.8 (C-3'/5'), 131.1 (C-2"/6"), and 114.5 (C-3"/5")], four sp^2 quaternary carbons [(δ_C 121.1 (C-1'), 157.8 (C-4'), 123.9 (C-1"), and 156.1 (C-4")], a methoxy group at δ_C 50.0 (4-OCH_3), and one sp^3 methylene at δ_C 42.3 (C-5). Additional signals included those of one carbonyl group at δ_C 166.2 (C-1), two sp^2 quaternary carbons at δ_C 139.1 (C-2) and 120.4 (C-3), and one dioxygenated sp^3 quaternary carbon at δ_C 108.4 (C-4), thus indicating the presence of a conjugated five-membered lactone ring. These data were in agreement with those observed for **10**, except for the replacement of the methylated carboxy group located at C-4 in **10** by a methoxy group in **7**, which accounted for the molecular weight difference of 28 amu observed between both compounds. In the HMBC spectrum of **7** (Figure 3.2.1), the correlations observed from the respective methoxy protons (4-OCH_3) to C-4; H-5 to C-4, C-1", C-2" and C-6"; 4'-OH to C-3', C-4' and C-5'; and 4"-OH to C-3", C-4" and C-5" corroborated the attachment of the methoxy group (4-OCH_3) at C-4 and allowed us to establish the planar structure of **7**. The presence of **7** in the crude EtOAc extract argues against the possibility that it is an artefact arising through methylation during the isolation procedure. Therefore, **7** was identified as the new natural product 3-hydroxy-5-(4'"-hydroxybenzyl)-4-(4'-hydroxyphenyl)-5-methoxyfuran-2-(5*H*)-one for which we propose the trivial name isobutyrolactone II. (Chen *et al*., 2015b)

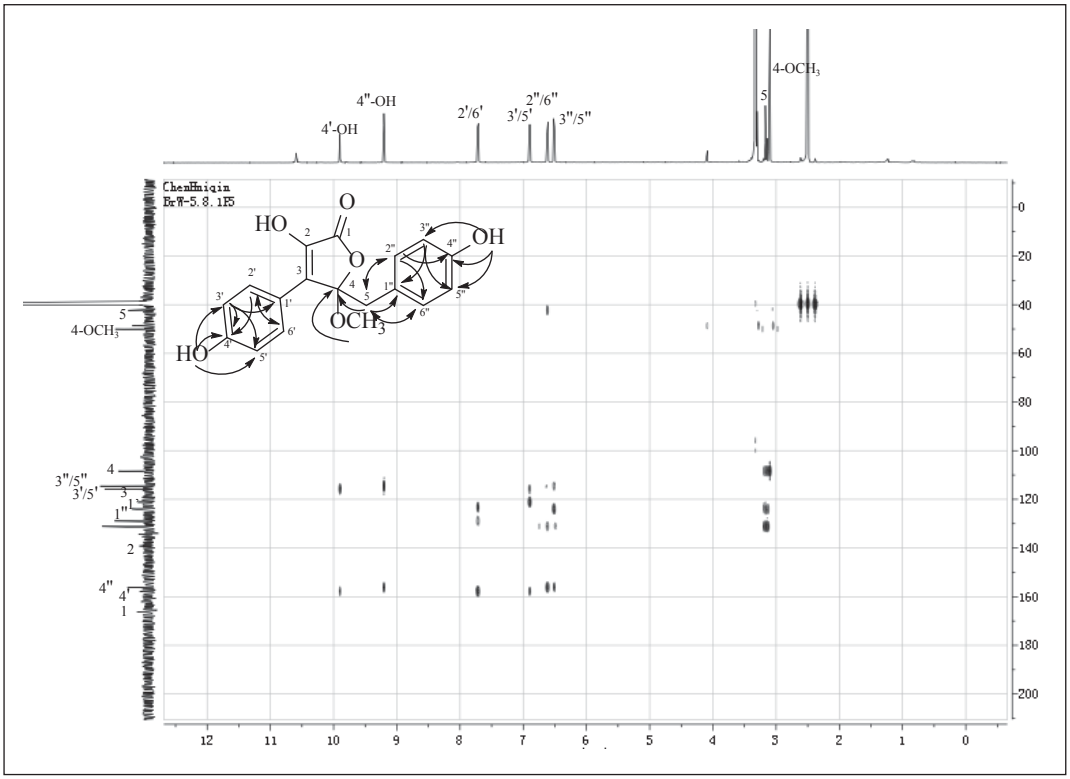

Figure 3.2.1 HMBC correlations of **7**.

Table 3.2.1 ^{1}H and ^{13}C NMR data of **7** and **8**. (Chen *et al*., 2015b)

No.	**7** (DMSO-d_6, δ in ppm, J in Hz)		**8** (DMSO-d_6, δ in ppm, J in Hz)	
	δ_H (600 MHz)	δ_C (150 MHz)	δ_H (600 MHz)	δ_C (150 MHz)
1		166.2		169.4
2		139.1		139.3
3		120.4		128.5
4		108.4		107.4
5	3.18 (1H, d, 14.0) 3.13 (1H, d, 14.0)	42.3	3.16 (1H, d, 14.0) 3.10 (1H, d, 14.0)	44.2
1'		121.1		123.7
2',6'	7.72 (2H, d, 8.8)	128.9	7.78 (2H, d, 8.8)	131.2
3',5'	6.90 (2H, d, 8.8)	115.8	6.87 (2H, d, 8.8)	116.3
4'		157.8		158.9
1"		123.9		126.5
2",6"	6.62 (2H, d, 8.5)	131.1	6.60 (2H, d, 8.5)	132.4
3",5"	6.51 (2H, d, 8.5)	114.5	6.49 (2H, d, 8.5)	115.5
4"		156.1		157.3
4-OCH_3	3.10 (3H, s)	50.0		
4-OH			not detected	
2-OH	10.59 (1H, s)		10.22 (1H, s)	
4'-OH	9.90 (1H, s)		9.78 (1H, s)	
4"-OH	9.20 (1H, s)		9.20 (1H, s)	

3.2.1.2 4-O-Demethylisobutyrolactone II (8, new compound)

4-O-Demethylisobutyrolactone II	
Biological Source	Co-cultivation of *Aspergillus terreus* and *Bacillus* sp.
Sample Code	BvW-5.8.1P1
Sample Amount	4.2 mg
Molecular Formula	$C_{17}H_{14}O_6$
Molecular Weight	314 g/mol
Solubility	MeOH
Physical Description	Yellow gum
Optical rotation	$[\alpha]^{20}_{D}$ +13.0 (*c* 0.2, MeOH)
HPLC Retention Time	18.53 min (standard gradient)

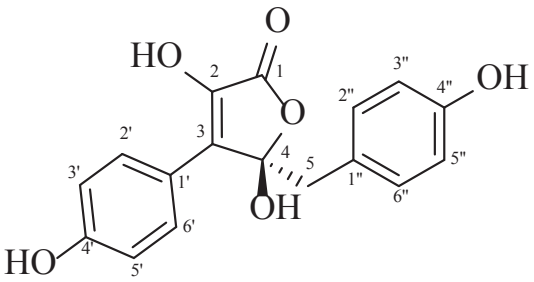

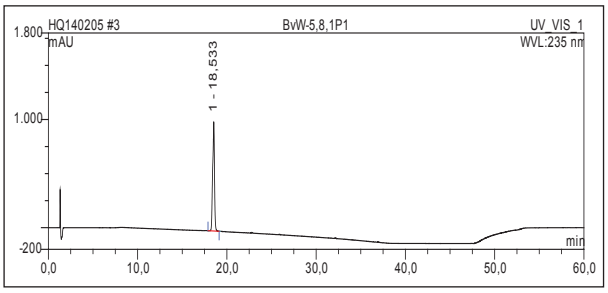

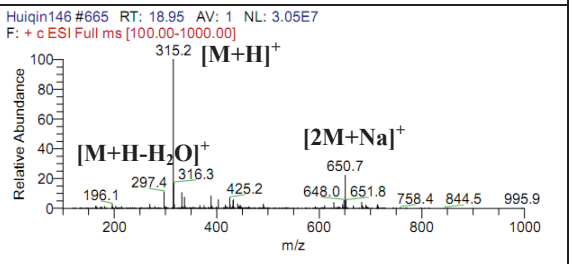

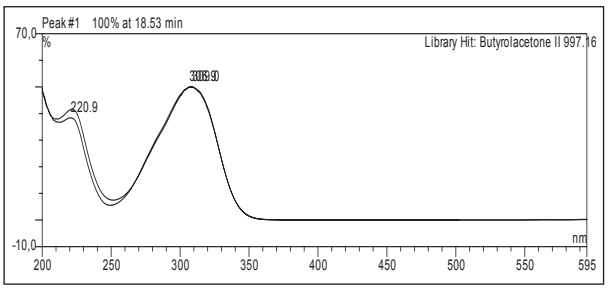

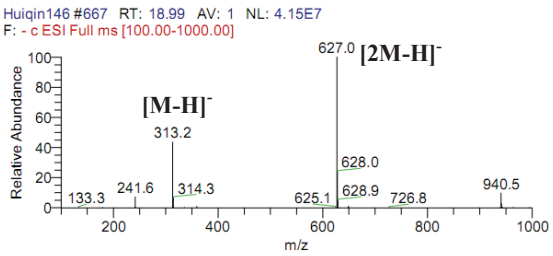

4-O-Demethylisobutyrolactone II (**8**) was isolated as a yellow gum. The molecular formula was determined as $C_{17}H_{14}O_6$ by HRESIMS (*m/z* 315.0863 $[M + H]^+$), indicating eleven degrees of unsaturation. Inspection of the ^1H and ^{13}C NMR data of **8** (Table 3.2.1) showed close structural similarity to those of **7**, apart from the absence of the methoxy group signal in **8**, which is in accordance with the decreased in the molecular weight by 14 amu compared to **7**. The structure of **8** was further confirmed by interpretation of the HMBC spectrum (Figure 3.2.2), which showed that all observed correlations corresponded to those observed in the spectrum of **7** except for the lacking methoxy group. Thus, **8** was identified as a new natural product for which we propose the trivial name 4-O-demethylisobutyrolactone II. (Chen *et al*., 2015b)

The absolute stereochemistry of the chiral center at C-4 of butyrolactones has been previously established as *R* through synthetic and spectroscopic studies (Nitta *et al*., 1983; Kiriyama *et al*., 1977; Parvatkar *et al*., 2009; Cazar *et al*., 2005; Niu *et al*., 2008). Based on the optical rotations of **7** ($[\alpha]^{20}_D$ +8.7, *c* 0.2, MeOH) and **8** ($[\alpha]^{20}_D$ +13.0, *c* 0.2, MeOH), which were on the positive side as observed in the literature for butyrolactones (Parvatkar *et al*., 2009; Cazar *et al*., 2005; Niu *et al*., 2008), as well as on their close biogenetic relationship, it is assumed that both compounds share the *R* configuration at C-4. (Chen *et al*., 2015b)

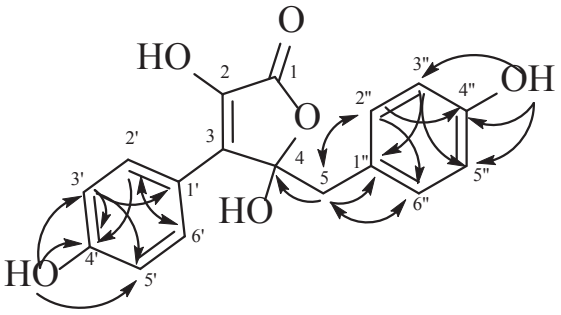

Figure 3.2.2 Key HMBC correlations of **8**.
(Chen *et al*., 2015b)

3.2.1.3 N-(Carboxymethyl)anthranilic acid (9, known compound)

N-(Carboxymethyl)anthranilic acid	
Biological Source	Co-cultivation of *Aspergillus terreus* and *Bacillus* sp.
Sample Code	BvW-10.7P3
Sample Amount	1.0 mg
Molecular Formula	$C_9H_9NO_4$
Molecular Weight	195 g/mol
Solubility	MeOH
Physical Description	Yellow amorphous solid
HPLC Retention Time	19.82 min (standard gradient)

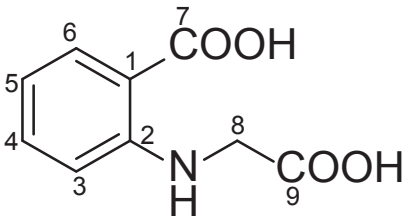

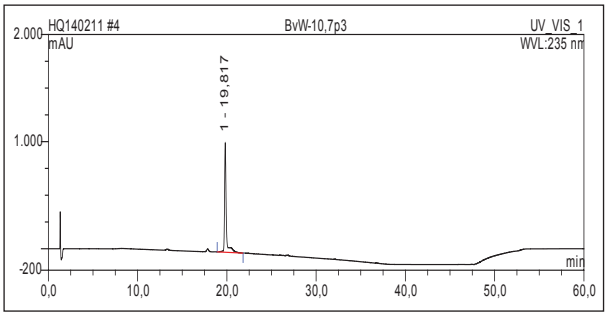

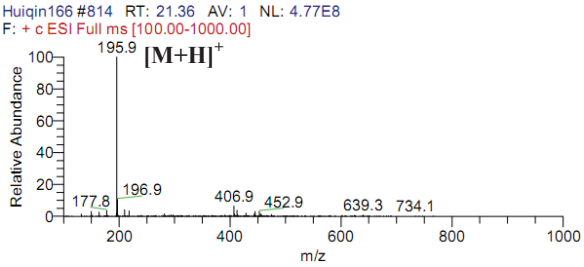

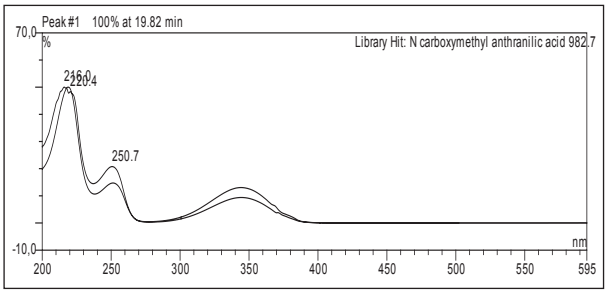

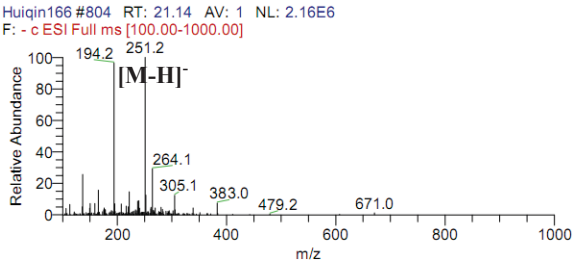

N-(carboxymethyl)anthranilic acid (**9**) was isolated as a yellow amorphous solid from EtOAc extracts of co-cultivation of *A. terreus* with *B. subtilis* or with *B. cereus* on solid rice medium. It displayed UV absorptions at λ_{max} (MeOH) 216, 250 and 345 nm. Positive and negative ESI-MS showed molecular ion peaks at *m/z* 195.9 $[M + H]^+$ and 194.2 $[M - H]^-$, respectively, indicating a molecular weight of 195 g/mol, and thus the presence of an odd number of nitrogen atoms in the structure. The ^1H NMR spectrum revealed four *ortho*-coupled phenyl protons at δ_H 7.91 (1H, dd, J = 7.9, 1.4 Hz, H-6), 7.36 (1H, td, J = 7.4, 1.6 Hz, H-4), 6.62 (1H, t, J = 8.4 Hz, H-5) and 6.61 (1H, d, J = 8.4 Hz, H-3), as well as a nitrogen-bearing methylene group, due to its downfield chemical shift at δ_H 4.01 (s, H_2-8). The HMBC cross-peaks from H-6 to C-7 (δ_C 171.3), C-2 (δ_C 151.3) and C-4 (δ_C 135.2); from H-4 to C-6 (δ_C 132.5); and from H-5 to C-3 (δ_C 111.9) were diagnostic of an anthranilic acid core structure. Moreover, the signals from H_2-8 to C-2 and C-9 (δ_C 173.6) together with the downfield chemical shift of H_2-8 indicated a carboxymethylene group connected at C-2 via a nitrogen bridge (Figure 3.2.3). Thus, **9** was identified as N-(carboxymethyl)anthranilic acid by comparison of its spectroscopic data with those in the literature. N-(carboxymethyl)anthranilic acid was first introduced as a synthetic compound in 1890 by Heumann and as a starting material for indigo synthesis (Wiklund, Romero and Bergman, 2003), while it was firstly reported as a natural metabolite by Ola *et al*. isolated from the co-cultivation of *Fusarium tricinctum* with *B. subtilis* (Ola *et al*., 2013).

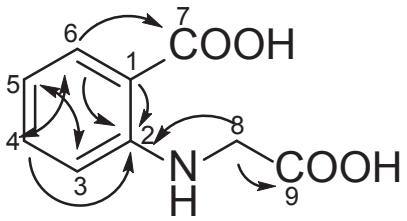

Figure 3.2.3 HMBC correlations of **9**.

Table 3.2.2 ^{1}H NMR data of **9** and N-(carboxymethyl)anthranilic acid (500 MHz for ^{1}H NMR, 125 MHz for ^{13}C NMR, in CD_3OD, δ in ppm, J in Hz).

Position	**9**		N-(carboxymethyl)anthranilic acid[a]	
	^{1}H NMR	HMBC	^{1}H NMR	^{13}C NMR
1				112.3
2				151.9
3	6.61 (d, 8.4)		6.6.1 (dd, 8.7, 1.0)	112.5
4	7.36 (td, 7.4, 1.6)	C-6 (δ_C 132.5)	7.36 (ddd, 8.7, 7.2, 1.6)	135.8
5	6.62 (t, 8.4)	C-3 (δ_C 111.9)	6.62 (ddd, 7.8, 7.2, 1.0)	116.4
6	7.91 (dd, 7.9, 1.4)	C-7 (δ_C 171.3), C-2 (δ_C 151.3) and C-4 (δ_C 135.2)	7.91 (dd, 7.9, 1.6)	133.4
7				171.9
8	4.01 (s)	C-2 and C-9 (δ_C 173.6)	4.01 (s)	45.5
9				174.1

[a] Ola *et al*., 2013

3.2.1.4 Butyrolactone II (10, known compound)

Butyrolactone II	
Biological Source	Co-cultivation of *Aspergillus terreus* and *Bacillus* sp.
Sample Code	W6-3.6P1, BvW-5.8.1P4, BvW-5.7.5P
Sample Amount	14.5 mg
Molecular Formula	$C_{19}H_{16}O_7$
Molecular Weight	356 g/mol
Solubility	MeOH
Physical Description	Yellow gum
HPLC Retention Time	21.10 min (standard gradient)

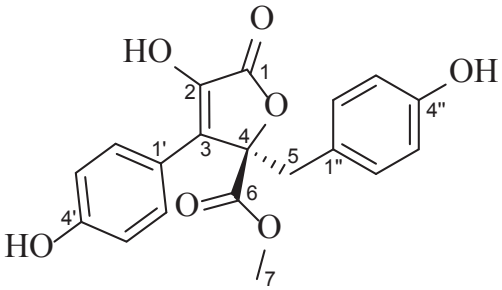

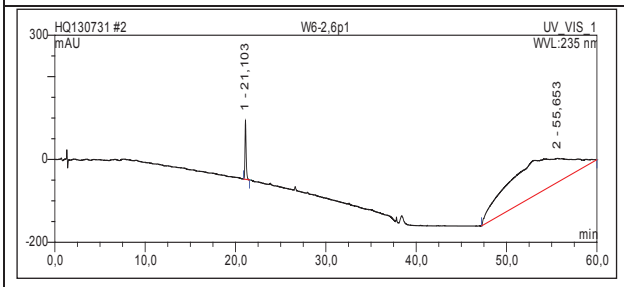

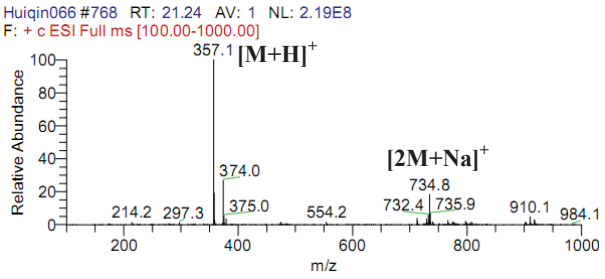

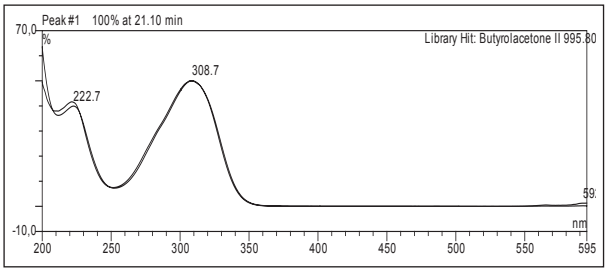

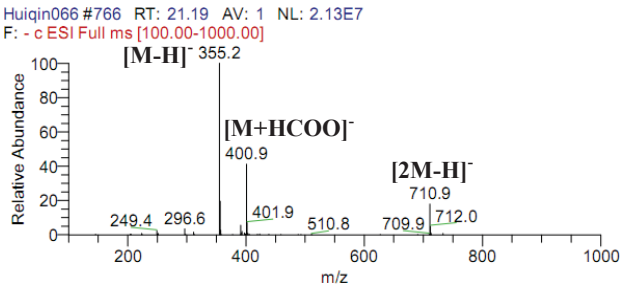

Butyrolactone II (**10**) was isolated as a yellow gum from the EtOAc extract of co-cultivation of *A. terreus* with *B. subtilis* or *B. cereus* on solid rice medium. The UV spectrum showed absorptions at λ_{max} (MeOH) 222 and 308 nm, suggesting the presence of a butyrolactone core structure. The molecular weight of 356 g/mol was deduced from the positive and negative ESI-MS pseudomolecular ion peaks at *m/z* 357.1 $[M + H]^+$, 734.8 $[2M + Na]^+$, 400.9 $[M + HCOO]^-$, 355.2 $[M - H]^-$ and 710.9 $[2M - H]^-$. The ^1H NMR spectrum displayed two *para*-substituted aromatic systems [δ_H 7.59 (2H, d, J = 8.8 Hz, H-2'/6'), 6.87 (2H, d, J = 8.8 Hz, H-3'/5'), 6.64 (2H, d, J = 8.5 Hz, H-2"/6"), 6.51 (2H, d, J = 8.5 Hz, H-3"/5")], one methoxy group at δ_H 3.78 (3H, s, OCH_3-7), and one methylene at δ_H 3.46 (2H, s, H_2-5). The identification of **10** was further confirmed by comparison of its UV, ^1H NMR, MS, and $[\alpha]_D$ data with those reported for butyrolactone II (Nitta *et al*., 1983), which was likewise reported from the same fungus.

3.2.1.5 Butyrolactone I (11, known compound)

Butyrolactone I	
Biological Source	Co-cultivation of *Aspergillus terreus* and *Bacillus* sp.
Sample Code	W6-2.5
Sample Amount	2.0 mg
Molecular Formula	$C_{24}H_{24}O_7$
Molecular Weight	424 g/mol
Solubility	MeOH
Physical Description	Purple gum
HPLC Retention Time	25.58 min (standard gradient)

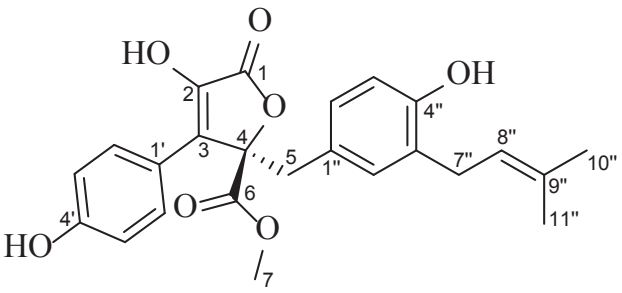

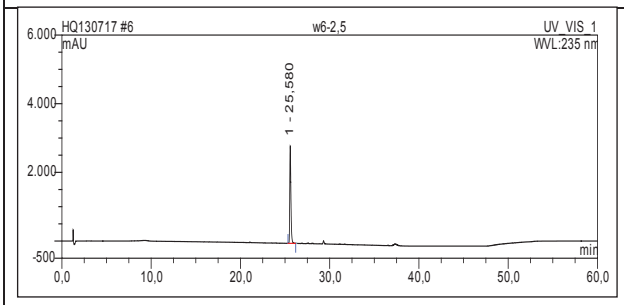

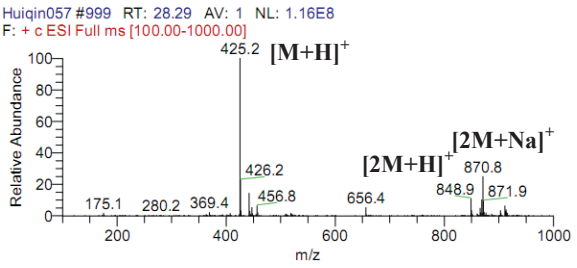

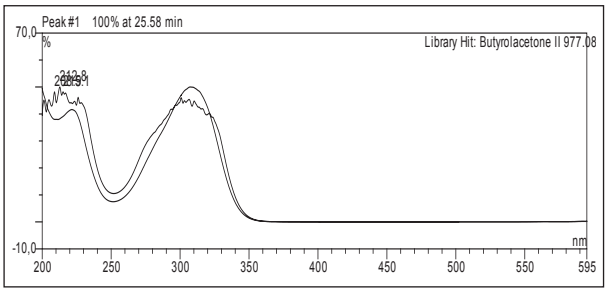

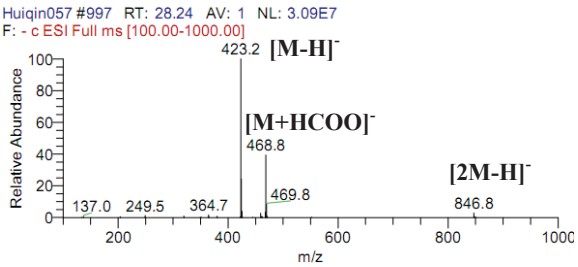

Butyrolactone I (**11**) was isolated as a purple gum from the EtOAc extract of co-cultivation of *A. terreus* with *B. subtilis* or with *B. cereus* on solid rice medium. It was the major compound detected in the analytical HPLC chromatogram. It displayed UV absorptions at λ_{max} (MeOH) 218 and 308 nm, showing high similarity to those of butyrolactone II (**10**). The molecular weight of 424 g/mol was deduced by the positive and negative ESI-MS pseudomolecular ion peaks at *m/z* 425.2 $[M + H]^+$, 848.9 $[2M + H]^+$, 870.8 $[2M + Na]^+$, 468.8 $[M + HCOO]^-$, 423.2 $[M - H]^-$ and 846.8 $[2M - H]^-$, showing a 68 amu increase compared to **10**. The ^1H NMR spectrum displayed one *para*-aromatic substituent and one ABX spin system with the protons at δ_H 7.67 (2H, d, J = 8.8 Hz, H-2'/6'), 6.96 (2H, d, J = 8.8 Hz, H-3'/5'), 6.62 (1H, dd, J = 8.1, 1.8 Hz, H-6"), 6.58 (1H, d, J = 8.1 Hz, H-5"), and 6.51 (1H, d, J = 1.8 Hz, H-2") in the structure instead of two *para*-substituent aromatic rings as in **10**. In addition, one methoxy group OCH_3-7 [δ_H 3.83 (3H, s)] and one methylene CH_2-5 [δ_H 3.51 (2H, d, J = 6.2 Hz)] were observed. The remaining signals in ^1H NMR spectrum of one methylene [δ_H 3.16 (2H, m, H-7")], one sp^2 methine [δ_H 5.15 (1H, t, J = 7.3 Hz, H-8")], and two methyl groups [δ_H 1.74 (3H, s, H_3-10") and 1.64 (3H, s, H_3-11")], indicated the presence of an isoprenyl group. Overall, the spectral properties and established substructures of **11** were identical to the known butyrolactone I, originally isolated from the same biological source (Kiriyama *et al*., 1977; Rao *et al*., 2000).

3.2.1.6 Butyrolactone III (12, known compound)

Butyrolactone III	
Biological Source	Co-cultivation of *Aspergillus terreus* and *Bacillus* sp.
Sample Code	BvW-5.5.3, BvW-5.4.7
Sample Amount	40.6 mg
Molecular Formula	$C_{24}H_{24}O_8$
Molecular Weight	440 g/mol
Solubility	MeOH
Physical Description	Yellow gum
HPLC Retention Time	23.51 min (standard gradient)

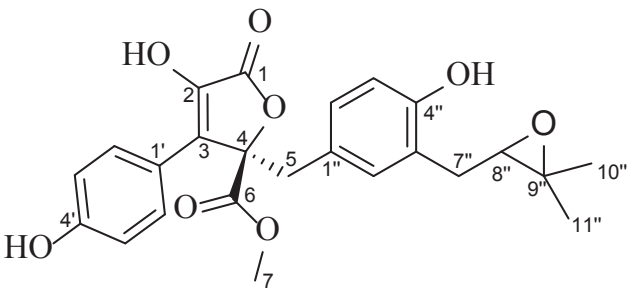

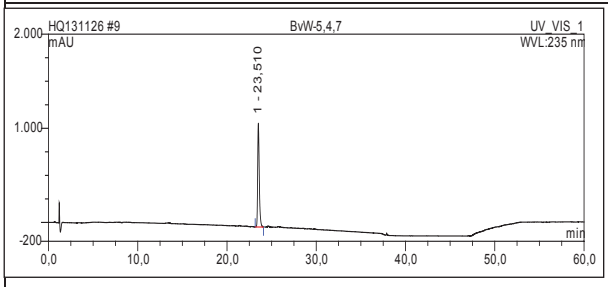

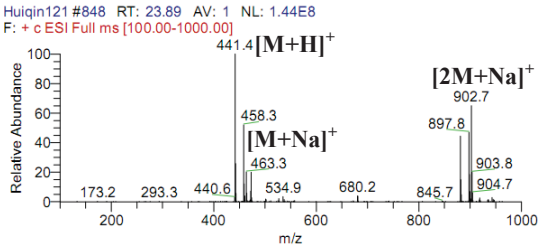

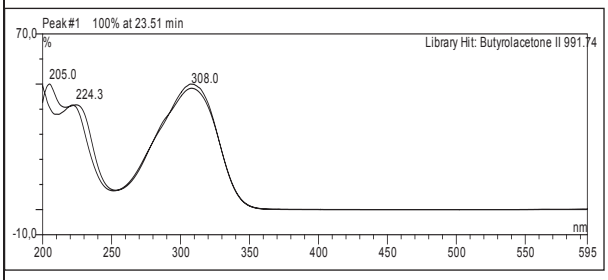

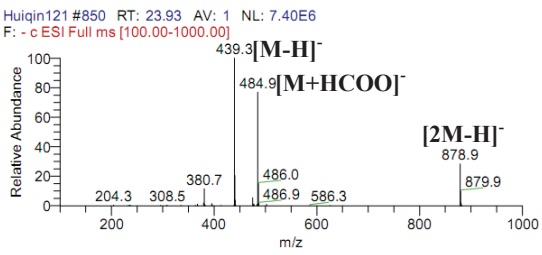

Butyrolactone III (**12**) was isolated as a yellow gum from the EtOAc extract of co-cultivation of *A. terreus* with *B. subtilis* or with *B. cereus* on solid rice medium. It displayed UV absorptions at λ_{max} (MeOH) 224 and 308 nm, characteristic of butyrolactone derivatives. The positive and negative ESI-MS ion peaks at *m/z* 441.4 $[M + H]^+$, 463.3 $[M + Na]^+$, 902.7 [2M + Na], 439.3 $[M - H]^-$, 484.9 $[M + HCOO]^-$ and 878.9 $[2M - H]^-$, indicated a molecular weight of 440 g/mol. The ^{1}H NMR data showed high similarity to those of **11**, as suggested by the proton signals on two different substituent aromatic rings [δ_H 7.63 (2H, d, J = 8.8 Hz, H-2'/6'), 6.94 (2H, d, J = 8.8 Hz, H-3'/5'), 6.61 (1H, dd, J = 8.3, 2.1 Hz, H-6''), 6.54 (1H, d, J = 8.3 Hz, H-5''), 6.55 (1H, d, J = 2.1 Hz, H-2'')], one methoxyl group at δ_H 3.85 (3H, s, OCH_3-7), and two methyl groups at δ_H 1.33 (3H, s, H_3-10'') and 1.24 (3H, s, H_3-11''). In addition, the double bond C-8''/9'' in **11** was replaced by an epoxide group in **12**, as suggested by the remaining downfield resonance at δ_H 3.73 (1H, m, H-8'') and by its molecular formula. Comparison of the obtained UV, MS and ^{1}H NMR data with those reported in the literature established **12** as butyrolactone III, which is a common metabolite of *A. terreus* (Kiriyama *et al*., 1977; Rao *et al*., 2000).

3.2.1.7 Butyrolactone VI (13, known compound)

Butyrolactone VI	
Biological Source	Co-cultivation of *Aspergillus terreus* and *Bacillus* sp.
Sample Code	W6-6P, W6-8.4P, BvW-5.5.2P2
Sample Amount	2.3 mg
Molecular Formula	$C_{24}H_{26}O_9$
Molecular Weight	458 g/mol
Solubility	MeOH
Physical Description	Yellow gum
HPLC Retention Time	23.44 min (standard gradient)

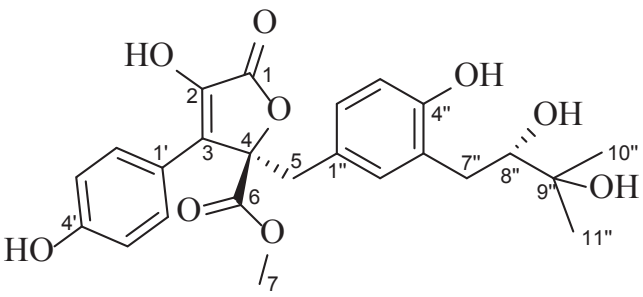

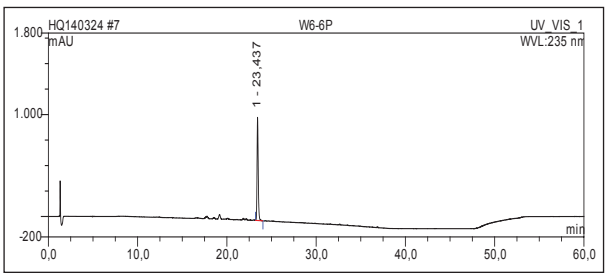

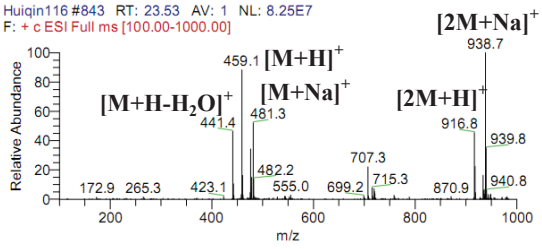

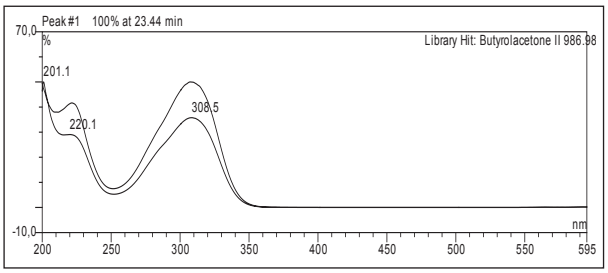

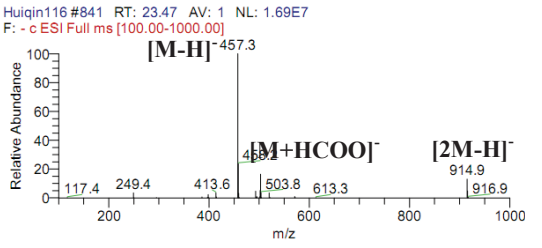

Butyrolactone VI (**13**) was isolated as a yellow gum from the EtOAc extract of co-cultivation of *A. terreus* with *B. subtilis* or with *B. cereus* on solid rice medium. It displayed UV absorptions at λ_{max} (MeOH) 220 and 308 nm, typical for butyrolactone derivatives. Positive and negative ESI-MS showed molecular ion peaks at *m/z* 441.4 $[M + H - H_2O]^+$, 459.1 $[M + H]^+$, 481.3 $[M + Na]^+$, 916.8 $[2M + H]^+$, 938.7 $[2M + Na]^+$, 457.3 $[M - H]^-$, 503.0 $[M + HCOO]^-$ and 914.9 $[2M - H]^-$, indicating a molecular weight of 458 g/mol. The butyrolactone skeleton of **13** was futher supported by the ^{1}H NMR data at δ_H 7.58 (2H, d, *J* = 8.8 Hz, H-2'/6'), 6.87 (2H, d, *J* = 8.8 Hz, H-3'/5'), 6.62 (1H, d, *J* = 2.0 Hz, H-2"), 6.52 (1H, d, *J* = 8.2 Hz, H-5"), 6.49 (1H, d, *J* = 8.2, 2.0 Hz, H-6"), 3.79 (3H, s, OCH_3-7), 1.18 (3H, s, H_3-10") and 1.17 (3H, s, H_3-11"). The molecular weight difference of 18 amu observed between **12** and **13**, suggested that **13** was formed by epoxide hydrolysis of **12**. This conclusion was further corroborated by the ion peak of 441.4 $[M + H - H_2O]^+$ observed in the ESI-MS. Based on the aforementioned data and by comparison with the literature (Nuclear *et al*., 2010), **13** was identified as butyrolactone VI, which is a common metabolite of *A. terreus*.

Table 3.2.3 ^{1}H NMR data of **10 - 13** (500 MHz, in CD_3OD, δ in ppm, *J* in Hz).

Position	**10** (δ_H)	**11** (δ_H)	**12** (δ_H)	**13** (δ_H)
5	3.46 (s)	3.51 (d, 6.2)	3.51 (br. s)	3.49 (br. s)
7	3.78 (s)	3.83 (s)	3.85 (s)	3.79 (s)
2'/6'	7.59 (d, 8.8)	7.67 (d, 8.8)	7.63 (d, 8.8)	7.58 (d, 8.8)
3'/5'	6.87 (d, 8.8)	6.96 (d, 8.8)	6.94 (d, 8.8)	6.87 (d, 8.8)
2"	6.64 (d, 8.5)	6.51 (d, 1.8)	6.55 (d, 2.1)	6.62 (d, 2.0)
3"	6.51 (d, 8.5)			
5"	6.51 (d, 8.5)	6.58 (d, 8.1)	6.54 (d, 8.3)	6.52 (d, 8.2)
6"	6.64 (d, 8.5)	6.62 (dd, 8.1, 1.8)	6.61 (dd, 8.3, 2.1)	6.49 (d, 8.2, 2.0)
7"		3.16 (2H, m)	2.87 (m)	2.70 (dd, 14.0, 2.0)
			2.59 (m)	2.51 (dd, 14.0, 10.0)
8"		5.15 (t, 7.3)	3.73 (m)	3.49 (dd, 10.1, 2.1)
10"		1.74 (s)	1.33 (s)	1.18 (s)
11"		1.64 (s)	1.24 (s)	1.17 (s)

3.2.1.8 Terrein (14, known compound)

Terrein	
Biological Source	Co-cultivation of *Aspergillus terreus* and *Bacillus* sp.
Sample Code	BvW-6crystal
Sample Amount	7.3 mg
Molecular Formula	$C_8H_{10}O_3$
Molecular Weight	154 g/mol
Solubility	MeOH
Physical Description	White crystal
HPLC Retention Time	7.84 min (standard gradient)

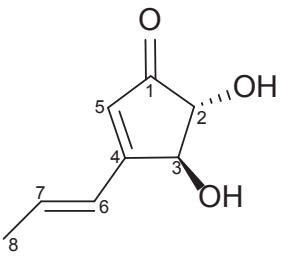

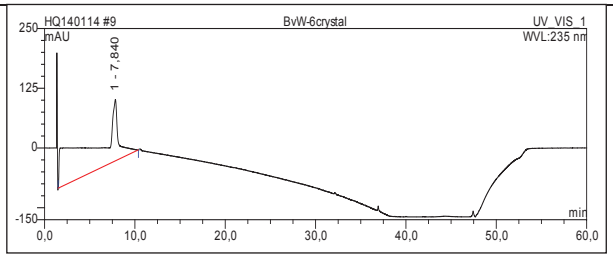

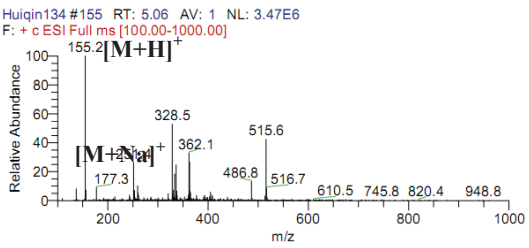

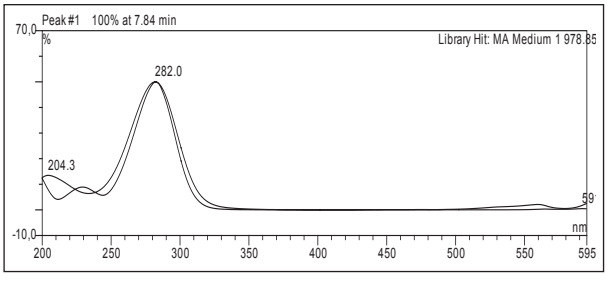

No ionisation in negative mode.

Terrein (**14**) was isolated as a white crystal from the EtOAc extract of co-cultivation of *A. terreus* with *B. subtilis* or with *B. cereus* on solid rice medium. It showed UV absorption $\lambda_{(max)}$ at 282 nm. ESI-MS analysis gave only positive ionization at *m/z* 155.2 $[M + H]^+$ and 177.3 $[M + Na]^+$, which indicated a molecular weight of 154 g/mol. The ^{1}H NMR spectrum exhibited one *E*-configured double bond [δ_H 6.84 (1H, m, H-7) and 6.44 (1H, d, J = 15.8 Hz, H-6)], according to the large coupling constant $^3J_{6,7}$ = 15.8 Hz, and one methyl group at δ_H 1.94 (3H, dd, J = 6.8, 1.6 Hz, H_3-8). In addition, two oxygenated methines were observed, based on their downfield chemical shifts at δ_H 4.67 (1H, s, H-2) and 4.07 (1H, d, J = 2.6 Hz, H-3). The UV, MS and ^{1}H NMR spectra of **14** were in agreement with published data for terrein (Dunn, Entwistle and Johnstone, 1975), which was previously reported from *A. terreus* (Raistrick and Smith, 1935), and *Penicillium raistrickii* (Grove, 1954). Terrein has shown to inhibit plant growth (Phattanawasin, *et al*., 2007), melanin biosynthesis (Park *et al*., 2004), and inflammation in human dental pulp cells (Lee *et al*., 2008), as well as to have antibiotic (Ghisalberti, Narbey and Rowland, 1990), anti-proliferative (Kim *et al*., 2007), and antitumor (Arakawa *et al*., 2008) activities.

3.2.1.9 Dihydroterrein (15, known compound)

Dihydroterrein	
Biological Source	Co-cultivation of *Aspergillus terreus* and *Bacillus* sp.
Sample Code	BvW-5.5.1.2
Sample Amount	1.29 mg
Molecular Formula	$C_8H_{12}O_3$
Molecular Weight	156 g/mol
Solubility	MeOH
Physical Description	Yellow amorphous solid
HPLC Retention Time	10.62 min (standard gradient)

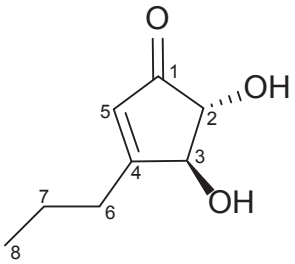

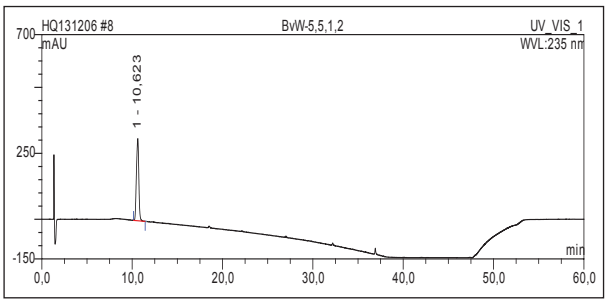

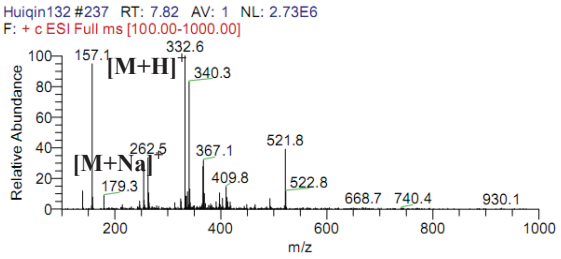

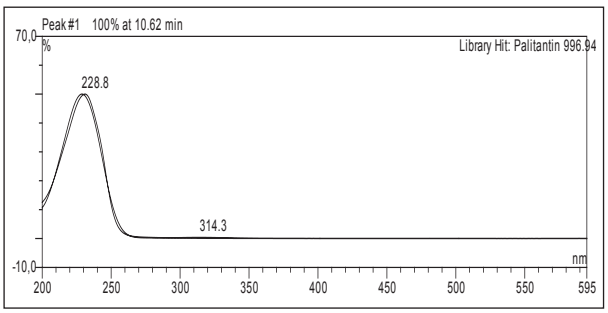

No ionisation in negative mode.

Dihydroterrein (**15**) was isolated as a yellow solid from the EtOAc extract of co-cultivation of *A. terreus* with *B. subtilis* or with *B. cereus* on solid rice medium. It displayed UV absorption $\lambda_{(max)}$ at 229 nm. The positive ESI-MS mode ionization at *m/z* 157.1 $[M + H]^+$ and 179.3 $[M + Na]^+$ suggested a molecular weight of 156 g/mol, thus revealing 2 amu increase compared to **14**. The ^{1}H NMR spectrum of **15** suggested the same 2,3-dihydroxycyclopent-4-en-1-one core structure as in **14**, with the corresponding protons at δ_H 6.00 (1H, s, H-5), 4.50 (1H, d, J = 2.5 Hz, H-3), and 4.07 (1H, d, J = 2.5 Hz, H-2). Thus, it was assumed that the double bond between C-6 and C-7 in the side chain of **14** was reduced in **15**, which is in accordance with the upfield chemical shifts at δ_H 2.51 (2H, m, H_2-6), 1.72 (1H, m, H-7) and 1.66 (1H, m, H-7), together with the signal of the terminal methyl group at δ_H 1.05 (3H, t, J = 7.3 Hz, H_3-8). The structure of **15** was further confirmed by comparison of its UV, ^{1}H NMR, and mass spectral data with those reported in the literature for dihydroterrein (Hosoe *et al*., 2009).

Table 3.2.4 ^{1}H NMR data of terrein (**14**) and dihydroterrein (**15**) (δ in ppm, J in Hz).

Position	**14** (500MHz, CD_3OD)	Terrein [PMR (D_2O)]	**15** (500MHz, CD_3OD)	Dihydroterrein[a] (400 MHz, $CDCl_3$)
2	4.67 (br. s)	5.08 (d, 2.5)	4.07 (d, 2.5)	4.25 (d, 2.8)
3	4.07 (d, 2.6)	4.50 (d, 2.5)	4.50 (d, 2.5)	4.63 (d, 1.6)
5	6.00 (s)	6.38 (s)	6.00 (s)	5.96 (s)
6	6.44 (d, 15.8)	6.71 (d, 17)	2.51 (2H, m)	2.47 (2H, m)
7	6.84 (m)	7.09 (m, 17, 6)	1.72 (m) 1.66 (m)	1.61 (2H, m)
8	1.94 (dd, 6.8, 1.6)	2.17 (d, 6)	1.05 (t, 7.3)	0.98 (t, 7.2)

[a] Hosoe *et al*., 2009

3.2.1.10 Orsellinic acid (16, known compound)

Orsellinic acid	
Biological Source	Co-cultivation of *Aspergillus terreus* and *Bacillus* sp.
Sample Code	BvW-5.8.1p2
Sample Amount	2.1 mg
Molecular Formula	$C_8H_8O_4$
Molecular Weight	168 g/mol
Solubility	MeOH
Physical Description	Yellow amorphous solid
HPLC Retention Time	17.83 min (standard gradient)

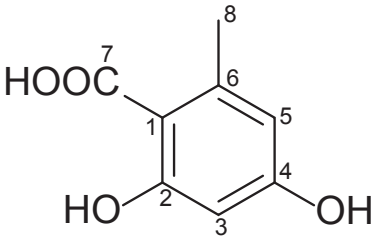

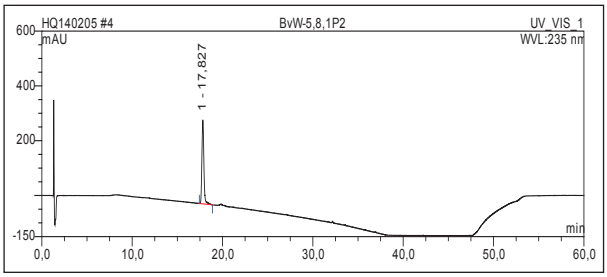

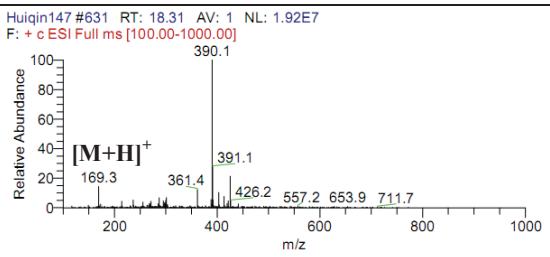

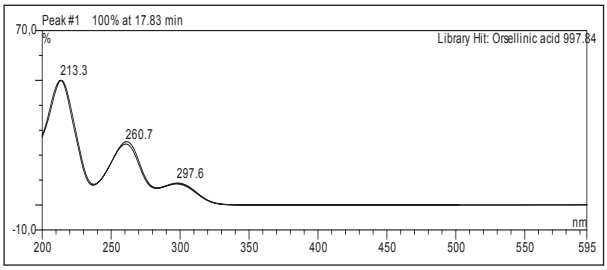

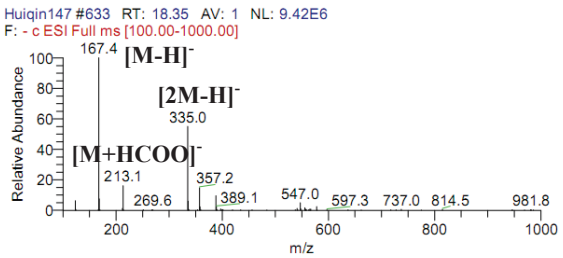

Orsellinic acid (**16**) was isolated as a yellow amorphous solid from the EtOAc extract of co-cultivation of *A. terreus* with *B. subtilis* or with *B. cereus* on solid rice medium. It showed UV absorptions at λ_{max} (MeOH) at 213, 260 and 297 nm. Positive and negative ions at *m/z* 169 $[M + H]^+$, 167.4 $[M - H]^-$, 213.1 $[M + HCOO]^-$ and 335.0 $[2M - H]^-$ indicated the molecular weight of 168 g/mol. The ^{1}H NMR spectrum revealed two *meta*-coupled peaks at δ_H 6.19 (1H, d, J = 2.0 Hz, H-5) and 6.14 (1H, d, J = 2.0 Hz, H-3), according to their coupling constants, in addition to an aromatic methyl signal at δ_H 2.52 (3H, s, H_3-8). The structure of **16** was conclusively determined by further literature comparison, and was identified as orsellinic acid (2,4-dihydroxy-6-methylbenzoic acid) based on its UV, ESI-MS and ^{1}H NMR data (Table 3.2.5) (Xu *et al*., 2014; Van Eijk, 1969).

Table 3.2.5 ^{1}H NMR data of **16** and orsellinic acid (δ in ppm, J in Hz).

Position	**16** (500MHz, CD_3OD)	Orsellinic acid[a] (60 Mc, Acetone)
3	6.14 (d, 2.0)	6.32 (m)
5	6.19 (d, 2.0)	6.32 (m)
8	2.52 (s)	2.56 (s, unsharp)
2-OH, 4-OH, 7-COOH		9.12-12.62 (s, broad and flat)

[a] Van Eijk, 1969

3.2.1.11 Terreinol (17, known compound)

Terreinol	
Biological Source	Co-cultivation of *Aspergillus terreus* and *Bacillus* sp.
Sample Code	BvW-4.8p
Sample Amount	2.0 mg
Molecular Formula	$C_{13}H_{14}O_5$
Molecular Weight	250 g/mol
Solubility	MeOH
Physical Description	Yellow amorphous solid
HPLC Retention Time	20.79 min (standard gradient)

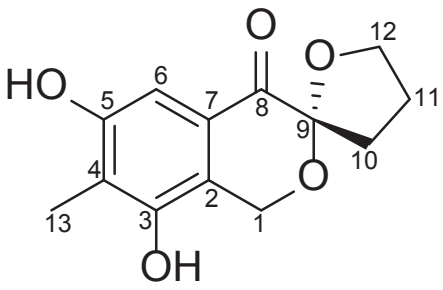

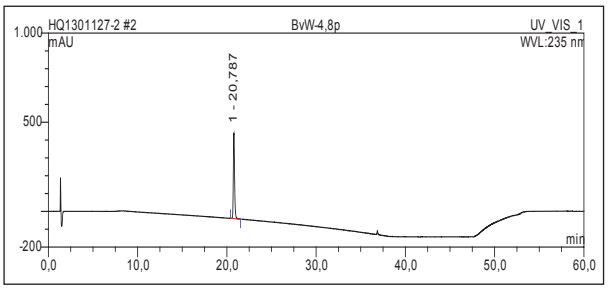

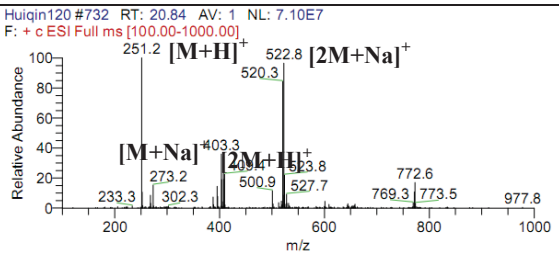

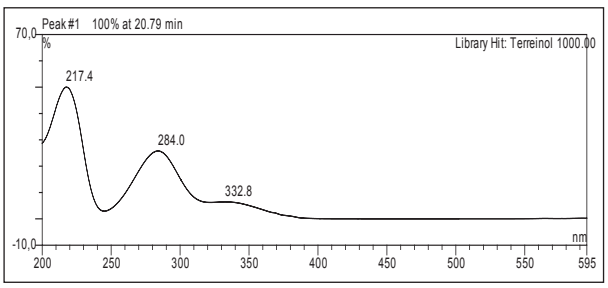

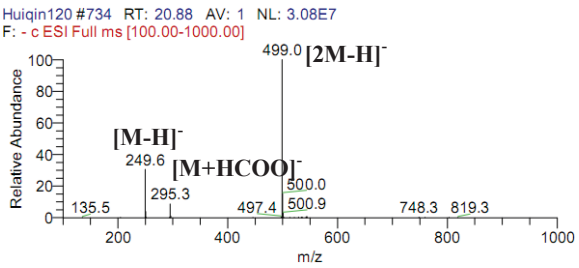

Terreinol (**17**) was isolated as a yellow amorphous solid from the EtOAc extract of co-cultivation of *A. terreus* with *B. subtilis* or with *B. cereus* on solid rice medium. It displayed UV absorptions at λ_{max} (MeOH) at 217 and 284 nm. The positive and negative ESI-MS ion peaks at *m/z* 251.2 $[M + H]^+$, 273.2 $[M + Na]^+$, 522.8 $[2M + Na]^+$, 249.6 $[M - H]^-$, 295.3 $[M + HCOO]^-$ and 499.0 $[2M - H]^-$ indicated a molecular weight of 250 g/mol. In the ^1H NMR spectrum of **17**, one singlet aromatic proton at δ_H 7.02 (1H, s, H-6) suggested the presence of a *penta*-substituted aromatic ring. Two doublets at δ_H 4.99 (1H, d, J = 15.6 Hz, H-1a) and 4.79 (1H, d, J = 15.6 Hz, H-1b) were assigned to an oxygenated methylene group, which was visualized as an AX spin system in the ^1H–^1H COSY spectrum. In addition, the COSY spectrum showed a saturated spin system composed of three methylenes at δ_H 4.13 (1H, td, J = 14.5, 7.5 Hz, H-12a), 4.03 (1H, dd, J = 14.5, 7.1 Hz, H-12b), 2.69 (1H, dt, J = 12.8, 8.8 Hz, H-10a), 2.08 (2H, overlapping, H_2-11) and 1.95 (1H, m, H-10b). The remaining signal at δ_H 2.18 (3H, s, H_3-13) was assigned to an aromatic methyl group according to its chemical shift and integration. The structure of **17** was confirmed by comparison of its UV, MS, and ^1H NMR data with published data for terreinol isolated from *A. terreus* (Table 3.2.6) (Macedo, Porto and Marsaioli, 2004).

Table 3.2.6 ^1H NMR data for terreinol **17**.

Position	**17** (CD_3OD, δ_H in ppm, J in Hz)	Terreinol (CD_3OD, δ_H in ppm, J in Hz)[a]
1	4.99 (1H, d, 15.6)	4.94 (1H, d, 15.7)
	4.79 (1H, d, 15.6)	4.73 (1H, d, 15.7)
6	7.02 (1H, s)	6.97 (1H, s)
10	2.69 (1H, dt, 12.8, 8.8)	2.64 (1H, dt, 12.6, 8.8)
	1.95 (1H, m)	1.89 (1H, ddd, 12.6, 8.2, 4.5)
11	2.08 (H_2-11, overlapping)	2.13 (1H, overlapping)
		2.04 (1H, m)
12	4.13 (1H, td, 14.5, 7.5)	4.06 (1H, m)
	4.03 (1H, dd, 14.5, 7.1)	3.97 (1H, dd, 14.6, 7.7)
13	2.18 (3H, s)	2.13 (3H, s)

[a] Macedo, Porto and Marsaioli, 2004

3.2.1.12 Terretonin A (18, known compound)

Terretonin A	
Biological Source	Co-cultivation of *Aspergillus terreus* and *Bacillus* sp.
Sample Code	W6-2.3 crystal
Sample Amount	0.78 mg
Molecular Formula	$C_{26}H_{32}O_8$
Molecular Weight	472 g/mol
Solubility	$CHCl_3$
Physical Description	White needle crystal
HPLC Retention Time	27.08 min (standard gradient)

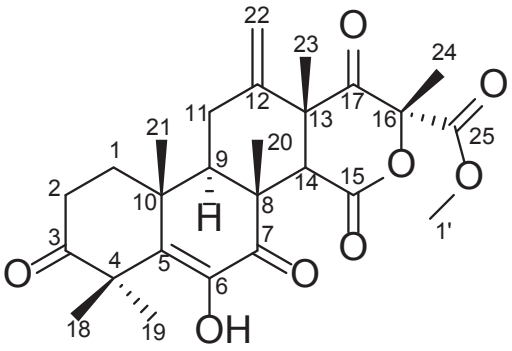

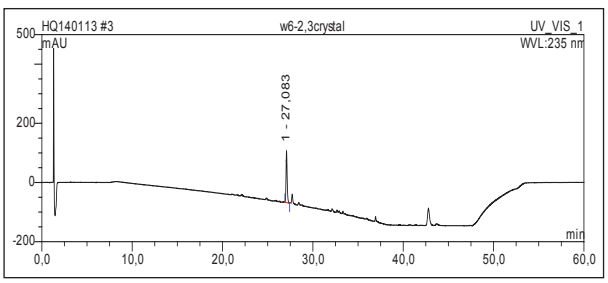

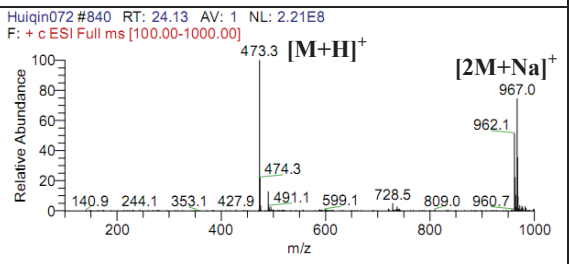

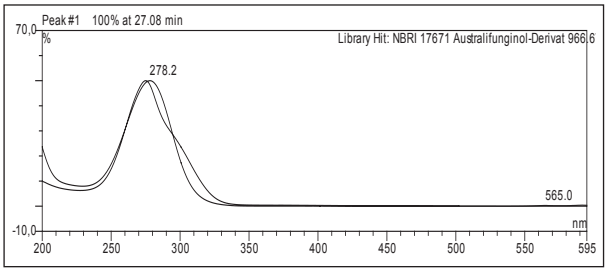

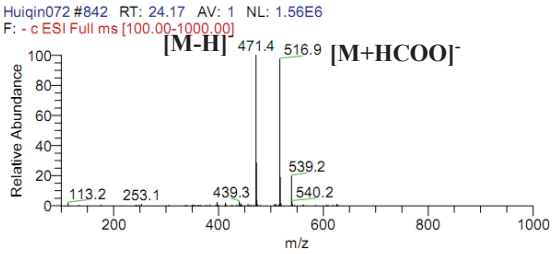

Terretonin A (**18**) was isolated as a white needle crystal from the EtOAc extract of co-cultivation of *A. terreus* with *B. subtilis* or with *B. cereus* on solid rice medium. It displayed UV absorption at λ_{max} (MeOH) 278.2 nm. The positive and negative ESI-MS ion peaks at *m/z* 473.3 $[M + H]^+$, 967.0 $[2M + Na]^+$, 471.4 $[M - H]^-$ and 516.9 $[M + HCOO]^-$ indicated a molecular weight of 472 g/mol. The ^1H NMR spectrum revealed a vinylidene moiety [δ_H 5.17 (1H, s, H-22a) and 4.98 (1H, s, H-22b)], one methoxy group [δ_H 3.82 (3H, s, OCH_3-1')] and six methyl groups [δ_H 1.83 (3H, s, H_3-20), 1.73 (3H, s, H_3-24), 1.47 (3H, s, H_3-19), 1.46 (3H, s, H_3-18), 1.43 (3H, s, H_3-23) and 1.11 (3H, s, H_3-21)]. In addition, several upfield methyl and methylene proton resonances were observed, indicating the terpenoid nature of **18**. The obtained data were identical to those reported for the known meroterpenoid terretonin A, for which the absolute stereochemistry was determined by X-ray crystallographic analysis (Li *et al*., 2005). Terretonin A is another important type of mycotoxin produced by *A. terreus*, belonging to a structurally complex class of natural products called meroterpenoid (Guo *et al*., 2012).

3.2.1.13 Terretonin (19, known compound)

Terretonin	
Biological Source	Co-cultivation of *Aspergillus terreus* and *Bacillus* sp.
Sample Code	W6-4.2 crystal, BvW-5.2 crystal
Sample Amount	24.9 mg
Molecular Formula	$C_{26}H_{32}O_9$
Molecular Weight	488 g/mol
Solubility	$CHCl_3$
Physical Description	White needle crystal
HPLC Retention Time	25.27 min (standard gradient)

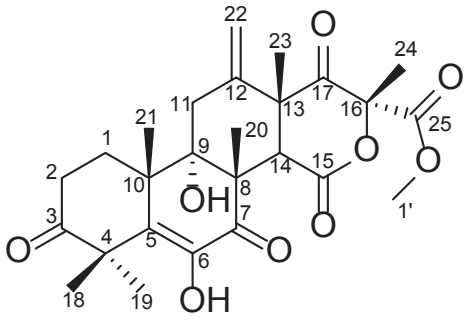

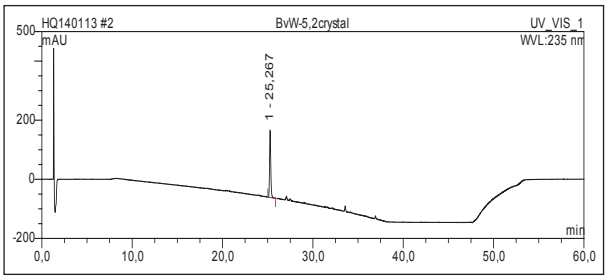

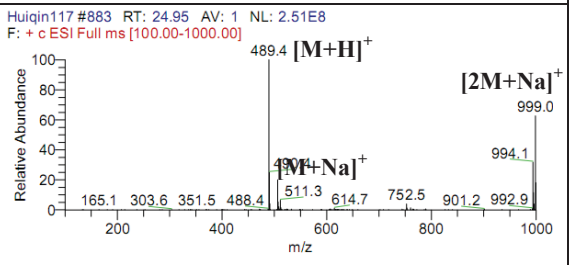

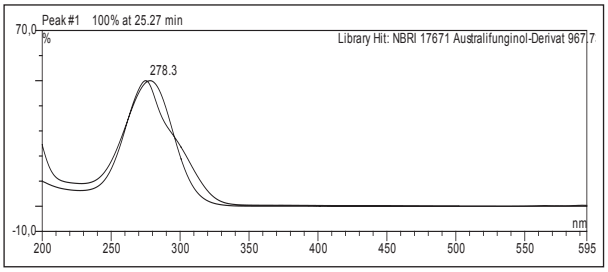

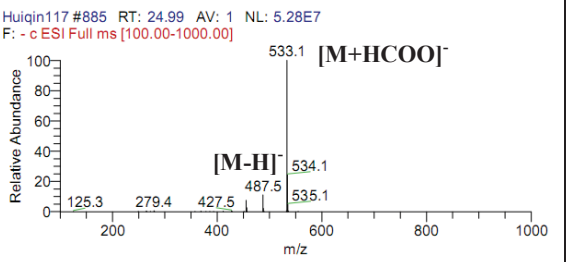

Terretonin (**19**) was isolated as white needle crystals from the EtOAc extract of co-cultivation of *A. terreus* with *B. subtilis* or with *B. cereus* on solid rice medium. It displayed UV absorption at λ_{max} (MeOH) 278.3 nm. The positive and negative ESI-MS ion peaks at *m/z* 489.4 $[M + H]^+$, 511.3 $[M + Na]^+$, 999.0 $[2M + Na]^+$, 487.5 $[M - H]^-$ and 533.1 $[M + HCOO]^-$

indicated a molecular weight of 488 g/mol, and thus 16 amu more than the molecular weight of **18**. Comparison of the ^{1}H NMR spectrum of **19** with that of **18** showed high similarity, apart from the absence of H-9, indicating the presence of a hydroxy-substitution at C-9, as supported by the molecular formula of **19**. On the basis of the foregoing evidence, along with comparison with reported data (Springer *et al*., 1979), the structure of **19** was deduced as terretonin. Terretonin has been isolated from different species of *Aspergillus* and was shown to be biosynthesized by a mixed polyketide-terpenoid pathway (McIntyre *et al*., 1989).

Table 3.2.7 ^{1}H NMR data for terretonin A, **18** and **19**.

Position	Terretonin A[a] ($CDCl_3$, 600MHz δ_H in ppm, *J* in Hz)	**18** ($CDCl_3$, 500 MHz δ_H in ppm, *J* in Hz)	**19** ($CDCl_3$, 500 MHz δ_H in ppm, *J* in Hz)
1	2.19 (1H, dd, 13.6, 9.1)	2.18 (1H, dd, 13.6, 8.7)	2.23 (1H, dd, 12.2)
	1.72 (1H, dd, 13.8, 10.6)	1.70 (1H, overlapping)	1.76 (1H, dd, 13.6, 8.4)
2	2.70 (1H, dd, 13.8, 9.0)	2.69 (1H, dd, 19.1, 8.8)	2.71 (1H, dd, 19.1, 8.8)
	2.56 (1H, dd, 14.1, 10.6)	2.54 (1H, overlapping)	2.52 (1H, m)
9	1.55 (1H, dd, 12.8, 2.4)	1.54 (1H, dd, 12.8, 2.6)	
11	2.51 (1H, dd, 13.8, 12.8)	2.51 (1H, overlapping)	2.96 (1H, d, 14.3)
	2.34 (1H, dd, 13.8, 2.4)	2.33 (1H, dd, 13.7, 2.6)	2.26 (1H, d, 14.3)
14	2.84 (1H, s)	2.84 (1H, s)	3.54 (1H, s)
18	1.47 (3H, s)	1.46 (3H, s)	1.47 (3H, s)
19	1.48 (3H, s)	1.47 (3H, s)	1.47 (3H, s)
20	1.85 (3H, s)	1.83 (3H, s)	1.92 (3H, s)
21	1.12 (3H, s)	1.11 (3H, s)	1.21 (3H, s)
22	5.17 (1H, br. s)	5.17 (1H, br. s)	5.46 (1H, br. s)
	5.00 (1H, br. s)	4.98 (1H, br. s)	5.08 (1H, br. s)
23	1.45 (3H, s)	1.43 (3H, s)	1.44 (3H, s)
24	1.75 (3H, s)	1.73 (3H, s)	1.71 (3H, s)
1'	3.84 (3H, s)	3.82 (3H, s)	3.79 (3H, s)

[a] Li *et al*., 2005

3.2.1.14 Aspulvinone E (20, known compound)

	Aspulvinone E
Biological Source	Co-cultivation of *Aspergillus terreus* and *Bacillus* sp.
Sample Code	BvW-5.8.3
Sample Amount	1.9 mg
Molecular Formula	$C_{17}H_{12}O_5$
Molecular Weight	296 g/mol
Solubility	MeOH
Physical Description	Yellow amorphous solid
HPLC Retention Time	23.18 min (standard gradient)

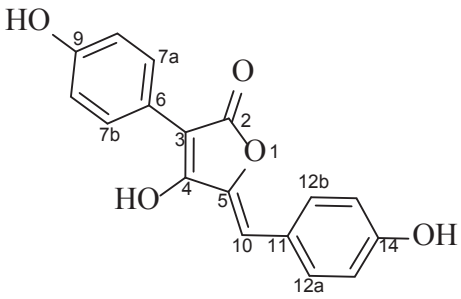

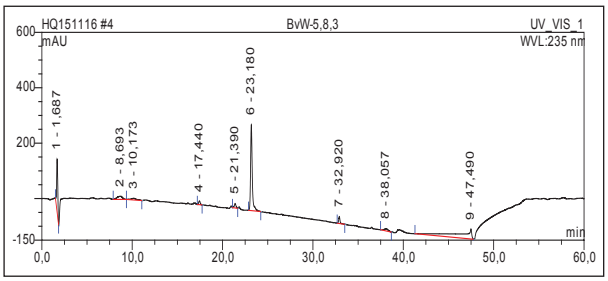

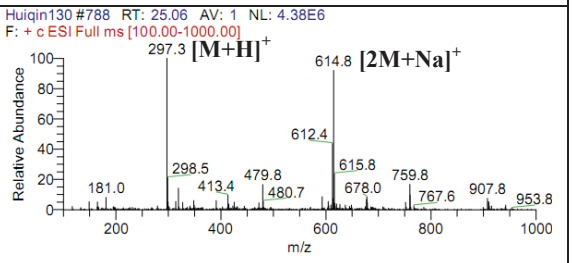

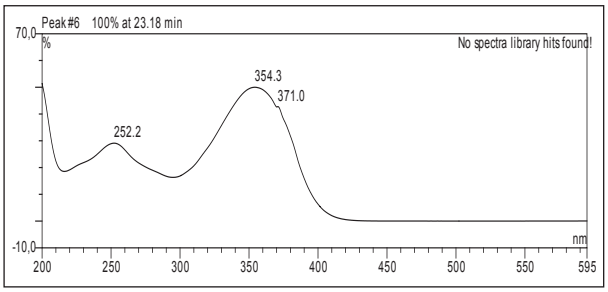

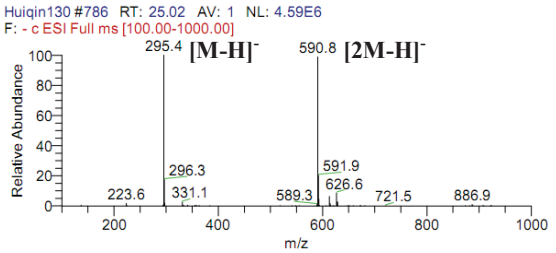

Aspulvinone E (**20**) was isolated as a yellow solid from the EtOAc extract of co-cultivation of *A. terreus* with *B. subtilis* or with *B. cereus* on solid rice medium. It displayed UV absorption at λ_{max} (MeOH) 362 nm. The positive and negative ESI-MS ion peaks at *m/z* 297.3 $[M + H]^+$, 614.8 $[2M + Na]^+$, 295.4 $[M - H]^-$ and 590.8 $[2M - H]^-$ indicated a molecular weight of 296 g/mol. The ^1H NMR spectrum exhibited only five aromatic protons, including two *para*-substituent aromatic systems [δ_H 7.59 (2H, d, J = 8.7 Hz, H-7a/7b), 7.40 (2H, d, J = 8.7 Hz, H-12a/12b), 6.92 (2H, d, J = 8.7 Hz, H-13a/13b), 6.78 (2H, d, J = 8.7 Hz, H-8a/8b)] and one singlet olefinic proton [δ_H 5.94 (1H, s, H-10)]. The remaining resonances were attributed to a trisubstituted five-membered lactone ring (Table 3.2.8). The identification of **20** was further confirmed by comparison of its UV, ^1H NMR, MS, and $[\alpha]_D$ data with those reported for aspulvinone E (Gao *et al*., 2013), which was previously reported from *Aspergillus* species. Aspulvinone A, possessing a butenolide moiety substituted by a phenyl group at C-3 and a benzyl group at C-5, is produced as a pigment by *Aspergillus* fungi. So far, more than 40 natural congeners have been reported, displaying *Z*-configuration for the exocyclic double bond, apart from isoaspulvinone *E* exhibiting *E*-configuration (Gao *et al*., 2013). It was shown that these two compounds were stable in the dark, while they were converted into each other in the presence of light, indicating that they are photointerconvertible (Gao *et al*., 2013).

Table 3.2.8 ^1H NMR data for **20**, aspulvinone E and isoaspulvinone E.

Position	**20** (CD_3OD, 500 MHz δ_H in ppm, J in Hz)	Aspulvinone E[b] (DMSO-*d*, 600 MHz, δ_H in ppm, J in Hz)	Isoaspulvinone E[b] (DMSO-*d*, 600 MHz, δ_H in ppm, J in Hz)
7a/7b	7.59 (2H, d, 8.7)	7.80 (2H, d, 7.7)	7.47 (2H, d, 7.7)
8a/8b	6.78 (2H, d, 8.7)[a]	6.82 (2H, d, 7.7)	6.80 (2H, d, 7.7)
10	5.94 (1H, s)	6.58 (1H, s)	6.64 (1H, s)
12a/12b	7.40 (2H, d, 8.7)	7.58 (2H, d, 7.7)	7.63 (2H, d, 7.7)
13a/13b	6.92 (2H, d, 8.7)[a]	6.86 (2H, d, 7.7)	6.75 (2H, d, 7.7)

[a] signals can be interchanged

[b] Gao *et al*., 2013

3.2.1.15 3-Hydroxy-5-(4-hydroxybenzyl)-4-(4-hydroxyphenyl)furan-2(5*H*)-one (21, known compound)

3-Hydroxy-5-(4-hydroxybenzyl)-4-(4-hydroxyphenyl)furan-2(5*H*)-one	
Biological Source	Co-cultivation of *Aspergillus terreus* and *Bacillus* sp.
Sample Code	BvW-5.8.1P3
Sample Amount	1.6 mg
Molecular Formula	$C_{17}H_{14}O_5$
Molecular Weight	298 g/mol
Solubility	MeOH
Physical Description	Gray amorphous solid
HPLC Retention Time	21.15 min (standard gradient)

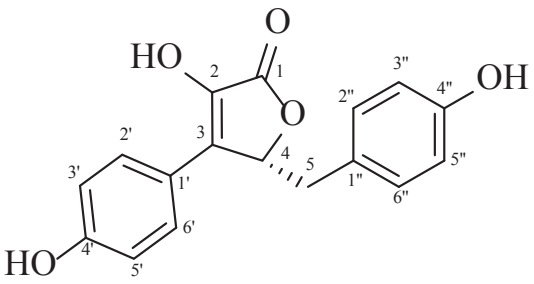

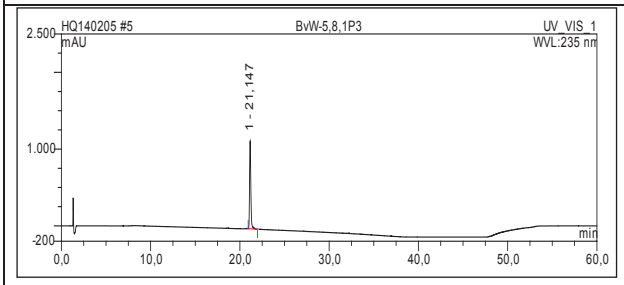

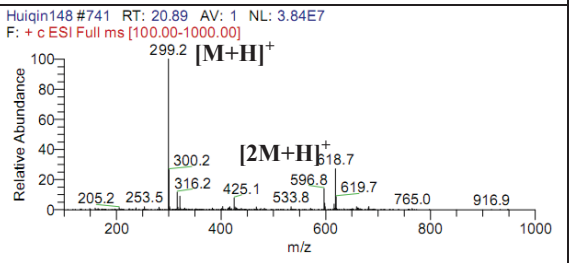

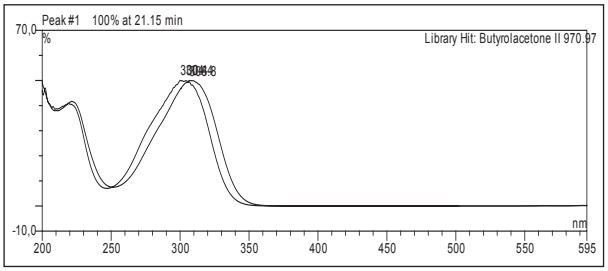

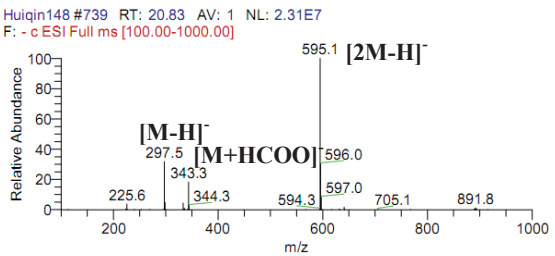

3-Hydroxy-5-(4-hydroxybenzyl)-4-(4-hydroxyphenyl)furan-2(5*H*)-one (**21**) was isolated as a gray amorphous solid from the EtOAc extract of co-cultivation of *A. terreus* with *B. subtilis* or with *B. cereus* on solid rice medium. The UV spectrum showed high similarity to those of butyrolactones with λ_{max} (MeOH) at 308 nm. The positive and negative ESI-MS ion peaks at *m/z* 299.2 $[M + H]^+$, 596.8 $[2M + H]^+$, 297.5 $[M - H]^-$, 343.3 $[M + HCOO]^-$ and 595.1 $[2M - H]^-$ suggested its molecular weight as 298 g/mol, indicating a 16 amu decrease in comparison with **8**. In the ^{1}H NMR spectrum of **21**, two AA'BB' aromatic systems were observed [δ_H 7.62 (2H, d, *J* = 8.8 Hz, H-3'/5'), 6.93 (2H, d, *J* = 8.8 Hz, H-2'/6'), 6.82 (2H, d, *J* = 8.5 Hz, H-2"/6"), and 6.63 (2H, d, *J* = 8.5 Hz, H-3"/5")]. The remaining signals were assigned to a methine proton at δ_H 5.62 (1H, dd, *J* = 5.5, 3.5 Hz, H-4) and two methylene protons at 3.28 (1H, dd, *J* = 14.6, 3.5 Hz, H-5a) and 2.91 (1H, dd, *J* = 14.6, 5.5 Hz, H-5b). By comparison of the UV, ^{1}H NMR, MS, and $[\alpha]_D$ data with data published in the literature, the structure of **21** was deduced as 3-hydroxy-5-(4-hydroxybenzyl)-4-(4-hydroxyphenyl)furan-2(5*H*)-one (Cotelle *et al*., 2003), previously reported from *A. terreus*.

Table 3.2.9 ^{1}H NMR data for **21** and 3-hydroxy-5-(4-hydroxybenzyl)-4-(4-hydroxyphenyl)furan-2(5*H*)-one.

Position	**21** (CD_3OD, 500 MHz δ_H in ppm, *J* in Hz)	literature[a] (Acetone-d_6, 200 MHz, δ_H in ppm, *J* in Hz)
4	5.62 (dd, 5.5, 3.5)	5.59(dd, 6.0, 3.3)
5	3.28 (dd, 14.6, 3.5)	3.27 (dd, 14.5, 3.3)
	2.91 (dd, 14.6, 5.5)	2.84 (dd, 14.5, 6.0)
2'/6'	6.93 (d, 8.8)	6.98 (d, 8.8)
3'/5'	7.62 (d, 8.8)	7.61 (d, 8.8)
2"/6"	6.82 (d, 8.5)	6.87 (d, 8.5)
3"/5"	6.63 (d, 8.5)	6.66 (d, 8.5)

[a] Cotelle *et al*., 2003

3.2.1.16 Results from co-cultivation experiments

In this study, we reported the metabolic response of the soil derived fungus *A. terreus* during co-cultivation with *B. subtilis*, *B. cereus*, *S. coelicolor* or with *S. lividans*. The strain of *A. terreus* is well known for the production of butyrolactones (Nuclear *et al*., 2010). When *A. terreus* was cultured axenically on solid rice medium, average yields of the main butyrolactone derivatives per culture flask were 0.57 mg for butyrolactone II (**10**), 117.1 mg for butyrolactone I (**11**), 19.6 mg for butyrolactone III (**12**), and 0.86 mg for butyrolactone VI (**13**). During co-cultivation of *A. terreus* with *B. subtilis*, with autoclaved *B. subtilis* or with *B. cereus* a strong enhancement of butyrolactone accumulation was observed (Table 3.2.1.9). During co-cultivation with *B. subtilis*, the average production of butyrolactones per flask reached 1.94 mg for butyrolactone II (**10**), 290.3 mg for butyrolactone I (**11**), 56.87 mg for butyrolactone III (**12**), and 2.04 mg for butyrolactone VI (**13**), which accounted for a 2.5-3.0 fold increase of the latter metabolites compared to axenic fungal controls (Table 3.2.10). Interestingly, when *A. terreus* was co-cultivated with autoclaved *B. subtilis*, a similar induction of butyrolactone accumulation was observed, which resulted in an average production per flask of 2.16 mg for butyrolactone II (**10**), 390.6 mg for butyrolactone I (**11**), 30.6 mg for butyrolactone III (**12**), and 1.39 mg for butyrolactone VI (**13**) (1.5-3.3 fold increase). These data indicate that even heat sterilized bacterial biomass and culture media cause an induction of fungal natural products accumulation similar to adding live bacterial cultures. Co-culturing of *A. terreus* with *B. cereus* resulted in a similar induction of butyrolactone accumulation as observed before, accounting for a 1.8-3.3 fold increase compared to controls, which is in accordance with the aforementioned data (Table 3.2.10). (Chen *et al*., 2015b)

A similar trend was observed with regard to the induction of orsellinic acid (**16**) and terrein (**14**) during co-cultivation of *A. terreus* with *B. subtilis* or with *B. cereus*. The latter compound, which is a typical constituent of *A. terreus*, was strongly enhanced during co-cultivation, leading to an up to 34-fold increase during co-cultivation of *A. terreus* with *B. subtilis*, with autoclaved *B. subtilis* or with *B. cereus*, respectively. However, no clear induction was detected for dihydroterrein (**15**) compared to the fungal controls, indicating that the effects of

co-culturing are not uniform for all fungal compounds. (Chen *et al*., 2015b)

In addition to the increase of constitutively present metabolites, two new compounds isobutyrolactone II (**7**) and 4-O-demethylisobutyrolactone II (**8**) that were only observed in co-cultures of *A. terreus* with *B. subtilis*, with autoclaved *B. subtilis* or with *B. cereus*, as well as the known N-(carboxymethyl)anthranilic acid (**9**) that was only detected when co-culturing *A. terreus* with *B. subtilis,* were isolated. (Figure 3.2.4) (Chen *et al*., 2015b)

Table 3.2.10 Yield of induced metabolites per flask during co-culture of *A. terreus* and *Bacillus* sp. (n = 4) vs axenic controls of *A. terreus* (n = 4). (Chen *et al*., 2015b)

compound	Control[a] (mg)	*A. terreus* vs. *B. subtilis* (mg)	Increase (fold)	*A. terreus* vs. autoclaved *B. subtilis* (mg)	Increase (fold)	*A. terreus* vs. *B. cereus* (mg)	increase (fold)
7	n.d.[b]	2.33 ± 0.35		2.89 ± 0.47		3.01± 0.42	
8	n.d.	1.57 ± 1.79		2.15 ± 1.18		1.45± 0.98	
9	n.d.	1.61 ± 0.00011		n.d.		n.d.	
10	0.65 ± 0.05	1.94 ± 0.001	3.0	2.16 ± 0.009	3.3	2.13±0.07	3.3
11	117.1 ± 0.27	290.3 ± 6.68	2.5	390.6 ± 6.68	3.3	439.4 ± 37.1	3.7
12	19.59 ± 2.81	56.87 ± 4.35	2.9	30.64 ± 2.27	1.5	44.13 ± 2.36	2.3
13	0.86 ± 0.24	2.04 ± 0.31	2.4	1.39 ± 0.20	1.6	1.57± 0.38	1.8
14	11.7 ± 6.66	380.4 ± 72.2	32.5	184.5 ± 31.1	15.7	397.5 ± 185.9	33.9
15	0.28 ± 0.31	0.33 ± 0.35	1.2	n.d.		0.27 ± 0.29	1.0
16	0.36 ± 0.23	1.68 ± 0.29	4.8	0.97 ± 0.09	2.7	0.99 ± 0.18	2.8

[a] *A. terreus* axenic control, [b] not detected

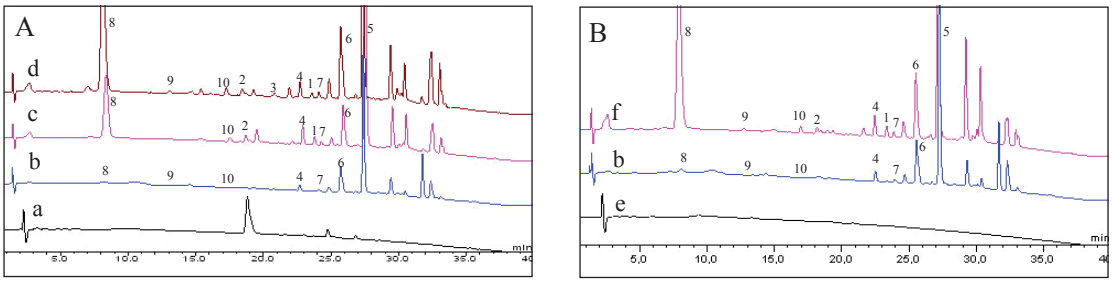

Figure 3.2.4 HPLC chromatograms of EtOAc extracts from co-culture experiments (detection at UV 235 nm): A) (a) *B. subtilis* control, (b) *A. terreus* control, (c) co-culture of *A. terreus* with autoclaved *B. subtilis*, (d) co-culture of *A. terreus* with viable *B. subtilis*; B) (b) *A. terreus* control, (e) *B. cereus* control, (f) co-culture of *A. terreus* with *B. cereus*. (Chen *et al*., 2015b)

When *A. terreus* was co-cultured with autoclaved *B. subtilis*, two different procedures were carried out. The first procedure was culture the bacteria on rice for four days first, then followed by autoclaving and adding *A. terreus* grown on malt agar to the rice medium which contained dead bacteria. The second procedure was by adding a 20 mL volume of autoclaved bacteria and prepared fungus to the rice medium at the same time. Interestingly, only the first procedure showed a clear effect on the induction of secondary metabolite production. (Figure 3.2.5)

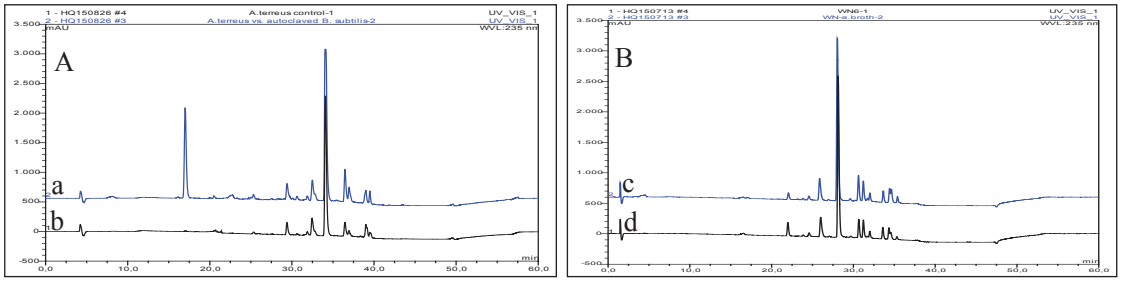

Figure 3.2.5 HPLC chromatograms of EtOAc extracts from co-culture with autoclaved *B. subtilis* experiments (detection at UV 235 nm): A) (c) co-culture of *A. terreus* with autoclaved *B. subtilis* with four days growing on rice, (b) *A. terreus* control; B) (c) co-culture of *A. terreus* with autoclaved *B. subtilis* broth, (d) *A. terreus* control.

In a second set of experiments, *A. terreus* was co-cultured with *S. lividans* or with *S. coelicolor*. These actinomycetes occur both in soil and in plants (Meschke *et al*., 2012; Adegboye *et al*., 2012; Mellado, 2011; Burkholder and Giles, 1947). In contrast to the results obtained during co-cultivation of *A. terreus* with *B. subtilis* or with *B. cereus*, no induction of fungal metabolites was observed during the co-cultures with both *Streptomyces* species (Figure 3.2.6), indicating that the response of *A. terreus* toward different bacteria may be a specific rather than a general reaction towards prokaryotes, which is in accordance with our previously reported results (Chen *et al*., 2015b; Ola *et al*., 2013).

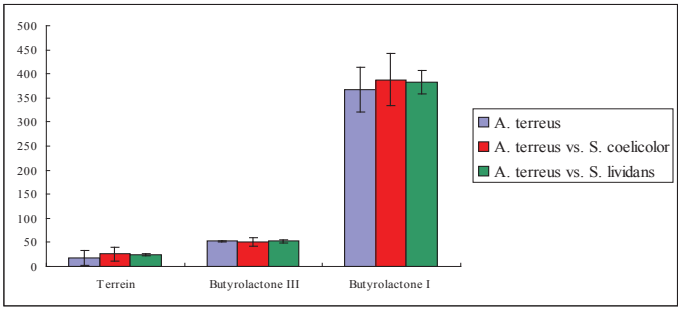

Figure 3.2.6 Yield of three main compounds produced by *A. terreus* during co-cultivation

All isolated compounds were tested for their antibacterial activities against *B. subtilis* and *B. cereus*, but only **11** and **20** showed weak inhibition of *B. cereus*, with MICs of 64 μg/mL. The isolated compounds were further examined for their effects on the growth of the L5178Y mouse lymphoma cell line employing the MTT assay. Terrein (**14**) showed moderate cytotoxicity with 80% inhibition of the respective cell line at a dose of 10 μg/mL. The remaining compounds exhibited no activity. Interestingly, the biosynthesis of **14** was most strongly induced among all the isolated compounds, which highlights the value of the co-cultivation approach as an effective strategy to access bioactive secondary metabolites from microorganisms. (Chen *et al*., 2015b)

3.2.2 Inducing secondary metabolite production by medium engineering

In order to study the effect of culture media on the induction of secondary metabolites from fungi, rice, liquid Wickerham medium and white beans were used for cultivation of *A. terreus*. Interestingly, HPLC analysis showed distinct chromatograms. From the liquid Wickerham medium culture, apart from four compounds likewise detected in the rice medium (butyrolactone I, butyrolactone II, butyrolactone VI and terrein), another seven compounds **22** – **28** were isolated, which were not observed in the rice medium culture. Among these compounds, **22** and **23** were stereoisomers as determined by their CD spectra, whereas **24** was a racemic mixture according to chiral HPLC analysis. From the bean culture, butyrolatone I, II, III, together with **29** and **30** were isolated.

3.2.2.1 (2*R*, 1'*S*)-Dihydroisoflavipucine (22, known compound)

(2*R*, 1'*S*)-Dihydroisoflavipucine	
Biological Source	*Aspergillus terreus*
Sample Code	WN6-L-1.10P3, WN6-L-1.9P3
Sample Amount	5.4 mg
Molecular Formula	$C_{12}H_{17}NO_4$
Molecular Weight	239 g/mol
Solubility	MeOH
Physical Description	White needle-like crystals
Optical rotation	-95.8 (*c* 0.1, MeOH)
HPLC Retention Time	19.84 min (standard gradient)

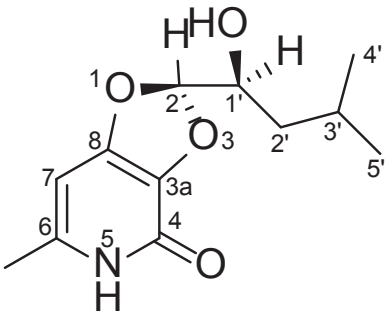

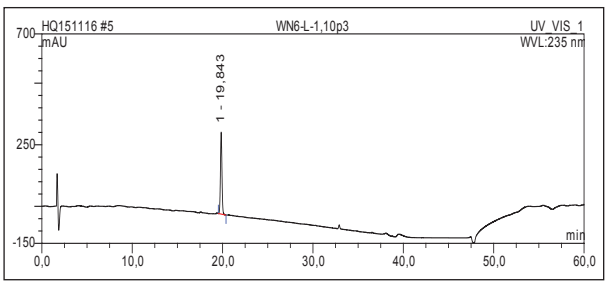

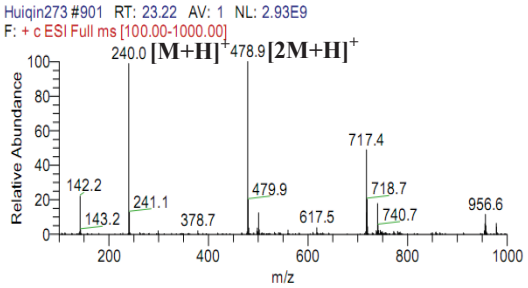

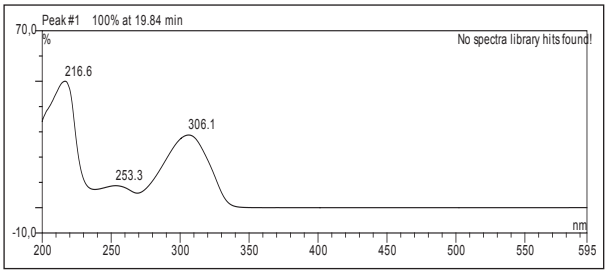

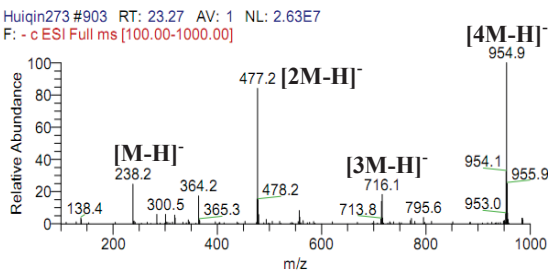

(2*R*, 1'*S*)-Dihydroisoflavipucine (**22**) was isolated as white needle-like crystals from the liquid Wickerham medium culture of *A. terreus*. It displayed UV absorptions at λ_{max} (MeOH) 219 and 301 nm. The positive and negative ESI-MS ion peaks at *m/z* 240.0 $[M + H]^+$, 478.9 $[2M + H]^+$, 238.2 $[M - H]^-$, 477.2 $[2M - H]^-$, 716.1 $[3M - H]^-$ and 954.9 $[4M - H]^-$ indicated a molecular weight of 239 g/mol, containing an odd number of nitrogen atoms in the structure. The ^{1}H NMR spectrum showed three methyl groups, including one aromatic methyl at δ_H 2.27 (3H, d, J = 0.75 Hz, H_3-6-CH_3) and two aliphatic methyl signals at δ_H 0.98 (3H, d, J = 6.7 Hz, H_3-4') and 0.94 (3H, d, J = 6.6 Hz, H_3-5'). The remaining signals in the ^{1}H NMR spectrum were assigned to one olefinic proton at δ_H 6.12 (1H, d, J = 0.75 Hz, H-7), three methines and one methylene group. The ^{13}C NMR spectrum exhibited three methyl carbons at 18.8 (C-6-CH_3), 24.0 (C-5') and 21.8 (C-4'). In addition, C-1' was suggested to be oxygenated, according to the downfield chemical shift at δ_C 70.5 (C-1'). In the HMBC spectrum of **22**, the correlations (Figure 3.2.7) from H-7 to C-3a (δ_C 132.7), C-6, C-6-CH_3 and C-8 (δ_C 157.9), as well as from H_3-6-CH_3 to C-7 (δ_C 95.0) and C-6 (δ_C 143.5), indicated a methylated 2-pyridone moiety. In addition, the correlations from H-2 [δ_H 6.06 (1H, d, J = 3.0 Hz)] to C-3a and C-8, together with the chemical shift of C-2 (δ_C 115.8), suggested a dioxygenated heterocyclic core. The remaining dihydro-isopentenyl moiety was connected to C-2 based on the HMBC correlations from H-1' to C-2' (δ_C 40.4) and C-3' (δ_C 25.2), from H_3-4' to C-2', C-3' and C-5', and from H_3-5' to C-2' (Figure 3.2.7). The identification of **22** was further confirmed by comparison of its UV, ^{1}H NMR, MS, and $[\alpha]_D$ data with those reported for dihydroisoflavipucine, for which the absolute configuration (2*R*, 1'*S*) was determined by CD calculations and X-ray crystallization analysis (Loesgen *et al*., 2011).

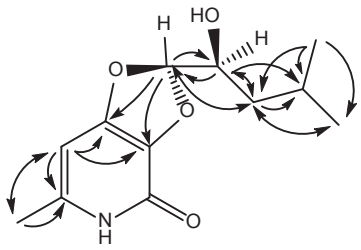

Figure 3.2.7 HMBC correlations of **22**.

3.2.2.2 (2*S*, 1'*S*)-Dihydroisoflavipucine (23, new compound)

(2*S*, 1'*S*)-Dihydroisoflavipucine	
Biological Source	*Aspergillus terreus*
Sample Code	WN6-L-1.10P2, WN6-L-1.9P2
Sample Amount	2.7 mg
Molecular Formula	$C_{12}H_{17}NO_4$
Molecular Weight	239 g/mol
Solubility	MeOH
Physical Description	White needle-like crystals
Optical rotation	+ 17 (*c* 0.1, MeOH)
HPLC Retention Time	19.6 min (standard gradient)

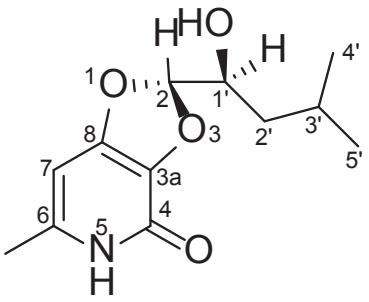

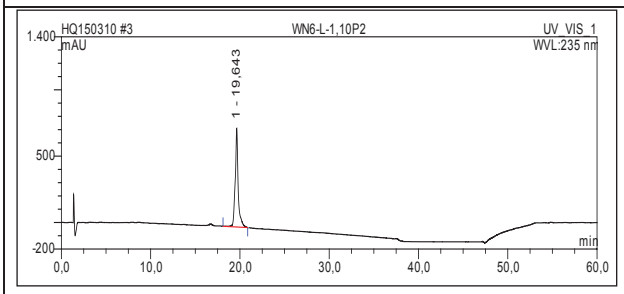

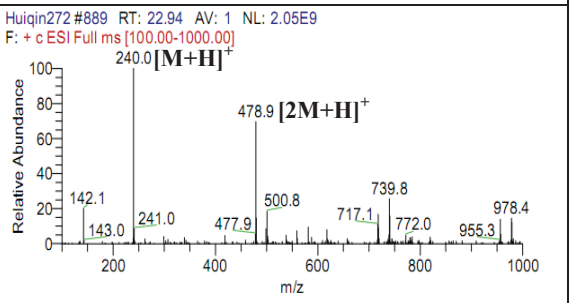

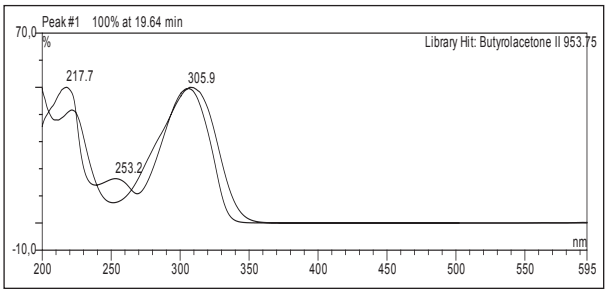

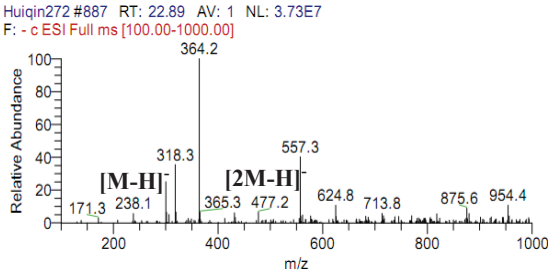

(2*S*, 1'*S*)-Dihydroisoflavipucine (**23**) was isolated as white needle-like crystals from the liquid Wickerham medium culture of *A. terreus*. It exhibited UV absorptions at λ_{max} (MeOH) 218, 253, and 306 nm, showing high similarity to the UV spectrum of **22**. The molecular formula was determined as $C_{12}H_{17}NO_4$ on the basis of the pseudomolecular ion peak at *m/z* 452.2795 $[M + H]^+$ observed in the HRESIMS spectrum. Due to the high similarity of the ^1H, ^{13}C, and HMBC NMR data of **23** to those of **22** (Table 3.2.11, Figure 3.2.8), the planar structure of **23** was deduced to be identical to that of **22**. However, **23** was assumed to be a stereoisomer of **22**, due to the different retention times observed from Dionex HPLC analysis and their opposite optical rotations. Extensive analysis of the CD spectra of compounds **22** and **23** (Figure 3.2.9) further suggested that both compounds are diastereomers differing at the configuration of the chiral center at C-2. Thus, the structure of **23** was identified as (2*S*, 1'*S*)-dihydroisoflavipucine.

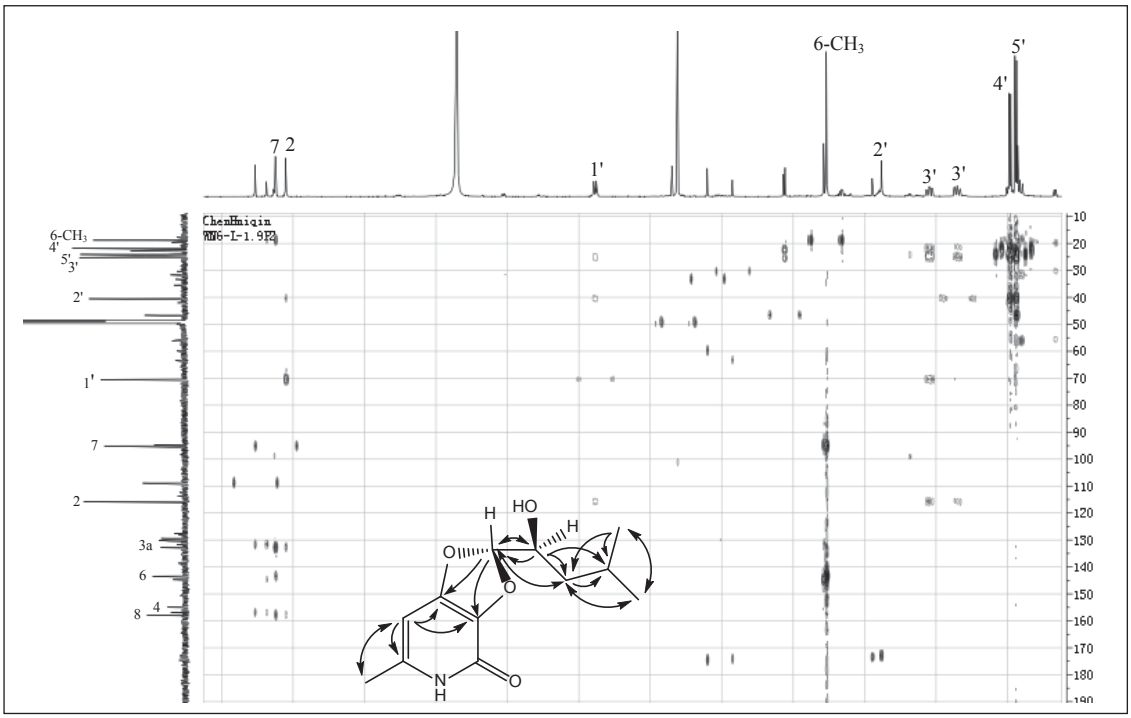

Figure 3.2.8 HMBC correlations of **23**.

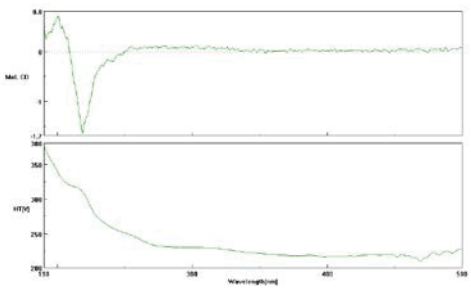

22: Cell: cm, Conc.: 9.17*10^{-4}, Solv.: AcN

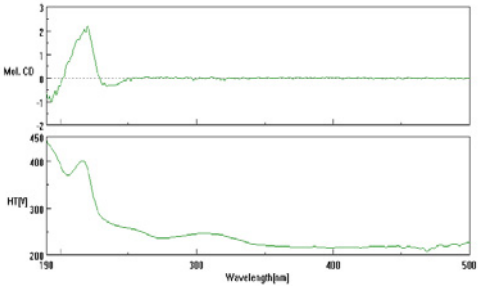

23: Cell: mm, Conc.: 9.19*10^{-4}, Solv.: AcN

Figure 3.2.9 CD spectra of **22** and **23**.

Table 3.2.11 ^{1}H and ^{13}C NMR data of **22** and **23** (δ in ppm, J in Hz).

Position	literature[a]		**22**		**23**	
	^{1}H NMR[b]	^{13}C NMR[c]	^{1}H NMR[d]	^{13}C NMR[e]	^{1}H NMR[d]	^{13}C NMR[e]
2	6.00 (d, 3.5)	114.1	6.06 (d, 3.0)	115.8	6.05 (d, 3.0)	115.8
3a		130.7		132.7		132.8
4		156.5		155.0		155.0
6		142.7		143.5		143.4
6-CH_3	2.36 (s)	19.3	2.27 (d, 0.75)	18.8	2.27 (d, 0.4)	18.8
7	5.69 (s)	94.2	6.12 (d, 0.75)	95.0	6.12 (d, 0.6)	95.1
8		153.9		157.9		157.9
1'	3.92 (ddd, 10.0, 4.0, 4.0)	69.8	3.88 (dt, 10.4, 3.0)	70.5	3.89 (dt, 10.5, 3.0)	70.5
2'	1.57 (ddd, 10.0, 4.0, 4.0)	39.6	1.57 (ddd, 14.0, 10.5, 4.6)	40.4	1.55 (ddd, 14.0, 10.5, 4.6)	40.5
	1.37 (ddd, 10.0, 4.0, 4.0)		1.34 (ddd, 13.9, 9.5, 3.1)		1.35 (ddd, 13.8, 9.5, 3.1)	
3'	1.88 (m)	24.0	1.89 (m)	25.2	1.89 (m)	25.2
4'	0.91 (d, 6.5)		0.98 (d, 6.7)	21.8	0.98 (d, 6.7)	21.8
5'	0.95 (d, 6.5)		0.94 (d, 6.6)	24.0	0.94 (d, 6.6)	24.0

[a] Loesgen *et al*., 2011; [b] in $CDCl_3$, at 600 MHz; [c] in $CDCl_3$, at 150.8 MHz

[d] in CD_3OD, at 600 MHz; [e] in CD_3OD, at 150 MHz

3.2.2.3 WN6-L-1.9P4 (24, known compound)

Biological Source	*Aspergillus terreus*
Sample Code	WN6-L-1.9P4, WN6-L-1.10P4
Sample Amount	1.4 mg
Molecular Formula	$C_{13}H_{19}NO_5$
Molecular Weight	269 g/mol
Solubility	MeOH
Physical Description	Yellow powder
HPLC Retention Time	20.69 min (standard gradient)

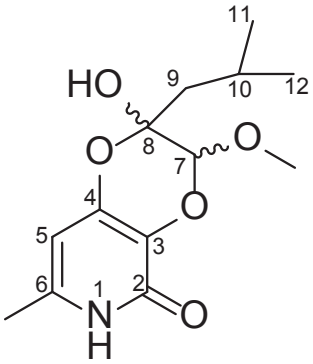

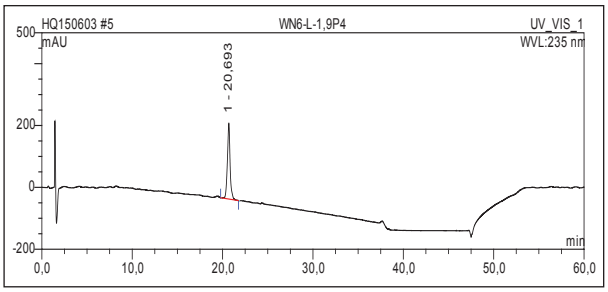

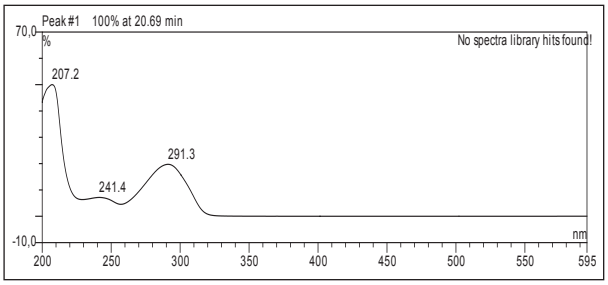

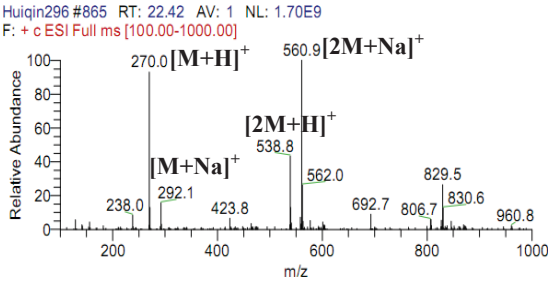

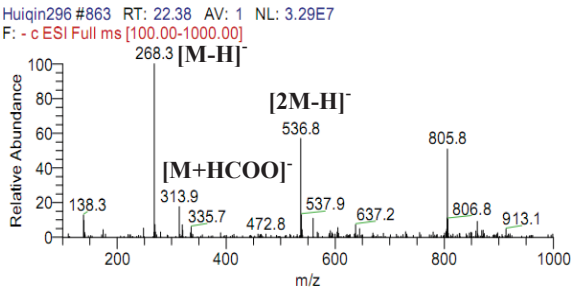

WN6-L-1.9P4 (**24**) was isolated as a yellow powder from the liquid Wickerham medium culture of *A. terreus*. It displayed UV absorptions at λ_{max} (MeOH) 207 and 291 nm. Positive and negative ESI-MS ion peaks at *m/z* 270.0 $[M + H]^+$, 292.1 $[M + Na]^+$, 538.8 $[2M + H]^+$, 560.9 $[M + Na]^+$, 268.3 $[M - H]^-$, 313.9 $[M + HCOO]^-$ and 536.8 $[2M - H]^-$ indicated a molecular weight of 269 g/mol. The ^{1}H NMR spectrum presented one methoxy group at δ_H 3.45 (3H, s, H_3-7-OCH_3), three methyl groups, including one methyl group located at C-6 of the 2-pyridone moiety [δ_H 2.20 (3H, d, J = 0.73 Hz, H_3-6-CH_3)], and another two methyl groups at δ_H 1.05 (3H, d, J = 6.6 Hz, H_3-11) and 0.98 (3H, d, J = 6.6 Hz, H_3-12). The latter were connected to the highly oxygenated carbon C-8 (δ_C 96.9) based on the coupling constants and the HMBC correlations from H_3-11 to C-12 (δ_C 23.4) and C-9 (δ_C 44.1), from H_3-12 to C-11 (δ_C 22.6) and C-9, and from H_2-9 to C-8, C-11 and C-12. The remaining singlet signal at δ_H 5.85 (s, H-5) was located at C-5 of the 2-pyridone moiety, as supported by the HMBC correlations from H-5 to C-3 (δ_C 149.2), C-4 (δ_C 124.0), C-6 (δ_C 137.3) and C-6-CH_3 (δ_C 16.9), and from H_3-6 to C-5 (δ_C 99.8) (Figure 3.2.8). The structure was confirmed by comparison of the UV, ^{1}H NMR and mass spectral data with the literature, in which **24** was reported as an intermediate during the synthesis of flavipucine (Girotra, Patchett and Wendler, 1977). In this study, it can't be excluded that this compound was an artifact due to the methanol and trifuoroacetic acid used during the isolation. In addition, **24** was isolated as a mixture of isomers differing at the stereogenic centers C-7 and C-8, as supported by the ^{1}H NMR spectrum [H-7 (δ_H 4.96/4.90), H_3-7-OCH_3 (δ_H 3.52/3.45), H-10 (δ_H 1.96/2.04) and H_2-9 (δ_H 1.82, 1.75/1.58, 1.52)], as well as by chiral HPLC analysis (Figure 3.2.11), which is in accordance with literature data (Girotra, Patchett and Wendler, 1977).

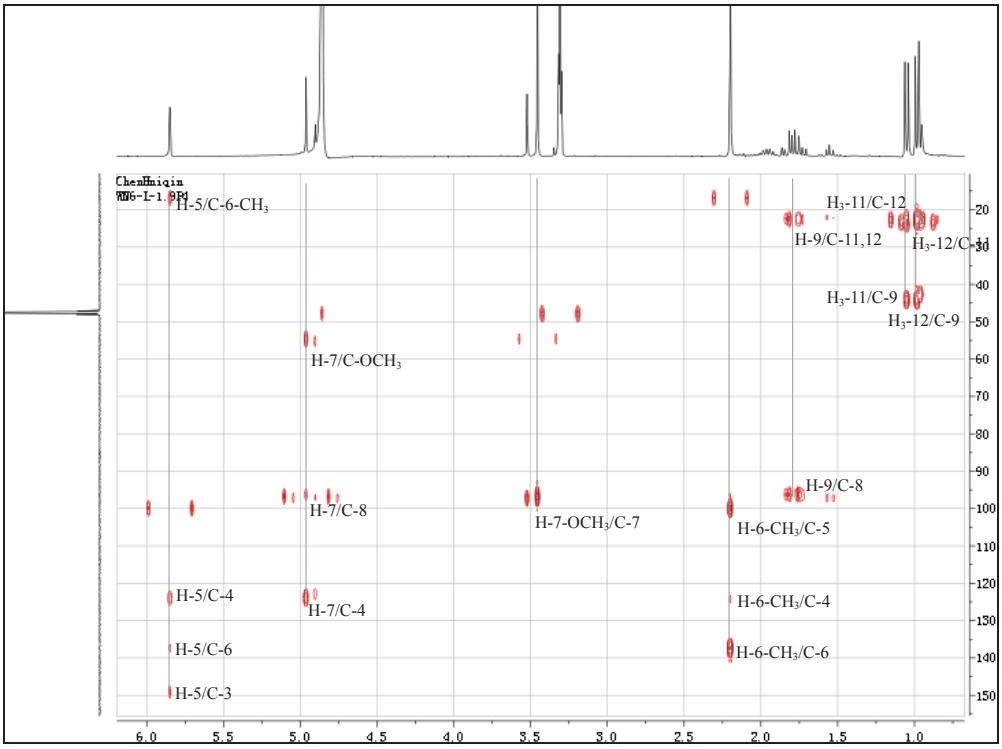

Figure 3.2.10 HMBC correlations of **24**.

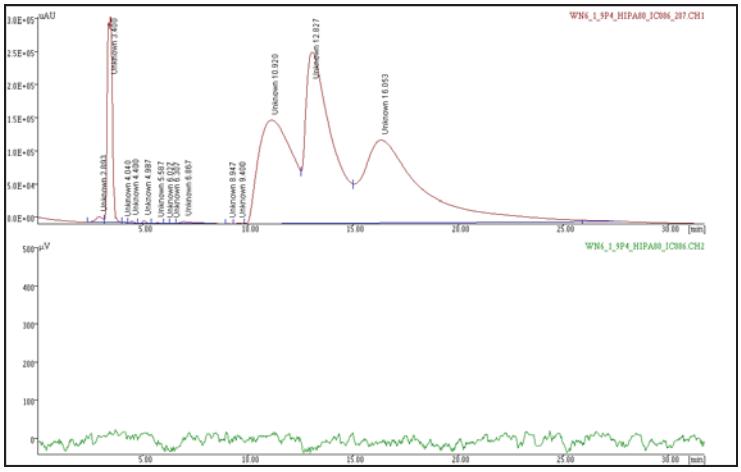

Figure 3.2.11 Compound **24** on chiral HPLC analysis.

3.2.2.4 *Cis*-4,6-Dihydroxymellein (25, known compound)

***Cis*-4,6-Dihydroxymellein**	
Biological Source	*Aspergillus terreus*
Sample Code	WN6-L-1.7P1
Sample Amount	0.79 mg
Molecular Formula	$C_{10}H_{10}O_5$
Molecular Weight	210 g/mol
Solubility	MeOH
Physical Description	White needle-like crystals
Optical rotation	$[\alpha]^{20}_{D}$ +3.0 (*c* 0.15, MeOH)
HPLC Retention Time	10.56 min (standard gradient)

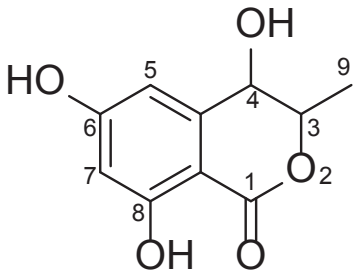

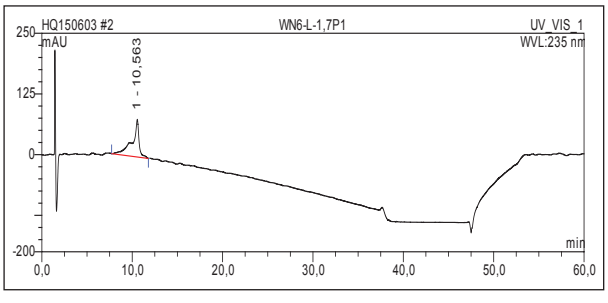

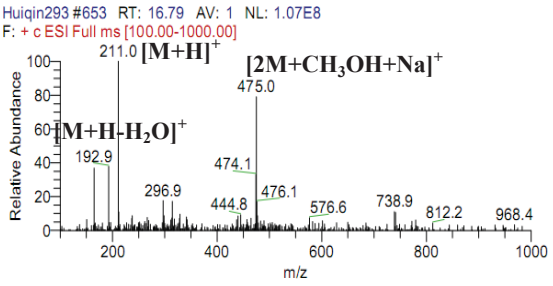

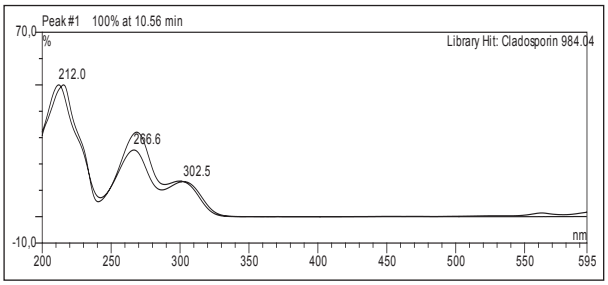

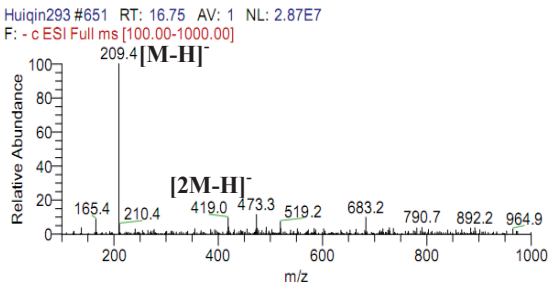

Cis-4,6-Dihydroxymellein (**25**) was isolated as white needle-like crystals from the liquid Wickerham medium culture of *A. terreus*. It displayed UV absorptions at λ_{max} (MeOH) 212, 266 and 302 nm. ESI-MS showed positive and negative pseudomolecular ion peaks at *m/z* 211.0 $[M + H]^+$, 209.4 $[M - H]^-$, 419.0 $[2M - H]^-$ and 475.0 $[2M + CH_3OH + Na]^+$, indicating a molecular weight of 210 g/mol. The ^1H NMR spectrum exhibited signals typical for *meta*-coupled aromatic protons at δ_H 6.42 (1H, d, J = 2.2 Hz, H-5) and 6.31 (1H, d, J = 2.2 Hz, H-7), as supported by their coupling constants and chemical shifts. In addition, one methyl group at δ_H 1.48 (3H, d, J = 6.6 Hz, H-9) and two oxygenated protons at δ_H 4.63 (1H, qd, J = 6.6, 2.2 Hz, H-3) and 4.45 (1H, d, J = 2.2 Hz, H-4) were attributed to a 3,4-dihydro-isocoumarin moiety. The configuration between H-3 and H-4 was assigned as *cis*, which is in accordance with their small coupling constant ($^3J_{H3, H4}$ = 2.2 Hz). By the way, the *trans*- configuration was assigned to the compound with a coupling constant [$^3J_{H3, H4}$ (3 - 4 Hz)]. It has been reported that in the *cis*- compound, the two vicinal hydrogen atoms of the lactonic ring occupy necessarily one pseudo-axial and the other pseudo-equatorial position, while in the case of *trans*- isomer, a relatively small value of the ^3J coupling constant (3.3 Hz) was accounted for the contribution of the conformation having both H_3 and H_4 in the pseudo-equatorial position, and relatively large coupling constant (4 Hz) was observed when both of them located in the pseudo-axial position. (Table 3.2.12) (Avantaggiato et al. 1999)

The structure of **25** was further confirmed by comparison of its UV, ^1H NMR, and mass spectral data with those reported in the literature for *cis*-dihydroxymellein (Avantaggiato *et al*., 1999; Assante *et al*., 1977; Takenaka *et al*., 2011b).

Table 3.2.12 ^1H NMR data for **25**, *cis*- and *trans*- dihydroxymellein (300 MHz, δ_H in ppm, J in Hz)

Position	**25** (CD_3OD)	*Cis*-dihydroxymellein (CD_3OD)	*Cis*-dihydroxymellein (H_2O)	*Trans*-dihydroxymellein (H_2O)
3	4.63 (qd, 6.6, 2.2)	4.63 (qd, 6.5, 2.5)	4.25 (qd, 6.5, 2.3)	4.28 (qd, 6.6, 3.3)
4	4.45 (d, 2.2)	4.45 (d, 2.5)	5.38 (dd, 2.3, 0.9)	5.45 (dd, 3.3, 0.9)
5	6.42 (d, 2.2)	6.41 (d, 2.0)	6.52 (dd, 1.8, 0.9)	6.50 (dd, 1.8, 0.9)
7	6.31 (d, 2.2)	6.30 (d, 2.0)	6.39 (d, 1.8)	6.38 (d, 1.8)
9	1.48 (d, 6.6)	1.47 (d, 6.5)	1.37 (d, 6.5)	1.37 (d, 6.6)

3.2.2.5 *Cis*-4-Hydroxy-6-methoxymellein (26, known compound)

***Cis*-4-Hydroxy-6-methoxymellein**	
Biological Source	*Aspergillus terreus*
Sample Code	WN6-L-1.5P2
Sample Amount	1.25 mg
Molecular Formula	$C_{11}H_{12}O_5$
Molecular Weight	224 g/mol
Solubility	MeOH
Physical Description	White, amorphous powder
Optical rotation	$[\alpha]^{20}_{D}$ + 2.43 (*c* 2.0, MeOH)
HPLC Retention Time	17.85 min (standard gradient)

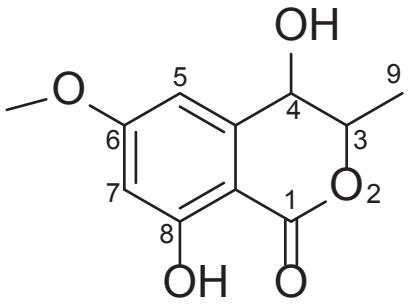

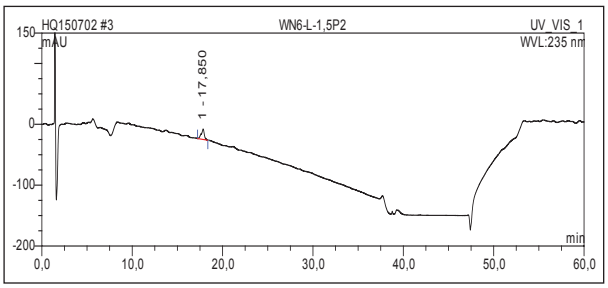

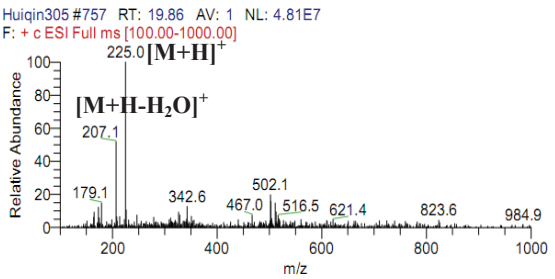

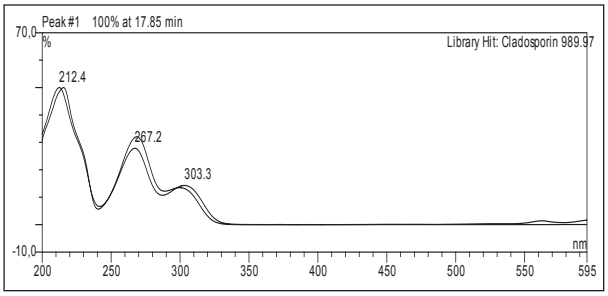

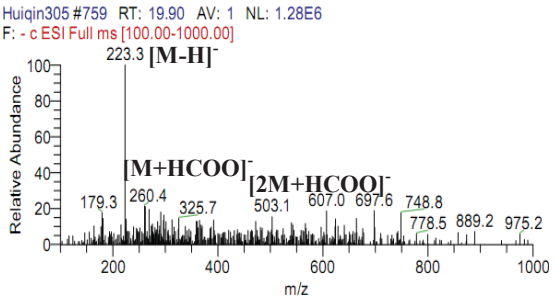

Cis-4-Hydroxy-6-methoxymellein (**26**) was isolated as a white, amorphous powder from the liquid Wickerham medium culture of *A. terreus*. The UV spectrum of **26** showed absorptions at λ_{max} (MeOH) 212, 267 and 303 nm, showing high similarity to those of **25**. Its molecular weight was established as 224 g/mol based on the positive and negative ESI-MS pseudomolecular ion peaks observed at *m/z* 207.1 $[M + H - H_2O]^+$, 225.0 $[M + H]^+$, 223.3 $[M - H]^-$, 260.4 $[M + HCOO]^-$ and 503.1 $[2M + HCOO]^-$. The ^{1}H NMR spectrum of **26** showed close similarity to that of **25**, including two aromatic protons at δ_H 6.54 (H, d, J = 2.2 Hz, H-5) and 6.51 (1H, d, J = 2.2 Hz, H-7), two methine protons at δ_H 4.68 (1H, dq, J = 6.5, 2.3 Hz, H-3) and 4.46 (1H, d, J = 2.2 Hz, H-4), as well as one methyl group at δ_H 1.37 (3H, d, J = 6.5 Hz, H-9). The main difference between **25** and **26** was the presence of an additional methoxy group at δ_H 3.83 (3H, s, H-6-OCH_3) in the ^{1}H NMR spectrum of the latter, which is in accordance with the increase in the molecular weight of 14 amu compared to **25**. Moreover, the relative configuration between H-3 and H-4 was assigned as *cis* on the basis of their small ^3J coupling constant ($^3J_{H3,\ H4}$ = 2.2 Hz). The UV, MS, and ^{1}H NMR data of **26** were in agreement with data published for 4-hydroxy-6-methoxymellein in the literature (Takesue *et al*., 2014; Takenaka, Hamada and Tanahashi, 2011), previously isolated from *Graphis* sp..

3.2.2.6 *Cis*-3,4-Dihydro-4,8-dihydroxy-6,7-dimethoxy-3-methylisocoumarin (27, known compound)

***Cis*-3,4-Dihydro-4,8-dihydroxy-6,7-dimethoxy-3-methylisocoumarin**	
Biological Source	*Aspergillus terreus*
Sample Code	WN6-L-1.4P2, WN6-L-1.5P1
Sample Amount	1.0 mg
Molecular Formula	$C_{12}H_{14}O_6$
Molecular Weight	254 g/mol
Solubility	MeOH
Physical Description	White, amorphous powder
Optical Rotation	$[\alpha]^{20}_D$ -1.39 (*c* 0.15, MeOH)
HPLC Retention Time	14.93 min (standard gradient)

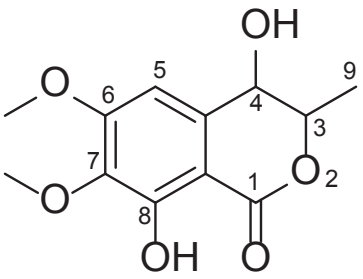

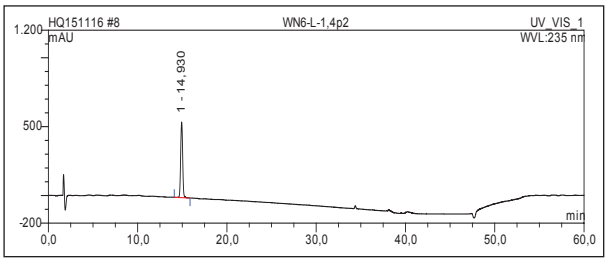

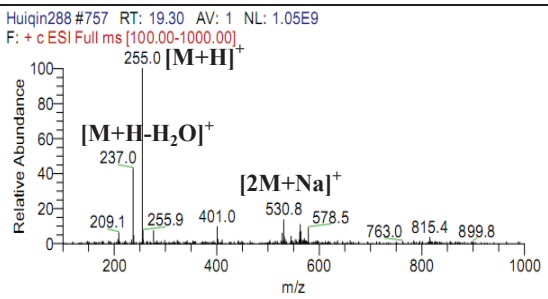

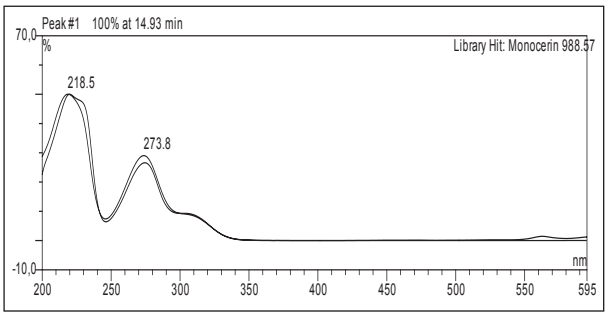

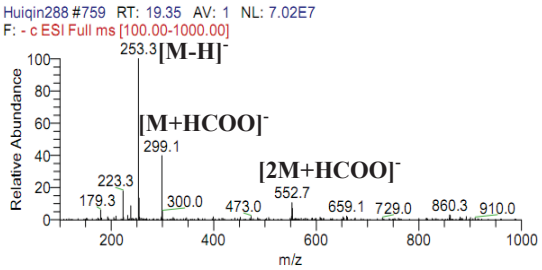

Cis-3,4-Dihydro-4,8-dihydroxy-6,7-dimethoxy-3-methlisocoumarin (**27**) was isolated as a white, amorphous powder from the liquid Wickerham medium culture of *A. terreus*. The UV spectrum of **27** displayed UV absorptions at λ_{max} (MeOH) 218 and 273 nm, characteristic for isocoumarin derivatives. The positive and negative ESI-MS pseudomolecular ion peaks at *m/z* 237.0 $[M + H - H_2O]^+$, 255.0 $[M + H]^+$, 530.8 $[2M + Na]^+$, 253.3 $[M - H]^-$, 299.1 $[M + HCOO]^-$ and 552.7 $[2M + HCOO]^-$ indicated a molecular weight of 254 g/mol. Comparison of the ^{1}H NMR spectrum of **27** with that of **26** showed high similarity, apart from the absence of an aromatic proton (H-7) and the presence of a methoxy group (7-OCH_3) instead. The identification of **27** was further confirmed by comparison of its UV, ^{1}H NMR, and MS data with those reported for *cis*-3,4-dihydro-4,8-dihydroxy-6,7-dimethoxy-3-methylisocoumarin, which was likewise reported from the same fungus as a root growth promoter (Arai *et al.*, 1983; Shimada *et al*., 2004).

Table 3.2.13 ^{1}H NMR data for **26** and **27**.

Position	**26** (DMSO, 300 MHz, *J* in Hz)	**27** (H_2O, 300 MHz, *J* in Hz)
3	4.68 (dq, 6.5, 2.3)	4.67 (qd, 6.6, 2.2)
4	4.46 (d, 2.2)	4.51 (d, 2.2)
5	6.54 (d, 2.2)	6.71 (s)
7	6.51 (d, 2.2)	
9	1.37 (d, 6.5)	1.50 (d, 6.6)
6-OCH_3	3.83 (s)	3.81 (s)
7-OCH_3		3.95 (s)

3.2.2.7 1-(2',3'-Dihydroxyphenyl)ethanone (28, known compound)

1-(2',3'-Dihydroxyphenyl)ethanone	
Biological Source	*Aspergillus terreus*
Sample Code	WN6-L-1.6P, WN6-L-1.4P5, WN6-L-1.5P3, WN6-L-1.7P3
Sample Amount	5.4 mg
Molecular Formula	$C_8H_8O_3$
Molecular Weight	152 g/mol
Solubility	MeOH
Physical Description	White needle-like crystals
HPLC Retention Time	27.79 min (standard gradient)

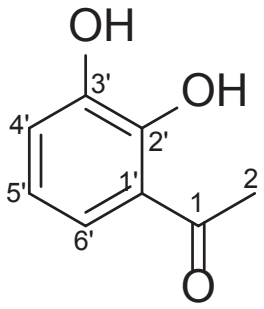

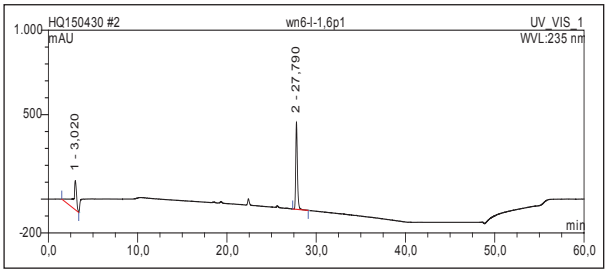

No ionisation in positive mode.

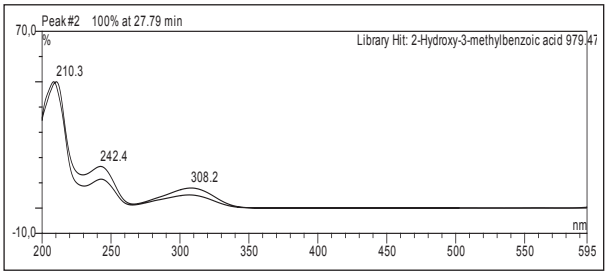

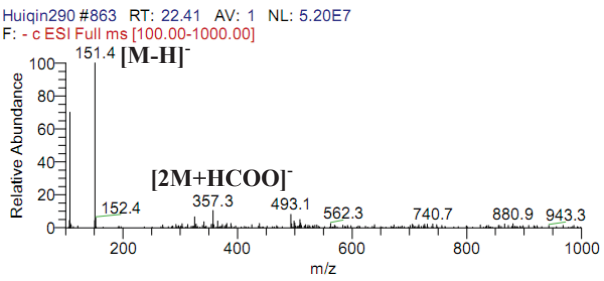

1-(2',3'-Dihydroxyphenyl)ethanone (**28**) was isolated as white needle-like crystals from the liquid Wickerham medium culture of *A. terreus*. It displayed UV absorptions at λ_{max} (MeOH) 210, 242 and 308 nm. Its molecular weight was determined as 152 g/mol according to the observed negative pseudomolecular ion peaks at *m/z* 151.4 $[M - H]^-$ and 357.3 $[2M + HCOO]^-$, whereas no ionisation was observed in the positive mode. The ^{1}H NMR spectrum showed three downfield signals, including one signal at δ_H 7.05 (1H, t, J = 8.0 Hz, H-5') and two overlapped signals at 6.60 (2H, d, J = 8.0 Hz, H-4'/6'), consistent with a 1,2,3-substituent phenyl moiety. The remaining signal at δ_H 2.58 (3H, s, H_3-2) was assigned to a methyl carbonyl group. On the basis of above data, 1-(2',3'-dihydroxyphenyl)ethanone or 1-(2',6')-dihydroxyphenyl)ethanone were proposed to the structure. Considering the symmetry of the structure of 1-(2',6')-dihydroxyphenyl)ethanone, H-4' and H-6' were overlapping completely, which was different from the separate signals observed in the ^{1}H NMR. This assignment was further corroborated by the published data for 1-(2',3'-dihydroxyphenyl)ethanone. (Ghaffarzadeh and Ahmadi, 2014).

Table 3.2.14 ^{1}H NMR data for **28** and 1-(2',3'-dihydroxyphenyl)ethanone.

Position	**28** (CD_3OD, 300 MHz, J in Hz)	1-(2',3'-dihydroxyphenyl)ethanone[a] ($CDCl_3$, 500 MHz, J in Hz)
2	2.58 (s, 3H)	2.78 (s, 3H)
4'	6.60 (d, 8.0, overlapping)	6.42 (d)
5'	7.05 (t, 8.0)	7.25 (m)
6'	6.60 (d, 8.0, overlapping)	6.42 (d)

[a] Ghaffarzadeh and Ahmadi, 2014

3.2.2.8 Asterrelenin (29, known compound)

Asterrelenin	
Biological Source	*Aspergillus terreus*
Sample Code	WN6-B-9P0P1, WN6-L-1.4P6, WN6-B-9P2
Sample Amount	9.1 mg
Molecular Formula	$C_{25}H_{25}N_3O_4$
Molecular Weight	431 g/mol
Solubility	MeOH
Physical Description	Colorless crystals
Optical rotation	$[\alpha]^{20}_D$ + 184.9 (*c* 0.2, MeOH)
HPLC Retention Time	24.18 min (standard gradient)

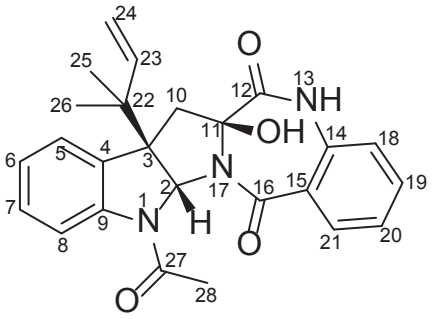

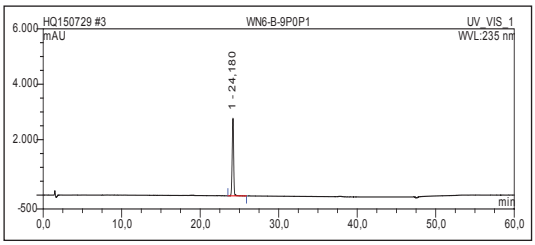

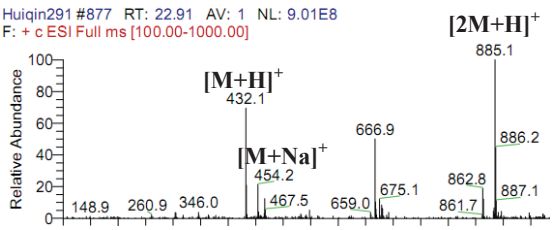

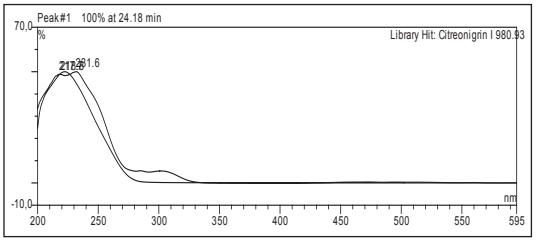

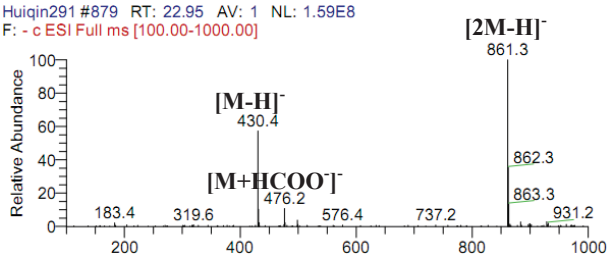

Asterrelenin (**29**) was isolated as colorless crystals from the ethyl acetate extract of the white beans culture of *A. terreus*. It showed UV absorption at λ_{max} (MeOH) 218 nm. Positive and negative ESI-MS showed molecular ion peaks at *m/z* 432.1 $[M + H]^+$, 454.2 $[M + Na]^+$, 884.1 $[2M + H]^+$, 430.4 $[M - H]^-$, 476.2 $[M + HCOO]^-$ and 861.3 $[2M - H]^-$ indicating a molecular

weight of 431 g/mol, and thus the presence of an odd number of nitrogen atoms in the structure. The ^{1}H NMR spectrum of **29** revealed the presence of two *ortho*-substituted aromatic moieties [δ_H 7.90 (1H, dd, J = 8.0, 1.4 Hz, H-5), 7.73 (1H, d, J = 7.1 Hz, H-8), 7.44 (1H, br. t, J = 7.4 Hz, H-7), 7.43 (1H, dd, J = 7.6, 0.9 Hz, H-21), 7.23 (1H, t, J = 7.6 Hz, H-6), 7.16 (1H, td, J = 7.6, 1.0 Hz, H-19), 7.13 (1H, br. t, J = 7.5 Hz, H-20) and 6.93 (1H, d, J = 7.7 Hz, H-18)], which were further confirmed by their respective ^{1}H–^{1}H COSY and HMBC correlations (Figure 3.2.12). An additional methyl carbonyl group was observed at δ_H 2.70 (1H, s, H-28), whereas a broad singlet at δ_H 6.34 (1H, br. s, H-2) was assigned to a nitrogen bearing carbon, due to its downfield chemical shift. Moreover, the ^{1}H–^{1}H COSY spectrum indicated a spin system corresponding to the fragment CH_2(24)CH(23)CH(22)CH_3(25)CH_3(26), as supported by the HMBC correlations from H-23 to C-22 (δ_C 40.5), as well as from both H_3-25 and H_3-26 to C-22 and C-23 (δ_C 144.1). Further HMBC correlations from H_3-25 and H_3-26 to C-3 (δ_C 57.6) corroborated the attachment of the respective substructure at C-3. Thus, **29** was identified as asterrelenin, an indole alkaloid previously reported from *A. terreus* (Li *et al*., 2005). The absolute configuration of asterrelenin was previously deduced by X-ray crystallographic analysis (Li *et al*., 2005). The large positive optical rotation ($[\alpha]^{20}_D$ + 184.9) of **29** was also consistent with reported data, thus suggesting the same absolute configuration as in asterrelenin.

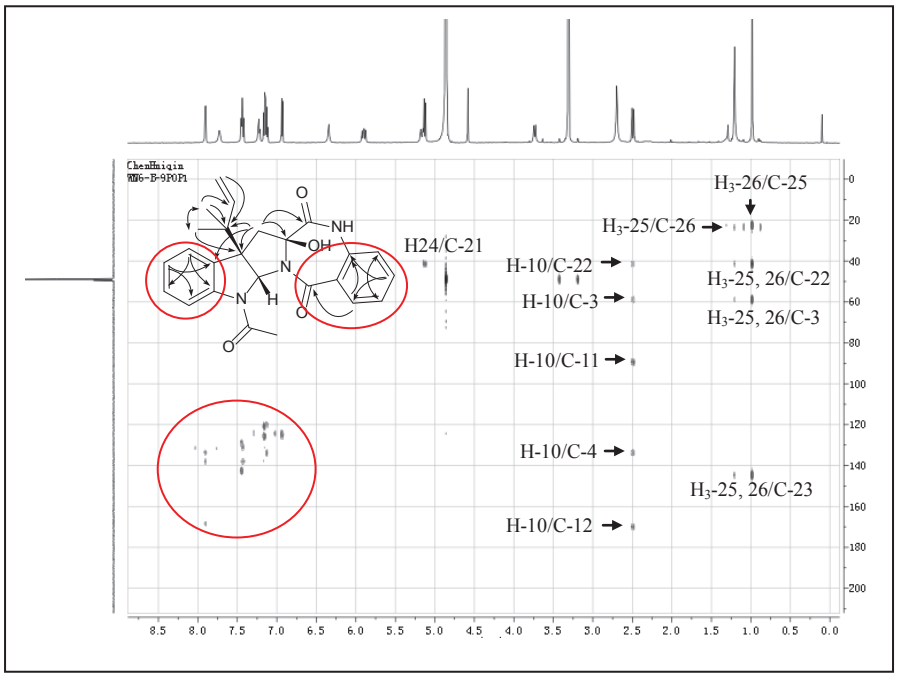

Figure 3.2.12 HMBC correlations of compound **29**

3.2.2.9 Acetylaszonalenin (30, known compound)

Acetylaszonalenin	
Biological Source	*Aspergillus terreus*
Sample Code	WN6-B-9P4
Sample Amount	1.2 mg
Molecular Formula	$C_{25}H_{25}N_3O_3$
Molecular Weight	415 g/mol
Solubility	MeOH
Physical Description	Yellow crystals
HPLC Retention Time	25.71min (standard gradient)

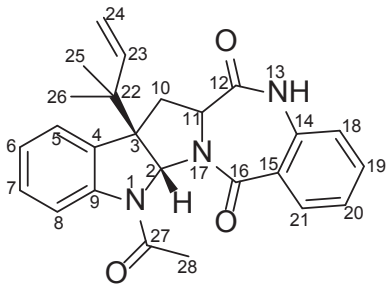

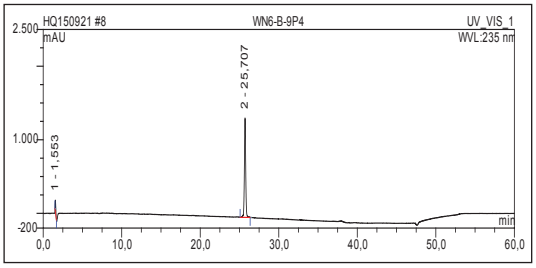

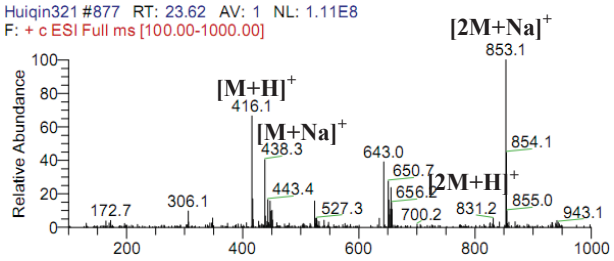

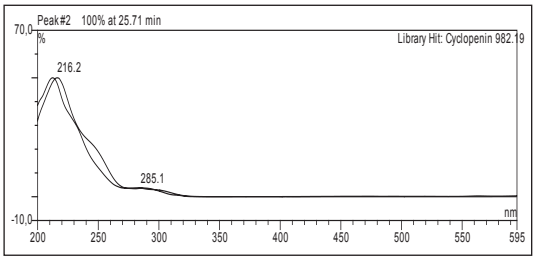

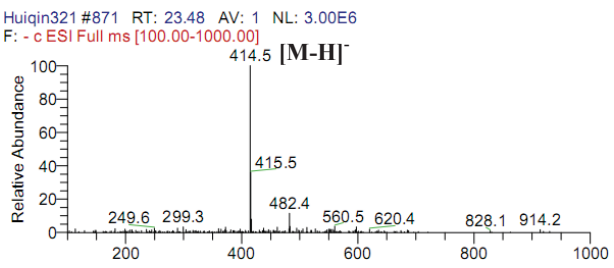

Acetylaszonalenin (**30**) was isolated as yellow crystals from the ethyl acetate extract of the solid bean culture of *A. terreus*. The UV spectrum showed the same pattern as that of **29**. Positive and negative ESI-MS ion peaks at *m/z* 416.1 $[M + H]^+$, 438.3 $[M + Na]^+$, 831.2 [2M

+ H]$^+$, 853.1 [2M + Na]$^+$, and 414.5 [M - H]$^-$ indicated a molecular weight of 415 g/mol. Comparison of the ^{1}H NMR spectrum of **30** with that of **29** showed high similarity, apart from the absence of the hydroxy group at C-11 and the presence of a methine proton (δ_H 4.26, H-11) instead, as supported by the molecular formula of **30**. Based on the data mentioned above, along with comparison with published data, the structure of **30** was deduced as acetylaszonalenin, previously reported from the same species (Ellestad, Mirando and Kunstmann, 1973).

Table 3.2.15 ^{1}H NMR data for **29** and **30**.

Position	Asterrelenin[a] ($CDCl_3$, 600 MHz, *J* in Hz)	**29** (CD_3OD, 600 MHz, *J* in Hz)	**30** (CD_3OD, 300 MHz, *J* in Hz)
2	6.18 (s)	6.34 (br. s)	6.21 (br. s)
5	7.82 (dd, 7.8, 1.4)	7.90 (dd, 8.0, 1.4)	7.93 (dd, 8.0, 1.4)
6	7.05 (td, 7.6, 0.9)	7.23 (t, 7.6)	7.15 (td, 7.5, 1.2)
7	7.41 (td, 7.6, 1.4)	7.44 (br. t, 7.4)	7.51 (dd, 7.1, 1.1)
8	7.61 (dd, 6.7, 1.1)	7.73 (br. d, 7.1)	7.72 (br. d, 8.3)
10	3.57 (d, 13.6)	3.74 (d, 13.6)	3.13 (d, 13.5)
	2.41 (d, 13.6)	2.49 (d, 13.8)	2.68 (dd, 13.3, 9.6)
11			4.26 (dd, 9.6, 0.8)
18	6.90 (dd, 8.0, 1.3)	6.93 (d, 7.7)	7.00 (dd, 8.1, 0.8)
19	7.16 (td, 8.2, 0.9)	7.16 (td, 7.6, 1.0)	7.24 (m)
20	7.11 (td, 7.4, 0.9)	7.13 (br. t, 7.5)	7.24 (m)
21	7.37 (dd, 7.6, 0.9)	7.43 (dd, 7.6, 0.9)	7.49 (td, 7.1, 1.6)
23	5.87 (17.6, 10.6)	5.90 (dd, 17.3, 10.7)	5.91 (dd, 17.4, 10.8)
24	5.09 (d, 17.6)	5.17 (d, 17.6)	5.15 (dd, 17.3, 0.8)
	5.07 (d, 10.6)	5.13 (d, 10.9)	5.12 (dd, 10.8, 1.1)
25	1.08 (s)	1.21 (s)	1.21 (s)
26	0.86 (s)	0.98 (s)	0.99 (s)
28	2.59 (s)	2.70 (s)	2.68 (s)

[a] Li *et al*., 2005

3.2.2.10 HPLC analysis of fungal cultures in different media

Three media (rice, liquid Wickerham medium, and white beans) were used to ferment *A. terreus*, and different chemical patterns were observed by comparison of the HPLC profiles of the respective ethyl acetate extracts. Accordingly, the proportion of purple pigments (peaks shown in the frame) was significantly increased when *A. terreus* was cultured on white beans medium, and observed as a major peak in the mycelium part of liquid Wickerham medium

culture. Unfortunately, these peaks were impossible to be identified due to its decomposition in short time. The peaks indicated by the arrow were identified as dihydroisoflavipucines, and were only observed in the broth of liquid Wickerham medium culture. Another main component, terrein, was obtained in a large amount on rice and in liquid Wickerham medium cultures (not in the detected range due to its weak absorption under UV 235 nm), whereas it could not be obtained when *A. terreus* was cultivated on white beans culture.

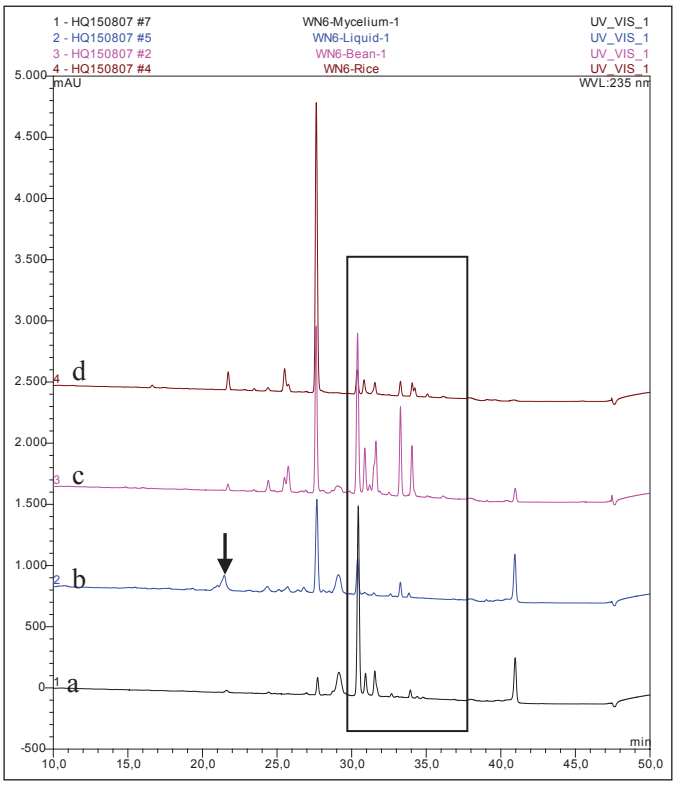

Figure 3.2.13 HPLC chromatograms of the EtOAc extracts from *A. terreus* cultured in three different media: a) mycelium of *A. terreus* in liquid Wickerham medium culture; b) liquid part of *A. terreus* in liquid Wickerham medium culture; c) *A. terreus* was cultured on white beans; d) *A. terreus* was cultured on rice.

3.2.2.11 Bioactivity assay of isolated compounds from *A. terreus*

All isolated compounds were submitted to several bioassays. Butyrolactone II (**11**) and aspulvinone E (**20**) showed weak inhibition of *B. cereus* with MICs 64 μg/mL, respectively, while asterrelenin (**29**) showed weak inhibition of *Mycobacterium tuberculosis* with MIC 100 μg/mL (Table 3.2.14). For the results from cytotoxicity assays, terrein (**14**) showed moderate

cytotoxicity with 80% inhibition of the murine lymphoma cell line L5178Y at a dose of 10 μg/ml (Table 3.2.16), while **29** and acetylaszonalenin (**30**) showed weak cytotoxicity against human ovarian cancer A2780 sens cell line at the concentration of 10^2 μM (Figure 3.2.14).

3.2.16 Bioactivities of compounds **7**-**30**.

compound	Cytotoxicity	Anti-bacteria (MIC)	
	L5178Y	*B. cereus*	*M. tuberculosis*
11		64 μg/mL	
14	80% inhibition (10 μg/ml)		
20		64 μg/mL	
29			100 μg/mL

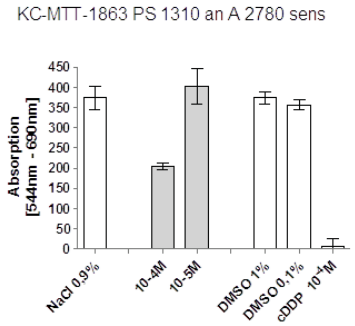

29

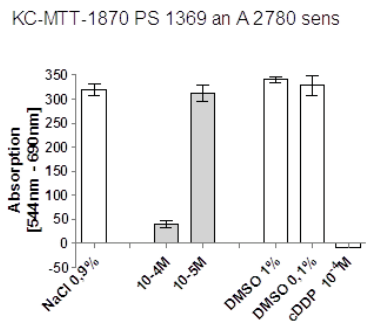

30

Figure 3.2.14 Cytotoxic activity of **29** and **30** against A2780 sens cell line.

3.2.3 Inducing secondary metabolite production by epigenetic modifiers

Suberoylanilide hydroxamic acid (SAHA) and 5-azacytidine (5-Aza) were applied to liquid Wickerham medium culture of *A. terreus*. However, no accumulation of secondary metabolites was observed after analysis of the respective HPLC chromatograms.

3.3 Compounds isolated from two sponge-derived *Penicillium sp*. strains (IO1 and IO2).

Penicillium species play an important role in food and drug production, as well as in medicine, with the genus containing over 300 species (Cannon and Kirk, 2007). Importantly, the antibiotic penicillin and the antifungal drug griseofulvin were obtained from the genus *Penicillium*. Herein, two *Penicillium* sp. strains IO1 and IO2 were isolated from the Mediterranean sponge *Ircinia oros*. They were identified as different strains according to the different HPLC chromatograms of the EtOAc crude extracts from solid rice cultures. When cultured independently, a new fusarielin analogue (**31**) together with the known compounds griseofulvin (**32**) and dechlorogriseofulvin (**33**) were isolated from the *Penicillium* sp. strain IO1, while three known compounds dehydrocurvularin (**34**), curvularin (**35)**, and trichodimerol (**36**) were isolated from the *Penicillium* sp. strain IO2.

The structure of the new compound **31** was unambiguously elucidated by comprehensive spectroscopic analysis (1D and 2D NMR), and mass spectrometry, as well as by comparison with the literature, while the absolute configuration of **31** was determined on the basis of TDDFT ECD calculations. (Chen *et al*., 2015c)

Co-cultivation of both *Penicillium* strains IO1 and IO2 was found to induce the accumulation of the known norlichexanthone (**37**) and monocerin (**38**) that were not detected in either of the two axenic fungal controls, whereas another two compounds griseophenone B (**39**) and echinulin (**40**) were isolated incidentally from the co-culture, which were not observed in the HPLC chromatograms due to the small amounts. (Chen *et al.*, 2015a)

3.3.1 Secondary metabolites from *Penicillium* sp. strain IO1

3.3.1.1 Fusarielin I (31, new compound)

Fusarielin I	
Biological Source	*Penicillium* sp. strain IO1
Sample Code	%40 Hex22-31P1(M)
Sample Amount	5.2 mg
Molecular Formula	$C_{22}H_{32}O_4$
Molecular Weight	360 g/mol
Solubility	MeOH
Physical Description	Pale yellow gel
Optical rotation	$[\alpha]^{20}_D$ -108 (*c* 0.1, MeOH)
HPLC Retention Time	32.29 min (standard gradient)

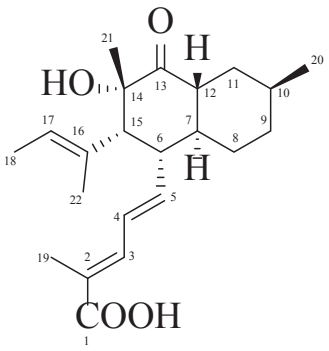

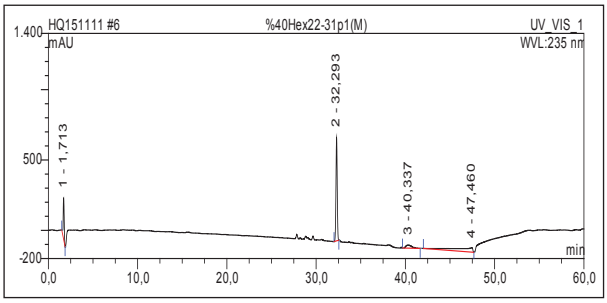

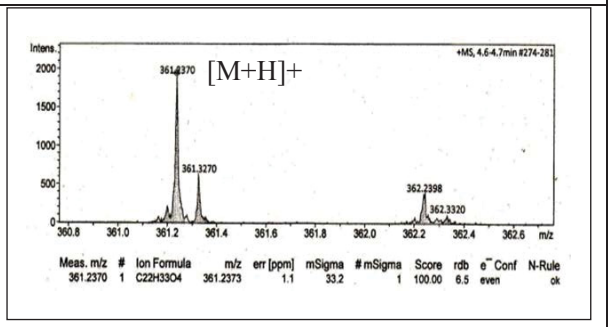

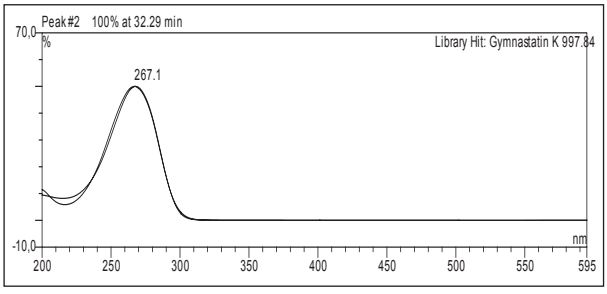

Fusarielin I (**31**) was isolated as a pale yellow gel. The molecular formula was determined as $C_{22}H_{32}O_4$ on the basis of a prominent ion peak at *m/z* 361.2369 $[M + H]^+$ observed in the HRESIMS spectrum, indicating seven degrees of unsaturation. The ^{1}H NMR spectrum of **31** revealed the presence of three tertiary methyl groups at δ_H 1.94 (3H, d, J = 1.5 Hz, H_3-19), 1.55 (3H, s, H_3-21) and 1.50 (3H, s, H_3-22), two secondary methyl groups at δ_H 1.58 (3H, d, J = 6.0 Hz, H_3-18) and 1.01 (3H, d, J = 7.0 Hz, H_3-20), and four olefinic protons at δ_H 7.13 (1H, dd, J = 11.4, 1.5 Hz, H-3), 6.51 (1H, dd, J = 15.0, 11.4 Hz, H-4), 5.70 (1H, dd, J = 15.0, 9.8 Hz, H-5) and 5.01 (1H, m, H-17) (Table 3.3.1). The ^{13}C NMR spectrum showed a total of 22 resonances (Table 3.3.1) assigned to eight sp^2 carbons [including two carbonyl groups at δ_C 216.5 (C-13) and 171.9 (C-1)], five methyl groups [δ_C 29.1 (C-21), 18.1 (C-20 and C-22), 13.5 (C-18) and 12.7 (C-19)], eight aliphatic sp^3 carbons (including three methylenes and five methines), and one oxygenated quaternary carbon at δ_C 78.5 (C-14), as supported by the DEPT and HSQC spectra. (Chen, *et al*., 2015a)

Detailed analysis of the ^{1}H–^{1}H COSY spectrum disclosed the presence of a continuous spin system starting from H-3 and sequentially extending until H-12 with H-10 further correlating with an aliphatic methyl (H_3-20) (Figure 3.3.1a). In addition, COSY correlations from H-6 to H-15 and from H-7 to H-12 were observed. The HMBC correlations from H-15 (δ_H 2.76) to C-13, C-14, C-6 (δ_C 49.3), and C-7 (δ_C 45.8); H_3-21 to C-13, C-14 and C-15 (δ_C 66.0); and H-12 (δ_H 2.60) to C-6 and C-13 further extended this substructure from C-12 to C-15 (Figure 3.3.1a), thus indicating the presence of a decalone ring similar to that of fusarielins and rapiculin. (Sørensen *et al.*, 2013; Nozawa *et al.*, 1991) Further HMBC correlations from H-4 to C-2 (δ_C 127.0), C-3 (δ_C 139.5), and C-6, and from H_3-19 to C-1, C-2, and C-3 corroborated the presence of a 2-methylpenta-2,4-dienoic acid moiety and its connection to the decalone moiety at C-6. Moreover, a but-2-en-2-yl group was attached at C-15, as supported by the COSY correlation between H-17 and H_3-18, as well as by the HMBC correlations from H_3-22 to C-15, C-16 (δ_C 133.8), and C-17 (δ_C 125.6) (Figure 3.3.1a), thereby rationalizing the remaining element of unsaturation. Thus, the planar structure of **31** was established. (Chen, *et al*., 2015a)

The geometry of the double bonds in the 2-methylpenta-2,4-dienoic acid side chain was deduced as *E* based on the ROESY correlation between H_3-19 and H-4 and the large coupling constant between H-4 and H-5 ($^3J_{4,\ 5}$ = 15.0 Hz), respectively. Likewise, the ROESY correlation between H_3-22 and H_3-18 indicated the 16*E* configuration for the double bond in the but-2-en-2-yl group (Figure 3.3.1b). (Chen, *et al*., 2015a)

Accordingly, the relative configuration of the stereocenters for the decalone moiety of **31** was deduced by analysis of the coupling constants and the ROESY spectrum (Figure 3.3.1b). The axial orientations of H-12, H-7, and H-6 were suggested by the large vicinal coupling constants ($^3J_{6,\ 7}$ = $^3J_{7,\ 12}$ = 11.6 Hz), hence indicating the presence of a trans-decalone ring as observed in fusarielins (Sørensen *et al*. 2013). This was further corroborated by the absence of a cross-peak between H-7 and H-12 in the ROESY spectrum of **31**. Moreover, the relatively small coupling constant between H-6 and H-15 ($^3J_{6,\ 15}$ = 5.4 Hz) revealed the equatorial orientation for the latter and subsequently the axial orientation for the but-2-en-2-yl group. The ROESY spectrum further showed correlations of H-12 to H_3-20, H_3-21, and H-6, which further confirmed the co-facial orientation of these protons and the (6*S**,7*S**,10*S**,12*R**,14*S**,15*R**) relative configuration (Figure 3.3.1b). (Chen *et al.*, 2015a)

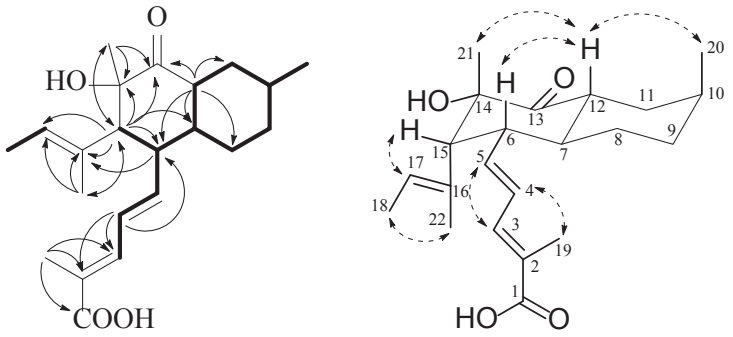

(a) (b)

Figure 3.3.1 (a) ^{1}H–^{1}H COSY (bold lines) and key HMBC (arrows) correlations of **31**.
(b) Key ROESY correlations of **31**.
(Chen *et al.*, 2015a)

Table 3.3.1 1D and 2D NMR spectral data of **31** at 600 (^{1}H) and 150 (^{13}C) MHz (in CD_3OD, δ in ppm). (Chen *et al.*, 2015a)

No.	δ_C	δ_H (J in Hz)	HMBC
1	171.9, qC		
2	127.0, qC		
3	139.5, CH	7.13, dd (11.4, 1.5)	1, 2, 5, 19
4	128.5, CH	6.51, dd (15.0, 11.4)	2, 3, 6
5	145.3, CH	5.70, dd (15.0, 9.8)	2, 3, 6, 7
6	49.3, CH	2.88, ddd (11.6, 9.8, 5.4)	4, 5, 7, 8, 15, 16
7	45.8, CH	1.75, qd (11.6, 2.7)	6, 8, 9, 12
8	28.14, CH_2	1.51, m 1.31, m	
9	32.0, CH_2	1.50, m	
10	28.10, CH	2.12, m	
11	32.5, CH_2	1.80, dd (13.6, 1.8) 1.32, m	9, 10, 12
12	44.9, CH	2.60, td (11.6, 2.9)	6, 7, 8, 11, 13
13	216.5, qC		
14	78.5, qC		
15	66.0, CH	2.76, d (5.4)	5, 6, 7, 13, 14, 16, 17, 21, 22
16	133.8, qC		
17	125.6, CH	5.01, m	
18	13.5, CH_3	1.58, d (6.0)	16, 17
19	12.7, CH_3	1.94, d (1.5)	1, 2, 3
20	18.1, CH_3	1.01, d (7.0)	9, 10, 11
21	29.1, CH_3	1.55, s	13, 14, 15
22	18.1, CH_3	1.50, s	15, 16, 17

The conformers differed in the orientation of the C-15 substituent and the carboxyl group (Figure 3.3.2). All the conformers reproduced an intense negative CE at 266 nm, and the Boltzmann-weighted TDDFT-ECD spectra computed with three functionals (B3LYP, BH&HLYP, PBE0) and TZVP basis set for (6*S*,7*S*,10*S*,12*R*,14*S*,15*R*)-**31** gave good agreement with the experimental ECD spectrum, although the intensity of the 218 positive CE was underestimated (Figure 3.3.3). (Chen *et al.*, 2015a)

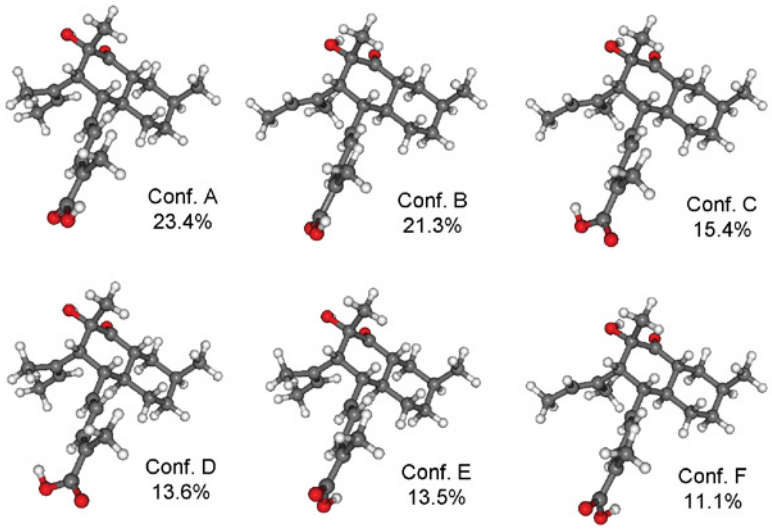

Figure 3.3.2. Structures and populations of the conformers of (6*S*,7*S*,10*S*,12*R*,14*S*,15*R*)-**31** obtained by the B3LYP/6-31G(d) reoptimization of the initial MMFF conformers in the gas phase. (Chen *et al.*, 2015a)

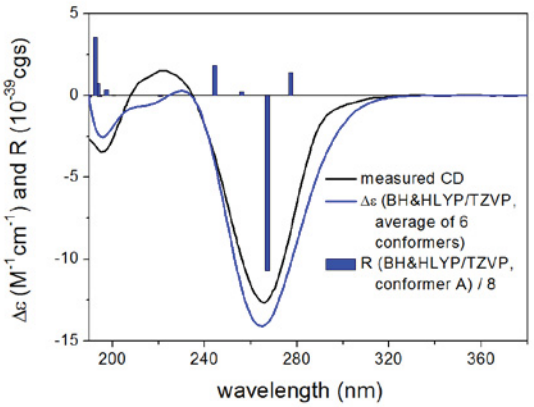

Figure 3.3.3 Comparison of the experimental ECD of **31** (black) with the Boltzmann-weighted BH&HLYP/TZVP ECD spectra of (6*S*,7*S*,10*S*,12*R*,14*S*,15*R*)-**31** (blue) computed for the 6 B3LYP/6-31G(d) gas phase conformers. Bars represent the computed rotational strength of the lowest-energy conformer. (Chen *et al.*, 2015a)

In order to improve the agreement, the reoptimization of the MMFF conformers of (6*S*,7*S*,10*S*,12*R*,14*S*,15*R*)-**31** was also carried out at B97D/TZVP level with PCM for acetonitrile, which afforded 14 conformers above 2% population (Figure 3.3.4). The Boltzmann-weighted TDDFT-ECD spectra of these conformers also reproduced the positive 218 CE of the experimental spectrum with the BH&HLYP/TZVP method providing the best agreement, which allowed determining the absolute configuration as (6*S*,7*S*,10*S*,12*R*,14*S*,15*R*) (Figure 3.3.5). (Chen *et al.*, 2015a)

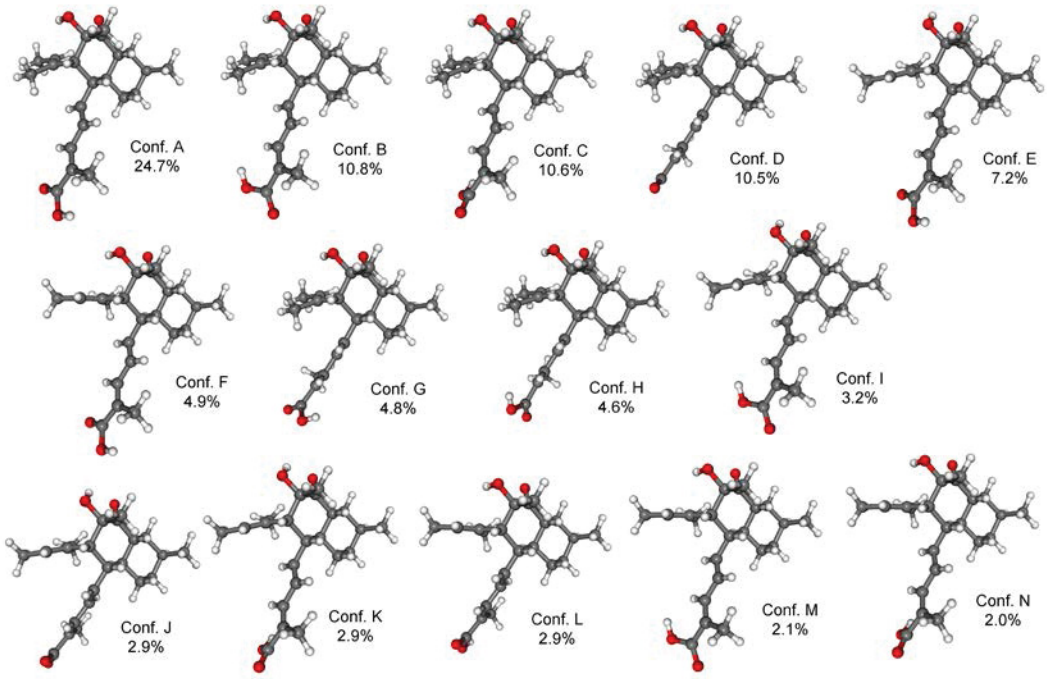

Figure 3.3.4 Structures and populations of the conformers of (6*S*,7*S*,10*S*,12*R*,14*S*,15*R*)-**31** obtained by the B97D/TZVP reoptimization of the initial MMFF conformers with PCM for acetonitrile. (Chen *et al.*, 2015a)

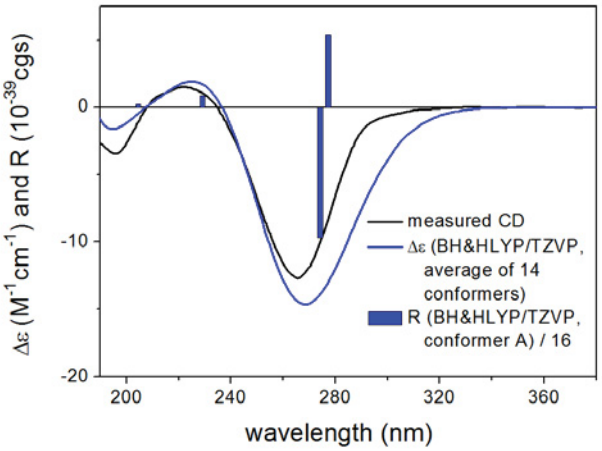

Figure 3.3.5 Comparison of the experimental ECD of **31** (black) with the Boltzmann-weighted BH&HLYP/TZVP ECD spectra of (6*S*,7*S*,10*S*,12*R*,14*S*,15*R*)-**31** (blue) computed for the 14 B97D/TZVP (PCM for acetonitrile) conformers. Bars represent the computed rotational strength of the lowest-energy conformer. (Chen *et al.*, 2015a)

The ECD calculations also revealed that the negative 266 nm CE is governed by the π–π* transition of the C-6 and C-15 side-chains (Figure 3.3.6). On the basis of the above data, **31** was identified as a new natural product, for which the name fusarielin I is proposed. (Chen *et al.*, 2015a)

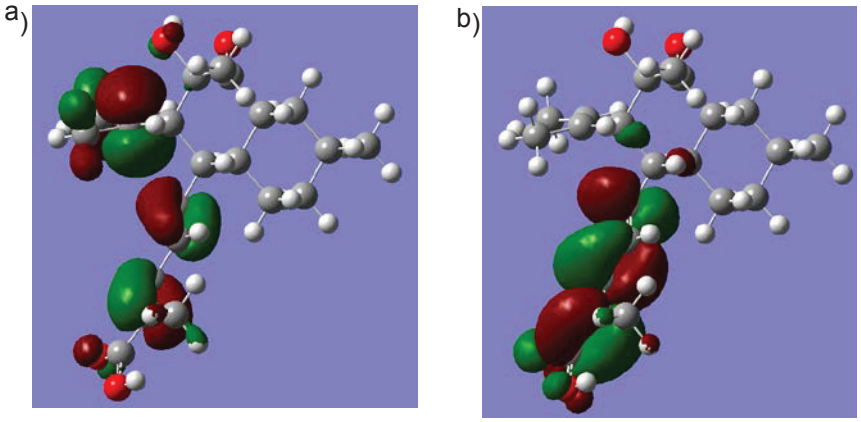

Figure 3.3.6. Kohn-Sham orbitals of **31** responsible for the 266 nm negative π-π* [HOMO-1 (a)→LUMO (b)] transitions extracted from B3LYP/TZVP calculation of the lowest-energy B97D/TZVP (PCM model for acetonitrile) solution conformer and plotted with an isovalue of 0.032. (Chen *et al.*, 2015a)

3.3.1.2 Griseofulvin (32, known compound)

Griseofulvin	
Biological Source	*Penicillium* sp. strain IO1
Sample Code	Fr %100 EtOAc Peak1, Cocul 100DCM
Sample Amount	136.74 mg
Molecular Formula	$C_{17}H_{17}ClO_6$
Molecular Weight	352 g/mol
Solubility	$CHCl_3$
Physical Description	Yellow powder
Optical rotation	$[\alpha]^{20}_D$ +92
HPLC Retention Time	24.82 min (standard gradient)
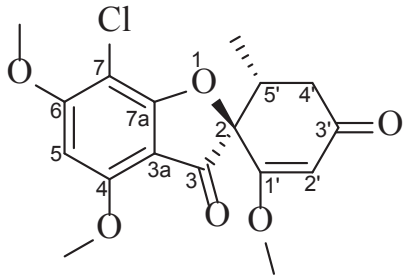	
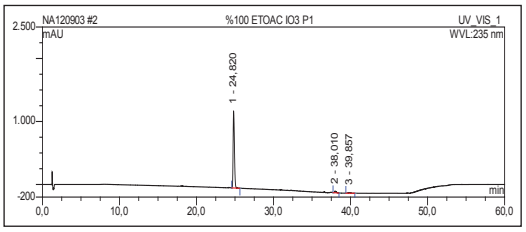	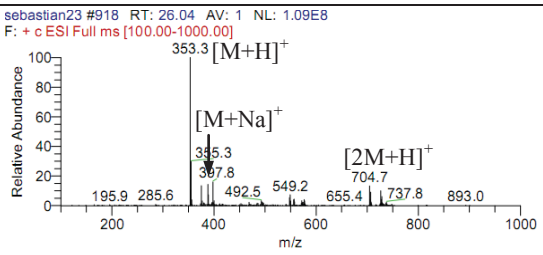
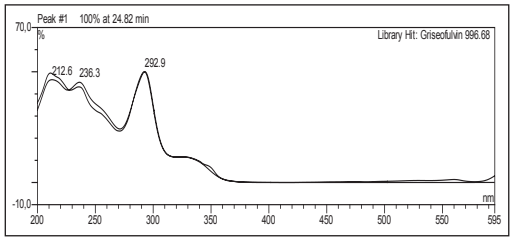	No ionisation in negative mode.

Griseofulvin (**32**) was isolated as a yellow powder from *Penicillium* sp. strain IO1. The UV spectrum gave the supposed structure of griseofulvin from the spectrum library with absorptions at λ_{max} (MeOH) 212, 236 and 292 nm. The optical rotation was $[\alpha]^{20}_D$ +92. Its molecular weight was determined as 352 g/mol based on the pseudomolecular ion peak

observed at *m/z* 353.3 $[M + H]^+$, 375 $[M + Na]^+$ and 704.7 $[2M + H]^+$ upon positive ionisation by ESI-MS, which was consistent with the molecular weight of griseofulvin. The ion peaks at *m/z* 353.3 and 355.3 with the ratio of 3:1 were characteristic for the presence of a chlorine atom in the structure. The ^{1}H NMR spectrum showed the presence of one aromatic proton at δ_H 6.42 (1H, s, H-5), one olefinic proton at δ_H 5.63 (1H, s, H-2'), three methoxy groups at δ_H 4.04 (3H, s, 4-OCH_3), 3.98 (3H, s, 6-OCH_3) and 3.69 (3H, s, 1'-OCH_3), of which both 4-OCH_3 and 6-OCH_3 were assigned to the aromatic ring. Additionally one methyl group was detected at δ_H 0.92 (3H, d, J = 6.4 Hz, 5'-CH_3), as well as three aliphatic protons, including one methylene group at δ_H 2.86 (1H, m, overlapping, H-4'a) and 2.43 (1H, dd, J = 15.4, 3.3 Hz, H-4'b),] and one methine proton at δ_H 2.86 (1H, m, overlapping, H-5'), which were connected to each other as deduced by the ^{1}H–^{1}H COSY spectrum. These signals were identical to the reported data for griseofulvin (Table 3.3.2) (Park *et al.*, 2005). Furthermore the optical rotation value of **32** ($[\alpha]^{20}_D$ +92) was in accordance with that of griseofulvin both measured in the same solvent and at a similar concentration, confirming the same configuration. Based on the above mentioned data, **32** was elucidated as griseofulvin.

Griseofulvin is used orally as an antifungal drug for infections of the skin, hair and nails. It is produced by many species of *Penicillium,* such as *P. griseofulvum*, *P. patulum*, *P. urticae*, *P. nigricans*, and *P. sclerotigenum*, and also by species of other genera, e.g. *Aspergillus versicolor, Streptomyces albolongus* and *Xylaria* species.

Table 3.3.2 ^{1}H NMR comparison of **32** and griseofulvin.

Position	**32**	Griseofulvin[b]
	δ_H (CD_3OD, 500 MHz, J in Hz)	δ_H ($CDCl_3$, 500 MHz, J in Hz)
4-OCH_3	4.04 (s)[a]	4.04 (s)
5	6.42 (s)	6.14 (s)
6-OCH_3	3.98 (s)[a]	4.04 (s)
1'-OCH_3	3.69 (s)	3.63 (s)
2'	5.63 (s)	5.55 (s)
4'	2.43 (dd, 15.4, 3.3)	2.44 (dd, 16.7, 4.6)
	2.86 (m, overlapping)	3.04 (dd, 16.0, 3.5)
5'	2.86 (m, overlapping)	2.86 (m)
5'-CH_3	0.92 (d, 6.4)	0.97 (d, 6.8)

[a] could be exchanged, [b] Park *et al.*, 2005

3.3.1.3 Dechlorogriseofulvin (33, known compound)

Dechlorogriseofulvin	
Biological Source	*Penicillium* sp. strain IO1
Sample Code	%40 Hex IO3 32-39 P1
Sample Amount	5.32 mg
Molecular Formula	$C_{17}H_{18}O_6$
Molecular Weight	318 g/mol
Solubility	$CHCl_3$, MeOH
Physical Description	Yellow powder
Optical rotation	$[\alpha]^{20}_D$ +119
HPLC Retention Time	23.39 min (standard gradient)

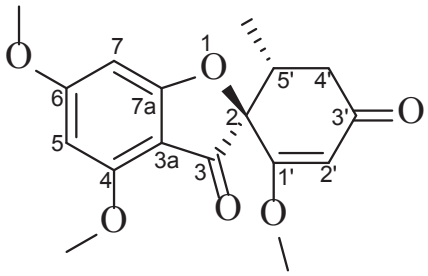

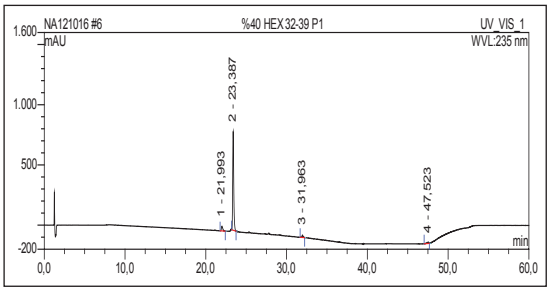

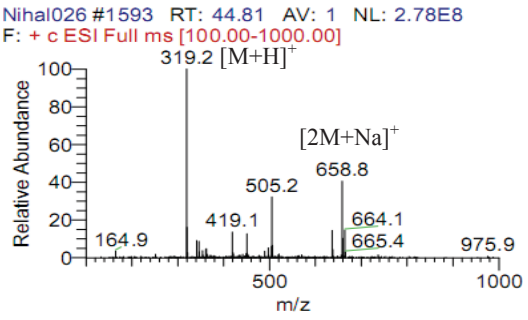

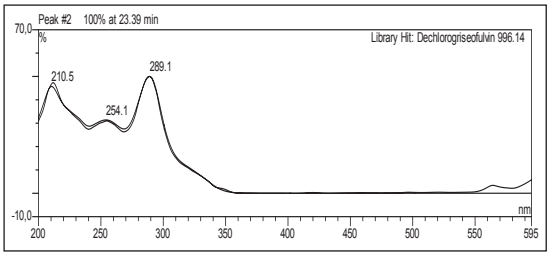

No ionisation in negative mode.

Dechlorogriseofulvin (**33**) was isolated as a yellow powder from *Penicillium* sp. strain IO1. It displayed UV absorptions at λ_{max} (MeOH) 210, 254 and 289 nm, which were in accordance with dechlorogriseofulvin. The positive molecular ion peaks at *m/z* 319.2 $[M + H]^+$ and 658.8 $[2M + Na]^+$ indicated the molecular weight of 318 g/mol, 34 amu less than that of **32**, which is in agreement with the chlorine atom replaced by a proton. Comparison of the ^{1}H NMR spectrum of **33** with those of **32** indicated the signals to be similar, except for one more aromatic proton in **33**, In addition, the coupling constant of H-5/7 (^3J = 1.8 Hz) implied a *meta*-position of these two protons, that further confirmed the replacement of the chlorine atom (Cl-7) of **32** by a proton (H-7) in **33**. The remaining protons included those of one olefinic proton at δ_H 5.61 (1H, s, H-2'), three methoxy groups at δ_H 3.92 (3H, s, 4-OCH_3), 3.89 (3H, s, 6-OCH_3) and 3.68 (3H, s, 1'-OCH_3), one methyl group at 0.92 (3H, d, J = 6.6 Hz, 5'-CH_3), as well as three aliphatic protons, which composed one methylene group at δ_H 2.91 (1H, dd, J = 16.7, 13.4 Hz, H-4'a) and 2.41 (1H, dd, J = 16.7, 4.7 Hz, H-4'b), and one methine proton at δ_H 2.77 (1H, m, H-5') (Table 3.3.3). All spectroscopic and spectrometric data were in excellent agreement with those reported for dechlorogriseofulvin (Park *et al.*, 2005).

Table 3.3.3 ^{1}H NMR data comparison of **33** and dechlorogriseofulvin.

Position	**33**	Dechlorogriseofulvin[a]
	δ_H (CD_3OD, 500 MHz, J in Hz)	δ_H ($CDCl_3$, 500 MHz, J in Hz)
4-OCH_3	3.92 (s)	3.63 (s)
5	6.35 (d, 1.8)	6.24 (d, 1.8)
7	6.20 (d, 1.8)	6.05 (d, 1.7)
6-OCH_3	3.89 (s)	3.90 (s)
1'-OCH_3	3.68 (s)	3.91 (s)
2'	5.61 (s)	5.55 (s)
4'	2.41 (dd, 16.7, 4.7)	2.41 (dd, 16.8, 4.7)
	2.91 (dd, 16.7, 13.4)	3.05 (dd, 16.8, 13.4)
5'	2.77 (m)	2.75 (m)
5'-CH_3	0.92 (d, 6.6)	0.97 (d, 6.7)

[a] Park *et al*., 2005

3.3.2 Secondary metabolites from *Penicillium* sp. strain IO2.

3.3.2.1 Dehydrocurvularin (34, known compound)

Dehydrocurvularin	
Biological Source	*Penicillium* sp. strain IO2
Sample Code	%40 Hex SS6 29-53 mp(4), IO2 60Hex S3
Sample Amount	5.32 mg
Molecular Formula	$C_{16}H_{18}O_5$
Molecular Weight	290 g/mol
Solubility	MeOH
Physical Description	Yellow powder
Optical rotation	$[\alpha]^{20}_{D}$ -44
HPLC Retention Time	21.85 min (standard gradient)

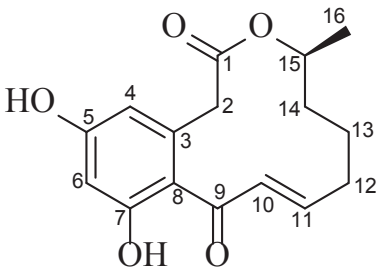

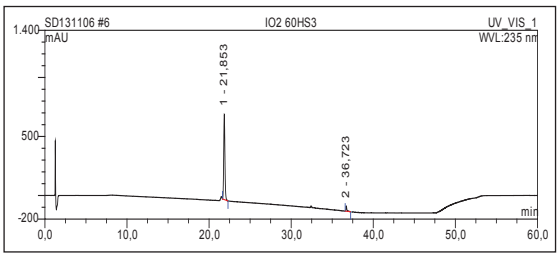

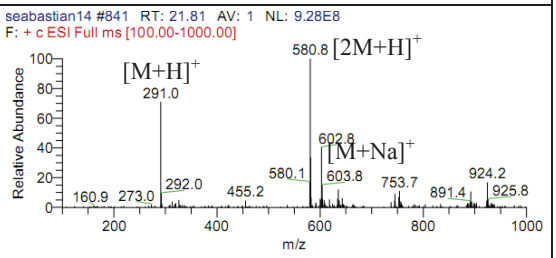

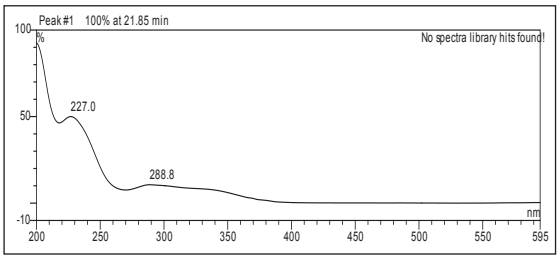

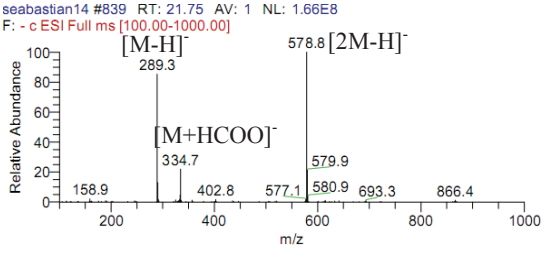

Dehydrocurvularin (**34**) was isolated as a yellow powder from *Penicillium* sp. strain IO2. It showed UV absorptions at λ_{max} (MeOH) 227 and 288 nm. Its molecular weight was established as 290 g/mol on the basis of the molecular ion peaks observed at *m/z* 291.0 $[M + H]^+$, 580.8 $[2M + H]^+$ and 603.8 $[2M + Na]^+$ in the positive mode and at *m/z* 289.3 $[M - H]^-$, 334.7 $[M + HCOO]^-$ and 578.8 $[2M - H]^-$ in the negative mode by ESI-MS analysis. Inspection of the ^{1}H NMR spectrum revealed the presence of two *meta*-positioned aromatic protons at δ_H 6.33 (1H, d, J = 2.0 Hz, H-4) and 6.29 (1H, d, J = 2.0 Hz, H-6), and two olefinic protons at δ_H 6.60 (1H, m, H-11) and 6.54 (1H, d, J = 15.4 Hz, H-10). One oxygen-substituted methine group was detected at δ_H 6.82 (1H, m, H-15), two separate methylene protons at δ_H 3.77 (H-2a) and 3.49 (H-2b), which displayed a geminal coupling with J = 16.8 Hz, one methyl group at δ_H 1.23 (3H, d, J = 6.5 Hz, H_3-16), as well as three additional methylene groups at δ_H 2.43 (1H, m, H-12a), 2.36 (1H, m, H-12b), and at 2.02 (1H, m, H-13a), 1.90 (1H, m, H-14a) and 1.62 (2H, m, H-13b/14b). From the ^{1}H–^{1}H COSY spectrum, the spin system beginning at H-10 and extending to H_3-16 was deduced according to the cross-peaks. The planar structure was determined by comparison of the UV, ESI and ^{1}H NMR (Table 3.3.4) data and by comparison with those reported for dehydrocurvularin (Greve *et al.*, 2008).

The geometry of the Δ^{10} double bond was assigned as *E* from the coupling constant of $^3J_{12, 13}$ = 15.4 Hz. The configuration of C-15 in published curvularins was determined on the basis of their optical rotation and CD spectra. The compounds with negative $[\alpha]_D$ value were consistent with a negative cotton effect due to the n-π* transition band of the lactone at 229-235 nm, while the enantiomer with positive value of $[\alpha]_D$ was consistent with the positive sign of the cotton effect in the CD spectra (Bicalho *et al.*, 2003; Greve *et al.*, 2008). In addition, based on the optical rotation of **34**, which is on the negative side, as observed for dehydrocurvularin, the *S* configuration was assigned to C-15. Dehydrocurvularin was reported before as a secondary metabolite from species of the genera *Penicillium*, *Curvularia*, and *Alternaria*.

3.3.2.2 Curvularin (35, known compound)

Curvularin	
Biological Source	*Penicillium* sp. strain IO2
Sample Code	%40 Hex SS6 29-53 MP 5, CoCul 20Hex S4 Semi2 IO2 40Hex S4 Semi6
Sample Amount	8.72 mg
Molecular Formula	$C_{16}H_{20}O_5$
Molecular Weight	292 g/mol
Solubility	MeOH
Physical Description	Colorless slice crystal
HPLC Retention Time	23.10 min (standard gradient)

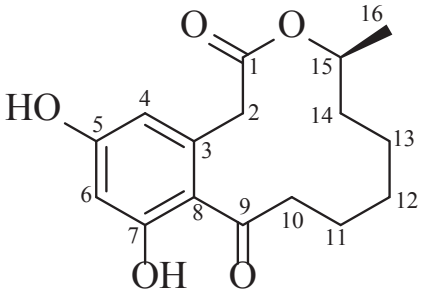

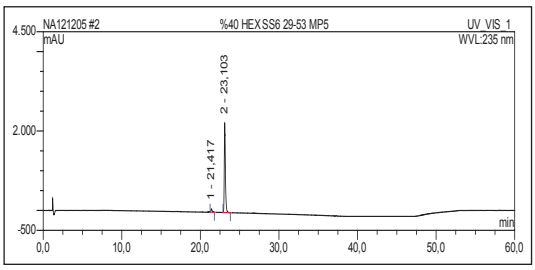

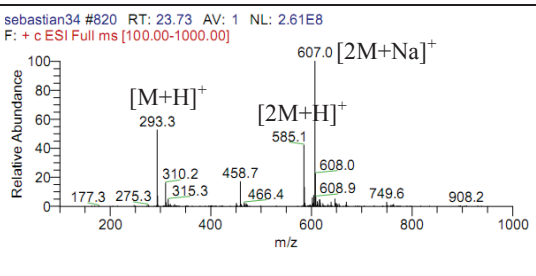

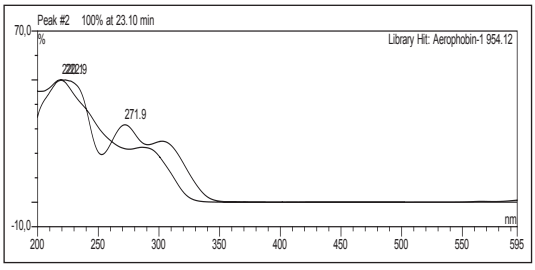

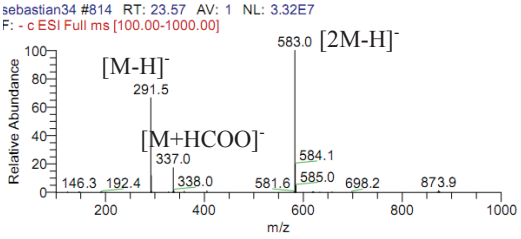

Curvularin (**35**) was isolated as a yellow powder from *Penicillium* sp. strain IO2. It showed UV absorptions at λ_{max} (MeOH) 222, 272 and 303 nm. Positive and negative ion peaks observed at *m/z* 293.3 $[M + H]^+$, 585.1 $[2M + H]^+$, and 607.0 $[2M + Na]^+$, and at 291.5 $[M - H]^-$, 337.0 $[M + HCOO]^-$ and 583.0 $[2M - H]^-$, respectively, indicated a molecular weight of 292 g/mol, with a 2 amu increase compared to **34**. The ^{1}H NMR spectrum of **35** exhibited two *meta*-coupled protons at δ_H 6.30 (1H, d, J = 2.2 Hz, H-6) and 6.26 (1H, d, J = 2.2 Hz, H-4), reminiscent of the signals in the aromatic moiety of **34**. In the macrolide substructure, one oxygen-substituted methine group at δ_H 4.96 (1H, m, H-15), two separated methylene protons at δ_H 3.90 (H-2a) and 3.67 (H-2b), which displayed geminal coupling with J = 15.8 Hz, one methyl group at δ_H 1.17 (3H, d, J = 6.3 Hz, H_3-16), as well as three further methylene groups (CH_2-12, CH_2-13 and CH_2-14) were observed (Table 3.3.4). However, the olefinic protons H-10/11 of **34** were not detectable in **35**. Instead, the ^{1}H NMR spectrum of **35** revealed two additional methylene groups at δ_H 3.25 (1H, ddd, J = 15.3, 8.8, 2.7 Hz, H-10a) and 2.79 (1H, ddd, J = 15.5, 9.7, 2.8 Hz, H-10b), and at δ_H 1.79 (1H, m, H-11a) and 1.61 (1H, m, H-11b), respectively. Based on the data mentioned above, as well as by comparison with the literature, **35** was assigned as curvularin (Bicalho *et al.*, 2003, Greve *et al.*, 2008).

Table 3.3.4 ^{1}H NMR data comparison of **34** and **35** (δ_H in ppm, J in Hz).

Position	**34** (CD_3OD, 500 MHz)	**35** (CD_3OD, 500 MHz)
2	3.77 (d, 16.8) 3.49 (d, 16.8)	3.90 (d, 15.8) 3.67 (d, 15.8)
4	6.33 (d, 2.0)	6.26 (d, 2.2)
6	6.29 (d, 2.0)	6.30 (d, 2.2)
10	6.54 (d, 15.4)	3.25 (ddd, 15.3, 8.8, 2.7) 2.79 (ddd, 15.5, 9.7, 2.8)
11	6.60 (m)	1.79 (m) 1.61 (m)
12	2.43 (m) 2.36 (m)	1.55-1.43 (m) 1.30-1.36 (m)
13	2.02 (m) 1.62 (m)	1.55-1.43 (m) 1.30-1.36 (m)
14	1.90 (m) 1.62 (m)	1.65-1.60 (m) 1.30-1.36 (m)
15	6.82 (m)	4.96 (m)
16	1.23 (d, 6.5)	1.17 (d, 6.3)

3.3.2.3 Trichodimerol (36, known compound)

Trichodimerol	
Biological Source	*Penicillium* sp. strain IO2
Sample Code	IO2 40Hex S3 Semi9
Sample Amount	7.12 mg
Molecular Formula	$C_{28}H_{32}O_8$
Molecular Weight	496 g/mol
Solubility	MeOH
Physical Description	Pale yellow powder
HPLC Retention Time	31.27 min (standard gradient)

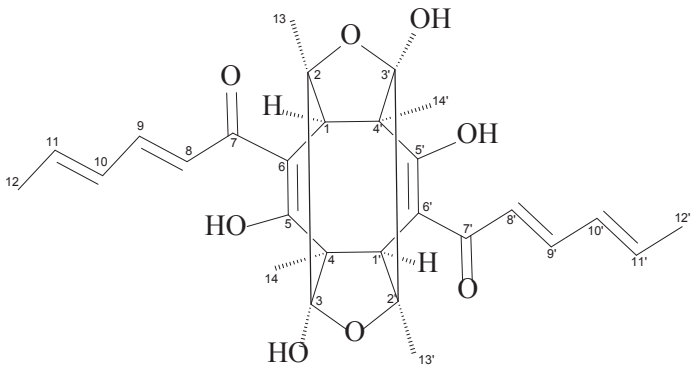

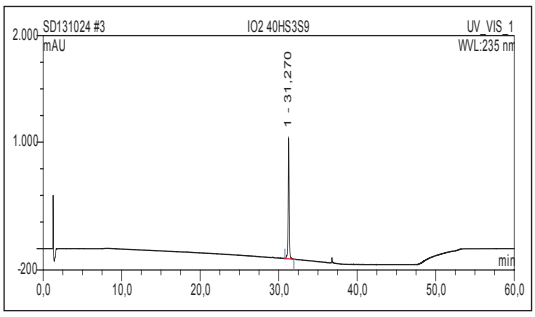

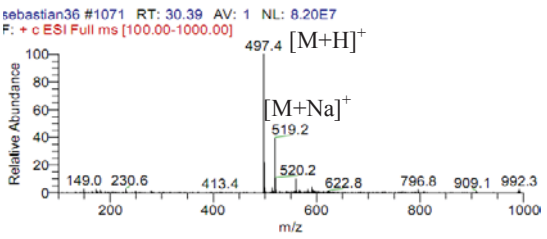

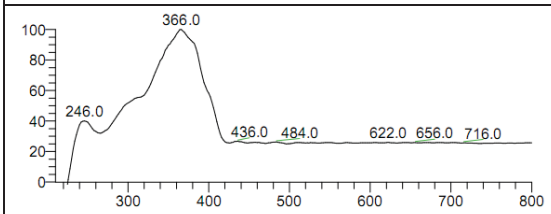

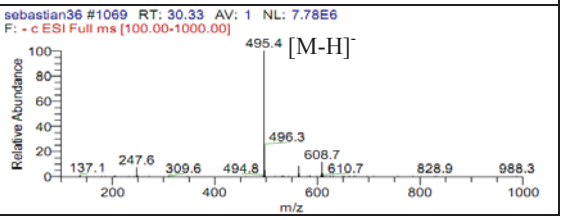

Trichodimerol (**36**) was isolated as a pale yellow powder from *Penicillium* sp. strain IO2 and showed UV absorption at λ_{max} (MeOH) 366 nm. Its molecular formula was established as $C_{28}H_{33}O_8$ according to the $[M + H]^+$ signal at 497.2171 (calc. for 497.2170) in the HRESIMS spectrum, indicating 13 degrees of unsaturation. The ^{13}C NMR spectrum showed 14 signals, suggesting the presence of a symmetrical structure. Accordingly, eight signals were observed in the ^1H NMR spectrum, which comprised four olefinic protons at δ_H 7.21 (1H, dd, J = 14.7, 11.0 Hz, H-9/9'), 6.43 (1H, m, overlapping, H-10/10'), 6.41 (1H, d, J = 14.3 Hz, H-8/8') and 6.27 (1H, m, H-11/11'), that all constituted the hexa-2,4-dienone side chains together with the methyl group at δ_H 1.85 (3H, d, J = 6.7 Hz, H-12/12'), as shown by the continuous ^1H–^1H COSY correlations extending from H-8/8' to H_3-12/12'. Moreover, one singlet methine at δ_H 3.04 (1H, s, H-1/1'), and two additional methyl groups at δ_H 1.26 (3H, s, H-14/14') and 1.25 (3H, s, H-13/13') were present in the ^1H NMR spectrum. The ^{13}C NMR spectrum showed the corresponding carbons of the side chain with one methyl group at δ_C 18.6 (C-12/12'), four sp^2 methine groups at δ_C 142.5 (C-9/9'), 140.0 (C-11/11'), 131.1 (C-10/10'), and 119.3 (C-8/8'), and one carbonyl group at δ_C 174.8 (C-7/7') (Table 3.3.5). These substructures were confirmed by interpretation of the HMBC spectrum, showing correlations from H_3-12/12' to C-10/10' and C-11/11', from H-11/11' to C-9/9', C-10/10' and C-12/12', from H-9/9' to C-8/8', C-10/10' and C-11/11', and from H-8/8' to C-7/7'. As deduced from the DEPT experiment, two additional sp^2 carbons were present in the molecule at δ_C 200.5 (C-5/5') and 103.5 (C-6/6'). The remaining carbons were attributed to two methyl groups at δ_C 21.4 (C-13/13') and 19.5 (C-14/14'), one methylene group at δ_C 56.4 (C-1/1'), as well as three methine groups, including one monooxygenated and one dioxygenated carbon at δ_C 78.6 (C-2/2') and 104.1 (C-3/3'). These functionalities accounted for 7 of the 13 degrees of unsaturation, and thus 5 rings were assigned in the structure. Compound **36** was finally determined as trichodimerol on the basis of UV, MS, ^1H NMR, ^{13}C NMR, ^1H–^1H COSY and HMBC data (Andrade, Ayer and Mebe, 1992). Trichodimerol, belong to bisorbicillinoids, firstly was isolated from *Trichoderma* sp., and later was found in cultures of species belonging to the genera *Penicillium* and *Phialocephala*.

Table 3.3.5 ^{1}H and ^{13}C NMR data comparison of **36** and trichodimerol.

Position	**36** (DMSO-d_6 , J in Hz)		Trichodimerol[a] ($CDCl_3$, J in Hz)	
	^{1}H (500 MHz)	^{13}C (125 MHz)	^{1}H (360 MHz)	^{13}C (75.5 MHz)
1/1'	3.04 (s)	56.4	3.00 (s)	57.6
2/2'		78.6		78.9
3/3'		104.1		104.1
4/4'		59.4		58.9
5/5'		200.5		197.9
6/6'		103.5		102.8
7/7'		174.8		176.0
8/8'	6.41 (d, 14.3)	119.3	6.11-6.34 (m)	118.6
9/9'	7.21 (dd, 14.7, 11.0)	142.5	7.32 (dd, 15.5, 10.0)	143.6
10/10'	6.43 (m, overlapping)	131.1	6.11-6.34 (m)	131.0
11/11'	6.27 (m)	140.0	6.11-6.34 (m)	140.3
12/12'	1.85 (d, 6.7)	18.6	1.89 (d, 6.5)	18.7
13/13'	1.25 (s)	21.4	1.43 (s)	21.3
14/14'	1.26 (s)	19.5	1.46 (s)	18.9

[a] Andrade *et al.*, 1992

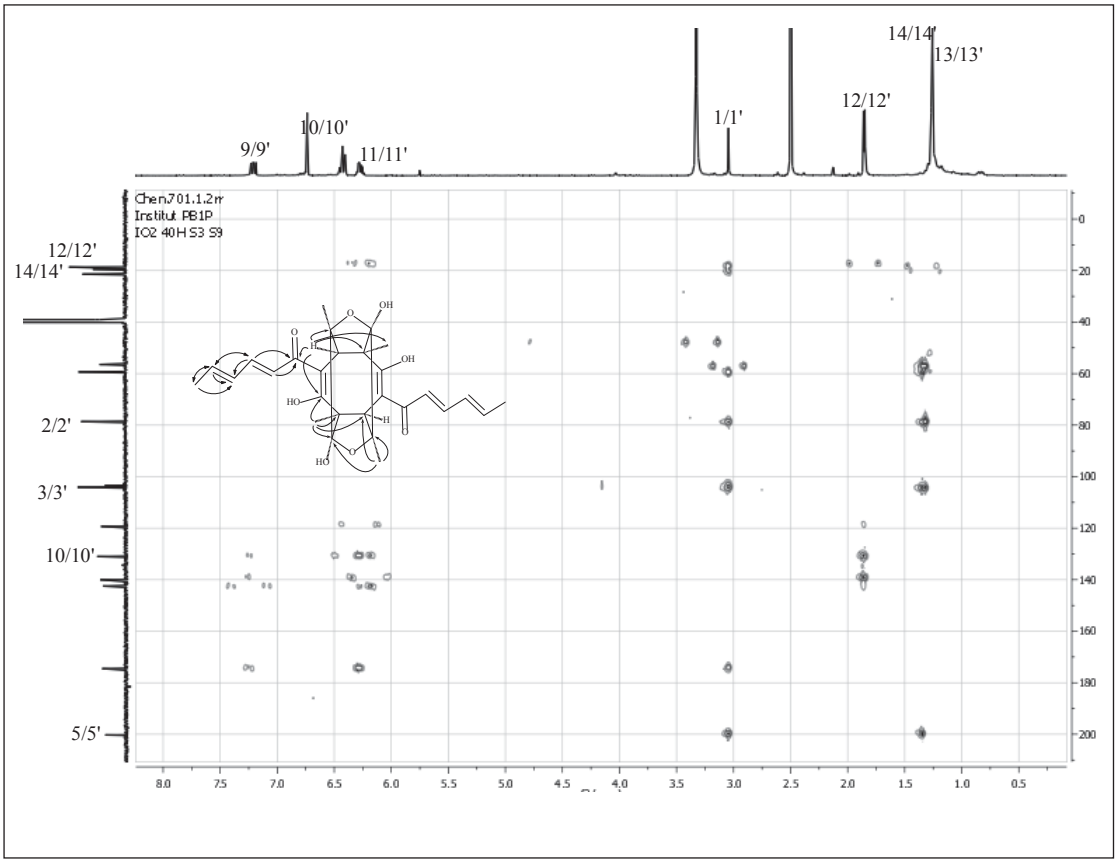

Figure 3.3.7 HMBC spectrum of **36**.

3.3.3 Experiment of co-cultivation of two *Penicillium* sp. strains IO1 and IO2.

3.3.3.1 Norlichexanthone (37, known compound)

Norlichexanthone	
Biological Source	Co-culture of *Penicillium* sp. strains IO1 and IO2
Sample Code	CoCul 40 Hex S7
Sample Amount	19.8 mg
Molecular Formula	$C_{14}H_{10}O_5$
Molecular Weight	258 g/mol
Solubility	MeOH
Physical Description	Yellow amorphous solid
HPLC Retention Time	30.47 min (standard gradient)

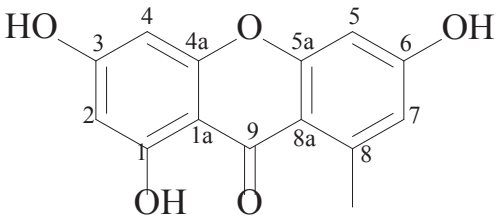

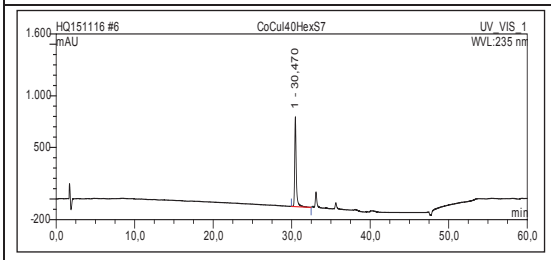

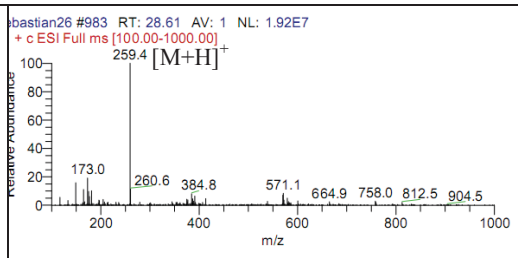

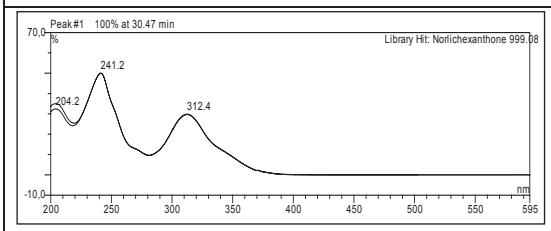

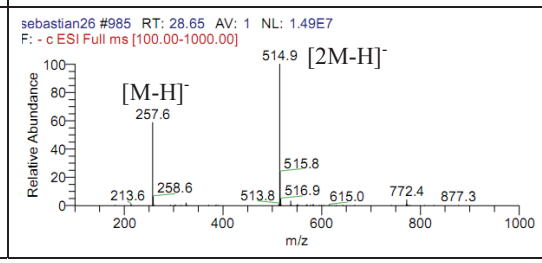

Norlichexanthone (**37**) was isolated as a yellow amorphous solid from the co-cultivation experiment of the *Penicillium* sp. strains IO1 and IO2. The UV spectrum showed absorptions at λ_{max} (MeOH) 241 and 312 nm, characteristic of xanthone derivatives. The molecular weight of 258 g/mol was indicated by the signals observed in the positive ESI mode at 259.4 $[M + H]^+$ and in the negative ESI mode at 257.6 $[M - H]^-$ and 514.9 $[2M - H]^-$. The ^1H NMR spectrum presented two pairs of *meta*-coupled protons at δ_H 6.63 (1H, br. s, H-7), 6.62 (1H, br. s, H-5), 6.26 (1H, d, J = 2.1 Hz, H-4) and 6.11 (1H, d, J = 2.1 Hz, H-2), one phenolic methyl group at δ_H 2.71 (1H, s, 8-CH_3), and three hydroxy groups at δ_H 13.4 (1H, s, 1-OH), and 10.9 (2H, s, 3/6-OH). In addition, fourteen carbons were observed in the ^{13}C NMR spectrum of **37**. These consisted of four methine carbons at δ_C 110.8 (C-7), 100.5 (C-5), 97.8 (C-2) and 93.2 (C-4) and eight quaternary carbons. The remaining carbons were assigned to one methyl group at δ_C 22.9 (C-8) and one carbonyl group at δ_C 181.4 (C-9). The substitution pattern of **37** was deduced from the HMBC spectrum (Figure 3.3.8), which exhibited correlations from the methyl group 8-CH_3 to C-7, C-8 (δ_C 142.7) and C-8a (δ_C 116.1), from H-2 to C-1a (δ_C 102.1) and C-3 (δ_C 164.7), from H-4 to C-2, C-3 (δ_C 164.7), C-1a (δ_C 102.1) and C-4a (δ_C 156.5), from H-5 to C-5a (δ_C 162.8), C-6 (δ_C 158.7) and C-8a (δ_C 116.1), and from H-7 to C-5. Therefore, based on the above-mentioned data and by comparison with the literature (Broadbent, Mabelis and Spencer, 1975; Yang, *et al*., 2013), compound **37** was determined as norlichexanthone.

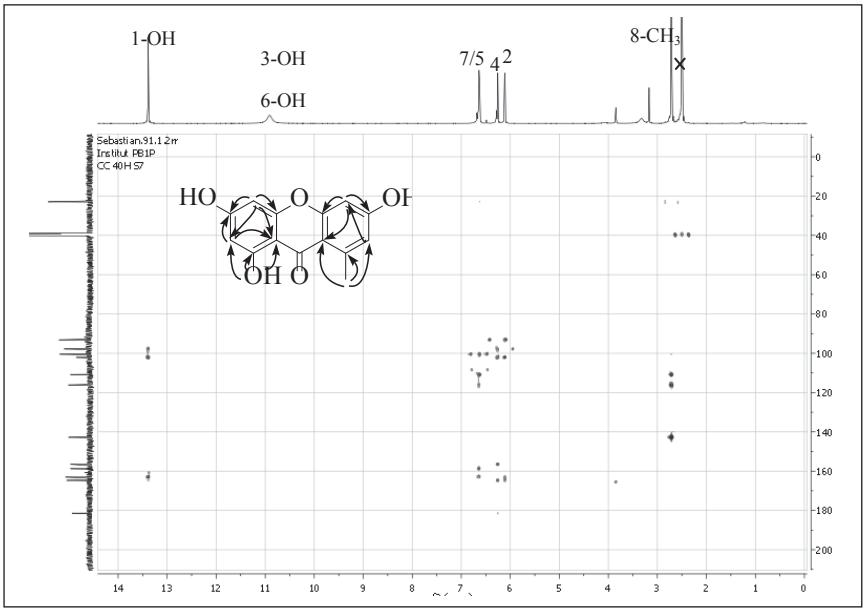

Figure 3.3.8 HMBC spectrum of **37**.

Table 3.3.6 ^{1}H and ^{13}C NMR data comparison of **37** and norlichexanthone.

Position	**37** (DMSO-d_6 , J in Hz)		norlichexanthone[a] (Acetone-d_6, J in Hz)
	^{1}H (500 MHz)	^{13}C (125 MHz)	^{1}H (300 MHz)
1		56.4	
1a		78.6	
2	6.11 (1H, d, 2.1)	104.1	6.16 (1H, d, 2.0)
3		59.4	
4	6.26 (1H, d, 2.1)	200.5	6.27 (1H, d, 2.0)
4a		103.5	
5	6.62 (1H, br s)	174.8	6.67 (1H, s)
5a		119.3	
6		142.5	
7	6.63 (1H, br s)	131.1	6.67 (1H, s)
8		140.0	
8a		18.6	
9		21.4	
8-CH_3	2.71 (3H, s)		2.76 (3H, s)
1-OH	13.4 (1H, s)		13.41 (1H, s)
3-OH	10.9 (1H, s)		9.65 (1H, s)
6-OH	10.9 (1H, s)		9.65 (1H, s)

[a] Yang *et al*., 2013

3.3.3.2 Monocerin (38, known compound)

Monocerin	
Biological Source	Co-culture of *Penicillium* sp. strains IO1 and IO2
Sample Code	%40 Hex IO3 32-39 P2, Co-Cul 20Hex S3
Sample Amount	14.5 mg
Molecular Formula	$C_{16}H_{20}O_6$
Molecular Weight	308 g/mol
Solubility	MeOH
Physical Description	Yellow gel
HPLC Retention Time	25.41 min (standard gradient)

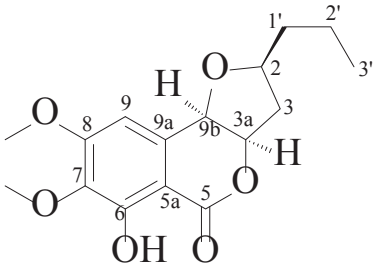

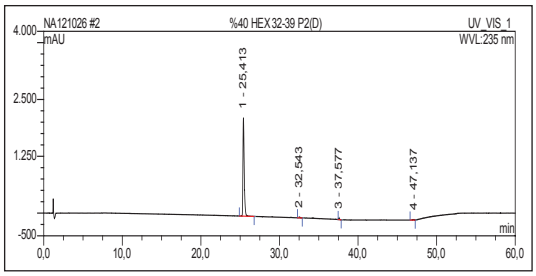

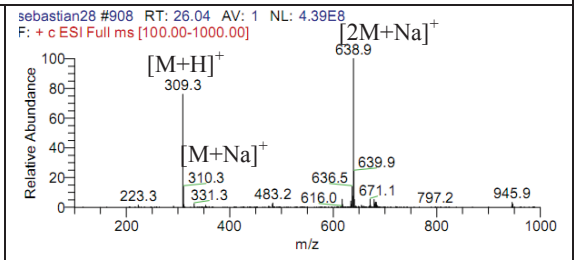

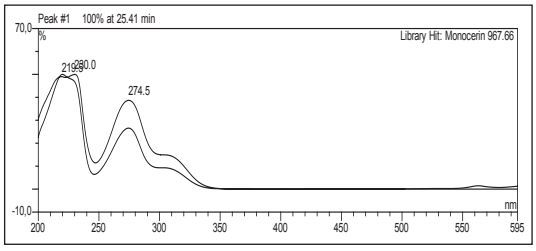

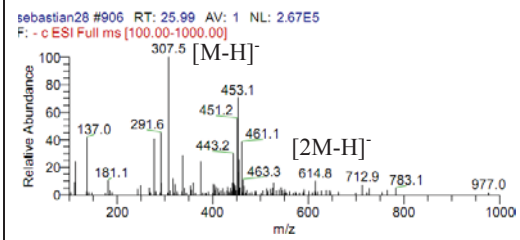

Monocerin (**38**) was isolated as a yellow gel from co-cultivation experiments of the two *Penicillium* sp. strains IO1 and IO2. It displayed UV absorptions at λ_{max} (MeOH) 219 and 274 nm. Positive and negative ESI-MS ionization peaks were detected at 309.3 $[M + H]^+$, 331.3 $[M + Na]^+$, 638.9 $[2M + Na]^+$, 307.5 $[M - H]^-$ and 614.8 $[2M - H]^-$, indicating a molecular weight of 308 g/mol. The ^{1}H NMR spectrum of **38** showed one singlet phenylic proton at δ_H 6.78 (1H, s, H-9), two methoxy groups at δ_H 3.96 (3H, s, 7-OCH_3) and 3.83 (3H, s, 8-OCH_3), which were assigned to the phenylic moiety due to their downfield chemical shifts, one methyl group at δ_H 0.93 (3H, d, J = 7.4 Hz, H_3-3'), as well as a series of aliphatic protons (Table 3.3.7). The latter belonged to a spin system, which was connected sequentially as CH_3(3')CH_2(2')CH_2(1')CH(2)CH_2(3)CH(3a)CH(9b) by the cross-peaks in the ^{1}H–^{1}H COSY spectrum. By further comparison with monocerin, the aforementioned data were consistent with those reported in the literature (Fang *et al*., 2013). Monocerin is a dihydroisocoumarin obtained from several fungal species such as *Drechslera monoceras*, *D. ravenelii*, *Exserohilum turcicum* and *Fusarium larvarum*. Due to its interesting biological properties as antifungal, insecticidal, plant pathogenic, and phytotoxic agent, this natural product has been subjected to total synthesis studies (Fang *et al*., 2013; Dillon, Simpson and Sweeney, 1992; Cassidy *et al*., 2006).

Table 3.3.7 ^{1}H NMR data comparison of **38** and monocerin.

Position	**38** δ_H (CD_3OD, 500 MHz, J in Hz)	Monocerin[b] δ_H ($CDCl_3$, 500 MHz, J in Hz)
2	4.14 (m)	4.13 (dt, 14.8, 6.3)
3	2.66 (ddd, 14.5, 8.5, 5.8)	2.60 (ddd, 14.6, 8.5, 6.2)
	2.05 (dd, 14.4, 5.5)	2.17 (dd, 14.5, 5.8)
3a	5.11 (d, 3.5)	5.06 (dd, 5.3, 3.0)
7-OCH_3	3.96 (s)[a]	3.96 (s)
8-OCH_3	3.83 (s)[a]	3.90 (s)
9	6.78 (s)	6.60 (s)
9b	4.65 (d, 2.2)	4.55 (d, 3.0)
1'	1.55 (m)	1.64-1.52 (m)
	1.61 (m)	1.74-1.66 (m)
2'	1.35 (m)	1.50-1.29 (2H, m)
	1.44 (m)	
3'	0.93 (d, 7.4)	0.92 (d, 7.3)

[a] could be exchanged, [b] Fang *et al.*, 2013

3.3.3.3 Griseophenone B (39, known compound)

Griseophenone B	
Biological Source	Co-culture of *Penicillium* sp. strains IO1 and IO2
Sample Code	%40 Hex IO3 53-65
Sample Amount	0.2 mg
Molecular Formula	$C_{16}H_{15}ClO_6$
Molecular Weight	338 g/mol
Solubility	MeOH
HPLC Retention Time	23.45 min (standard gradient)

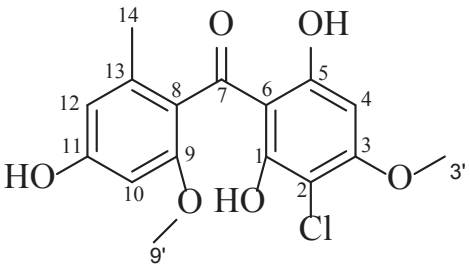

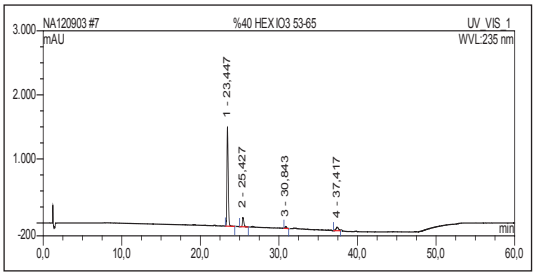

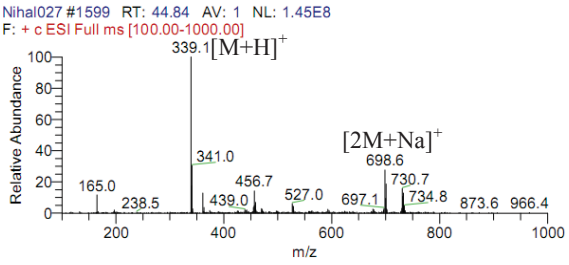

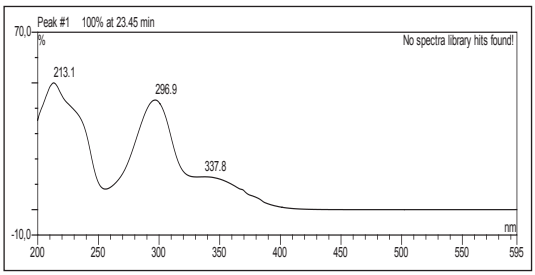

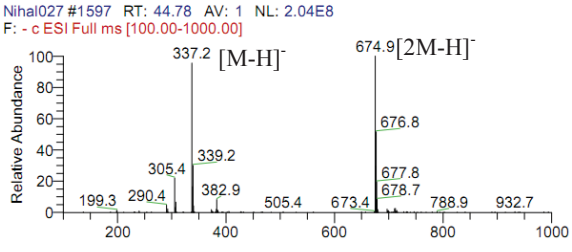

Griseophenone B (**39**) was isolated from the co-cultivation experiment of the two *Penicillium* sp. strains IO1 and IO2 on solid rice medium. It showed UV absorptions at λ_{max} (MeOH) 213 and 296 nm. The positive and negative ESI-MS spectrum of **39** showed the presence of molecular ion peaks at *m/z* 339.1 and 341.0 $[M + H]^+$, as well as at *m/z* 337.2 and 339.2 $[M - H]^-$, respectively, with the characteristic isotope pattern (3:1 ratio) caused by one chloro atom in the molecule. The ^{1}H NMR spectrum of **39** showed the presence of three aromatic protons including one *meta*-coupled pair, which appeared as doublets at δ_H 6.26 (1H, d, J = 2.0 Hz, H-10) and 6.24 (1H, d, J = 2.0 Hz, H-12), and one singlet proton at δ_H 6.04 (H-4). Furthermore, three methyl signals were detected as singlets, two of which were assigned as aromatic methoxy groups according to their downfield chemical shifts at δ_H 3.88 (OCH_3-3') and 3.65 (OCH_3-9'), whereas the third one was determined as an aromatic methyl group at δ_H 2.08 (CH_3-14). The structure of **39** was conclusively determined by further literature comparison, and was identified as griseophenone B on the basis of the UV, ESI-MS and ^{1}H NMR data (Table 3.3.8) (Cacho *et al*., 2013).

Table 3.3.8 ^{1}H NMR data comparison of **39** and griseophenone B.

Position	**39**	Griseophenone B[a]
	δ_H (CD_3OD, 500 MHz, J in Hz)	δ_H ($(CD_3)_2CO$, 500 MHz, J in Hz)
3'	3.88 (s)	3.90 (s)
4	6.04 (s)	6.16 (s)
9'	3.65 (s)	3.63 (s)
10	6.26 (d, 2.0)	6.32 (d, 1.8)
12	6.24 (d, 2.0)	6.31 (d, 1.8)
14	2.08 (s)	2.08 (s)

[a] Cacho *et al.*, 2013

3.3.3.4 Echinulin (40, known compound)

Echinulin	
Biological Source	Co-culture of *Penicillium* sp. strains IO1 and IO2
Sample Code	Fr %100 EtOAc Peak 2
Sample Amount	0.6 mg
Molecular Formula	$C_{29}H_{39}N_3O_2$
Molecular Weight	461 g/mol
Solubility	MeOH
HPLC Retention Time	33.83 min (standard gradient)

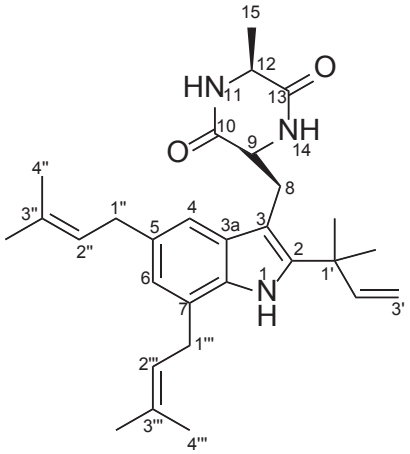

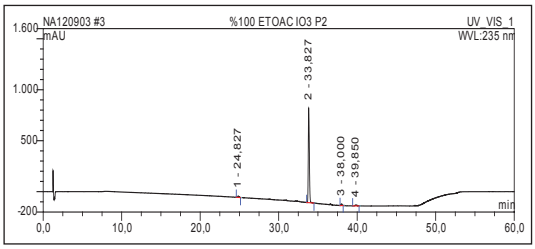

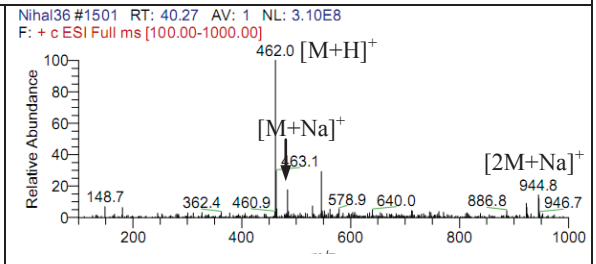

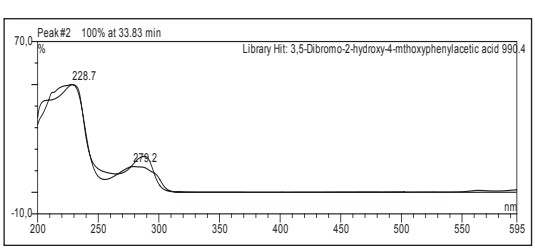

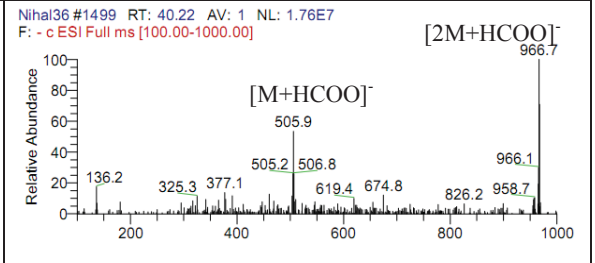

Echinulin (**40**) was isolated from co-cultivation experiments of *Penicillium* sp. strains IO1 and IO2. It showed UV absorptions at λ_{max} (MeOH) 228 and 279 nm. Positive and negative

ion peaks given by the ESI-MS spectrum at 462.0 $[M + H]^+$, 484 $[M + Na]^+$, 944.8 $[2M + Na]^+$, 505.9 $[M + HCOO]^-$ and 966.7 $[2M + HCOO]^-$ indicated a molecular weight of 461 g/mol. The odd number of the molecular weight suggested the presence of an odd number of nitrogen atoms in its structure. The ^{1}H NMR spectrum presented two *meta*-coupled aromatic proton singlets of an indole system at δ_H 7.13 (H-4) and 6.80 (H-6). Moreover, analysis of the ^{1}H NMR and HSQC spectra revealed the presence of seven methyl groups (H_3-15, 1'-CH_3 x 2, H_3-4", H_3-5", H_3-4'", and H_3-5'"), two methine groups (H-9 and H-12), three olefinic protons (H-2', H-2", H-2'"), three methylene groups, as well as three amine protons (NH-1, NH-11, and NH-14) (Table 3.3.9). Detailed analysis of 1D and 2D NMR data of **40**, indicated the presence of a tetrasubstituted indole moiety together with a diketopiperazine system in the structure. Moreover, two prenyl subunits were located at C-5 and C-7 of the indole moiety. Each subunit was determined according to their HMBC correlations. The former showed correlations from H-4" (δ_H 1.735) to C-2" (δ_C 124.3), C-3" (δ_C 131.3) and C-5" (δ_C 17.88), from H-5" (δ_H 1.74) to C-2" (δ_C 124.3), C-3" and C-4" (δ_C 25.8), and from H-1" (δ_H 3.39) to C-5 (δ_C 132.2), C-2" and C-3", while the latter subunit showed correlations from H-4'" (δ_H 1.81) to C-2'" (δ_C 122.8), C-3'" (δ_C 132.9) and C-5'" (δ_C 17.9), and from H-5'" (δ_H 1.87) to C-2'" (δ_C 122.8), C-3'" and C-4'" (δ_C 25.7). The 3-methylbut-1-en substituent of the indole core located at C-2 was deduced from the HMBC correlations from H_2-3' (δ_H 5.16 and 5.15) to C-1' (δ_C 39.1) and C-2' (δ_C 145.6), and from both geminal methyl groups (δ_H 1.51 x 2) to C-2 (δ_C 141.2), C-1' (δ_C 39.1) and C-2' (δ_C 145.6). The last substituent was identified as an alanine anhydride moiety, as deduced from the presence of two secondary amine protons at δ_H 5.83 (NH-11) and 5.65 (NH-14), and an additional methyl group at δ_H 1.53 (d, J = 7.0 Hz, CH_3-15) further coupled to a methine proton at δ_H 4.09 (q, J = 7.0 Hz, H-12). The latter was positioned by its HMBC correlations to C-12 (δ_C 50.8) and to one of the two carbonyl functions at C-13 (δ_C 167.6). The alanine anhydride function was linked via a methylene bridge (δ_H 3.66 and 3.19, H_2-8) to C-3 of the indole core, as supported by the cross-peaks in the HMBC spectrum showing correlations to C-2 (δ_C 141.2), C-3 (δ_C 103.9), C-3a (δ_C 128.7) and C-9 (δ_C 54.4). The structure was finally determined as echinulin based on the above-mentioned interpretation as well as by comparison with the literature (Sohn, Lee and Oh, 2013).

Table 3.3.9 ^{1}H NMR data comparison of **40** and echinulin (Sohn *et al.*, 2013).

Position	**40**			Echinulin[a]	
	^{1}H NMR ($CDCl_3$, 600 MHz, *J* in Hz)	HSQC	HMBC	^{1}H NMR ($CDCl_3$, 400 MHz, *J* in Hz)	^{13}C NMR ($CDCl_3$, 100 MHz, *J* in Hz)
1-NH	8.04 (s)			8.06 (s)	
2					141.3
3					104.0
3a					128.9
4	7.13 (br s)	115.0	C-5 (δ_C 132.2), C-1' (δ_C 34.5)	7.14 (s)	115.0
5					133.8
6	6.80 (br s)	122.8	C-4 (δ_C 115.0), C-5 (δ_C 132.2), C-1' (δ_C 34.5), C-1''' (δ_C 31.3)	6.81 (s)	122.8
7					123.4
7a					132.2
8	3.66 (dd, 14.7, 3.7) 3.19 (dd, 14.8, 11.7)	29.2	C-2 (δ_C 141.2), C-3 (δ_C 103.9), C-3a (δ_C 128.7), C-9 (δ_C 54.4)	3.65 (dd, 14.6, 3.7) 3.19 (dd, 14.6, 11.7)	29.4
9	4.41 (m)	54.4		4.41 (m)	54.5
10					168.5
11-NH	5.83 (s)			6.48 (s)	
12	4.09 (q, 6.3)	50.8		4.10 (q, 7.3)	50.8
13					167.8
14-NH	5.65 (s)			5.69 (s)	
15	1.53 (d, 7.0)	19.8	C-12 (δ_C 50.8), C-13 (δ_C 167.6)	1.54 (d, 7.6)	19.8
1'			C-2' (δ_C 145.6)		38.9
1'-CH_3	1.51 (s, 2 × CH_3)	27.8	C-2 (δ_C 141.2), C-1' (δ_C 39.1), C-2' (δ_C 145.6)	1.51 (s, 2 × CH_3)	27.9 27.8
2'	6.10 (dd, 17.4, 10.6)	145.6	C-1'-CH_3 (δ_C 27.8)	6.10 (dd, 17.2, 10.6)	145.7
3'	5.16 (d, 17.4) 5.15 (d, 10.5)	112.3	C-1' (δ_C 39.1), C-2' (δ_C 145.6)	5.16 (d, 18.3) 5.15 (d, 10.3)	112.3
1''	3.39 (d, 7.3)	34.5	C-5 (δ_C 132.2), C-2'' (δ_C 124.3), C-3'' (δ_C 131.3)	3.39 (d, 7.3)	34.6
2''	5.35 (m)	124.3		5.34 (m)	124.5
3''					131.6
4''	1.735 (s)	25.8	C-2'' (δ_C 124.3), C-3'' (δ_C 131.3), C-5'' (δ_C 17.88)	1.735 (s)	25.7
5''	1.74 (s)	17.88	C-2'' (δ_C 124.3), C-3'' (δ_C 131.3), C-4'' (δ_C 25.8)	1.74 (s)	17.88
1'''	3.53 (d, 7.2)	31.3	C-7 (δ_C 123.2)	3.53 (d, 7.3)	31.4
2'''	5.42 (m)	122.8		5.42 (m)	
3'''					132.9
4'''	1.81 (s)	25.7	C-2''' (δ_C 122.8), C-3''' (δ_C 132.9), C-5''' (δ_C 17.9)	1.81 (s)	25.8
5'''	1.87 (s)	17.9	C-2''' (δ_C 122.8), C-3''' (δ_C 132.9), C-4''' (δ_C 25.7)	1.87 (s)	17.9

3.3.4 Bioactivity assay of isolated compounds

All compounds analyzed in this study were submitted to a cellular cytotoxicity (MTT) assay employing the L5178Y mouse lymphoma cell line. Compounds **34** and **38** exhibited significant cytotoxicity with IC_{50} values of 4.7 and 8.4 μM, respectively, compared to kahalalide F used as positive control (IC_{50} 4.3 μM).

3.3.5 Co-cultivation of the two *Penicillium* sp. strains IO1 and IO2

Co-cultivation of the two *Penicillium* sp. strains IO1 and IO2 induced the production of two known compounds norlichexanthone (**37**) and monocerin (**38**), which were not detected in either of the axenic fungal controls (Figure 3.3.9).

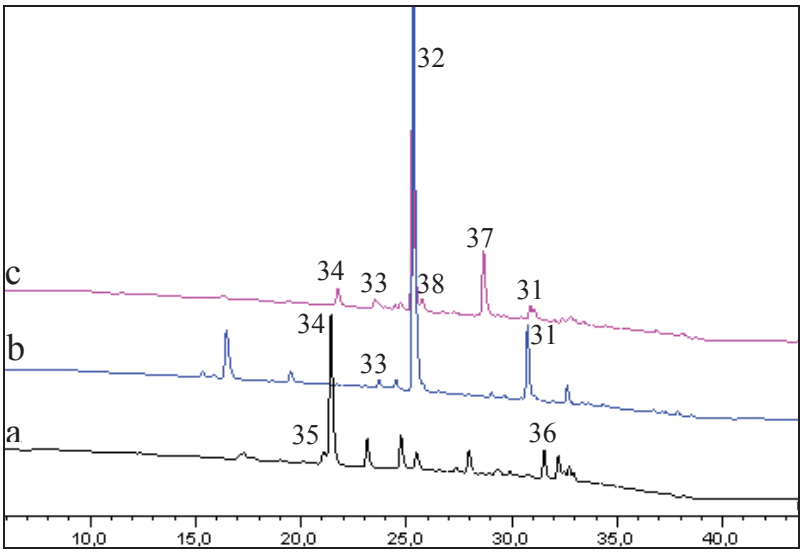

Figure 3.3.9 HPLC chromatograms (intensity [mAU*min] against time [min]) of EtOAc extracts from co-cultivation experiments (UV detection at 235 nm): (a) *Penicillium* sp. IO2 control, (b) *Penicillium* sp. IO1 control, (c) co-cultivation of *Penicillium* sp. IO1 and IO2.

3.4 Compounds isolated from endophytic fungus *Alternaria alternata* originated from the rainforest plant *Antiaris africana*

A. alternata was isolated from leaves of the rainforest plant *A. africana* collected in Cameroon in October 2013. From the ethyl acetate extract following fermentation on rice, six compounds, including two new stereoisomers, (5*S*)-altersetin (**41)** and altersetin-2 (**42)** were isolated.

3.4.1 (5*S*)-Altersetin (41, known compound)

(5*S*)-Altersetin	
Biological Source	*Alternaria alternata*
Sample Code	FR-9.2P1, FR-9.3.3P1, FR3-1.6P1, FR-1.2P6
Sample Amount	6.5 mg
Molecular Formula	$C_{24}H_{33}NO_4$
Molecular Weight	399 g/mol
Solubility	MeOH, Acetone
Physical Description	Yellow gum
Optical Rotation	$[\alpha]^{20}_{D}$ -288.3 (*c* 0.2, MeOH)
HPLC Retention Time	36.98 min (standard gradient)

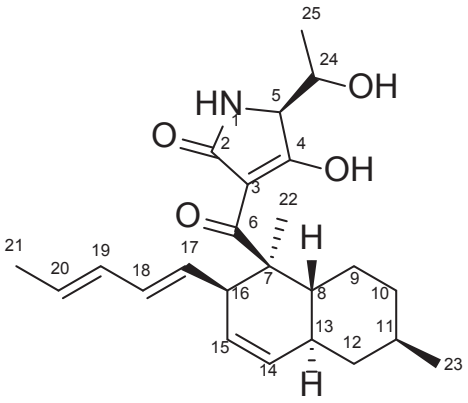

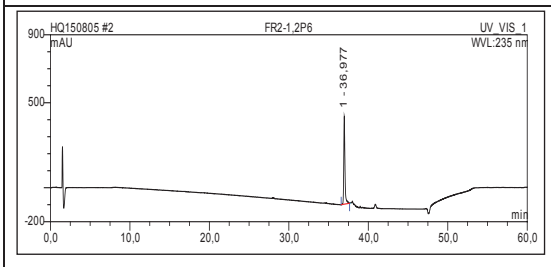

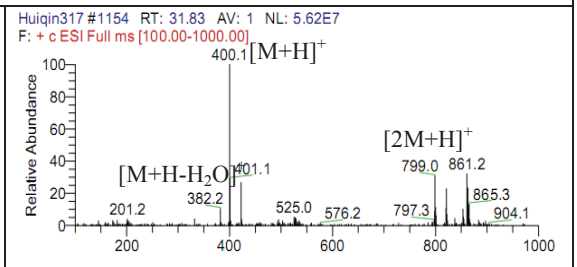

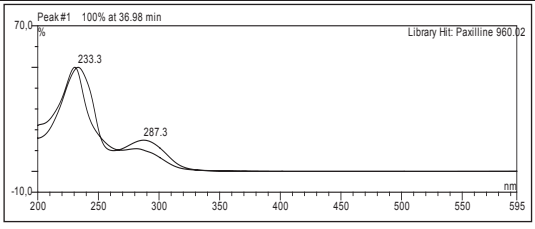

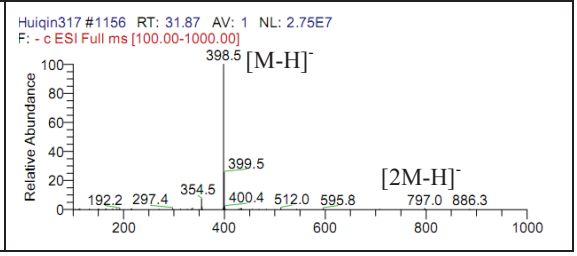

(5*S*)-Altersetin (**41**) was obtained as a yellow gum from the ethyl acetate extract of the rice

culture of *A. alternata,* displaying UV absorption at λ_{max} (MeOH) 233 and 287 nm, and an $[\alpha]^{20}_{D}$ value of -288.3 (*c* 0.2, MeOH). Its molecular weight was established as 399 g/mol on the basis of the ion peaks observed at *m/z* 400.1 $[M + H]^+$ and 799.0 $[2M + H]^+$ in the positive ESI-MS mode, as well as at *m/z* 398.5 $[M - H]^-$ and 797.0 $[2M - H]^-$ in the negative ESI-MS mode. The signals in the ^{1}H NMR spectrum of **41** were assigned to four methyl groups, six olefinic methines, three aliphatic methylenes, and six aliphatic methines. Moreover, an exchangeable signal was observed at δ_H 9.25 (s) and was attributed to NH. The ^{13}C NMR spectrum confirmed the corresponding carbon signals and revealed in addition two carbonyl groups (C-2 and C-6) and one oxygenated olefinic carbon (C-3). Detailed analysis of the HMBC spectrum (Figure 3.4.1) revealed a trisubstituted decalin moiety. Accordingly, the methyl groups CH_3-22 and CH_3-23 were located at C-7 and C-11, respectively, as deduced by the HMBC correlations from CH_3-23 [δ_H 0.89 (3H, d, J = 6.5 Hz)] to C-10 (δ_C 35.4), C-11 (δ_C 32.9) and C-12 (δ_C 41.7), as well as from CH_3-22 [δ_H 1.37 (1H, br. s)] to C-7 (δ_C 48.4), C-8 (δ_C 39.2), and C-16 (δ_C 44.0). Moreover, an exocylic all-*trans*-diene residue connected to C-16 was supported by the correlations from CH_3-21 [δ_H 1.64 (3H, d, J = 6.6 Hz)] to C-19 (δ_C 131.4) and C-20 (δ_C 128.0); from H-20 [δ_H 5.51 (1H, dt, J = 13.6, 6.5 Hz)] to C-21 (δ_C 17.8) and C-18 (δ_C 131.4); from H-18 [δ_H 5.72 (1H, dd, J = 14.1, 11.1 Hz)] to C-16 (δ_C 44.6), C-17 (δ_C 130.3) and C-20; as well as from H-17 [δ_H 5.22 (1H, dd, J = 13.8, 9.3 Hz)] to C-7 and C-16. The remaining ^{1}H and ^{13}C residues were attributed to a tetramic acid moiety (Royles *et al*. 1995), adjacent to C-7 of the decalin ring via a carbonyl bridge. The relative configuration of **41** was assigned by ^3J coupling constants and by the ROESY spectrum (Figure 3.4.2). All-*trans*-diene residues were indicated by the large coupling constants between the respective olefinic protons ($^3J_{19,20}$ = 13.6 Hz, $^3J_{17,18}$ = 14.0 Hz), as well as by the cross-peaks between H_3-21/H-19 and H-19/H-17 in the ROESY spectrum. In addition, the ROESY cross peaks between H-16/H-22, H-22/H-13, H-22/ H-12β, H-11/ H-13, and H-11/ H-12β suggested the *syn* relationship of these protons, whereas the cross peak between H-8 and H-17 positioned these protons on the other side of the plane, thus indicating a *trans*-decalin moiety. The structure of **41** was further corroborated by the very similar experimental UV, MS, ECD spectral data compared with those published for altersetin, previously reported from the same species (Hellwig *et al*., 2002).

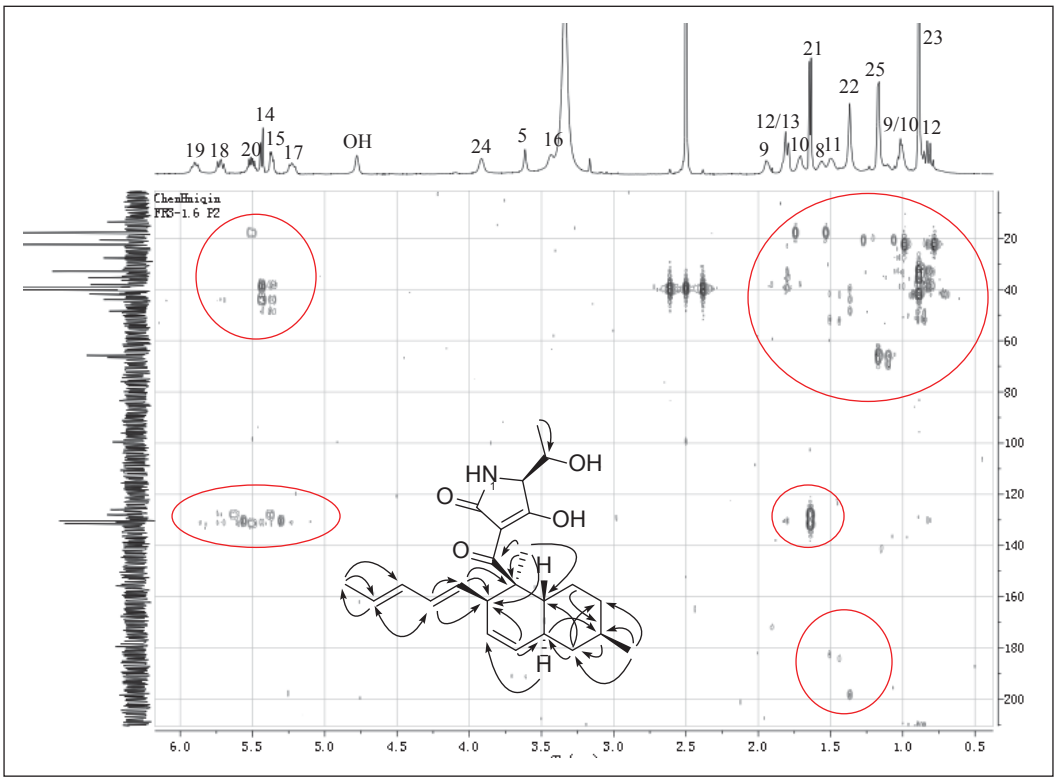

Figure 3.4.1 HMBC correlations of **41**.

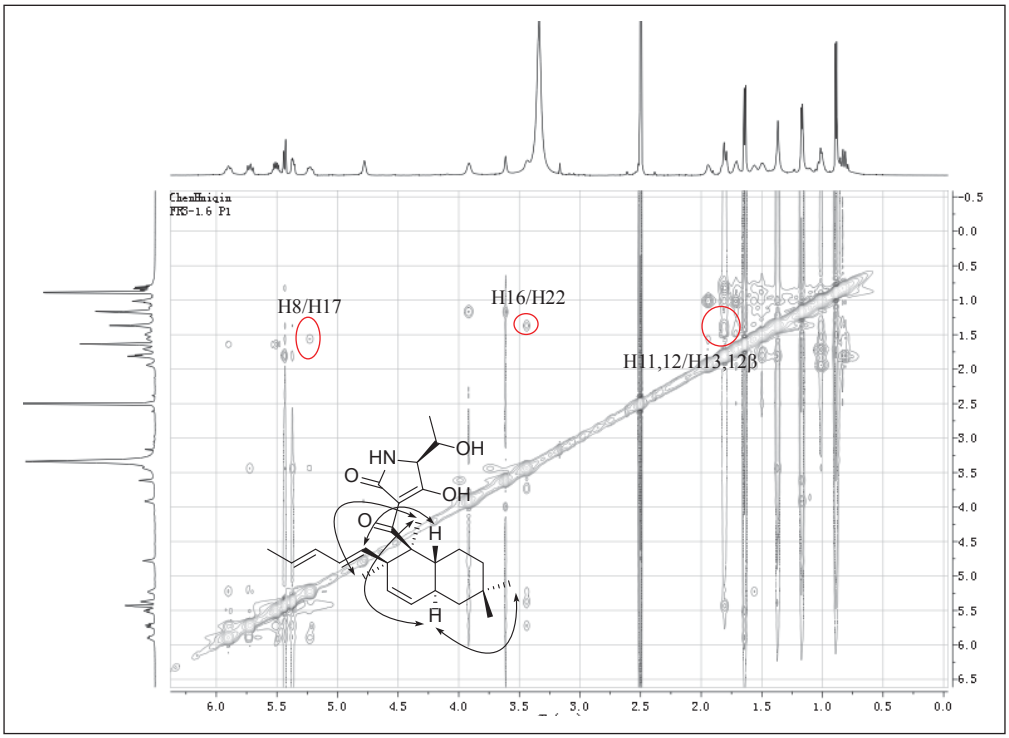

Figure 3.4.2 Key ROESY correlations of **41**.

3.4.2 Altersetin-2 (42, new compound)

Altersetin-2	
Biological Source	*Alternaria alternata*
Sample Code	FR-9.2P2, FR-9.3.3P2, FR3-1.6P2, FR-1.2P7
Sample Amount	4.5 mg
Molecular Formula	$C_{24}H_{33}NO_4$
Molecular Weight	399 g/mol
Solubility	MeOH, Acetone
Physical Description	Yellow gum
Optical Rotation	$[\alpha]^{20}_{D}$ -54.4 (*c* 0.2, MeOH)
HPLC Retention Time	37.94 min (standard gradient)

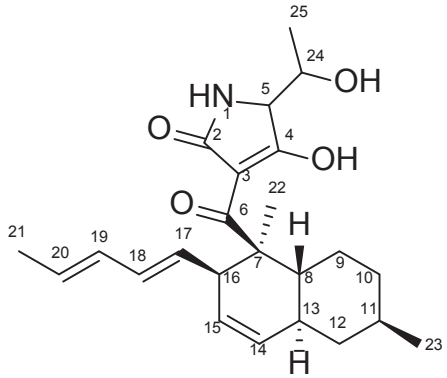

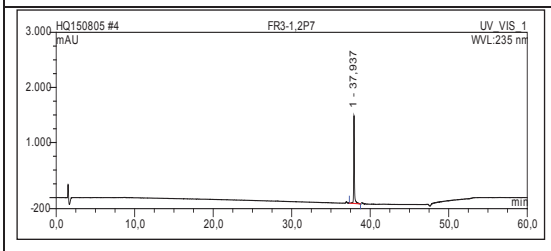

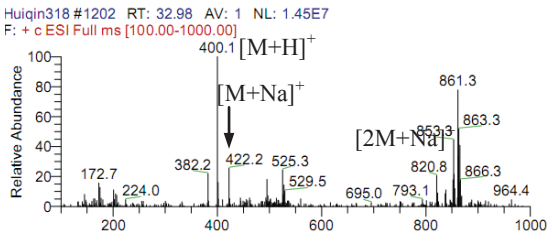

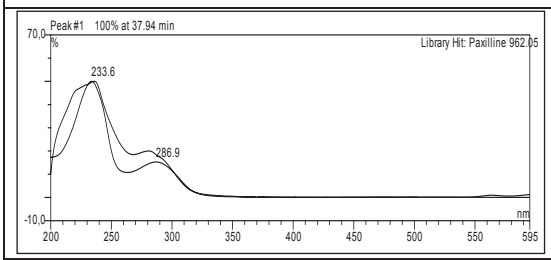

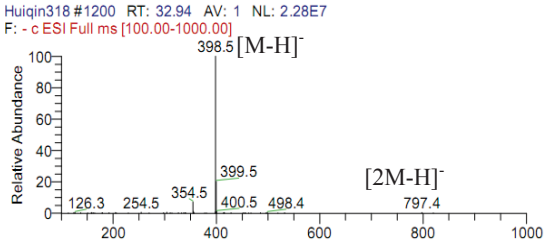

Altersetin-**2** (**42**) was obtained as a yellow gum from the ethyl acetate extract of the rice

culture of *A. alternata,* displaying the same UV absorption as **41**. The molecular formula of $C_{24}H_{34}NO_4$ was given by the HRESIMS, in accordance with the ion peak at *m/z* 400.2478 [M + H]$^+$ (cal. 400.2482). Detailed analysis of the MS, ^{1}H NMR and HMBC spectra of **42** allowed us to establish the same planar structure as that of **41**. However, the different retention times observed in the HPLC chromatogram suggested that **42** was a stereoisomer of **41**, which was corroborated by the similar chemical shifts of the corresponding protons in the ^{1}H NMR spectrum measured in DMSO-d_6 or acetone-d_6. Accordingly, H-5 shifted downfield from δ_H 3.61 (**41**) to δ_H 3.89 (**42**), and CH_3-25 shifted upfield from δ_H 1.17 (**41**) to δ_H 0.90 (**42**). These NMR data together with the different high-wavelength ECD transitions of **42** compared to **41**, may suggest a different absolute configuration at C-5. Moreover, the decalin moiety of **42** was found to have the same relative stereochemistry as that of **41** based on the respective ROESY correlations. Thus, **42** was tentatively assigned as the C-5 epimer of **41** and was given the name altersetin-2.

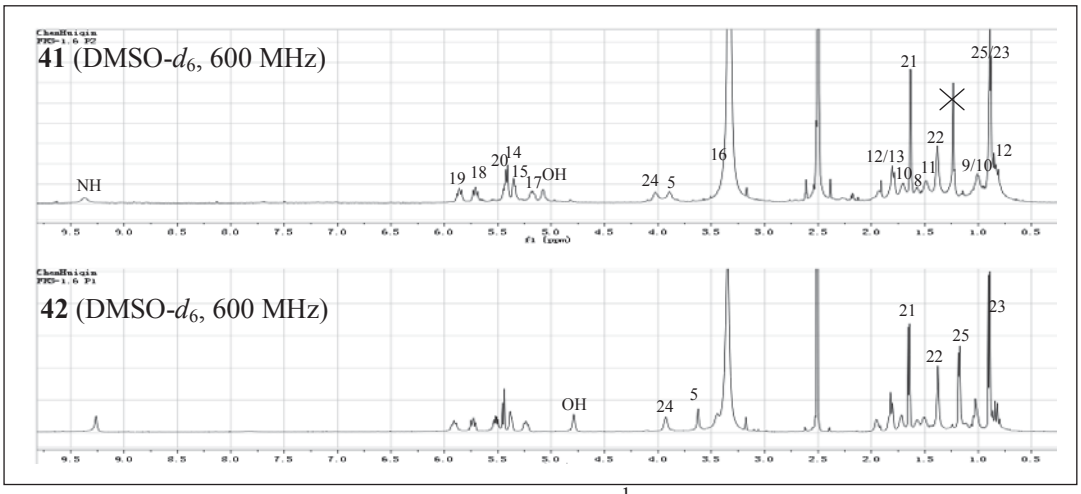

Figure 3.4.3 Comparison of ^{1}H NMR of **41** and **42**.

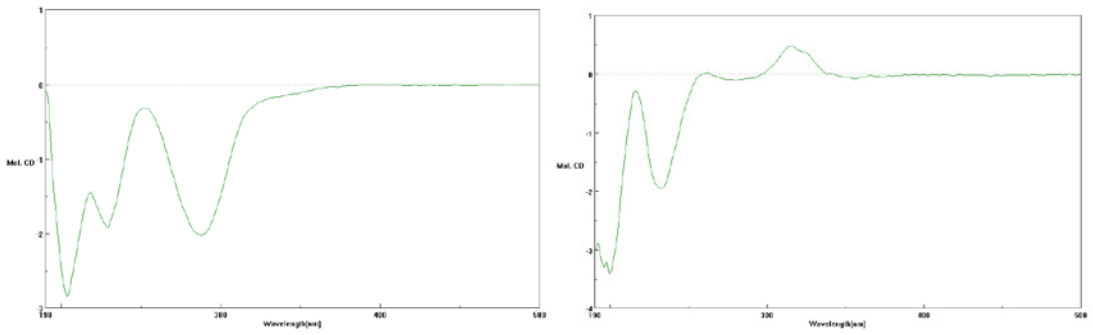

41 **42**

Figure 3.4.4 ECD spectra of **41** and **42**.

Table 3.4.1 ^{1}H NMR data comparison of **41**, **42** and (5*S*)-altersetin (in DMSO-d_6).

Position	**42** (600 MHz)	**41** (600 MHz)	(5*S*)-altersetin (400 MHz)[a]
NH	9.37 (br. s)	9.25 (br. s)	9.20 (br. s)
5	3.89 (br. s)	3.61 (br. s)	3.61 (br. s)
8	1.57 (m)	1.56 (m)	1.56 (m)
9	1.93 (m)	1.94 (m)	1.90 (m)
	1.00 (m)	1.02 (m)	1.03 (m)
10	1.70 (m)	1.71 (m)	1.70 (m)
	1.00 (m)	1.02 (m)	1.00 (m)
11	1.49 (m)	1.50 (m)	1.50 (m)
12	1.79 (m)	1.80 (m)	1.80 (m)
	0.83 (m)	0.82 (m)	0.80 (m)
13	1.79 (m)	1.80 (m)	1.80 (m)
14	5.41 (m, overlapping)	5.44 (d, 9.9)	5.45 (dm)
15	5.34 (m)	5.37 (m)	5.35 (m)
16	ca. 3.45 (overlapping)	3.44 (m, overlapping)	3.45 (m)
17	5.17 (dd, 12.5, 9.4)	5.22 (dd, 13.8, 9.3)	5.24 (dd)
18	5.71 (dd, 13.5, 10.9)	5.72 (dd, 14.1, 11.1)	5.70 (dd)
19	5.86 (dd, 13.5, 11.9)	5.90 (m)	5.90 (dd)
20	5.43 (m, overlapping)	5.51 (dt, 13.6, 6.5)	5.50 (dq)
21	1.63 (d, 6.0)	1.64 (d, 6.6)	1.64 (d)
22	1.38 (br. s)	1.37 (br. s)	1.35 (s)
23	0.89 (d, 6.2)	0.89 (d, 6.5)	0.85 (d)
24	4.03 (br. s)	3.91 (br. s)	3.91 (m)
25	0.90 (d, 5.4)	1.17 (d, 6.3)	1.17 (d)
24-OH	5.07 (s)	4.78 (br. s)	

[a] Hellwig *et al*., 2002

3.4.3 Altertoxin II (43, known compound)

Altertoxin II	
Biological Source	*Alternaria alternata*
Sample Code	FR-2.1, FR-2.2
Sample Amount	1.2 mg
Molecular Formula	$C_{20}H_{14}O_6$
Molecular Weight	350 g/mol
Solubility	DMSO
Physical Description	Reddish brown powder
HPLC Retention Time	25.97 min (standard gradient)

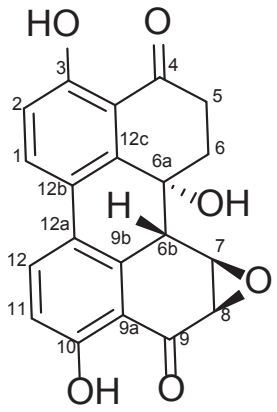

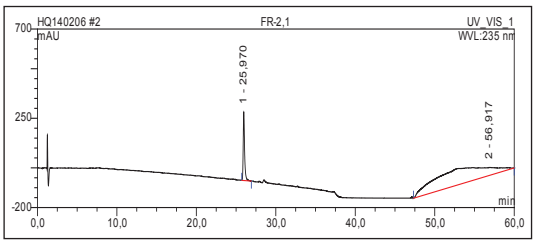

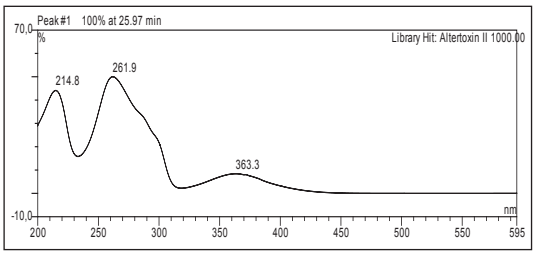

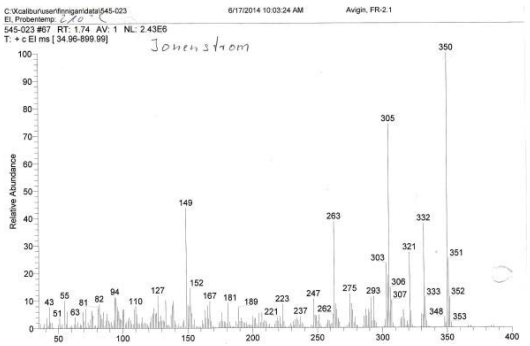

Altertoxin II (**43**) was obtained as a reddish brown powder from the ethyl acetate extract of the rice culture of *A. alternata,* giving UV absorptions at λ_{max} (MeOH) 214 and 262 nm. No ionisation was observed in the positive or the negative ESI-MS mode, whereas the base peak of 350 $[M]^+$ in the EI-MS spectrum indicated a molecular weight of 350 g/mol. The ^{1}H NMR spectrum presented three exchangeable protons, including one secondary hydroxy group at δ_H 5.60 (1H, s, 6a-OH) and two chelated phenolic hydroxy groups at δ_H 12.7 (1H, s, 3-OH) and 11.9 (1H, s, 10-OH). Two pairs of *ortho*-coupled protons [δ_H 8.17 (1H, d, J = 8.8 Hz, H-1), 8.08 (1H, d, J = 8.8 Hz, H-12), 7.08 (1H, d, J = 8.7 Hz, H-2) and 7.00 (1H, d, J = 8.7 Hz, H-11)] were observed in the spectrum, as indicated by their coupling constants and their strong ^{1}H–^{1}H COSY correlations. In addition, the fragments CH(6a)-CH(7)-CH(8) and CH_2(5)-CH_2(6) were assembled on the basis of the ^{1}H–^{1}H COSY spectrum. The above mentioned data led to assignment of the structure of **43** as altertoxin II from *Alternaria* sp. (Stack *et al*. 1986). Finally, the absence of vicinal coupling between H-6b [δ_H 3.60 (1H, s)] and H-7 [δ_H 3.77 (1H, m)] suggested that the dihedral angle between these protons is approximately 90^o as described for altertoxin II (Stack *et al*., 1986).

Table 3.4.2 ^{1}H NMR data comparison of **43** and altertoxin II.

Position	**43** δ_H (DMSO-d_6, 600 MHz, J in Hz)	altertoxin II[e] δ_H ($CDCl_3$, 360 MHz, J in Hz)
1	8.17 (d, 8.8)[c]	7.91 (d, 8.8)[a]
2	7.08 (d, 8.8)[d]	7.12 (d, 8.8)[b]
5	3.13 (ddd, 17.6, 13.6, 4.9) 2.70 (ddd, 17.6, 4.0, 2.4)	3.26 (ddd, 17.0, 14.4) 2.83 (ddd, 17.0, 3.2)
6	2.76 (ddd, 13.3, 4.9, 2.4) 2.46 (dd, 13.6, 4.0)	2.89 (ddd, 14.0, 4.2) 2.41 (dt, 14.3)
6a-OH	5.60 (s)	
6b	3.60 (s)	3.55 (d, 0.5)
7	3.77 (d, 3.7)	4.23 (d, 3.0)
8	4.38 (d, 3.7)	3.71 (dd, 3.0, 0.5)
11	7.00 (d, 8.7)[d]	7.07 (d, 8.8)[b]
12	8.08 (d, 8.8)[c]	7.86 (d, 8.8)[a]
3-OH	12.7 (s)	12.7 (s)
10-OH	11.9 (s)	12.1 (s)

[a-d] assignments in vertical columns may be interchanged

[e] Stack *et al*., 1986

3.4.4 Altertoxin I (44, known compound)

Altertoxin I	
Biological Source	*Alternaria alternata*
Sample Code	FR-4.2
Sample Amount	3.4 mg
Molecular Formula	$C_{20}H_{16}O_6$
Molecular Weight	352 g/mol
Solubility	DMSO
Physical Description	Yellow powder
HPLC Retention Time	25.35 min (standard gradient)

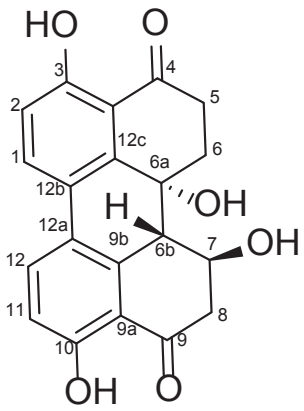

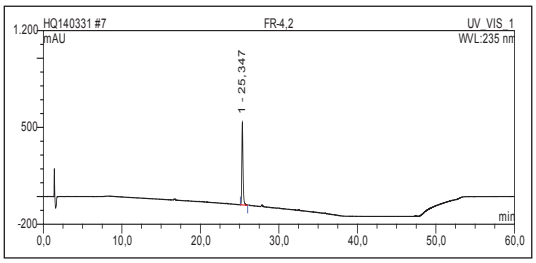

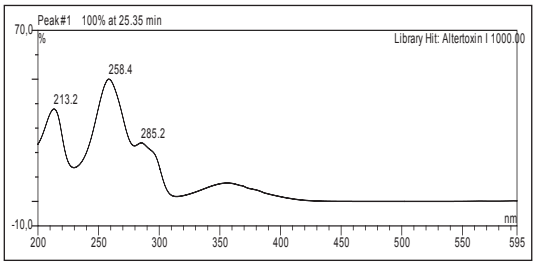

No ionisation in ESI-MS.

Altertoxin II (**44**) was obtained as a yellow powder from the ethyl acetate extract of rice culture of *A. alternata*. It displayed similar UV absorptions (λ_{max} 213 and 258 nm) compared to **43**, however, no ionization was observed in the ESI-MS spectrum. Comparison of the ^{1}H NMR spectrum of **44** with that of **43** suggested a close relationship between both structures. The main difference was the presence of one oxygenated methine proton H-7 [δ_H 4.52 (m)] and one methylene H_2-8 (δ_H 2.80 – 3.11) in **44** instead of an epoxide group between C-7 and C-8 as in **43**. The proposed structure was confirmed by further comparison of the UV and NMR data with published data for altertoxin II, previously reported from species of the genus *Alternaria* (Stack *et al*., 1986; Fleck *et al*., 2014).

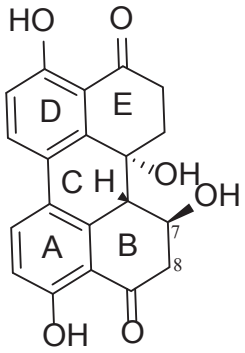

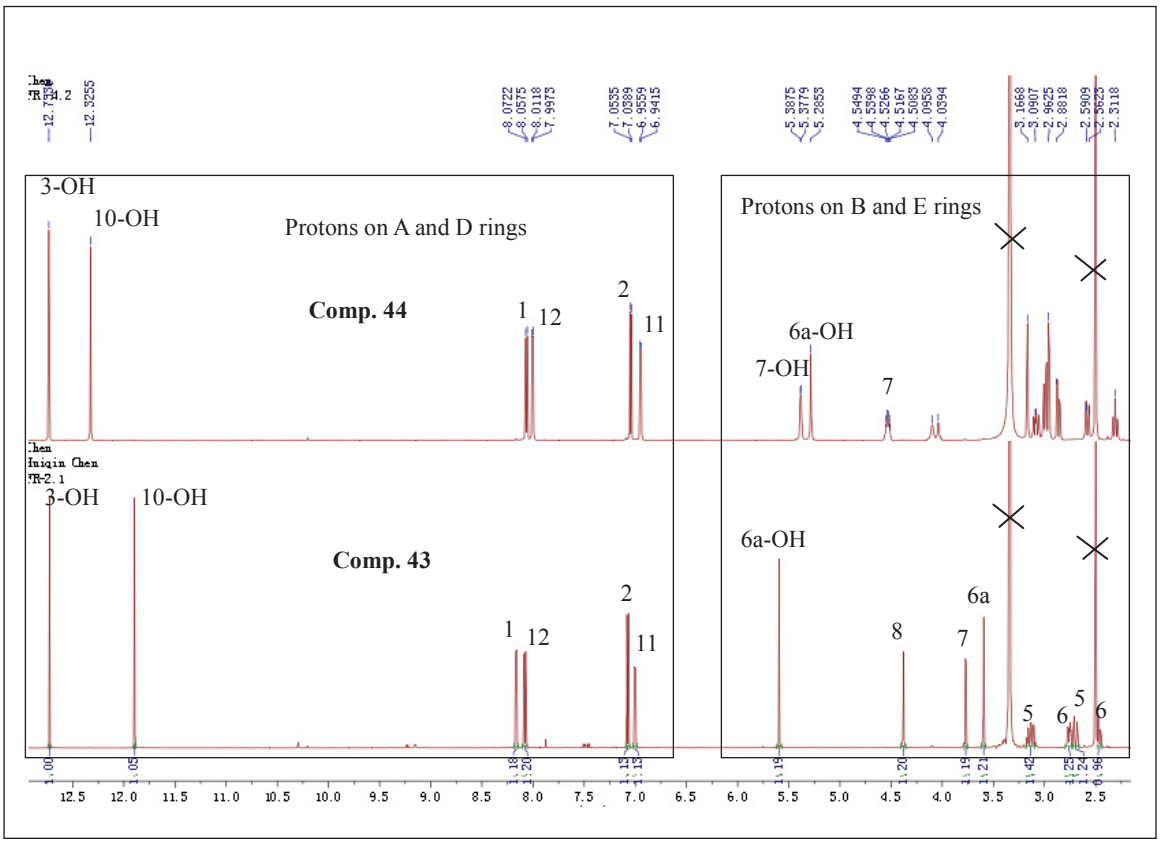

Figure 3.4.5 Comparison of ^{1}H NMR spectra of **43** and **44**.

3.4.5 Tenuazonic acid (45, known compound)

Tenuazonic acid	
Biological Source	*Alternaria alternata*
Sample Code	FR-2.7
Sample Amount	179.8 mg
Molecular Formula	$C_{10}H_{15}NO_3$
Molecular Weight	197 g/mol
Solubility	DMSO
Physical Description	Yellow gel
HPLC Retention Time	22.41 min (standard gradient)

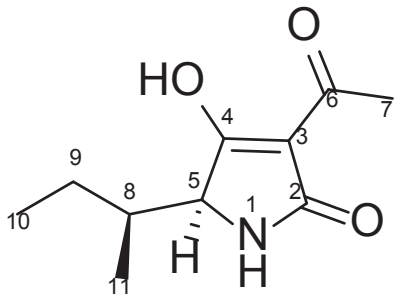

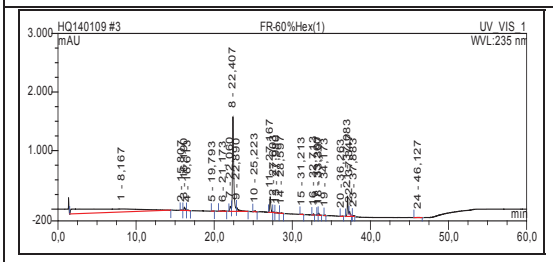

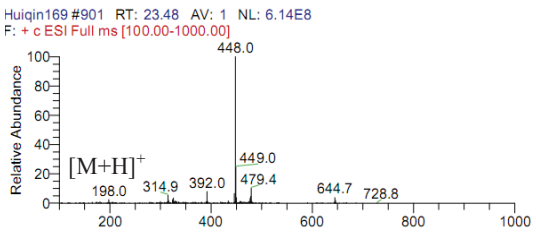

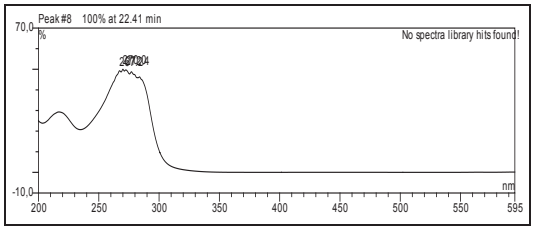

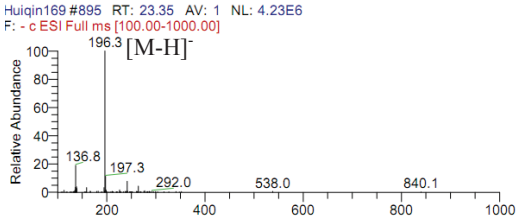

Tenuazonic acid (**45**) was obtained as a yellow gel from the ethyl acetate extract of rice cultures of *A. alternata*. It displayed UV absorption at λ_{max} (MeOH) 269 nm. The positive ion peak at *m/z* 198.0 $[M + H]^+$ and the negative ion peak at *m/z* 196.3 $[M - H]^-$, observed in the ESI-MS spectrum, indicated a molecular weight of 197 g/mol, suggesting an odd number of N-atoms in the structure of **45**. Seven signals were detected in the ^{1}H NMR spectrum, three of which were methyl groups connected to quaternary carbons, methine or methylene carbons according to the singlet [δ_H 2.41 (3H, s, CH_3-7)], doublet [δ_H 0.99 (3H, d, J = 7.0 Hz, CH_3-11)] or triplet [δ_H 0.90 (3H, t, J = 7.4 Hz, CH_3-10)] multiplicity of their signals, respectively. The singlet methyl group was assigned to a carbonyl due to the downfield chemical shift at δ_H 2.41 (3H, s, CH_3-7). Thus, based on the obtained UV, ESI-MS and ^{1}H NMR data and on comparison with the literature, **45** was assigned as tenuazonic acid (Hassan 2007). Tenuazonic acid is a major mycotoxin produced by *Alternaria* sp., and also reported from *Phoma sorghina*, *Pyricularia oryzae*, and *Aspergillus* sp. (Meronuck *et al*., 1972; Mikula *et al*., 2013). It shows one of the highest toxicities amongst all *Alternaria* mycotoxins (Weidenbörner, 2001), and therefore, it has received extensive investigations. So far, a number of tautomers have been reported, because tenuazonic acid is not stable and undergoes isomerization in solution (Siegel *et al*., 2010).

Table 3.4.3 ^{1}H NMR data comparison of **45** and tenuazonic acid.

Position	**45**	Tenuazonic acid[a]
	δ_H (CD_3OD, 600 MHz, J in Hz)	δ_H ($CDCl_3$, 500 MHz, J in Hz)
5	3.84 (br s)	3.77 (d, 3.4)
7	2.41 (s)	2.43 (s)
8	1.91 (m)	1.94 (m)
9	1.37 (m)	1.35 (m)
	1.24 (m)	1.23 (m)
10	0.90 (t, 7.4)	0.87 (t, 7.2)
11	0.99 (d, 7.0)	0.99 (d, 6.9)
NH		7.06 (s)

[a] Siegel *et al*., 2010

3.4.6 Methyl 2-carboxy-3-hydroxy-(*E*)-cinnamate and 3-[(methoxycarbonyl)methyl]-7-hydroxyphthalide (46 and 47, new compounds)

Methyl 2-carboxy-3-hydroxy-(*E*)-cinnamate	
Biological Source	*Alternaria alternata*
Sample Code	FR-9.6P2, FR-9.5, FR3-1.10, FR3-1.11
Sample Amount	4.0 mg
Molecular Formula	$C_{11}H_{10}O_5$
Molecular Weight	222 g/mol
Solubility	Methanol
Physical Description	Yellow gum
HPLC Retention Time	22.96 min (standard gradient)

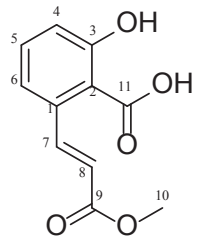

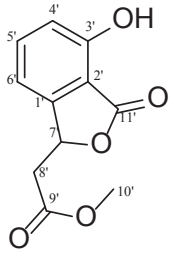

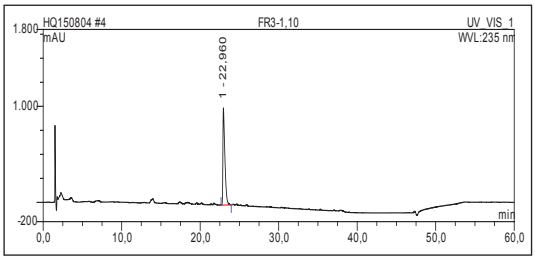

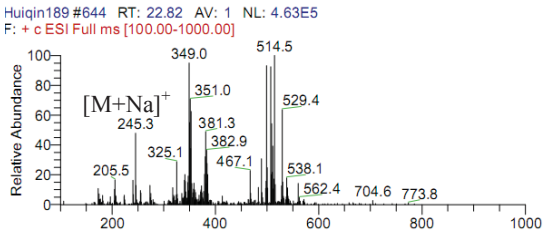

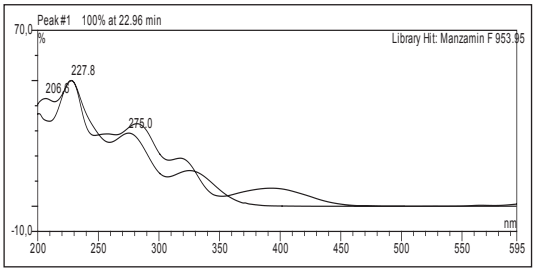

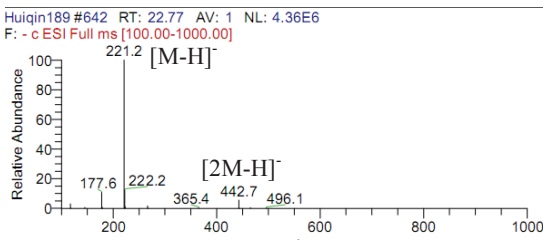

Methyl 2-carboxy-3-hydroxy-(*E*)-cinnamate (**46**) was obtained as a yellow gum from the ethyl acetate extract of the rice culture of *A. alternata*. It displayed UV absorptions at λ_{max} (MeOH) 227 and 275 nm. The molecular formula of **46** was established as $C_{11}H_{10}O_5$ based on

the prominent peak at *m/z* 223.0599 $[M + H]^+$ (cal. 223.0601) in the HRESIMS, thus comprising seven degrees of unsaturation. The ^{1}H NMR spectrum showed three phenyl protons at δ_H 7.25 (1H, t, *J* = 7.9 Hz, H-5), 6.95 (1H, t, *J* = 7.6 Hz, H-6) and 6.85 (1H, d, *J* = 8.2 Hz, H-4) characteristic of a 1,2,3-substituted phenyl moiety; two *E*-configured double bond protons at δ_H 8.72 (1H, d, *J* = 15.9 Hz, H-7) and 6.16 (1H, d, *J* = 15.9 Hz, H-8); and one methoxy group at δ_H 3.76 (3H, s, OCH_3). The ^{13}C NMR spectrum confirmed the presence of 11 carbons, including six aromatic carbons, two olefinic carbons, two carbonyl groups, and one methoxyl group.

The connection between the substituent groups and the benzene ring was determined by inspection of the HMBC spectrum. Accordingly, the cinnimate substructure was supported by the HMBC correlations from the olefinic proton H-7 to C-8 (δ_C 118.3) and C-9 (δ_C 169.5); from H-8 to C-1 (δ_C 139.1), C-7 (δ_C 149.6) and C-9; as well as from the phenyl proton H-6 to C-7. Moreover, the correlation from 10-OCH_3 [δ_H 3.76 (s)] to C-9 indicated that the terminal functional group of cinnimate was esterified. The remaining position at C-3 was hydroxylated, as suggested by the downfield chemical shift at 162.8 ppm and by the molecular formula. These data were in agreement with those reported for the known methyl 2-carboxy-3-methoxy-(*E*)-cinnamate (Trost, Rivers and Gold 1980), apart from the presence of an additional methoxyl group, which accounted for the difference in the molecular weight of 14 amu observed between both compounds. Therefore, **46** was identified as methyl 2-carboxy-3-hydroxy-(*E*)-cinnamate.

Interestingly, several weeks after keeping **46** in CD_3OD, the intensity of a serials of small peaks in the ^{1}H NMR increased gradually. By analyzing the ^{1}H, ^{13}C and HMBC data, the structure of the newly formed compound (**47**) was elucidated. It occupied the same 1,2,3-substituted aromatic part as **46**, whereas cyclized between the carboxyl group on C-2 and the side chain on C-1, as suggested by the correlations from H-5' [δ_H 7.55 (1H, t, *J* = 7.9 Hz)] and H-6' [δ_H 7.55 (1H, t, *J* = 7.9 Hz)] to C-7' (δ_C 78.3), from H-7' [δ_H 5.82 (1H, m)] to C-1' (δ_C 152.2) and C-10' (δ_C 171.2), and from H_2-8' [δ_H 3.09 (1H, dd, *J* = 16.6, 4.6 Hz) and 2.80 (1H, dd, *J* = 16.6, 8.0 Hz)] to C-1', C-7' (δ_C 78.3) and C-9' (δ_C 171.5) (Figure 3.4.6). Interestingly, **47** changed back to **46** when the NMR solvent was removed and replaced with DMSO-d_6 (Figure 3.4.7).

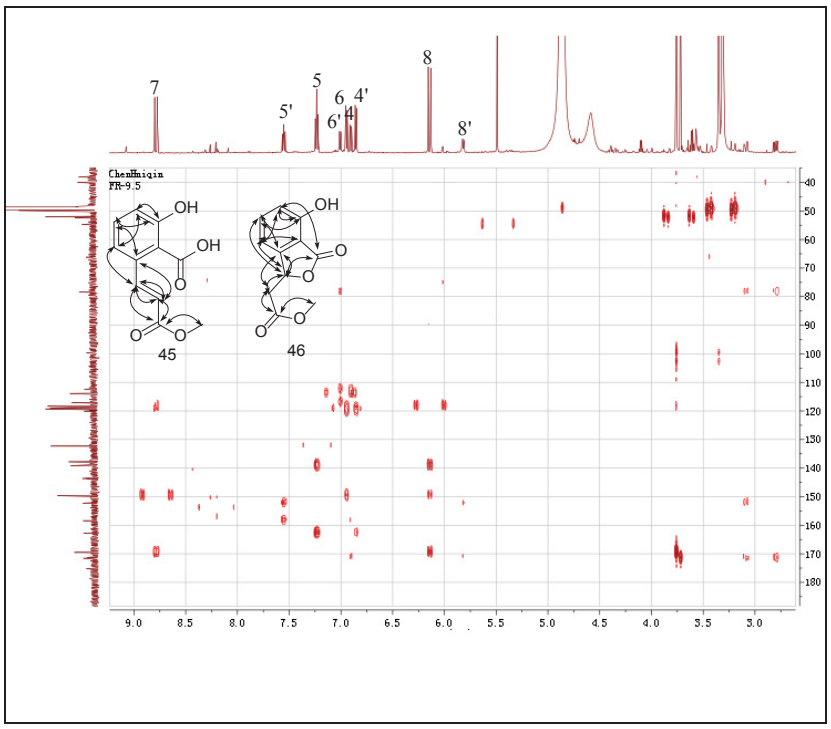

Figure 3.4.6 HMBC correlations of **46** and **47**.

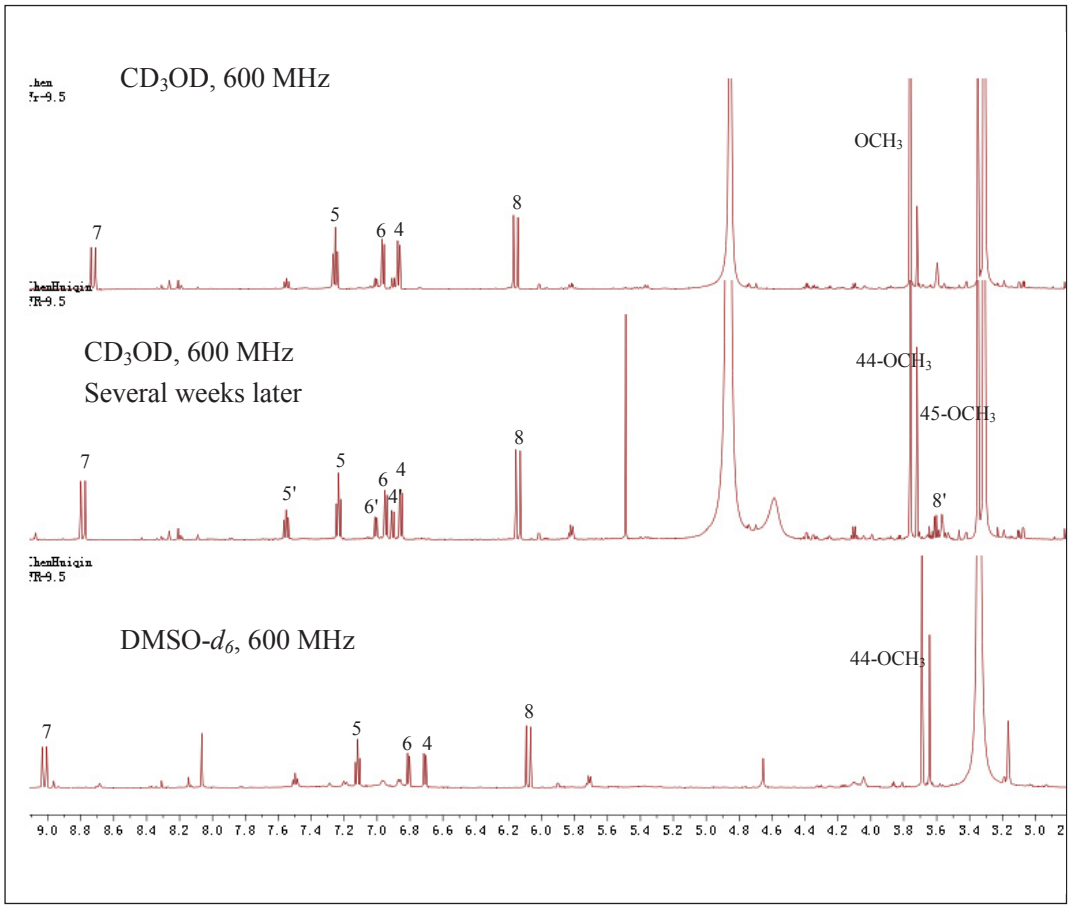

Figure 3.4.7 ^{1}H NMR spectra comparison of **46** in CD_3OD and DMSO-d_6.

Table 3.4.4 ^{1}H and ^{13}C NMR data of **46** and **47**.

	46			**47**	
Position	^{1}H NMR (DMSO-d_6, 600 MHz, *J* in Hz)	^{1}H NMR (CD_3OD, 600 MHz, *J* in Hz)	^{13}C NMR (CD_3OD, 150 MHz, *J* in Hz)	^{1}H NMR (CD_3OD, 600 MHz, *J* in Hz)	^{13}C NMR (CD_3OD, 150 MHz, *J* in Hz)
1			139.1		152.2
2					117.1
3			162.8		158.4
4	6.71 (d, 8.1)	6.85 (d, 8.2)	119.3	6.91 (d, 8.2)	112.5
5	7.12 (t, 7.8)	7.25 (t, 7.9)	132.3	7.55 (t, 7.9)	137.8
6	6.81 (t, 7.8)	6.95 (t, 7.6)	118.9	7.55 (t, 7.9)	113.9
7	9.02 (d, 16.0)	8.72 (d, 15.9)	149.6	5.82 (m)	78.3
8	6.08 (d, 16.0)	6.16 (d, 15.9	118.3	3.09 (dd, 16.6, 4.6) 2.80 (dd, 16.6, 8.0)	40.0
9			169.5		171.5
10					171.2
OCH_3	3.69 (s)	3.76 (s)	52.0	3.71 (s)	52.4

All isolated compounds were evaluated for their cytotoxicity toward L5178Y, A2780 sens, and A2780 CisR cancer cell lines, as well as for their antibacterial activities. Only compounds **41** and **43** showed activities, which presented in Table 3.4.5.

Table 3.4.5 Bioactivities of **41** and **43**.

		41 (MIC)	**43**
cytotoxicity	A2780 sens		active (C 0.1 mmol/L)
Anti-microbial activity [MIC (μg/mL)]	*S. aureus* ATCC 25923	50 μg/mL	
	S. aureus ATCC 700699	25 μg/mL	
	E. faecalis ATCC 29212	25 μg/mL	
	E. faecalis ATCC 51299	50 μg/mL	
	E. faecium ATCC 35667	50 μg/mL	
	E. faecium ATCC700221	50 μg/mL	
	Mycobacterium tuberculosis		MIC: 25 μg/mL

3.5 Known compounds isolated from soil-derived fungus *Penicillium paxilli*.

3.5.1 Structures and physical data of compounds from *P. paxilli*.

compound	Sample Code	Physical Description	Sample Amount	Molecular Formula	Molecular Weight	Structure	HPLC Retention Time (standard gradient)	UV spectrum
Paxilline (**48**)	W8-3.8.3	White amorphous solid	132.0 mg	$C_{27}H_{33}NO_4$	435 g/mol	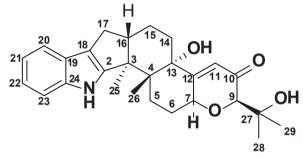	31.26 min	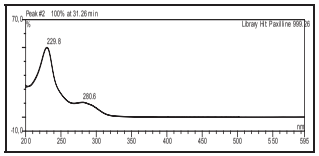
Dehydroxy paxilline (**49**)	W8-3.4.2P1	White amorphous solid	3.1 mg	$C_{27}H_{33}NO_3$	419 g/mol	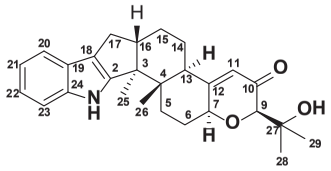	33.06 min	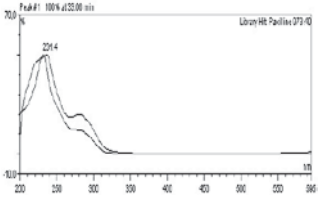
21-Isopentenylpaxilline (**50**)	W8-3.4.2P2	White amorphous solid	1.4 mg	$C_{32}H_{41}NO_4$	503 g/mol	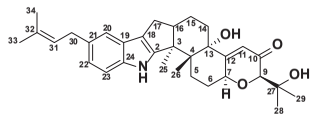	34.89 min	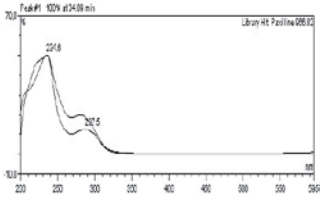

10β-hydroxy-13-desoxy paxilline (**51**)	W8-5.3P4	White amorphous solid	5.0 mg	$C_{27}H_{35}NO_3$	421 g/mol	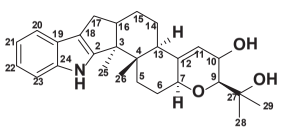	33.82 min	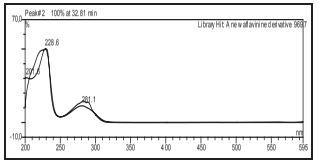
Paspaline (**52**)	W8-3.4.2P4	White amorphous solid	7.2 mg	$C_{28}H_{39}NO_2$	421 g/mol	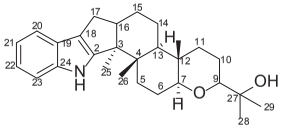	35.68 min	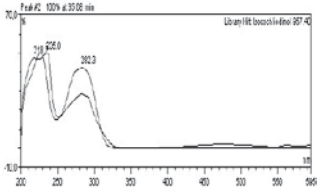
Emindole SB (**53**)	W8-3.4.2P5	White amorphous solid	5.1 mg	$C_{28}H_{39}NO$	405 g/mol	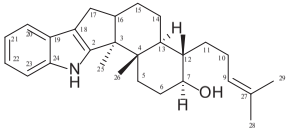	35.677 min	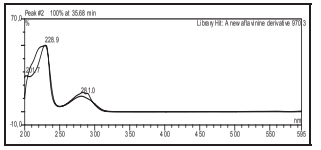
12-Carboxyl- Paspaline (**54**)	W8-5.3P3	White amorphous solid	11.7 mg	$C_{28}H_{37}NO_4$	451 g/mol	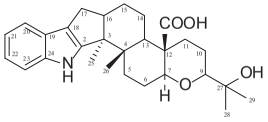	32.32 min	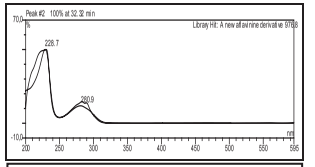
3-Deoxo-4b-deoxypaxilline (**55**)	W8-3.4.2p3	White amorphous solid	2.4 mg	$C_{27}H_{35}NO_2$	405 g/mol	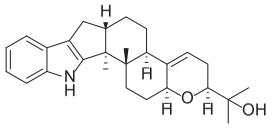	35.05	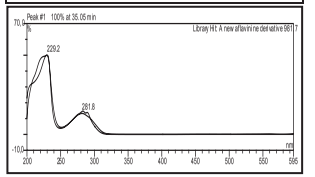
Pyrenocine B (**56**)	W8-7.3.2P2	White amorphous solid	9.8 mg	$C_{11}H_{14}O_5$	226 g/mol	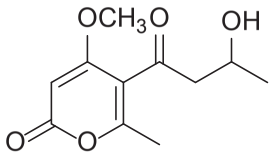	13.56 min	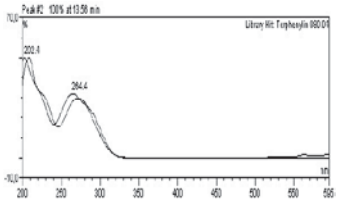

Pyrenocine A (**57**)	W8-4.2P1	White amorphous solid	13.3 mg	$C_{11}H_{12}O_4$	208 g/mol	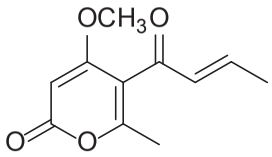	16.47 min	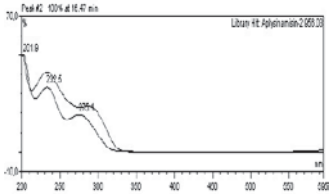
Citreo-γ-pyrone (**58**)	W8-9.2.2-1	Colorless crystal		$C_{11}H_{12}O_5$	224 g/mol	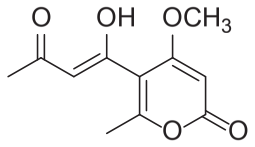	12.32 min	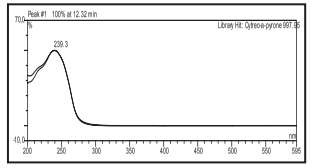
Citreo-α-pyrone (**59**)	W8-9.2.2-2	Colorless crystal		$C_{11}H_{12}O_5$	224 g/mol	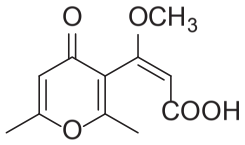		

3.5.2 Bioactivities of compounds from *P. paxilli*.

NO.	Sample name	Source	Cytotoxity		
			Mouse lymphoma cell line L5178Y (growth inhibition %)	Human ovarian cancer cell line A2780 sens	A2780 Cis*R*
48	W8-3.8.3 (Paxilline)	*Penicillium paxilli* Isolated from Sediment (Egypt)	45.6 (HQM089)	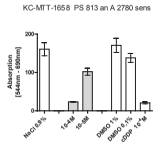	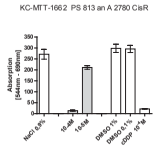
49	W8-3.4.2P1 (Dehydroxy paxilline)	*Penicillium paxilli* Isolated from Sediment (Egypt)	91.8 (HQM090) IC_{50}: 6.7 μM	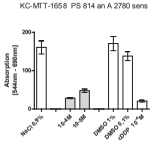 IC_{50} 6.4 μM	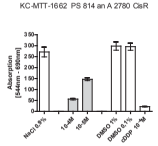 IC_{50} 1.1 μM
50	W8-3.4.2P2 (21-Isopentenylpaxilline)	*Penicillium paxilli* Isolated from Sediment (Egypt)	27.3 (HQM091)	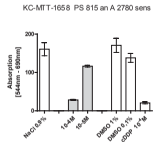 IC_{50} 105.6 μM	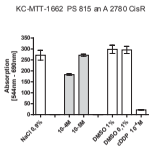
51	W8-5.3P4 (10β-hydroxy-13-desoxy paxilline)	*Penicillium paxilli* Isolated from Sediment (Egypt)	59.2 (HQM092)	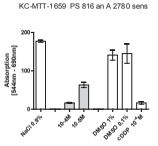 IC_{50} 24.5 μM	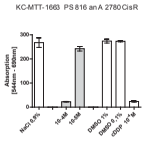

52	W8-3.4.2P4 (Paspaline)	*Penicillium paxilli* Isolated from Sediment (Egypt)	75.3 (HQM093) IC_{50} 3.2 μM	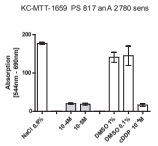	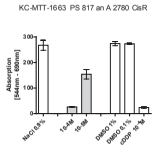
53	W8-3.4.2P5 (Emindole SB)	*Penicillium paxilli* Isolated from Sediment (Egypt)	29.5 (HQM094)	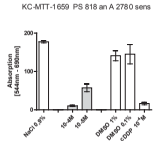	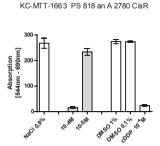
54	W8-5.3P3 (12-carboxyl- Paspaline)	*Penicillium paxilli* Isolated from Sediment (Egypt)	45.5 (HQM095)	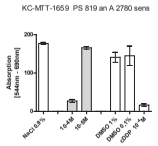	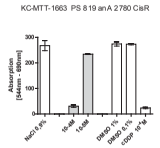
55	W8-3.4.2p3 (3-deoxo-4b-deoxypaxilline)	*Penicillium paxilli* Isolated from Sediment (Egypt)	35.1 (HQM096)	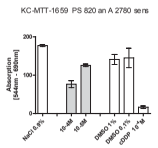	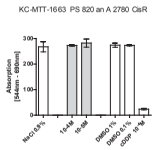
56	W8-7.3.2P2 (Pyrenocine B)	*Penicillium paxilli* Isolated from Sediment (Egypt)	98.4 (HQM097) IC_{50}: 4.9 μM IC_{50} 73.4 μM	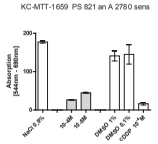	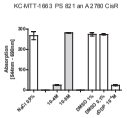

57	W8-4.2P1 (Pyrenocine A)	*Penicillium paxilli* Isolated from Sediment (Egypt)	113.7 (HQM098) IC_{50}: 1.1 μM	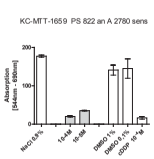	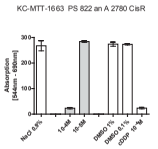 IC_{50} 22.0 μM

Results from antifungal (*Cladosporium cladosporioides*) and antibacterial (*S. aureus* ATCC) activity: inactive.

Result from antituberculosis:

HQT39: Paxilline (**48**) HQT47: Pyrenocine B (**56**) HQT40: Dehydroxy paxilline (**49**)

HQT48: Pyrenocine A (**57**) HQT43: Paspaline (**52**)

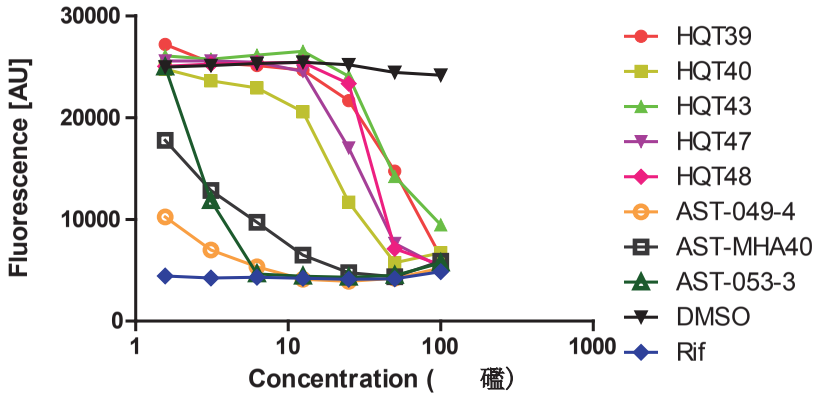

3.6 Known compounds isolated from endophytic fungus *Penicillium sclerotiorum* from mangrove plant *Aegialitis annulata*.

compound	Sample Code	Physical Description	Sample Amount	Molecular Formula	Molecular Weight	structure	HPLC Retention Time (standard gradient)	UV spectrum
(+)-Isorotiorin (**60**)	UvA-3.6p2 UvA-3.7P1	Yellow powder	11.3 mg	$C_{23}H_{23}ClO_5$	414	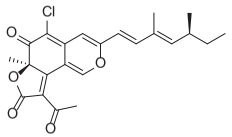	33.73 min	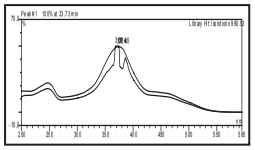
(+)-Sclerotiorin (**61**)	UvA-3.6P1	Yellow solid	3.6 mg	$C_{21}H_{23}ClO_5$	390	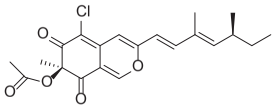	32.24 min	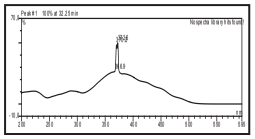
(+)-Isochromophilone VI (**62**)	UvA-10.1	Red solid	4.6 mg	$C_{23}H_{28}ClNO_5$	433	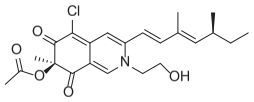	29.30 min	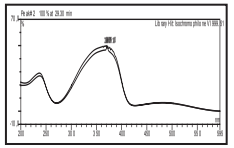
Isoharzianic acid (**63**)	UvA-12.2P2	Yellow gel	16.4 mg	$C_{19}H_{27}NO_6$	365	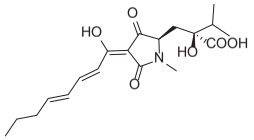	32.08 min	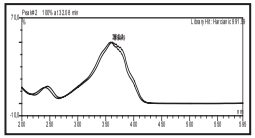
Harzianic acid (**64**)	UvA-12.2P1	Yellow gel	10.0 mg	$C_{19}H_{27}NO_6$	365	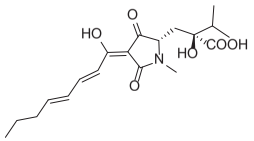	30.44 min	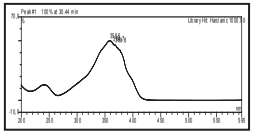

4 Discussion

4.1 Induction of new secondary metabolites by activation of silent biogenetic gene clusters in fungi

Screening of new bioactive secondary metabolites with pharmaceutical potential from fungi has played an important role in natural product research in recent decades (Scherlach and Hertweck, 2009). Herein, several approaches, including co-cultivation, "one strain many compounds" (OSMAC) approach, and epigenetic modification were employed to trigger the expression of silent biosynthetic pathways and to induce the secondary metabolite production from selected fungi.

4.1.1 Co-cultivation

Co-cultivation of microorganisms has repeatedly been shown to induce the formation of compounds that are not observed when the respective microorganisms are cultured under axenic conditions. For example, a new antibiotic pestalone was induced when the marine-derived fungus *Pestalotia* sp. was co-cultivated with a unicellular marine bacterium strain CNJ-328 (Cueto *et al*., 2001). Another example was the production of emericellamides A and B during co-culture of the marine-derived fungus *Emericella* sp. with the marine actinomycete *Salinispora arenicola* (Oh *et al*., 2007). This elicitation of natural product accumulation is believed to be caused by competition/ antagonism of different microorganisms and has been shown to be due to an activation of biogenetic gene clusters that remain silent under axenic conditions. There are two possible ways to achieve the crosstalk between microorganisms: one is through physical interaction, and the other way is through chemical signals secreted by one organism which can stimulate the assembly of natural products in the other organism (Scherlach and Hertweck, 2009). Herein, fungus-bacterium co-cultivation of *A. terreus* with *Bacillus* sp., as well as fungus-fungus co-cultivation of *Penicillium* sp. (strains IO1 and IO2), afforded the accumulation of new and/ or known compounds, which were not detected in the respective axenic cultures.

4.1.1.1 Secondary metabolite induction by co-cultivation of *A. terreus* with bacteria

A. terreus is well known for the production of butyrolactone derivatives (Guo *et al*., 2013; Haritakun *et al*., 2010; San-martin *et al*., 2011). Interestingly, co-cultivation of *A. terreus* with *B. subtilis* or with *B. cereus*, led to two new butyrolactone derivatives isobutyrolactone II (**7**) and 4-O-dimethylisobutyrolactone II (**8**) and to an up to 34-fold increase in the accumulation of constitutively present fungal natural products (Table 3.2.9). Furthermore, it is worth mentioning that compounds **7** and **8** were not only detected in co-cultures of *A. terreus* with live cultures of *B. subtilis* or with *B. cereus*, but also when *A. terreus* was cultured in the presence of autoclaved *B. subtilis*, indicating that the bacterial signaling, which leads to induction of fungal metabolites, is not due to heat labile molecules. (Chen *et al*., 2015b)

Isotope labeling and mutant strain experiments of *A. terreus* have shown that butyrolactones are biosynthesized by condensation of two *p*-hydroxyphenylpyruvic acid (HPPA) units involving NRPS-like enzymes terminating with a TE domain and missing the canonical C domain found in NRPS enzymes (Nitta *et al*., 1983; Guo *et al*., 2013). Based on the above data, the new products are assumed to be produced by *A. terreus*, and a plausible pathway for the biosynthesis of the butyrolactone derivatives (**7**, **8**, **10**-**13**, **21**) isolated in this study is proposed (Figure 4.1), which includes aldol condensation of two *p*-hydroxyphenylpyruvic acid (HPPA) methyl ester units, followed by ester cyclization to yield butyrolactone II (**10**). An alternate route for the production of **10** would be through methylation of the known butytolactone IV in the presence of S-adenosyl-methionine (SAM). Prenylation of **10** in the presence of dimethylallyl-pyrophosphate (DMAPP) and subsequent epoxidation would result in the formation of butyrolactone I (**11**) and butyrolactone III (**12**), respectively. Moreover, butyrolactone VI (**13**) would be formed by epoxide hydrolysis of **12**. Another biosynthetic route would include decarboxylation of butyrolactone IV followed by hydroxylation at C-4 to form compounds **21** and **8**, respectively. Finally, **7** is proposed to be biosynthesized from **8** through methylation in the presence of SAM (Figure 4.1). (Chen *et al*., 2015b)

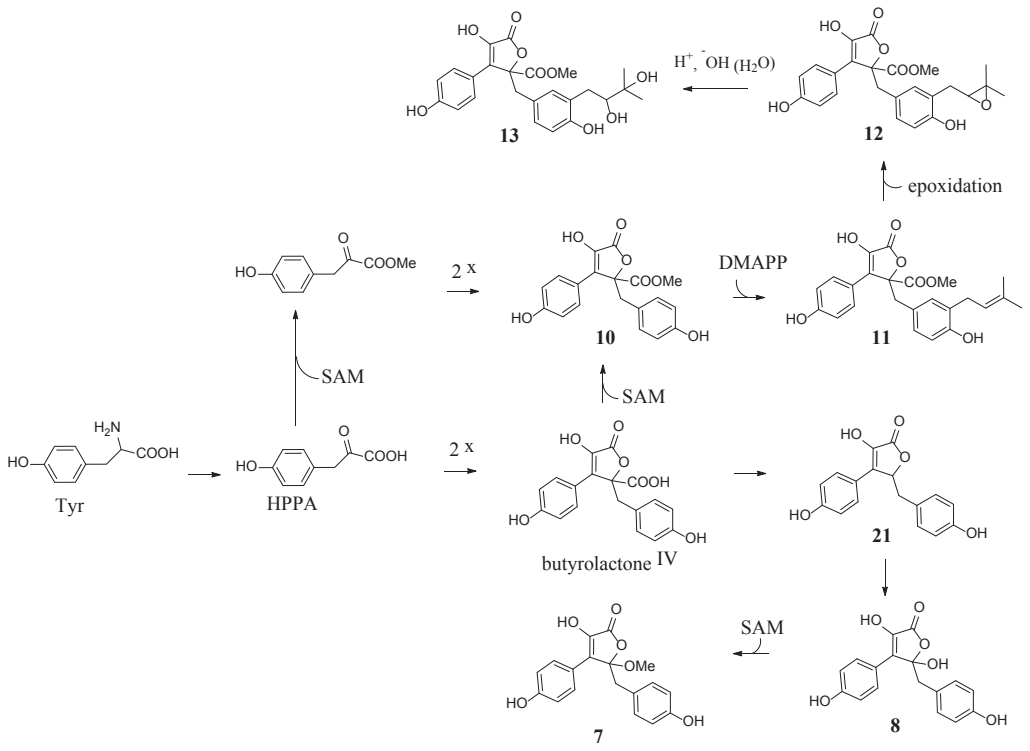

Figure 4.1 Proposed biosynthetic pathway leading to butyrolactones (Hosoe *et al*., 2009; Cazar *et al*., 2005).

Another induced compound, N-(carboxymethyl)anthranilic acid (**9**), was isolated from co-cultivation of *A. terreus* and *Bacillus* sp.. It was previously reported as an induced secondary metabolite produced during co-cultivation of *F. tricinctum* with *B. subtilis*, but was not detected in axenic cultures of *F. tricinctum* or of *B. subtilis* (Ola *et al*., 2013). In this study, **9** could only be detected in co-cultures of *A. terreus* with live *B. subtilis*, but not in co-cultures of *A. terreus* with *B. cereus* or with autoclaved *B. subtilis*. In addition, compound **9** is an anthranilic acid derivative, and anthranilic acid has been reported as a natural product produced by several bacterial species, such as *Streptomyces* sp. (Abdelfattah *et al*., 2012; Yang and Cordell, 1997) and *Paenibacillus polymyxa* (Lebuhn *et al*., 1997). Hence, it cannot be excluded that the producer of **9** is *B. subtilis*. (Chen *et al*., 2015b)

In addition to the induced compounds, some constitutively present compounds were accumulated during co-cultivation. Terrein (**14**), which is a typical metabolite of *A. terreus*, was strongly enhanced (34-fold increase) during co-cultivation of *A. terreus* with *B. subtilis*, with autoclaved *B. subtilis* or with *B. cereus*, respectively. Terrein has been reported to inhibit

plant growth and melanin biosynthesis, as well as to have antimicrobial, antiproliferative, and antioxidative activities (Park *et al*., 2004; Xu *et al*., 2012). *A. terreus*, as the only species of *Aspergillus* producing terrein, was exploited for investigation of terrein biosynthesis (Zaehle, *et al.* 2014). Interestingly, the essential gene for terrein biosynthesis (TerA) displayed unusual plasticity, yielding a mixture of 4-hydroxy-6-methylpyranone, orsellinic acid, and 2,3-dehydro-6-hydroxymellein by condensing acetyl-CoA with two, three, or four malonyl-CoA units, respectively. In addition, 6-hydroxymellein, formed by specific reduction of 2,3-dehydro-6-hydroxymellein, was identified as a key intermediate in the biosynthesis of terrein (Figure 4.2) (Zaehle *et al*., 2014). However, hydroxylation at position 7 of 2,3-dehydro-6-hydroxymellein and subsequent reduction yielded 6,7-dihydroxymellein, which was not converted into terrein (Figure 4.2) (Zaehle *et al*., 2014).

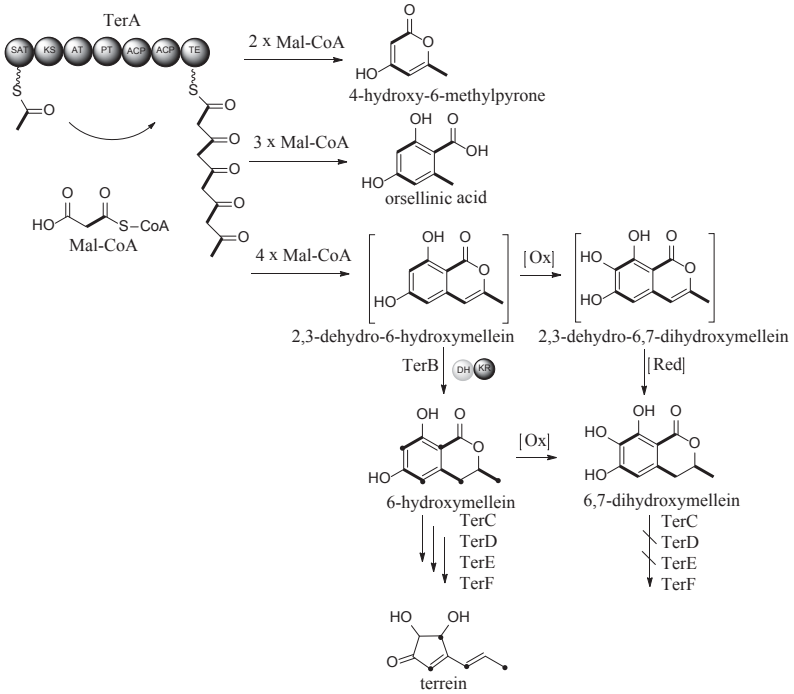

Figure 4.2 Biosynthetic pathway of terrein (Zaehle *et al*., 2014).

All isolated compounds were tested for their antibacterial activities against *B. subtilis* and *B. cereus*, but only butyrolactone II (**11**) and aspulvinone E (**20**) showed weak inhibition of *B. cereus* with MICs of 150.9 (64 μg/mL) and 216.2 (64 μg/mL) μM, respectively. The isolated compounds were further examined for their effects on the growth of L5178Y mouse lymphoma cells employing the MTT assay. Terrein (**14**) showed moderate cytotoxicity with 80% inhibition of the respective cell line at a dose of 10 μg/ml. The remaining compounds

exhibited no activity. Interestingly, the biosynthesis of **14** was most strongly induced among all the isolated compounds, which highlights the value of the co-cultivation approach as an effective strategy to access bioactive secondary metabolites from microorganisms. (Chen *et al*., 2015b)

4.1.1.2 Dynamic factors in co-cultivation metabolic response

During set up of co-cultivation experiments, various factors were considered to have critical influence on the accumulation of fungal metabolites. The strain *A. terreus*, which was used for our study, was co-cultured with different bacteria, including two *Bacillus* strains (*B. subtilis* and *B. cereus*), two *Streptomyces* strains (*S. lividans* and *S. coelicolor*), *Pseudomonas aeruginosa*, *Staphylococcus aureus*, and *Mycobacterium tuberculosis*. Both *Bacillus* strains, in addition to autoclaved *B. subtilis*, stimulated the accumulation of constitutively present fungal metabolites (Figure 3.2.4 and Table 3.2.10). However, no induction was observed during co-cultivation either with *S. lividans* or with *S. coelicolor* (Figure 3.2.6). Moreover, the autoclaved strains of *P. aeruginosa*, *S. aureus*, and *M. tuberculosis* were found to induce moderate accumulation of fungal metabolites (Figure 4.3). These results suggested that the response of *A. terreus* toward different bacteria may be a specific rather than a general reaction toward prokaryotes, which is in accordance with our previously reported results (Chen *et al*., 2015b; Ola *et al*., 2013).

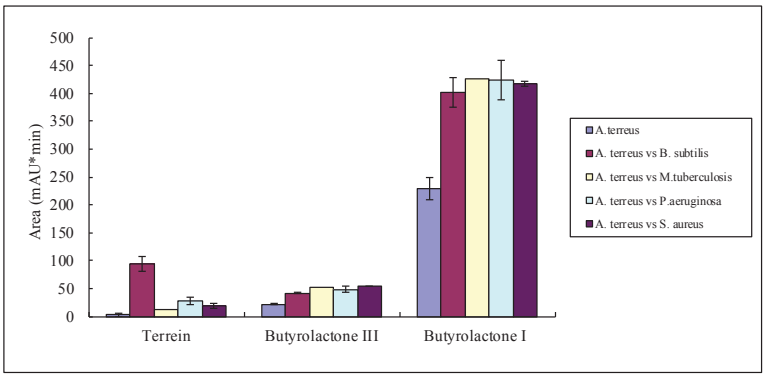

Figure 4.3 Yield of three main compounds produced by *A. terreus* during co-cultivation.

Interestingly, the accumulation of fungal metabolites of *A. terreus* was only detected following a four-day preincubation of the solid rice medium with *B. subtilis*. However, when *A. terreus* and *B. subtilis* were inoculated on rice medium at the same day, no effect was observed. Thus, the interspecies crosstalk during co-cultivation is a dynamic process that is

also influenced by the time of bacterium preincubation (Ola *et al*., 2013; Slattery *et al*., 2001).

4.1.1.3 Secondary metabolite induction by co-cultivation of two *Penicillium* sp.

Co-cultivation of two *Penicillium* strains IO1 and IO2 isolated from the Mediterranean sponge *Ircinia oros* was found to induce the accumulation of the known norlichexanthone (**37**) and monocerin (**38**), which were not detected in either of the fungal axenic controls. Interestingly, monocerin (**38**) exhibited significant cytotoxicity with an IC_{50} value of 8.4 μM, compared to kahalalide F as a positive control (IC_{50} 4.3 μM). Monocerin (**38**) was previously reported as an antifungal, insecticidal, and phytotoxic secondary metabolite from several fungal species (Sappapan *et al*., 2008; Zhang *et al*., 2008). The antimicrobial activity of norlichexanthone (**37**) against *Staphylococcus aureus, Sarcina ventriculi, Pseudomonas aeruginosa, Candida albicans, Aspergillus niger*, and *Fusarium oxysporum* was also described with MIC values similar to those of ampicillin (against bacteria) and nystatin (against fungi) (Liu *et al*., 2010). Therefore, it may be assumed that the production of **37** and **38** during co-cultivation is triggered by one of these fungi as a stress response to suppress the growth of its competitor. (Chen *et al*., 2015a)

4.1.2 OSMAC approach

"One strain-many compounds" (OSMAC) is a simple and effective approach for enhancing the chemical diversity of fungal metabolites by systematic alteration of the culture conditions of a given organism. It refers to the fact that a single microorganism can afford a wide range of compounds according to the environmental conditions (Bode *et al*., 2002; Reen *et al*., 2015). Therefore, a common strategy of the OSMAC approach is altering culture conditions, such as composition of the medium, pH and/or temperature that trigger the highest yield of bioactive secondary metabolites (Bode *et al*., 2002; Reen *et al*., 2015). For example, cultivation of the fungus *Gymnascella dankaliensis* on solid rice medium spiked with 3.5% NaCl led to the isolation of the chlorinated compounds gymnastatin A and B, whereas addition of KBr to the rice medium resulted in the accumulation of brominated metabolites lacking in fungal controls (Hammerschmidt *et al*., 2015). Herein, cultures of *A. terreus* on three different media (rice, bean and liquid Wickerham medium) displayed diverse HPLC

profiles obtained from the ethyl acetate extracts. Butyrolactones were the major compounds isolated from all of these three medium cultures. However, considerable amounts of N-containing compounds were isolated from liquid Wickerham medium and white beans cultures, affording dihydroisoflavipucine and asterrelenin, respectively, as the major constituents (Figure 3.2.13).

4.1.2.1 Dihydroisoflavipucine from liquid Wickerham medium culture

Dihydroisoflavipucine (**22**) was isolated as one of the major compounds from liquid Wickerham medium. Gressler, *et al.* (2011) provided the first insight into the biosynthesis of dihydroisoflavipucine on the basis of functional genetics, bioinformatics, and isotope labeling (Figure 4.3). Interestingly, it was shown that dihydroisoflavipucine is a PKS-NRPS hybrid metabolite. The pyridone moiety was derived from the polyketide pathway according to isotope-labeling experiments (Grandolini, Casinovi and Radics, 1987), whereas the side chain was derived from the amino acid leucine (Gressler *et al*., 2011). However, the study further illustrated that the production of dihydroisoflavipucine in *A. terreus* was induced by media with alkaline pH and/or by the presence of nitrogen sources, such as amino acids (Gressler *et al*., 2011). Thus, the high proportions of nitrogen-containing nutrients in liquid Wickerham medium (0.5% peptone), in addition to its slightly alkaline pH (7.2-7.4), may be important factors for the production of dihydroisoflavipucine as the main metabolite in *A. terreus*.

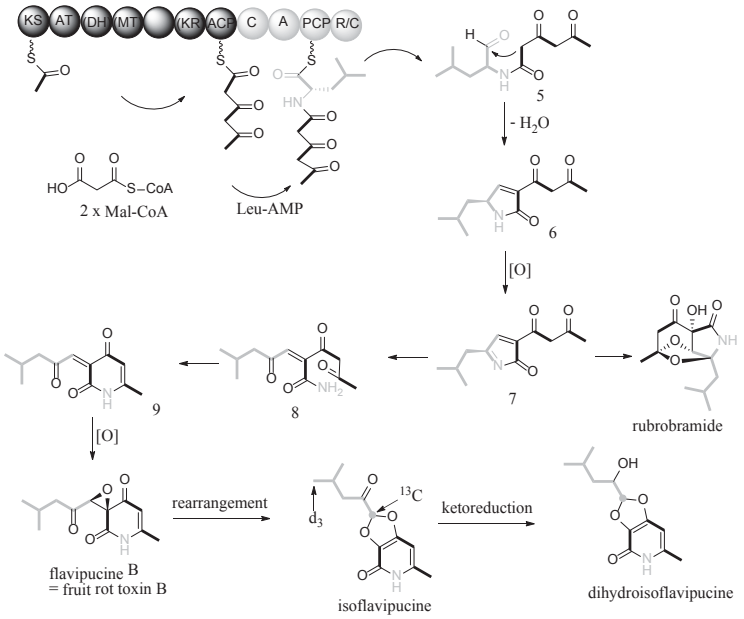

Figure 4.3 Proposed biosynthesis of isoflavipucine (Gressler *et al*., 2011).

In addition, three 6-hydroxymellein analogues (**25 - 27**) were isolated from liquid Wickerham medium cultures, while none of their analogues were detected or isolated from rice or white beans cultures.

4.1.2.2 Indole alkaloids from white beans medium culture

Two indole alkaloids asterrelenin (**29**) and acetylaszonalenin (**30**) were only obtained from white beans medium cultures of *A. terreus*. According to Yin, *et al*. (2009), L-tryptophan together with anthranilic acid, forms (*R*)-benzodiazepinedione, a cyclic dipeptide with a diketopiperazine structure, in the presence of a non-ribosomal peptide synthetase (AnaPS). Then, a dimethylallyl moiety is transferred to the indole ring of tryptophan, catalyzed by a non-ribosomal prenyltransferase (AnaPT), followed by the formation of an additional ring system with the diketopiperazine moiety to form aszonalenin. Finally, acetylaszonalenin is formed by acetylation at the N-position of the indole ring catalyzed by a non-ribosomal acetyltransferase (AnaAT), whereas asterrelenin is formed by hydroxylation of acetylaszonalenin at C-11. (Figure 4.4) (Yin *et al*., 2009) The above finding was consistent with the nutrient composition of the bean medium, which contains high concentrations of amino acids, including tryptophan. Thus, variation of medium composition may have a great impact on the quantity and diversity of fungal secondary metabolite production.

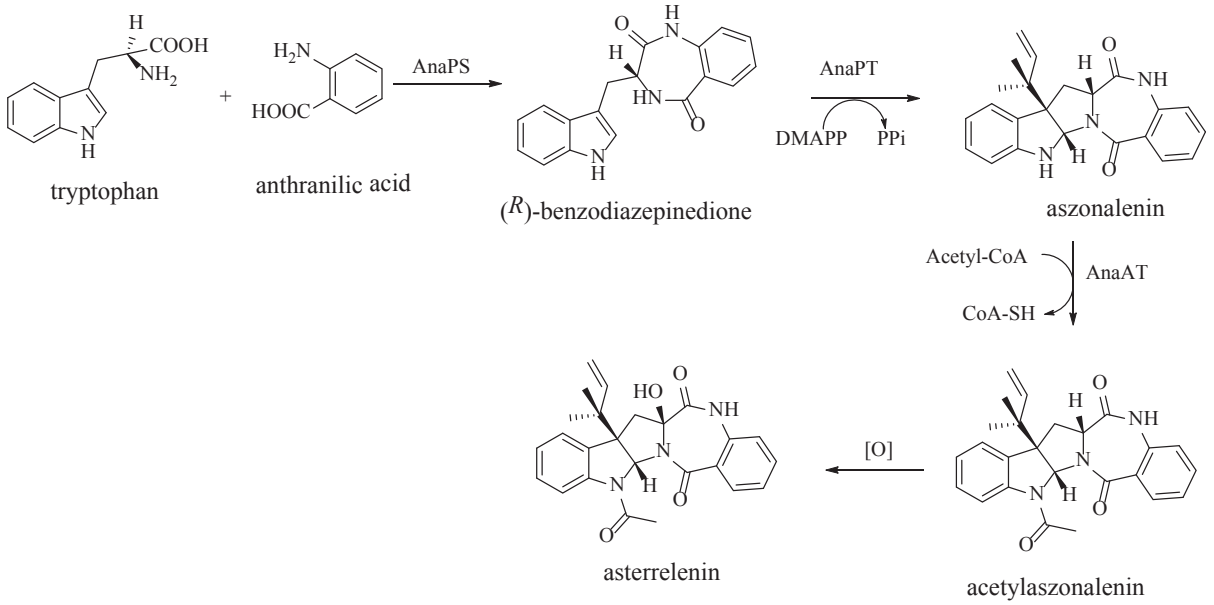

Figure 4.4 Proposed biosynthesis of acetylaszonalenin and asterrelenin (Yin *et al*., 2009).

4.1.3 Epigenetic modification

Epigenetic modifiers, such as the inhibitors of histone deacetylase (HDAC) or DNA methyltranferase (DNMT), have been used to activate the transcription of natural-product-encoding cryptic gene clusters through covalent modification of histones and/or DNA (Cichewicz, 2010). For example, addition of suberoylanilide hydroxamic acid (SAHA) to the culture medium of the entomopathogenic fungus *Cordyceps annullata*, clearly enhanced the production of secondary metabolites, including four new 2,3-dihydrobenzofurans, annullatins A-D, and a new aromatic polyketide annullatin E (Asai *et al*., 2012). Herein, the epigenetic modifiers 5-azacytidine and SAHA were added to liquid Wickerham medium for their impact on the induction of cryptic fungal secondary metabolite production. However, the HPLC profiles of the cultures treated with epigenetic modifiers were very similar to those of the axenic fungal cultures. It has been reported that the fungal reaction to epigenetic modifiers is rather specific and correlates with their concentration and/or preincubation time of the medium with the fungus (Williams *et al*., 2008). Thus, the different approaches for triggering the biosynthesis of new natural products are heavily dependent on the right conditions under which silent biosynthetic gene clusters are expressed (Scherlach and Hertweck, 2009).

4.2 Secondary metabolites produced by the endophytic fungus *T. harzianum*

4.2.1 Cytochalasins isolated from *T. harzianum*

Cytochalasins are characterized by a highly substituted hydrogenated isoindole ring to which typically a macrocyclic ring is fused. The latter may vary from 11-14 atoms and may be a carbocycle, a lactone, or a cyclic carbonate (Scherlach *et al*., 2010). The complex structure of cytochalasins is of biosynthetic interest as it includes constituents of mixed biogenetic origin. Isotope labeling experiments (Scherlach *et al*., 2010; Robert and Tamm, 1975; Lebet and Tamm, 1973) have shown that the macrocyclic ring originates from acetate/ malonate units, which are linked via the polyketide pathway. The methylene group C-12 and the two methyl groups C-16 and C-18 are introduced into the carbon backbone as C1- units from the *S*-methyl groups of *S*-adenosylmethionine. In addition, the perhydroisoindol-1-one moiety

commonly bears a benzyl group that originates from one phenylalanine unit. Interestingly, the presence of a *para*-hydroxy benzyl residue in 4'-hydroxyl-deacetyl-18-deoxycytochalasin H (**1)** suggests the incorporation of one tyrosine unit into the polyketide backbone, which is rarely encountered in this group of metabolites. (Chen *et al*., 2015c)

All isolated compounds were assayed for their cytotoxicity toward L5178Y, A2780 sens, and A2780 CisR cancer cell lines (Table 3.1.5). 18-Deoxycytochalasin H (**3)** showed the strongest activity toward L5178Y, A2780 sens, and A2780 CisR cancer cell lines (Table 3.1.5) with IC_{50} values of 0.19, 0.42, and 6.55 μM, respectively. Notably, deacetylation of the hydroxy group at C-21, as in **1** and deacetyl-18-deoxycytochalasin H (**2**), caused a significant decrease in the activity, indicating that the acetate group plays an important role in mediating cytotoxicity. A possible explanation for this observation lies in the contribution of the acetate group to an enhanced cellular uptake through increased membrane permeation. The presence of an additional hydroxyl substitutent in the aromatic ring, as in **1** compared with **2**, on the other side had no significant effect on the activity of these compounds. (Chen *et al*., 2015c)

4.2.2 Different patterns of compounds isolated from two independent fermentations of *T. harzianum*

During two independent fermentations of the endophytic fungus *T. harzianum*, different HPLC profiles of the respective extracts were observed. In the first fermentation, cytochalasins were the major compounds produced by this fungus, whereas, no cytochalasin analogues were detected during the second fermentation. Instead, several nonpolar aliphatic compounds were detected. The explanation probably lies in the metabolic change of the culture during storage on agar plates. In nature, fungi live in more complex environments with different sources of nutrients, competition between microbes, and symbiosis or contend with their hosts (Scherlach and Hertweck, 2009). On the other hand, fermentation of fungi under "luxurious" laboratory conditions (specific culture media and single strains) may lead to metabolic change and inactivation of biosynthetic gene clusters that are responsible for the production of specific bioactive secondary metabolites (Pettit, 2009; Reen, 2015).

5. Summary

Fungi play a crucial role in pharmaceutical industry and agriculture due to their potential to produce secondary metabolites with diverse chemical structures and biological activities. This dissertation investigates natural products from fungi from various biological sources: plant endophytes, sponge-associated and marine sediment derived fungi. Chemical investigations on fungi were mainly carried out in this thesis on rice culture, followed by various chromatographic separation techniques, whereas structure elucidation was based on mass spectrometry (MS) and nuclear magnetic resonance (NMR) data. The stereochemistry of chiral compounds was determined by comparison of their optical rotation with the literature or by ECD calculations. The isolated compounds were subjected to bioactivity assays, including antibiotic and cytotoxicity assays.

Furthermore, in order to activate silent biosynthetic gene clusters, several methods were employed to culture selected fungal strains. Medium optimization and co-cultivation with bacteria successfully induced new natural products and an increased accumulation of the constitutively presented metabolites in *A. terreus*. Co-cultivation of two *Penicillium* sp. strains isolated from the same host induced known compounds that were not present in either of the fungal axenic controls.

1. *Trichoderma harzianum*

The endophytic fungus *T. harzianum* was isolated from leaves of *C. nitida*. Six natural products, including one new cytochalasin 4'-hydroxy-deacetyl-18-deoxycytochalasin H (**1**) were isolated. Two subsequent fermentations gave different patterns of metabolites. Cytochalasins **1-3** showed potent cytotoxic activity against the murine lymphoma cell line L5178Y and human ovarian cancer cell lines A2780 sens and A2780 CisR with IC_{50} values between 0.19 and 6.97 μM.

2. *Aspergillus terreus*

A. terreus was isolated from a sediment sample collected from the saline lake in Wadi EI Natrun in Egypt. The first approach to trigger silent biosynthetic gene clusters through

co-cultivation with the bacteria *B. subtilis* or *B. cereus* on solid rice medium resulted in an up to 34-fold increase of the accumulation of constitutively present fungal natural products (**10** ─ **21**) compared to the axenic cultures of *A. terreus*. In addition, two new butyrolactone derivatives, isobutyrolactone II (**7**) and 4-O-demethylisobutyrolactone II (**8**), as well as the known N-(carboxymethyl)anthranilic acid (**9**) that were not present in axenic fungal or bacterial controls were strongly induced. However, co-cultivation with *S. lividans* or with *S. coelicolor* failed to induce changes in fungal natural product accumulation in contrast to co-cultures with *Bacillus* sp. The second approach of cultivation of *A. terreus* in different media resulted in the accumulation of seven distinct compounds from the liquid Wickerham medium culture, and two compounds, namely, asterrelenin (**29**) and acetylaszonalenin (**30**) from the white beans culture compared to the rice culture.

Bioassay results showed that compounds **11** and **20** weakly inhibited *B. cereus* with minimal inhibitory concentrations (MICs) of 64 μg/mL, and **14** showed moderate cytotoxicity against L5178Y cell line with growth inhibition of 80% at a dose of 10 μg/mL.

3. *Penicillium* sp. strains IO1 and IO2

Penicillium sp. (strains IO1 and IO2) were isolated from the Mediterranean sponge *I. oros*. A new fusarielin analogue fusarielin I (**31**) together with the known compounds griseofulvin (**32**) and dechlorogriseofulvin (**33**) were isolated from the rice culture of *Penicillium* sp. strain IO1. The absolute configuration of **31** was determined on the basis of TDDFT ECD calculations. Three known compounds dehydrocurvularin (**34**), curvularin (**35**), and trichodimerol (**36**) were isolated from *Penicillium* sp. strain IO2. Co-cultivation of both *Penicillium* strains resulted in the accumulation of the known norlichexanthone (**37**) and monocerin (**38**) that were not detected in either of the two axenic fungal controls. Compounds **39** and **40** showed pronounced cytotoxicity against L5178Y cell line with IC_{50} values of 8.4 and 4.7 μM, respectively.

4. *Alternaria alternata*

The endophytic fungus *A. alternata* was isolated from leaves of the Cameroon rainforest plant *A. africana*. Six compounds were isolated from the ethyl acetate extract of fermentation on

rice. The stereoisomers **41** and **42** applied to ECD spectroscopy showed similarity of **41** to the known altersetin, while the different high-wavelength ECD transitions of **42** may suggest different stereochemistry at C-5. The new methyl 2-carboxy-3-hydroxy-(*E*)-cinnamate (**46**) was observed to gradually cyclize to **47** in methanol.

5. *Penicillium paxillin*

P. paxillin was isolated from the sediment collected from Wadi EI Natrun lake, too. Ten known compounds, including eight paxillines and two pyrenocines were isolated from the rice culture, whereas two pyrones were induced when plant material was added to the rice medium. Cytotoxity tests showed that both pyrenocines A and B inhibited the growth of L5178Y and A2780 sens cell lines with IC_{50} values of 1.1 and 4.9 μM, respectively. Among paxillines, dehydroxy paxilline (**49**) presented the strongest cytotoxicity to all of the tested cell lines (L5178Y, A2780 sens and CisR) with IC_{50} values between 1.1and 6.7 μM.

6. *Penicillium sclerotiorum*

Five known compounds were isolated from the fungus *P. sclerotiorum*, which was isolated from the mangrove plant *A.annulata*.

In conclusion, sixty-four compounds were isolated and identified from six different sources of fungi, in which, seven were new natural products (Table 5.1). Different culture approaches successfully triggered the accumulation of distinct metabolites compared to axenic controls.

Table 5.1 Summary of the isolated compounds.

	Compound	Structure	Source	Comment
1	4'-Hydroxyl-deacetyl-18-deoxycytochalasin H	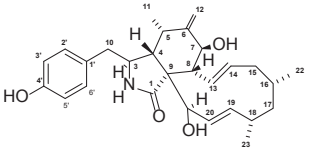	*T. harzianum*	new
2	Deacetyl-18-deoxycytochalasin H	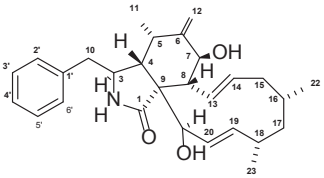	*T. harzianum*	known
3	18-Deoxycytochalasin H	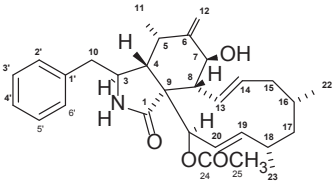	*T. harzianum*	known
4	Alternariol	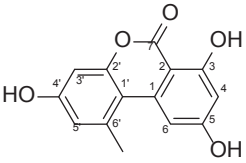	*T. harzianum*	known
5	Waol A	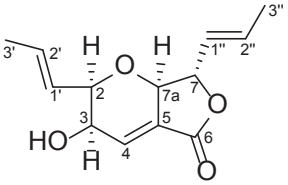	*T. harzianum*	known
6	Aspyridone A	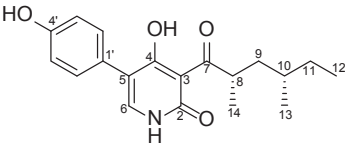	*T. harzianum*	known
7	Isobutyrolactone II	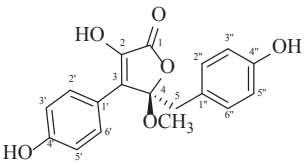	*A. terreus*	new
8	4-O-demethylisobutyrolactone II	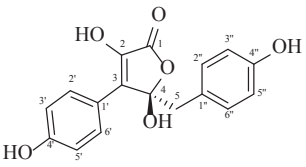	*A. terreus*	new
9	N-(carboxymethyl) anthranilic acid	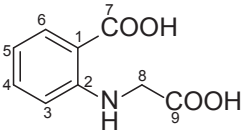	*A. terreus*	known

10	Butyrolactone II	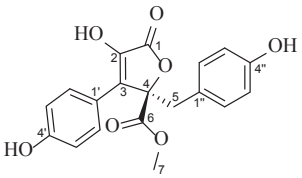	*A. terreus*	known
11	Butyrolactone I	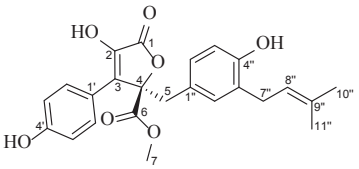	*A. terreus*	known
12	Butyrolactone III	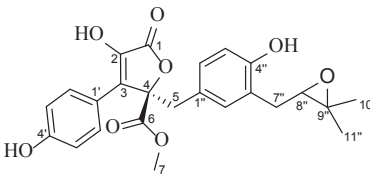	*A. terreus*	known
13	Butyrolactone VI	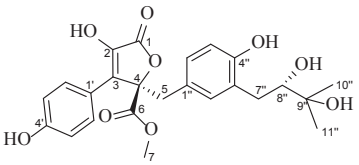	*A. terreus*	known
14	Terrein	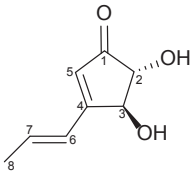	*A. terreus*	known
15	Dihydroterrein	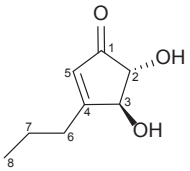	*A. terreus*	known
16	Orsellinic acid	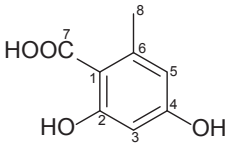	*A. terreus*	known
17	Terreinol	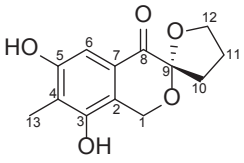	*A. terreus*	known

18	Terretonin A	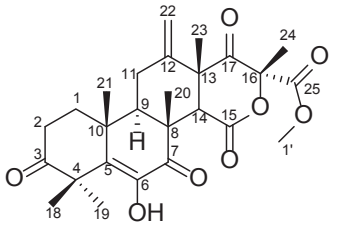	*A. terreus*	known
19	Terretonin	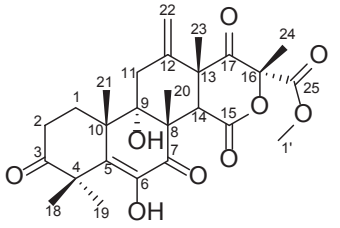	*A. terreus*	known
20	Aspulvinone E	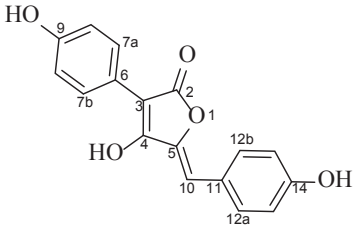	*A. terreus*	known
21	3-hydroxy-5-(4-hydroxybenzyl) -4-(4-hydroxyphenyl) furan-2(5*H*)-one	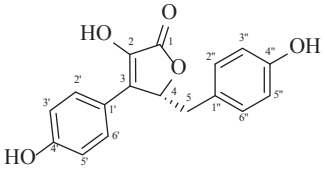	*A. terreus*	known
22	(2*R*, 1'*S*)-Dihydroisoflavipucine	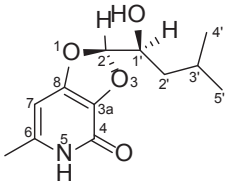	*A. terreus*	known
23	(2*S*, 1'*S*)-Dihydroisoflavipucine	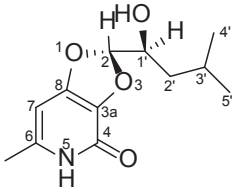	*A. terreus*	new
24		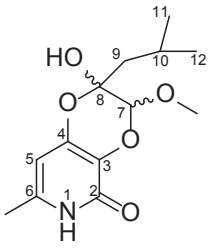	*A. terreus*	known

25	*Cis*-4,6-dihydroxymellein	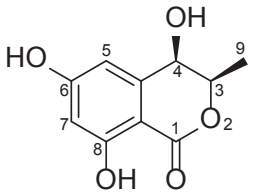	*A. terreus*	known
26	*Cis*-4-hydroxy-6-methoxymellein	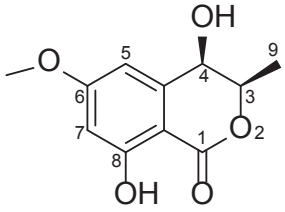	*A. terreus*	known
27	*Cis*-3,4-dihydro-4,8-dihydroxy-6,7-dimethoxy-3-methlisocoumarin	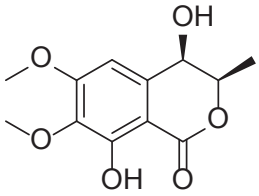	*A. terreus*	known
28	1-(2',3'-dihydroxyphenyl)ethanone	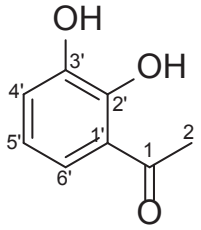	*A. terreus*	known
29	Asterrelenin	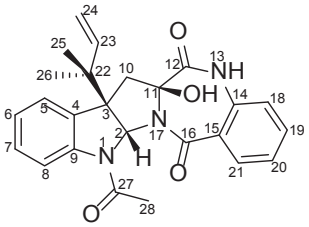	*A. terreus*	known
30	Acetylaszonalenin	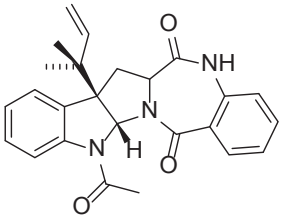	*A. terreus*	known
31	Fusarielin I	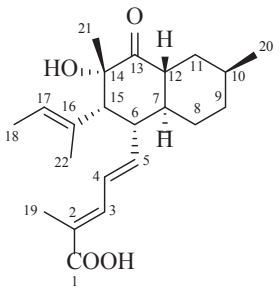	*Penicillium* sp. (strain IO1)	new

32	Griseofulvin	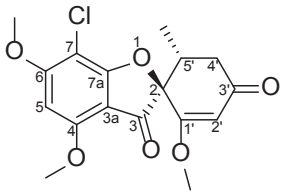	*Penicillium* sp. (strain IO1)	known
33	Dechlorogriseofulvin	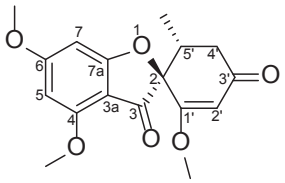	*Penicillium* sp. (strain IO1)	known
34	Dehydrocurvularin	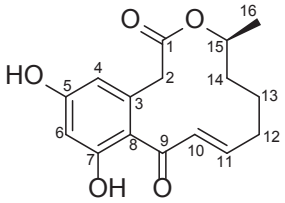	*Penicillium* sp. (strain IO2)	known
35	Curvularin	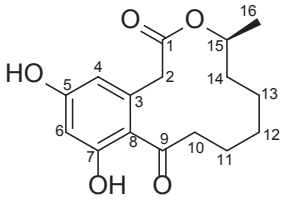	*Penicillium* sp. (strain IO2)	known
36	Trichodimerol	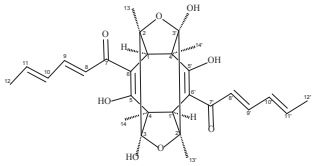	*Penicillium* sp. (strain IO2)	known
37	Norlichexanthone	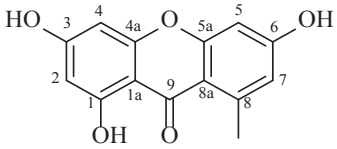	coculture of *penicillium* sp. strains IO1 and IO2	known
38	Monocerin	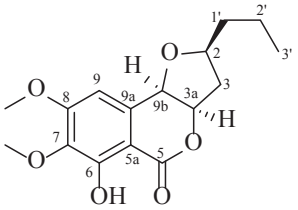	coculture of *penicillium* sp. strains IO1 and IO2	known
39	Griseophenone B	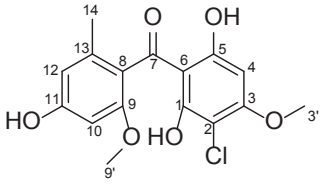	coculture of *penicillium* sp. strains IO1 and IO2	known

40	Echinulin	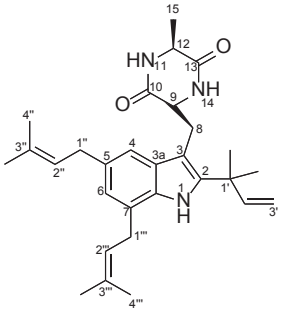	coculture of *penicillium* sp. strains IO1 and IO2	known
41	(5*S*)-Altersetin	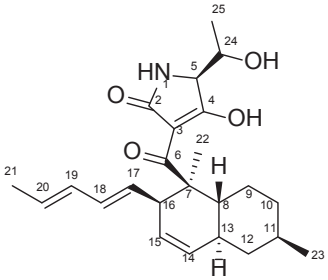	*A*. a*lternata*	known
42	Altersetin-2	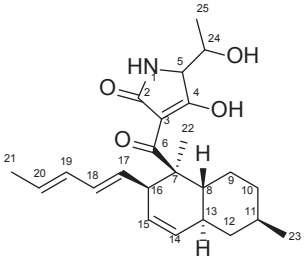	*A*. a*lternata*	new
43	Altertoxin II	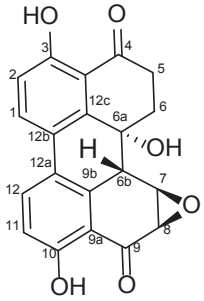	*A*. a*lternata*	known
44	Altertoxin I	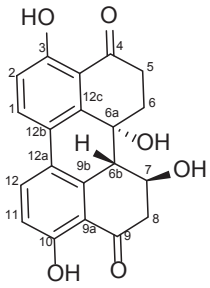	*A*. a*lternata*	known
45	Tenuazonic acid	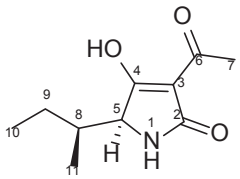	*A*. a*lternata*	known

46	Methyl 2-carboxy-3-hydroxy-(*E*)-cinnamate	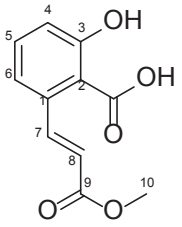	*A*. a*lternata*	new
47	3-[(methoxycarbonyl) methyl]-7-hydroxyphthalide	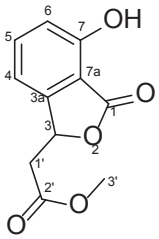	*A*. a*lternata*	new
48	Paxilline	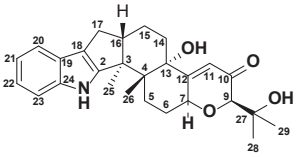	*P. paxilli*	known
49	Dehydroxy paxilline	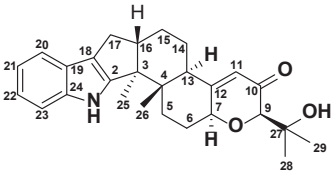	*P. paxilli*	known
50	21-Isopentenylpaxilline	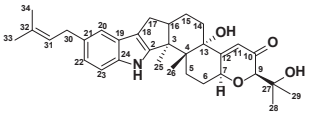	*P. paxilli*	known
51	10*β*-hydroxy-13-desoxy paxilline	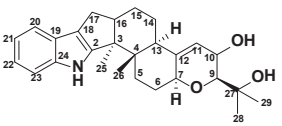	*P. paxilli*	known
52	Paspaline	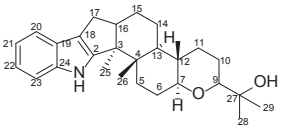	*P. paxilli*	known
53	Emindole SB	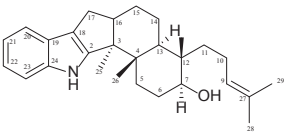	*P. paxilli*	known
54	12-carboxyl- Paspaline	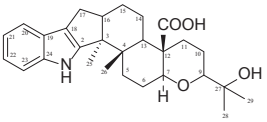	*P. paxilli*	known
55	3-deoxo-4b-deoxypaxilline	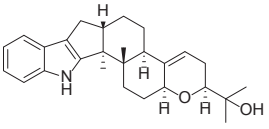	*P. paxilli*	known

56	Pyrenocine B	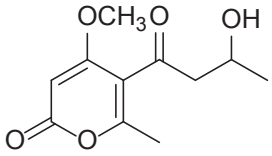	*P. paxilli*	known
57	Pyrenocine A	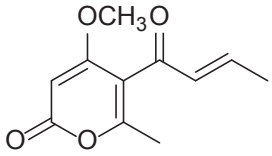	*P. paxilli*	known
58	Citreo-γ-pyrone	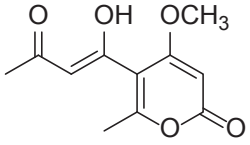	*P. paxilli*	known
59	Citreo-α-pyrone	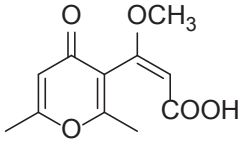	*P. paxilli*	known
60	(+)-Isorotiorin	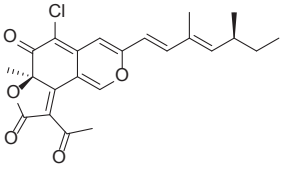	*P. sclerotiorum*	known
61	(+)-Sclerotiorin	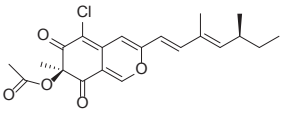	*P. sclerotiorum*	known
62	(+)-Isochromophilone VI	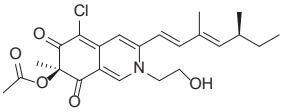	*P. sclerotiorum*	known
63	Isoharzianic acid	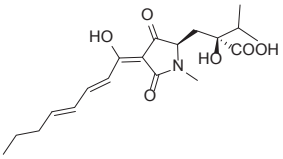	*P. sclerotiorum*	known
64	Harzianic acid	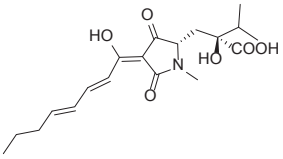	*P. sclerotiorum*	known

6. References

Abdelfattah, M. S., Toume, K., Arai, M. A., Masu, H., and Ishibashi, M. (2012) Katorazone, a new yellow pigment with a 2-azaquinone-phenylhydrazone structure produced by *Streptomyces* sp. IFM11299. *Tetrahedron Letter*, **53**, 3346-3348.

Adegboye, M. F., Babalola, O. O., Ngoma, L., and Okoh, A. I. (2012) Analysis of *Streptomyces* spp. native to Mahikeng soils in South Africa. *Journal of Pure and Applied Microbiology,* **6**(3), 1001-1010.

Alberts, A., Chen, J., Kuron, G., Hunt, V., Huff, J., Hoffman, C., Rothrock, J., Lopez, M., Joshua, H., and Harris, E. (1980) Mevinolin: a highly potent competitive inhibitor of hydroxymethylglutaryl-coenzyme A reductase and a cholesterol-lowering agent. *Proceedings of the National Academy of Sciences*, **77**, 3957-3961.

Alberts, A., MacDonald, J., Till, A., and Tobert, J. (1989) Lovastatin. *Cardiovascular Drug Reviews,* **7**, 89-109.

Aly, A. H., Debbab, A., and Proksch, P. (2011) Fungal endophytes: unique plant inhabitants with great promises. *Applied Microbiology and Biotechnology,* **90**(6), 1829-1845.

Aly, A., Debbab, A., and Proksch, P. (2013) Fungal endophytes–secret producers of bioactive plant metabolites. *Die Pharmazie-An International Journal of Pharmaceutical Sciences,* **68**, 499-505.

Andrade, R., Ayer, W. A., and Mebe, P. P. (1992) The metabolites of *Trichoderma longibrachiatum*. Part 1. Isolation of the metabolites and the structure of trichodimerol. *Canadian Journal of Chemistry,* **70**, 2526-2535.

Arai, K., Yoshimura, T., Itatani, Y., and Yamamoto, Y. (1983) Metabolic products of *Aspergillus terreus*. VIII. Astepyrone: a novel metabolite of the strain IFO 4100. *Chemical & Pharmaceutical Bulletin*, **31**(3), 925-933.

Arakawa, M., Someno, T., Kawada, M., and Ikeda, D. (2008) A new terrein glucoside, a novel inhibitor of angiogenin secretion in tumor angiogenesis. *The Journal of antibiotics,* **61**, 442-448.

Asai, T., Luo, D., Obara, Y., Taniguchi, T., Monde, K., Yamashita, K., and Oshima, Y. (2012) Dihydrobenzofurans as cannabinoid receptor ligands from *Cordyceps annullata*, an

entomopathogenic fungus cultivated in the presence of an HDAC inhibitor. *Tetrahedron Letters*, **53**(17), 2239-2243.

Assante, G., Locci, R., Camarda, L., Merlini, L., and Nasini, G. (1977) Screening of the genus *Cercospora* for secondary metabolites. *Phytochemistry,* **16**, 243-247.

Atta-Ur-Rahman, T. (2012) *Nuclear magnetic resonance: basic principles*. Springer Science & Business Media.

Avantaggiato, G., Solfrizzo, M., Tosi, L., Zazzerini, A., Fanizzi F., and Visconti, A. (1999) Isolation and characterization of phytotoxic compounds produced by *Phomopsis helianthi*. *Natural toxins,* **7**, 119-127.

Bacon, C. W., and White, J. (2000) *Microbial endophytes*. CRC Press.

Bandaranayake, W. M. (2002) Bioactivities, bioactive compounds and chemical constituents of mangrove plants. *Wetlands Ecology and Management,* **10**, 421-452.

Bartmańska, A. and Dmochowska-Gładysz, J. (2007) Transformation of steroids by *Trichoderma hamatum*. *Enzyme and Microbial Technology,* **40**, 1615-1621.

Bauer, A. W., Kirby, W. M. M., Sherriss, J. C., and Turck, M. (1966) Antibiotic susceptibility testing by a standardized single disc method. *American journal of clinical pathology*, **45** (4), 493-496.

Bergmann, S., Schümann, J., Scherlach, K., Lange, C., Brakhage, A. A., and Hertweck, C. (2007) Genomics-driven discovery of PKS-NRPS hybrid metabolites from *Aspergillus nidulans*. *Nature chemical biology,* **3**, 213-217.

Berova, N., Di Bari, L., and Pescitelli, G. (2007) Application of electronic circular dichroism in configurational and conformational analysis of organic compounds. *Chemical Society Reviews*, **36**(6), 914-931.

Bicalho, B., Gonçalves, R. A., Zibordi, A. P. M., Manfio, G. P., and Marsaioli, A. J. (2003) Antimicrobial compounds of fungi vectored by *Clusia* spp. (Clusiaceae) pollinating bees. *Zeitschrift für Naturforschung C,* **58**, 746-751.

Bode, H. B., Bethe, B., Höfs, R., and Zeeck, A. (2002) Big effects from small changes: possible ways to explore nature's chemical diversity. *ChemBioChem,* **3**, 619-627.

Borchardt, J. K. (2002) The beginnings of drug therapy: Ancient mesopotamian medicine. *Drug News Perspect,* **15**, 187-192.

Bovey, F. A., Mirau, P. A., and Gutowsky, H. (1988) *Nuclear magnetic resonance spectroscopy*, Elsevier.

Brakhage, A. A. (1998) Molecular regulation of *β*-lactam biosynthesis in filamentous fungi. *Microbiology and Molecular Biology Reviews,* **62**, 547-585.

Brakhage, A. A., and Schroeckh, V. (2011) Fungal secondary metabolites–strategies to activate silent gene clusters. *Fungal Genetics and Biology,* **48**, 15-22.

Brakhage, A. A., Spröte, P., Al-Abdallah, Q., Gehrke, A., Plattner, H., and Tuencher, A. (2004) Regulation of penicillin biosynthesis in filamentous fungi. *Molecular Biotechnolgy of Fungal beta-Lactam Antibiotics and Related Peptide Synthetases*, 45-90. Springer.

Broadbent, D., Mabelis, R. P., and Spencer, H. (1975) 3,6,8-Trihydroxy-1-methylxanthone–an antibacterial metabolite from *Penicillium patulum*. *Phytochemistry,* **14**, 2082-2083.

Brotzu, G. (1948) Ricerche su di un nuovo antibiotico. *Lavori dell'Instituto d'Igiene di Cagliari,* 1-11.

Burkholder, P. R. and Giles, N. H., (1947) Induced biochemical mutations in *Bacillus subtilis*. *American Journal of Botany*, **34**, 345-348.

Burns, E., Ifrach, I., Carmeli, S., Pawlik, J., and Ilan, M. (2003) Comparison of antipredatory sedimentary lipids. *Org Geochem,* **30**, 1-14.

Burres, N. S., Premachandran, U., Humphrey, P. E., Jackson, M., and Chen, R. H. (1992) A new immunosuppressive cytochalasin isolated from a *Pestalotia* sp.. *The Journal of antibiotics,* **45**, 1367-1369.

Cacho, R. A., Chooi, Y.-H., Zhou, H., and Tang, Y. (2013) Complexity generation in fungal polyketide biosynthesis: a spirocycle-forming P450 in the concise pathway to the antifungal drug griseofulvin. *ACS chemical biology,* **8**, 2322-2330.

Cannon, P. F. and Kirk, P. M. (2007) *Fungal families of the world*. Cabi.

Cantrell, D. A. and Smith, K. A. (1984) The interleukin-2 T-cell system: a new cell growth model. *Science,* **224**, 1312-1316.

Cassidy, J. H., Farthing, C. N., Marsden, S. P., Pedersen, A., Slater, M., and Stemp, G. (2006) A concise, convergent total synthesis of monocerin. *Organic & biomolecular chemistry,* **4**, 4118-4126.

Cazar, M. E., Schmeda-Hirschmann, G., and Astudillo, L. (2005) Antimicrobial butyrolactone

I derivatives from the Ecuadorian soil fungus *Aspergillus terreus* thorn. var terreus. *World Journal of Microbiology and Biotechnology*, **21**(6), 1067-1075.

Chen, H., Aktas, N., Konuklugil, B., Mándi, A., Daletos, G., Lin, W., Dai, H., Kurtán T., and Proksch, P. (2015a) A new fusarielin analogue from *Penicillium* sp. isolated from the Mediterranean sponge *Ircinia oros*. *Tetrahedron Letters,* **56**, 5317-5320.

Chen, H., Daletos, G., Abdel-Aziz, M. S., Thomy, D., Dai, H., Brötz-Oesterhelt, H., Lin W., and Proksch, P. (2015b) Inducing secondary metabolite production by the soil-dwelling fungus *Aspergillus terreus* through bacterial co-culture. *Phytochemistry Letters,* **12**, 35-41.

Chen, H., Daletos, G., Okoye, F., Lai, D., Dai H., and Proksch, P. (2015c) A new cytotoxic cytochalasin from the endophytic fungus *Trichoderma harzianum*. *Natural product communications,* **10**, 585-587.

Chiang, Y. M., Chang, S. L., Oakley, B. R., and Wang, C. C. C. (2011) Recent advances in awakening silent biosynthetic gene clusters and linking orphan clusters to natural products in microorganisms. *Current opinion in chemical biology*, **15**, 137-143.

Chin, Y. W., Balunas, M. J., Chai, H. B., and Kinghorn, A. D. (2006) Drug discovery from natural sources. *The AAPS journal,* **8**, E239-E253.

Chokpaiboon, S., Sommit, D., Bunyapaiboonsri, T., Matsubara, K., and Pudhom, K. (2011) Antiangiogenic effect of chamigrane endoperoxides from a Thai mangrove-derived fungus. *Journal of natural products,* **74**, 2290-2294.

Chung, Y. M., El-Shazly, M., Chuang, D. W., Hwang, T. L., Asai, T., Oshima, Y., Ashour, M. L., Wu, Y. C., and Chang, F. R. (2013) Suberoylanilide hydroxamic acid, a histone deacetylase inhibitor, induces the production of anti-inflammatory cyclodepsipeptides from *Beauveria felina*. *Journal of natural products,* **76**, 1260-1266.

Cichewicz, R. H. (2010) Epigenome manipulation as a pathway to new natural product scaffolds and their congeners. *Natural product reports,* **27,** 11-22.

Citron, C. A., Riclea, R., Brock, N. L., and Dickschat, J. S. (2011) Biosynthesis of acorane sesquiterpenes by *Trichoderma*. *RSC Advances,* **1**, 290-297.

Cotelle, P., Cotelle, N., Teissier, E., and Vezin, H. (2003) Synthesis and antioxidant properties of a new lipophilic ascorbic acid analogue. *Bioorganic & medicinal chemistry,* **11**,

1087-1093.

Cragg, G. M., Newman, D. J., and Snader, K. M. (1997) Natural products in drug discovery and development. *Journal of natural products,* **60**, 52-60.

Cueto, M., Jensen, P. R., Kauffman, C., Fenical, W., Lobkovsky, E., and Clardy, J. (2001) Pestalone, a new antibiotic produced by a marine fungus in response to bacterial challenge. *Journal of Natural Products*, **64**(11), 1444-1446.

de Macedo, F. C. and Marsaioli, A. J. (2005) Total structural assignment and absolute configuration of terreinol by 13C and 1H NMR. *Magnetic Resonance in Chemistry,* **43**, 251-255.

Debbab, A., Aly, A. H., and Proksch, P. (2012) Endophytes and associated marine derived fungi–ecological and chemical perspectives. *Fungal Diversity,* **57**, 45-83.

Debono, M., Turner, W. W., LaGrandeur, L., Burkhardt, F. J., Nissen, J. S., Nichols, K. K., Rodriguez, M. J., Zweifel, M. J., and Zeckner, D. J. (1995) Semisynthetic chemical modification of the antifungal lipopeptide echinocandin B (ECB): structure-activity studies of the lipophilic and geometric parameters of polyarylated acyl analogs of ECB. *Journal of medicinal chemistry,* **38**, 3271-3281.

Denning, D. W. (1997) Echinocandins and pneumocandins–a new antifungal class with a novel mode of action. *Journal of Antimicrobial Chemotherapy,* **40**, 611-614.

Dillon, M. P., Simpson, T. J., and Sweeney, J. B. (1992) Enantioselective synthesis of monocerin and fusarentin ethers: Antifungal and insecticidal fungal metabolites. *Tetrahedron letters,* **33**, 7569-7572.

Dombrowski, A. W., Bills, G. F., Sabnis, G., Koupal, L. R., Meyer, R., Ondeyka, J. G., Giacobbe, R. A., Monaghan, R. L., and Lingham, R. B. (1992) L-696,474, a novel cytochalasin as an inhibitor of HIV-1 protease. I. The producing organism and its fermentation. *The Journal of antibiotics,* **45**, 671-678.

Donia, M. and Hamann, M. T. (2003) Marine natural products and their potential applications as anti-infective agents. *The Lancet infectious diseases,* **3**, 338-348.

Doolittle, R. F., Feng, D. F., Tsang, S., Cho, G., and Little, E. (1996) Determining divergence times of the major kingdoms of living organisms with a protein clock. *Science,* **271**, 470-477.

Du, L., Zhu, T., Fang, Y., Liu, H., Gu, Q., and Zhu, W. (2007) Aspergiolide A, a novel anthraquinone derivative with naphtho [1,2,3-de] chromene-2,7-dione skeleton isolated from a marine-derived fungus *Aspergillus glaucus*. *Tetrahedron,* **63**, 1085-1088.

Dunn, A. W., Entwistle, I. D., and Johnstone, R. A. (1975) Terrein and other metabolites of *Phoma* species. *Phytochemistry,* **14**, 2081-2082.

Ebada, S. S., Edrada, R. A., Lin, W., and Proksch, P. (2008) Methods for isolation, purification and structural elucidation of bioactive secondary metabolites from marine invertebrates. *Nature protocols,* **3**, 1820-1831.

Elsässer, B., Krohn, K., Flörke, U., Root, N., Aust, H. J., Draeger, S., Schulz, B., Antus, S., and Kurtán, T. (2005) X‐ray Structure Determination, Absolute Configuration and Biological Activity of Phomoxanthone A. *European journal of organic chemistry*, **21**, 4563-4570.

Ellestad, G., Mirando, P., and Kunstmann, M. (1973) Structure of the metabolite LL-S490. beta. from an unidentified *Aspergillus* species. *The Journal of organic chemistry,* **38**, 4204-4205.

Endo, A. (1979) Monacolin K, a new hypocholesterolemic agent produced by a *Monascus* species. *The Journal of antibiotics,* **32**, 852-854.

Endo, A. (1985) Compactin (ML-236B) and related compounds as potential cholesterol-lowering agents that inhibit HMG-CoA reductase. *Journal of medicinal chemistry*, **28**, 401-405.

Fang, B., Xie, X., Li, H., Jing, P., Gu, J., and She, X. (2013) Asymmetric total synthesis of (+)-monocerin. *Tetrahedron Letters*, **54**, 6349-6351.

Fleck, S. C., Pfeiffer, E., Podlech, J., and Metzler, M. (2014) Epoxide Reduction to an Alcohol: A Novel Metabolic Pathway for Perylene Quinone-Type Alternaria Mycotoxins in Mammalian Cells. *Chemical research in toxicology*, **27**, 247-253.

Gao, H., Guo, W., Wang, Q., Zhang, L., Zhu, M., Zhu, T., Gu, Q., Wang, W., and Li, D. (2013) Aspulvinones from a mangrove rhizosphere soil-derived fungus *Aspergillus terreus* Gwq-48 with anti-influenza A viral (H1N1) activity. *Bioorganic & medicinal chemistry letters*, **23**, 1776-1778.

Gao, X. and Snider, B. B. (2004) Syntheses of (-)-TAN-2483A, (-)-Massarilactone B, and the fusidilactone B ring system. Revision of the structures of and syntheses of (±)-Waol A (FD-211) and (±)-Waol B (FD-212). *The Journal of organic chemistry*, **69**, 5517-5527.

Ghaffarzadeh, M. and Ahmadi, M. (2014) Catalytic application of fluorous silica gel in Fries rearrangement. *Journal of Fluorine Chemistry*, **160**, 77-81.

Ghisalberti, E., Narbey, M., and Rowland, C. (1990) Metabolites of *Aspergillus terreus* antagonistic towards the take-all fungus. *Journal of Natural Products*, **53**, 520-522.

Girotra, N., Patchett, A., and Wendler, N. (1977) Rearrangement of (+/-)-flavipucine and its diastereoisomer-chemistry of transformation product. *Heterocycles*, **6**, 1299-1305.

Grandolini, G., Casinovi, C. G., and Radics, L. (1987). On the biosynthesis of flavipucine. *The Journal of antibiotics*, **40**(9), 1339-1340.

Gressler, M., Zaehle, C., Scherlach, K., Hertweck, C., and Brock, M. (2011) Multifactorial Induction of an Orphan PKS-NRPS Gene Cluster in *Aspergillus terreus*. *Chemistry & Biology*, **18**, 198-209.

Greve, H., Schupp, P. J., Eguereva, E., Kehraus, S., Kelter, G., Maier, A., Fiebig, H. H., and König, G. M. (2008) Apralactone A and a New Stereochemical Class of Curvularins from the Marine Fungus *Curvularia* sp.. *European journal of organic chemistry*, **30**, 5085-5092.

Gross, J. H. (2004) *Mass spectrometry: a textbook*. Springer Science & Business Media.

Grove, J. (1954) The structure of terrein. *Journal of The Chemical Society Dec*, 4693-4694.

Grove, J. F., MacMillan, J., Mulholland, T., and Rogers, M. T. (1952) 762. Griseofulvin. Part IV. Structure. *Journal of the Chemical Society (Resumed)*, 3977-3987.

Gunatilaka, A. L. (2006) Natural Products from Plant-Associated Microorganisms: Distribution, Structural Diversity, Bioactivity, and Implications of Their Occurrence. *Journal of Natural Products*, **69**, 509-526.

Guo, C. J., Knox, B. P., Chiang, Y. M., Lo, H. C., Sanchez, J. F., Lee, K. H., Oakley, B. R., Bruno, K. S., and Wang, C. C. (2012) Molecular genetic characterization of a cluster in *A. terreus* for biosynthesis of the meroterpenoid terretonin. *Organic letters*, **14**, 5684-5687.

Guo, C. J., Knox, B. P., Sanchez, J. F., Chiang, Y. M., Bruno, K. S., and Wang, C.C.C. (2013)

Application of an efficient gene targeting system linking secondary metabolites to their biosynthetic genes in *Aspergillus terreus*. *Organic letter*, **15**, 3562-3565.

Hammerschmidt, L., Aly, A. H., Abdel-Aziz, M., Müller, W. E., Lin, W., Daletos, G., and Proksch, P. (2015). Cytotoxic acyl amides from the soil fungus *Gymnascella dankaliensis*. *Bioorganic & medicinal chemistry*, **23**(4), 712-719.

Haidle, A. M. and Myers, A. G. (2004) An enantioselective, modular, and general route to the cytochalasins: Synthesis of L-696,474 and cytochalasin B. *Proceedings of the National Academy of Sciences of the United States of America*, **101**, 12048-12053.

Haritakun, R., Rachtawee, P., Chanthaket, R., Boonyuen, N., and Isaka, M. (2010) Butyrolactones from the fungus *Aspergillus terreus* BCC 4651. *Chemical and Pharmaceutical Bulletin*, **58**, 1545-1548.

Harman, G. E. (2006) Overview of Mechanisms and Uses of *Trichoderma* spp. *Phytopathology*, **96**, 190-194.

Hassan, A. E. (2007) Novel Natural Products from Endophytic Fungi of Egyptian Medicinal Plants: Chemical and Biological Characterization.

Hellwig, V., Grothe, T., Mayer-Bartschmid, A., Endermann, R., Geschke, F. U., Henkel, T., and Stadler, M. (2002) Altersetin, a new antibiotic from cultures of endophytic *Alternaria* spp. Taxonomy, fermentation, isolation, structure elucidation and biological activities. *The Journal of antibiotics*, **55**, 881-892.

Hosoe, T., Moriyama, H., Wakana, D., Itabashi, T., Kawai, K. i., Yaguchi, T., Iizuka, T., Hoshi, K., Fukuyama, Y., Kouda, Y., and Lau, F. C. (2009) Inhibitory effects of dihydroterrein and terrein isolated from *Aspergillus novofumigatus* on platelet aggregation. *JSM Mycotoxins*, **59**, 75-82.

Hoye, T. R., Jeffrey, C. S., and Shao, F. (2007) Mosher ester analysis for the determination of absolute configuration of stereogenic (chiral) carbinol carbons. *Nature Protocols*, **2**, 2451-2458.

http://www.chem.uci.edu/~dmitryf/manuals/Fundamentals/CD%20spectroscopy.pdf

Huber, F. M. and Gottlieb, D. (1968) The mechanism of action of griseofulvin. *Canadian journal of microbiology*, **14**, 111-118.

Hyde, K. D., Jones, E. G., Leaño, E., Pointing, S. B., Poonyth, A. D., and Vrijmoed, L. L.

(1998) Role of fungi in marine ecosystems. *Biodiversity and Conservation*, **7**, 1147-1161.

Ishikawa, H. (1999) Mizoribine and mycophenolate mofetil. *Current medicinal chemistry*, **6**, 575-598.

Jimenez, J, L (2006) *Mechanisms of ion fragmentation. Mass spectrometry & Chromatography*.

Kharwar, R. N., Mishra, A., Gond, S. K., Stierle, A., and Stierle, D. (2011) Anticancer compounds derived from fungal endophytes: their importance and future challenges. *Natural product reports*, **28**, 1208-1228.

Kim, D. S., Cho, H. J., Lee, H. K., Lee, W. H., Park, E. S., Youn, S. W., and Park, K. C. (2007) Terrein, a fungal metabolite, inhibits the epidermal proliferation of skin equivalents. *Journal of dermatological science*, **46**, 65-68.

Kiriyama, N., Nitta, K., Sakaguchi, Y., Taguchi, Y., and Yamamoto, Y. (1977) Studies on the metabolic products of *Aspergillus terreus*. III. Metabolites of the strain IFO 8835. 1. *Chemical and Pharmaceutical Bulletin*, **25**, 2593-2601.

Kumar, A., Patil, D., Rajamohanan, P. R., and Ahmad, A. (2013) Isolation, purification and characterization of vinblastine and vincristine from endophytic fungus *Fusarium oxysporum* isolated from *Catharanthus roseus*. *PloS one*, **8**(9), e71805.

Kusari, S., Lamshöft, M., Zühlke, S., and Spiteller, M. (2008) An endophytic fungus from *Hypericum perforatum* that produces hypericin. *Journal of Natural Products*, **71**, 159-162.

Kusari, S., Singh, S., and Jayabaskaran, C. (2014) Biotechnological potential of plant-associated endophytic fungi: hope versus hype. *Trends in biotechnology*, **32**, 297-303.

Kusari, S., Verma, V. C., Lamshoeft, M., and Spiteller, M. (2012) An endophytic fungus from *Azadirachta indica* A. Juss. that produces azadirachtin. *World Journal of Microbiology and Biotechnology*, **28**, 1287-1294.

Kusari, S., Zühlke, S., and Spiteller, M. (2011) Effect of artificial reconstitution of the interaction between the plant *Camptotheca acuminata* and the fungal endophyte *Fusarium solani* on camptothecin biosynthesis. *Journal of natural products*, **74**,

764-775.

Latha, R. and Mitra, S. (2004) Mangrove fungi in India. *Current Science*, **86**, 1586.

Lebet, C. and Tamm, C. (1973) Biosynthesis of cytochalasins. II Building blocks of cytochalasun D. *Helvetica chimica acta*, **57**, 1785-1801.

Lebuhn, M., Heulin, T., and Hartmann, A. (1997) Production of auxin and other indolic and phenolic compounds by *Paenibacillus polymyxa* strains isolated from different proximity to plant roots. *FEMS Microbiology Ecology*, **22**(4), 325-334.

Lee, J. C., Yu, M. K., Lee, R., Lee, Y. H., Jeon, J. G., Lee, M. H., Jhee, E. C., Yoo, I. D., and Yi, H. K. (2008) Terrein reduces pulpal inflammation in human dental pulp cells. *Journal of endodontics*, **34**, 433-437.

Li, G. Y., Li, B. G., Yang, T., Yin, J. H., Qi, H. Y., Liu, G. Y., and Zhang, G. L. (2005) Sesterterpenoids, Terretonins AD, and an Alkaloid, Asterrelenin, from *Aspergillus terreus*. *Journal of natural products*, **68**, 1243-1246.

Li, H., Huang, H., Shao, C., Huang, H., Jiang, J., Zhu, X., Liu, Y., Liu, L., Lu, Y., and Li, M. (2011) Cytotoxic norsesquiterpene peroxides from the endophytic fungus *Talaromyces flavus* isolated from the mangrove plant *Sonneratia apetala*. *Journal of natural products*, **74**, 1230-1235.

Li, Y. Y., Wang, M. Z., Huang, Y. J., and Shen, Y. M. (2010) Secondary metabolites from *Phomopsis* sp. A123. *Mycology*, **1**, 254-261.

Lingham, R. B., Hsu, A., Silverman, K. C., Bills, G. F., Dombrowski, A., Goldman, M. E., Darked, P. L., Huang, L., Koch, G., and Ondeyka, J. G. (1992) L-696,474, a novel cytochalasin as an inhibitor of HIV-1 protease. III. Biological activity. *The Journal of antibiotics*, **45**, 686-691.

Guo, B., Li, H., and Zhang, L. (1998) Isolation of An Fungus Producting Vinbrastine. *Journal of Yunnan University (Natural Sciences)*, **20**(3), 214-215.

Liu, F., Cai, X. L., Yang, H., Xia, X. K., Guo, Z. Y., Yuan, J., Li, M. F., She, Z. G., and Lin, Y. C. (2010) The bioactive metabolites of the mangrove endophytic fungus *Talaromyces* sp. ZH-154 isolated from *Kandelia candel* (L.) Druce. *Planta medica*, **76**, 185-189.

Liu, H., Edrada-Ebel, R., Ebel, R., Wang, Y., Schulz, B., Draeger, S., Müller, W. E., Wray, V., Lin, W., and Proksch, P. (2009) Drimane sesquiterpenoids from the fungus *Aspergillus*

ustus isolated from the marine sponge *Suberites domuncula*. *Journal of natural products*, **72**, 1585-1588.

Loesgen, S., Bruhn, T., Meindl, K., Dix, I., Schulz, B., Zeeck, A., and Bringmann, G. (2011) (+)−Flavipucine, the Missing Member of the Pyridione Epoxide Family of Fungal Antibiotics. *European Journal of Organic Chemistry,* **26**, 5156-5162.

Lyko, F. and Brown, R. (2005) DNA methyltransferase inhibitors and the development of epigenetic cancer therapies. *Journal of the National Cancer Institute*, **97**, 1498-1506.

Macedo, F. C., Porto, A. L., and Marsaioli, A. J. (2004) Terreinol–a novel metabolite from *Aspergillus terreus*: structure and 13C labeling. *Tetrahedron letters*, **45**, 53-55.

Marmann, A., Aly, A. H., Lin, W., Wang, B., and Proksch, P. (2014) Co-cultivation–A powerful emerging tool for enhancing the chemical diversity of microorganisms. *Marine drugs*, **12**, 1043-1065.

McIntyre, C. R., Reed, D., Sadler, I. H., and Simpson, T. J. (1989) 1H and 13C nmr spectral assignment studies of terretonin, a toxic meroterpenoid metabolite of *Aspergillus terreus*. *Journal of the Chemical Society, Perkin Transactions 1*, **11**, 1987-1993.

Meronuck, R., Steele, J., Mirocha, C., and Christensen, C. (1972) Tenuazonic acid, a toxin produced by *Alternaria alternata*. *Applied microbiology*, **23**, 613-617.

Meschke, H., Walter, S., and Schrempf, H. (2012) Characterization and localization of prodiginines from *Streptomyces lividans* suppressing *verticillium dahliae* in the absence or presence of *Arabidopsis thaliana*. *Environmental microbiology*, **14**(4), 940-952.

Mikula, H., Horkel, E., Hans, P., Hametner, C., and Fröhlich, J. (2013) Structure and tautomerism of tenuazonic acid–A synergetic computational and spectroscopic approach. *Journal of hazardous materials*, **250**, 308-317.

Mishra, B. B. and Tiwari, V. K. (2011) Natural products: an evolving role in future drug discovery. *European journal of medicinal chemistry*, **46**, 4769-4807.

Newman, D. J., Cragg, G. M., and Snader, K. M. (2000) The influence of natural products upon drug discovery. *Natural product reports*, **17**, 215-234.

Newman D. J., Cragg, G. M., and Snader, K. M. (2003) Natural products as sources of new drugs over the period 1981-2002. *Journal of natural products*, **66**, 1022-1037.

Nitta, K., Fujita, N., Yoshimura, T., Arai, K., and Yamamoto, Y. (1983) Metabolic products of *Aspergillus terreus*. IX. Biosynthesis of butyrolactone derivatives isolated from strains IFO 8835 and 4100. *Chemical and pharmaceutical bulletin*, **31**, 1528-1533.

Niu, X. M., Dahse, H. M., Menzel, K. D., Lozach, O., Walther, G., Meijer, L., Grabley, S., and Sattler, I. (2008) Butyrolactone I derivatives from *Aspergillus terreus* carrying an unusual sulfate moiety. *Journal of natural products*, **71**, 689-692.

Nozawa, K., Nakajima, S., Udagawa, S. i., and Kawai, K. i. (1991) Isolation and structure of a new 1-decalone derivative, rapiculine, from *Ramichloridium apiculatum*. *Journal of the Chemical Society*, *Perkin Transactions 1*, **3**, 537-539.

Nozawa, O., Okazaki, T., Sakai, N., Komurasaki, T., Hanada, K., Morimoto, S., Chen, Z. X., He, B. M., and Mizoue, K. (1995) A Novel Bioactive. DELTA. lactone FD-211 Taxonomy, Isolation and Characterization. *The Journal of antibiotics*, **48**, 113-118.

Nuclear, P., Sommit, D., Boonyuen, N., and Pudhom, K. (2010) Butenolide and furandione from an endophytic *Aspergillus terreus*. *Chemical and Pharmaceutical Bulletin*, **58**, 1221-1223.

Nuetzmann, H. W., Reyes-Dominguez, Y., Scherlach, K., Schroeckh, V., Horn, F., Gacek, A., Schuemann, J., Hertweck, C., Strauss, J., and Brakhage, A. A. (2011) Bacteria-induced natural product formation in the fungus *Aspergillus nidulans* requires Saga/Ada-mediated histone acetylation. *Proceedings of the National Academy of Sciences*, **108**, 14282-14287.

Oh, D. C., Jensen, P. R., Kauffman, C. A., and Fenical, W. (2005) Libertellenones A-D: Induction of cytotoxic diterpenoid biosynthesis by marine microbial competition. *Bioorganic & medicinal chemistry*, **13**, 5267-5273

Oh, D. C., Kauffman, C. A., Jensen, P. R., and Fenical, W. (2007) Induced production of emericellamides A and B from the marine-derived fungus *Emericella* sp. in competing co-culture. *Journal of natural products*, **70**, 515-520.

Ola, A. R., Thomy, D., Lai, D., Brötz-Oesterhelt, H., and Proksch, P. (2013) Inducing secondary metabolite production by the endophytic fungus *Fusarium tricinctum* through coculture with *Bacillus subtilis*. *Journal of natural products*, **76**, 2094-2099.

Ondeyka, J., Hensens, O., Zink, D., Ball, R., Lingham, R., Bills, G., Dombrowski, A., and

Goetz, M. (1992) L-696,474, a novel cytochalasin as an inhibitor of HIV-1 protease. II. Isolation and structure. *The Journal of antibiotics*, **45**, 679-685.

Paranagama, P. A., Wijeratne, E. K., and Gunatilaka, A. L. (2007) Uncovering Biosynthetic Potential of Plant-Associated Fungi: Effect of Culture Conditions on Metabolite Production by *Paraphaeosphaeria quadriseptata* and *Chaetomium chiversii* (1). *Journal of natural products*, **70**, 1939-1945.

Parvatkar, R. R., D'Souza, C., Tripathi, A., and Naik, C. G. (2009) Aspernolides A and B, butenolides from a marine-derived fungus *Aspergillus terreus*. *Phytochemistry*, **70**, 128-132.

Park, S. H., Kim, D. S., Kim, W. G., Ryoo, I. J., Lee, D. H., Huh, C. H., Youn, S. W., Yoo, I. D., and Park, K. C. (2004) Terrein: a new melanogenesis inhibitor and its mechanism. *Cellular and Molecular Life Sciences CMLS*, **61**, 2878-2885.

Pettit, R. K. (2009) Mixed fermentation for natural product drug discovery. *Applied microbiology and biotechnology*, **83**, 19-25.

Pettit, R. K. (2011) Culturability and secondary metabolite diversity of extreme microbes: expanding contribution of deep sea and deep-sea vent microbes to natural product discovery. *Marine Biotechnology*, **13**, 1-11.

Pfaller, M., Boyken, L., Hollis, R., Messer, S., Tendolkar, S., and Diekema, D. (2005a) In vitro activities of anidulafungin against more than 2,500 clinical isolates of Candida spp., including 315 isolates resistant to fluconazole. *Journal of clinical microbiology*, **43**, 5425-5427.

Pfaller, M., Diekema, D., Boyken, L., Messer, S., Tendolkar, S., Hollis, R., and Goldstein, B. (2005b) Effectiveness of anidulafungin in eradicating Candida species in invasive candidiasis. *Antimicrobial agents and chemotherapy*, **49**, 4795-4797.

Phattanawasin, P., Pojchanakom, K., Sotanaphun, U., Piyapolrungroj, N., and Zungsontiporn, S. (2007) Weed growth inhibitors from *Aspergillus fischeri* TISTR 3272. *Natural product research*, **21**, 1286-1291.

Porras-Alfaro, A. and Bayman, P. (2011) Hidden fungi, emergent properties: endophytes and microbiomes. *Phytopathology*, **49**, 291.

Puri, S. C., Verma, V., Amna, T., Qazi, G. N., and Spiteller, M. (2005) An Endophytic Fungus

from *Nothapodytes foetida* that Produces Camptothecin. *Journal of natural products*, **68**, 1717-1719.

Raghukumar, C. (2008) Marine fungal biotechnology: an ecological perspective. *Fungal Diversity*, **31**, 19-35.

Raistrick, H. and Smith, G. (1935) Studies in the biochemistry of micro-organisms: the metabolic products of *Aspergillus terreus* Thom. A new mould metabolic product–terrein. *Biochemical Journal*, **29**, 606.

Rao, K., Sadhukhan, A., Veerender, M., Ravikumar, V., Mohan, E., Dhanvantri, S., Sitaramkumar, M., Babu, J. M., Vyas, K., and Reddy, G. (2000) Butyrolactones from *Aspergillus terreus*. *Chemical and Pharmaceutical Bulletin*, **48**, 559-562.

Reen, F. J., Romano, S., Dobson, A. D. W., and O' Gara, F. (2015) The sound of silence: activating silent bioysnthetic gene clusters in marine microorganisms. *Marine Drugs*, **13**, 4754-4783.

Reino, J. L., Guerrero, R. F., Hernández-Galán, R., and Collado, I. G. (2008) Secondary metabolites from species of the biocontrol agent *Trichoderma*. *Phytochemistry Reviews*, **7**, 89-123.

Ren, J., Xue, C., Tian, L., Xu, M., Chen, J., Deng, Z., Proksch, P., and Lin, W. (2009) Asperelines A−F, Peptaibols from the Marine-Derived Fungus *Trichoderma asperellum*. *Journal of natural products*, **72**, 1036-1044.

Rishton, G. M. (2008) Natural products as a robust source of new drugs and drug leads: past successes and present day issues. *The American journal of cardiology*, **101**, S43-S49.

Robert, J. L. and Tamm, C. (1975) Biosynthesis of cytochalasans. Part 5. The incorporation of deoxaphomin into cytochalasin B (phomin). *Helvetica chimica acta*, **58**, 2501-2504.

Rothweiler, W. and Tamm, C. (1966) Isolation and structure of phomin. *Experientia*, **22** (11), 750-752.

Royles, B. J. (1995) Naturally occurring tetramic acids: structure, isolation, and synthesis. *Chemical reviews*, **95**, 1981-2001.

Saleem, M., Ali, M. S., Hussain, S., Jabbar, A., Ashraf, M., and Lee, Y. S. (2007) Marine natural products of fungal origin. *Natural product reports*, **24**, 1142-1152.

San-martin, A., Rovirosa, J., Vaca, I., Vergara, K., Acevedo, L., Vina, D., Orallo, F., and

Chamy, M.C. (2011) New butyrolactone from a marine-derived fungus *Aspergillus* sp.. *Journal of the Chilean Chemical Society*, **56**(1), 625-627.

Sappapan, R., Sommit, D., Ngamrojanavanich, N., Pengpreecha, S., Wiyakrutta, S., Sriubolmas, N., and Pudhom, K. (2008) 11-Hydroxymonocerin from the plant endophytic fungus *Exserohilum rostratum*. *Journal of natural products*, **71**, 1657-1659.

Sauvage, E., Kerff, F., Terrak, M., Ayala, J. A., and Charlier, P. (2008) The penicillin-binding proteins: structure and role in peptidoglycan biosynthesis. *FEMS microbiology reviews*, **32**, 234-258.

Scherlach, K., Boettger, D., Remme, N., and Hertweck, C. (2010) The chemistry and biology of cytochalasans. *Natural product reports*, **27**, 869-886.

Scherlach, K. and Hertweck, C. (2009) Triggering cryptic natural product biosynthesis in microorganisms. *Organic & biomolecular chemistry*, **7**, 1753-1760.

Schroeckh, V., Scherlach, K., Nützmann, H. W., Shelest, E., Schmidt-Heck, W., Schuemann, J., Martin, K., Hertweck, C., and Brakhage, A. A. (2009) Intimate bacterial–fungal interaction triggers biosynthesis of archetypal polyketides in *Aspergillus nidulans*. *Proceedings of the National Academy of Sciences*, **106**, 14558-14563.

Selvin, J., Ninawe, A., Seghal Kiran, G., and Lipton, A. (2010) Sponge-microbial interactions: Ecological implications and bioprospecting avenues. *Critical reviews in microbiology*, **36**, 82-90.

Shang, Z., Li, X. M., Li, C. S., and Wang, B. G. (2012) Diverse Secondary Metabolites Produced by Marine Derived Fungus *Nigrospora* sp. MA75 on Various Culture Media. *Chemistry & biodiversity*, **9**, 1338-1348.

Shearer, C. A., Descals, E., Kohlmeyer, B., Kohlmeyer, J., Marvanová, L., Padgett, D., Porter, D., Raja, H. A., Schmit, J. P., and Thorton, H. A. (2007) Fungal biodiversity in aquatic habitats. *Biodiversity and Conservation*, **16**, 49-67.

Sheehan, J. C. and Henery-Logan, K. R. (1959) The total synthesis of penicillin V. *Journal of the American Chemical Society*, **81**, 3089-3094.

Shi, Q., Meroueh, S. O., Fisher, J. F., and Mobashery, S. (2011) A computational evaluation of the mechanism of penicillin-binding protein-catalyzed cross-linking of the bacterial

cell wall. *Journal of the American Chemical Society*, **133**, 5274-5283.

Shimada, A., Inokuchi, T., Kusano, M., Takeuchi, S., Inoue, R., Tanita M., and Fujioka, S. (2004) 4-Hydroxykigelin and 6-demethylkigelin, root growth promoters, produced by *Aspergillus terreus*. *Zeitschrift für Naturforschung C*, **59**, 218-222.

Shweta, S., Zuehlke, S., Ramesha, B., Priti, V., Kumar, P. M., Ravikanth, G., Spiteller, M., Vasudeva, R., and Shaanker, R. U. (2010) Endophytic fungal strains of *Fusarium solani*, from *Apodytes dimidiata* E. Mey. ex Arn (Icacinaceae) produce camptothecin, 10-hydroxycamptothecin and 9-methoxycamptothecin. *Phytochemistry*, **71**, 117-122.

Siegel, D., Merkel, S., Bremser, W., Koch, M., and Nehls, I. (2010) Degradation kinetics of the Alternaria mycotoxin tenuazonic acid in aqueous solutions. *Analytical and bioanalytical chemistry*, **397**, 453-462.

Skou, J. C. (1988) Overview: The Na, K-pump. *Methods in enzymology*, **156**, 1-25.

Sohn, J. H., Lee, D. S., and Oh, H. C. (2013) PTP1B inhibitory secondary metabolites from marine-derived fungal strains *Penicillium* spp. and *Eurotium* sp.. *Journal of microbiology and biotechnology*, **23**, 1206-1211.

Sørensen, J. L., Akk, E., Thrane, U., Giese, H., and Sondergaard, T. E. (2013) Production of fusarielins by *Fusarium*. *International journal of food microbiology*, **160**, 206-211.

Spratt, B. G. and Cromie, K. D. (1988) Penicillin-binding proteins of gram-negative bacteria. *Review of Infectious Diseases*, **10**, 699-711.

Springer, J. P., Dorner, J. W., Cole, R. J., and Cox, R. H. (1979) Terretonin, a toxic compound from *Aspergillus terreus*. *The Journal of Organic Chemistry*, **44**, 4852-4854.

Stack, M. E., Mazzola, E. P., Page, S. W., Pohland, A. E., Highet, R. J., Tempesta, M. S., and Corley, D. G. (1986) Mutagenic perylenequinone metabolites of *Alternaria alternata*: altertoxins I, II, and III. *Journal of natural products*, **49**, 866-871.

Strobel, G. A. (2003) Endophytes as sources of bioactive products. *Microbes and infection*, **5**, 535-544.

Strobel, G., Daisy, B., Castillo, U., and Harper, J. (2004) Natural Products from Endophytic Microorganisms. *Journal of natural products*, **67**, 257-268.

Survase, S. A., Kagliwal, L. D., Annapure, U. S., and Singhal, R. S. (2011) Cyclosporin A–A review on fermentative production, downstream processing and pharmacological

applications. *Biotechnology advances*, **29**, 418-435.

Taher, A. G. (1999) Inland saline lakes of Wadi El Natrun depression, Egypt. *International Journal of Salt Lake Research*, **8**, 149-169.

Takenaka, Y., Hamada, N., and Tanahashi, T. (2011a) Aromatic compounds from cultured lichen mycobionts of three *Graphis* species. *Heterocycles*, **83**, 2157-2164.

Takenaka, Y., Morimoto, N., Hamada, N., and Tanahashi, T. (2011b) Phenolic compounds from the cultured mycobionts of *Graphis proserpens*. *Phytochemistry*, **72**, 1431-1435.

Takesue, T., Fujita, M., Sugimura, T., and Akutsu, H. (2014) A Series of Two Oxidation Reactions of ortho-Alkenylbenzamide with Hypervalent Iodine (III): A Concise Entry into (3R, 4R)-4-Hydroxymellein and (3R, 4R)-4-Hydroxy-6-methoxymellein. *Organic letters*, **16**, 4634-4637.

Taniguchi, T., Monde, K., Nakanishi, K., and Berova, N. (2008). Chiral sulfinates studied by optical rotation, ECD and VCD: the absolute configuration of a cruciferous phytoalexin brassicanal C. *Organic & biomolecular chemistry*, **6**(23), 4399-4405.

Taylor, M. W., Radax, R., Steger, D., and Wagner, M. (2007) Sponge-associated microorganisms: evolution, ecology, and biotechnological potential. *Microbiology and molecular biology reviews*, **71**, 295-347.

Trost, B. M., Rivers, G. T., and Gold, J. M. (1980) Regiocontrolled synthesis of hydroxyphthalides. Synthesis of (±)-isoochracinic acid and a zealeranone intermediate. *The Journal of Organic Chemistry*, **45**, 1835-1838.

Thatoi, H., Behera, B. C., and Mishra, R. R. (2013) Ecological role and biotechnological potential of mangrove fungi: a review. *Mycology*, **4**, 54-71.

Van Eijk, G. (1969) Isolation and identification of orsellinic acid and penicillic acid produced by *Penicillium fennelliae* Stolk. *Antonie van Leeuwenhoek*, **35**, 497-504.

van Galen, Peter M. (2005) Mass spectrometry.

Vennila, R. and Muthumary, J. (2011) Taxol from Pestalotiopsis pauciseta VM1, an endophytic fungus of *Tabebuia pentaphylla*. *Biomedicine & Preventive Nutrition*, **1**, 103-108.

Vervoort, H. C., Drašković, M., and Crews, P. (2010) Histone deacetylase inhibitors as a tool to up-regulate new fungal biosynthetic products: Isolation of EGM-556, a

cyclodepsipeptide, from *Microascus* sp. *Organic letters*, **13**, 410-413.

Webster, N. S. and Taylor, M. W. (2012) Marine sponges and their microbial symbionts: love and other relationships. *Environmental Microbiology*, **14**, 335-346.

Weidenbörner, M. (2001) *Encyclopedia of food mycotoxins*. Springer Science & Business Media.

Wiklund, P., Romero, I., and Bergman, J. (2003) Products from dehydration of dicarboxylic acids derived from anthranilic acid. *Organic & biomolecular chemistry*, **1**, 3396-3403.

Williams, R. B., Henrikson, J. C., Hoover, A. R., Lee, A. E., and Cichewicz, R. H. (2008) Epigenetic remodeling of the fungal secondary metabolome. *Organic & biomolecular chemistry*, **6**, 1895-1897.

Wood, A. J., Rowinsky, E. K., and Donehower, R. C. (1995) Paclitaxel (taxol). *New England Journal of Medicine*, **332**, 1004-1014.

Xu, B., Yin, Y., Zhang, F., Li, Z., and Wang, L. (2012) Operating conditions optimization for (+)-terrein production in a stirred bioreactor by *Aspergillus terreus* strain PF-26 from marine sponge *Phakellia fusca*. *Bioprocess and biosystems engineering*, **35**, 1651-1655.

Xu, G. B., Wang, N. N., Bao, J. K., Yang, T., and Li, G. Y. (2014) New Orsellinic Acid Esters from Fungus *Chaetomium globosporum*. *Helvetica Chimica Acta*, **97**, 151-159.

Yang, J. X., Qiu, S. X., She, Z. G., and Lin, Y. C. (2013) New xanthone derivative from the marine fungus *Phomopsis* sp. (No. SK7RN3G1). *Chemistry of Natural Compounds*, **49**(2), 246-248.

Yang, S. W. and Cordell, G. A. (1997) Metabolism studies of indole derivatives using a staurosporine producer, *Streptomyces staurosporeus*. *Journal of natural products*, **60**, 44-48.

Yin, W. B., Grundmann, A., Cheng, J., and Li, S. M. (2009) Acetylaszonalenin biosynthesis in *Neosartorya fischeri* identification of the biosynthetic gene cluster by genomic mining and functional proof of the genes by biochemical investigation. *Journal of Biological Chemistry*, **284**, 100-109.

Zaehle, C., Gressler, M., Shelest, E., Geib, E., Hertweck, C., and Brock, M. (2014) Terrein biosynthesis in *Aspergillus terreus* and its impact on phytotoxicity. *Chemistry &*

biology, **21**, 719-731.

Zhang, D., Yang, X., Kang, J. S., Choi, H. D., and Son, B. W. (2008) Chlorohydroaspyrones A and B, antibacterial aspyrone derivatives from the marine-derived fungus *Exophiala* sp. *Journal of natural products*, **71**, 1458-1460.

Zhang, W., Krohn, K., Draeger, S., and Schulz, B. (2008) Bioactive isocoumarins isolated from the endophytic fungus *Microdochium bolleyi*. *Journal of natural products*, **71**, 1078-1081.

Zhang, Y., Zhu, T., Fang, Y., Liu, H., Gu, Q., and Zhu, W. (2007) Carbonarones A and B, New Bioactive g-Pyrone and a-Pyridone Derivatives from the Marine-derived Fungus *Aspergillus carbonarius*. *Journal of Antibiotics*, **60**, 153-157.

Zheng, C. J., Shao, C. L., Guo, Z. Y., Chen, J. F., Deng, D. S., Yang, K. L., Chen, Y. Y., Fu, X. M., She, Z. G., and Lin, Y. C. (2012) Bioactive hydroanthraquinones and anthraquinone dimers from a soft coral-derived *Alternaria* sp. fungus. *Journal of natural products*, **75**, 189-197.

Żwawiak, J. and Zaprutko, L. (2014) A brief history of taxol. *Journal of Medical Science*, **1**, 83.

7. Attachments

Attachment 1. The ^{1}H NMR spectrum of 4'-hydroxyl-deacetyl-18-deoxycytochalasin H (**1**, **new**) (600 MHz, CD_3OD)

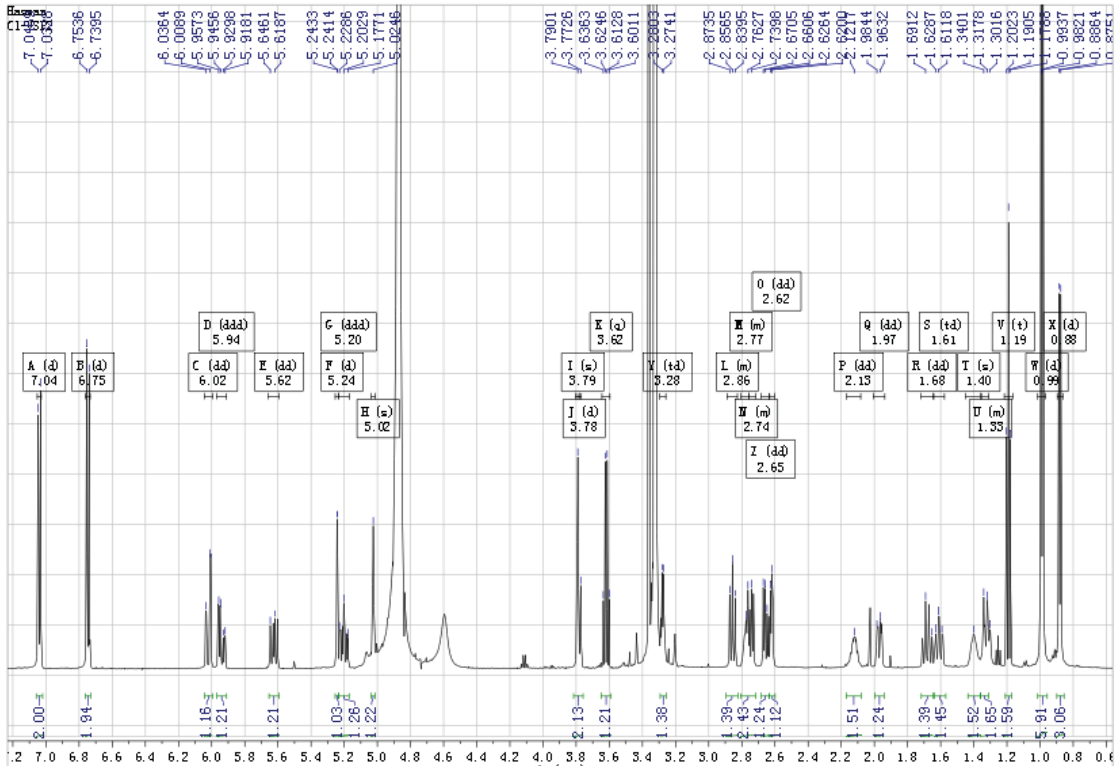

Attachment 2. The ^{1}H NMR spectrum of deacetyl-18-deoxycytochalasin H (**2**, **known**) (500 MHz, CD_3OD)

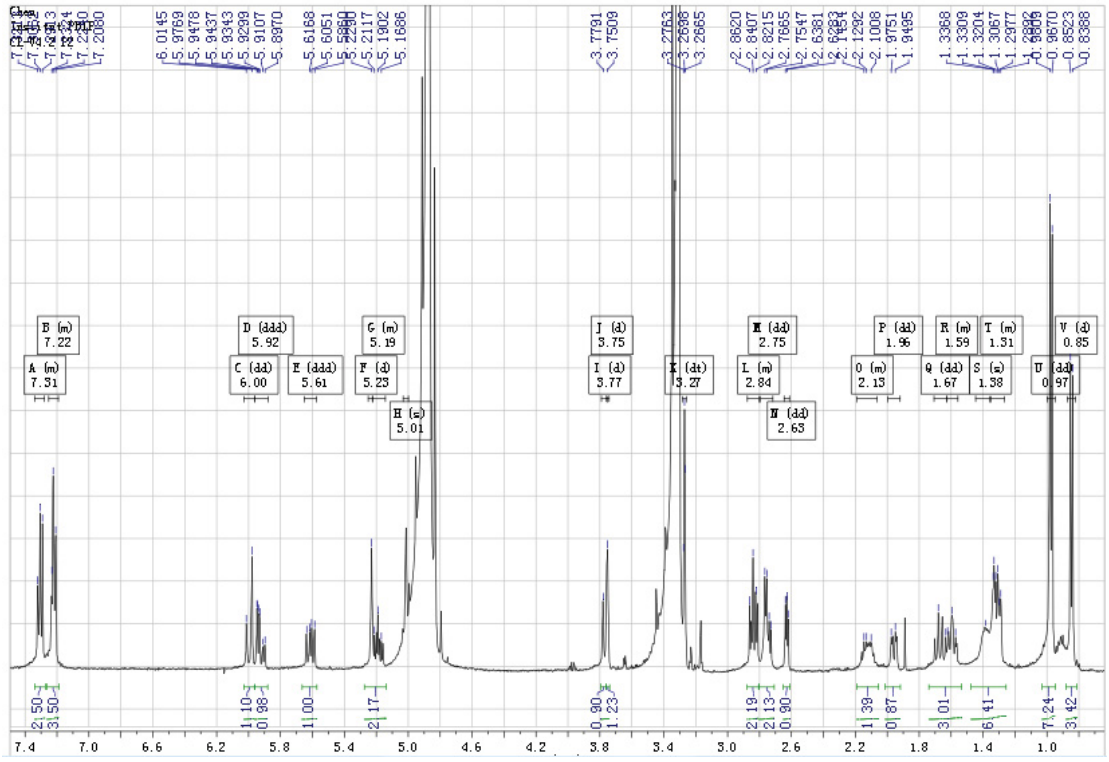

Attachment 3. The ^{1}H NMR spectrum of 18-deoxycytochalasin H (**3**, **known**) (500 MHz, CD_3OD)

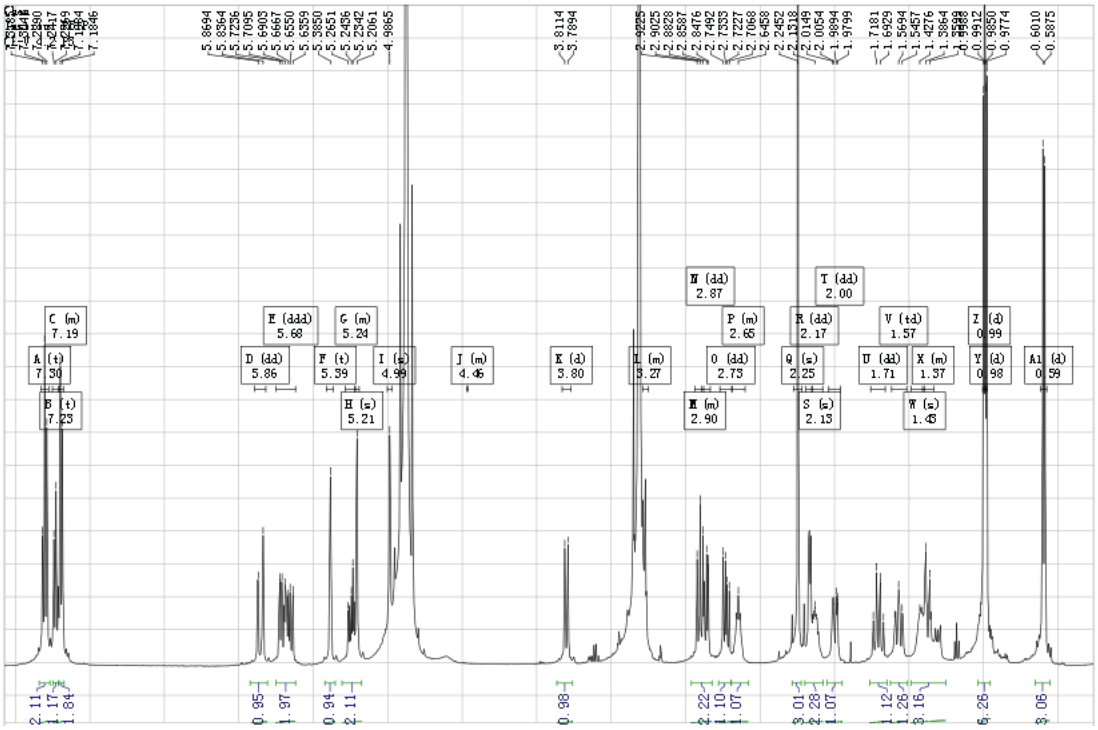

Attachment 4. The ^{1}H NMR spectrum of waol A (**5**, **known**) (500 MHz, CD_3OD)

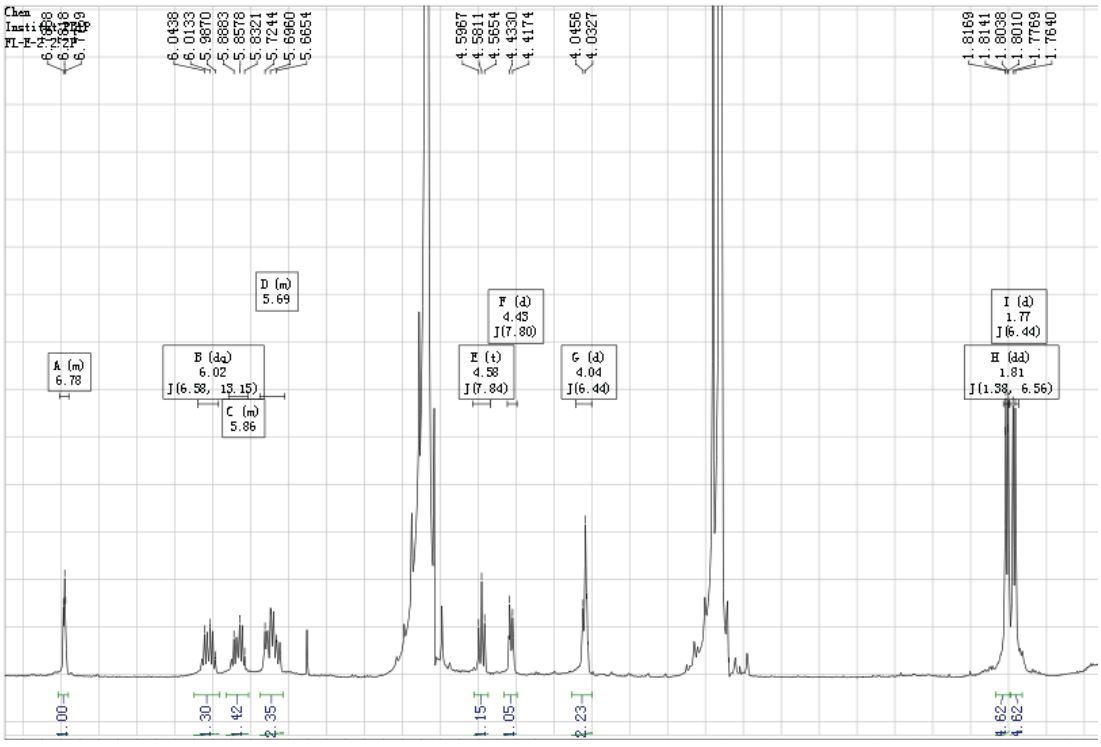

Attachment 5. The ^{1}H NMR spectrum of aspyridone A (**6**, **known**)
(500 MHz, DMSO)

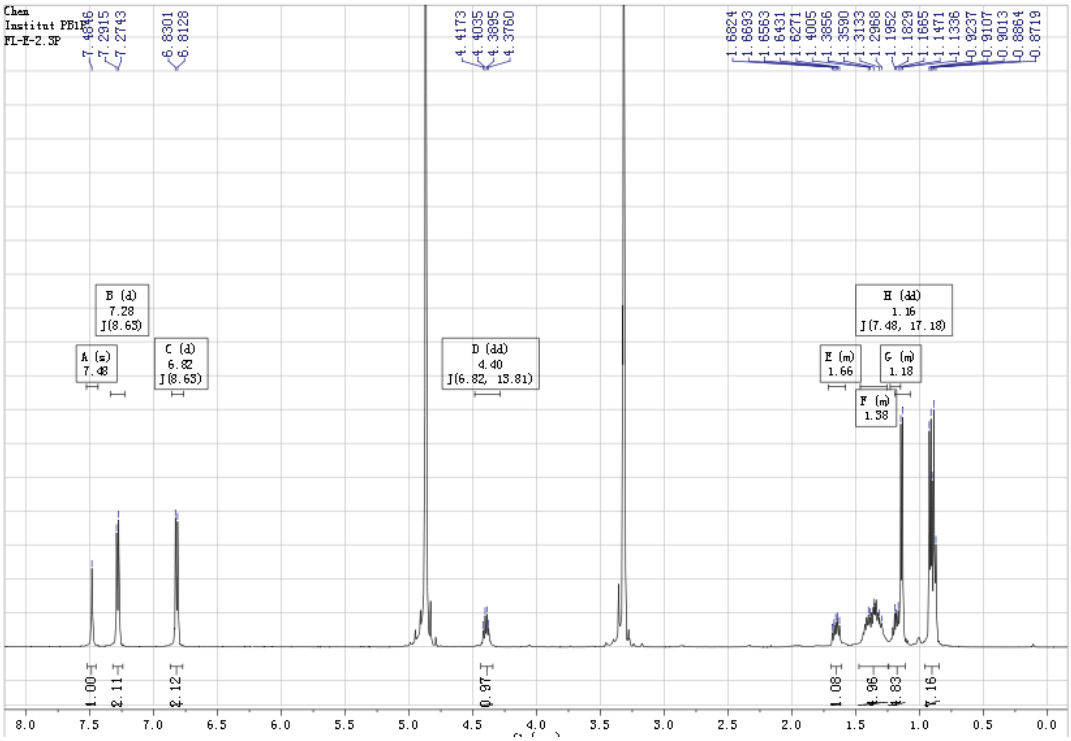

Attachment 6. The ^{1}H NMR spectrum of isobutyrolactone II (**7**, **new**)
(600 MHz, DMSO)

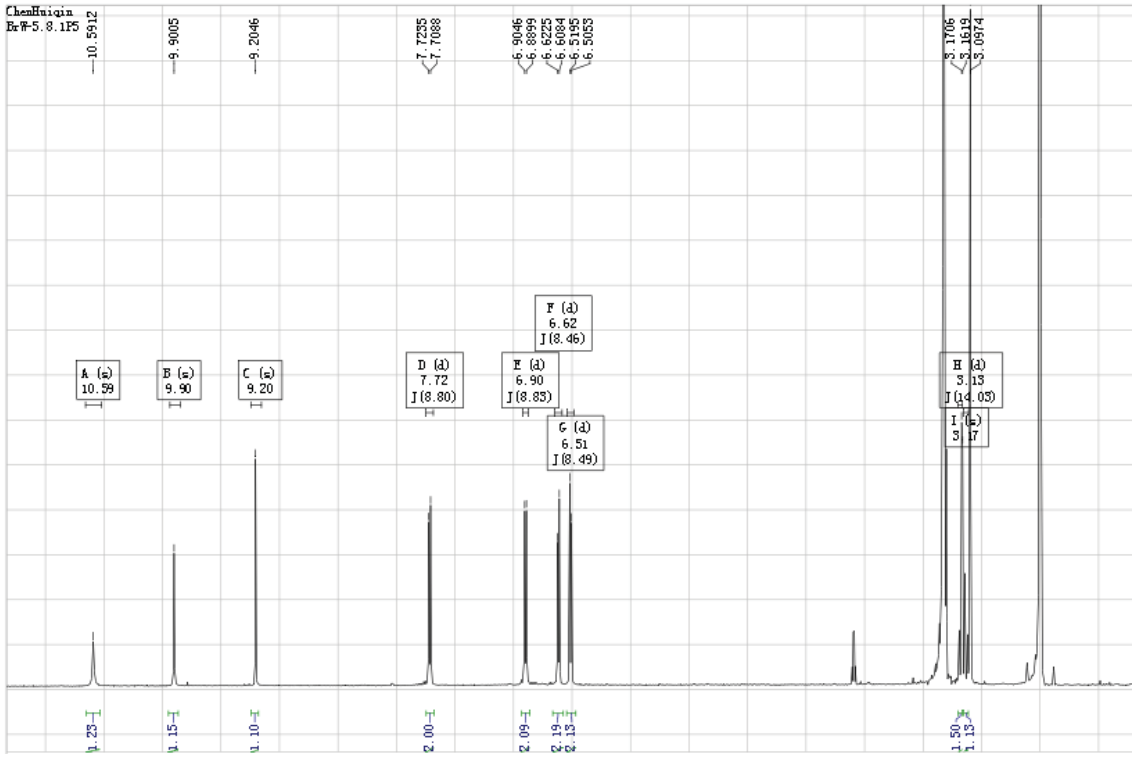

Attachment 7. The ^{1}H NMR spectrum of 4-O-demethylisobutyrolactone II (**8**, **new**) (600 MHz, DMSO)

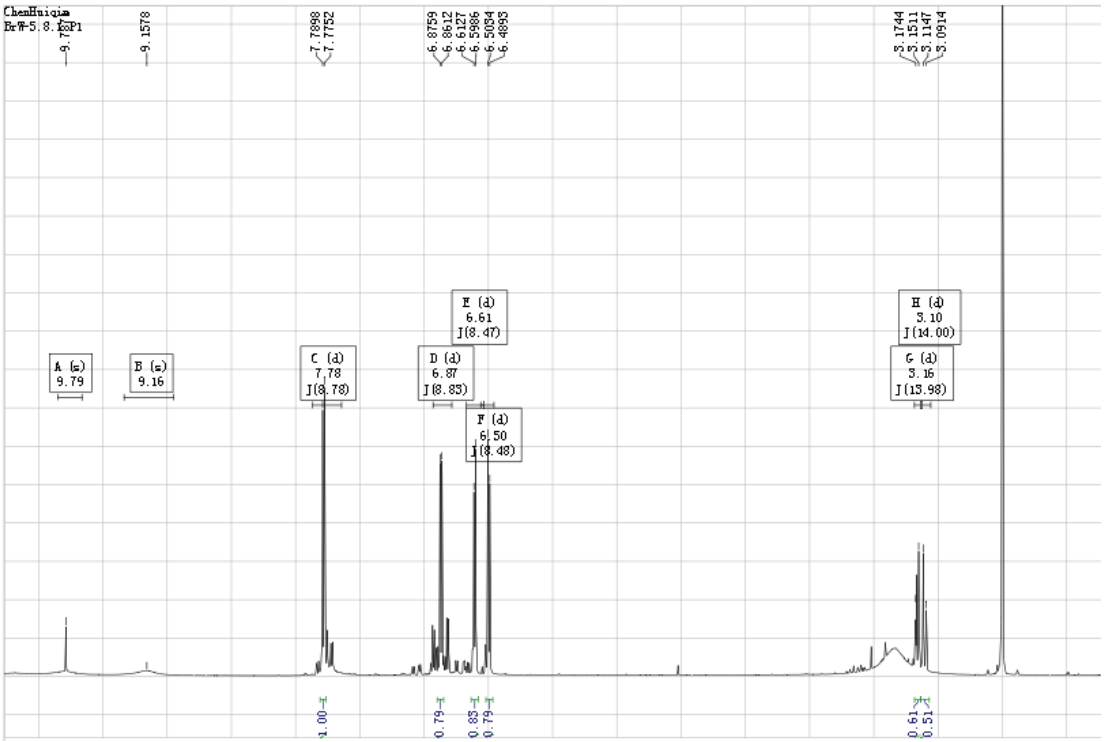

Attachment 8. The ^{1}H NMR spectrum of N-(carboxymethyl)anthranilic acid (**9**, **known**) (600 MHz, CD_3OD)

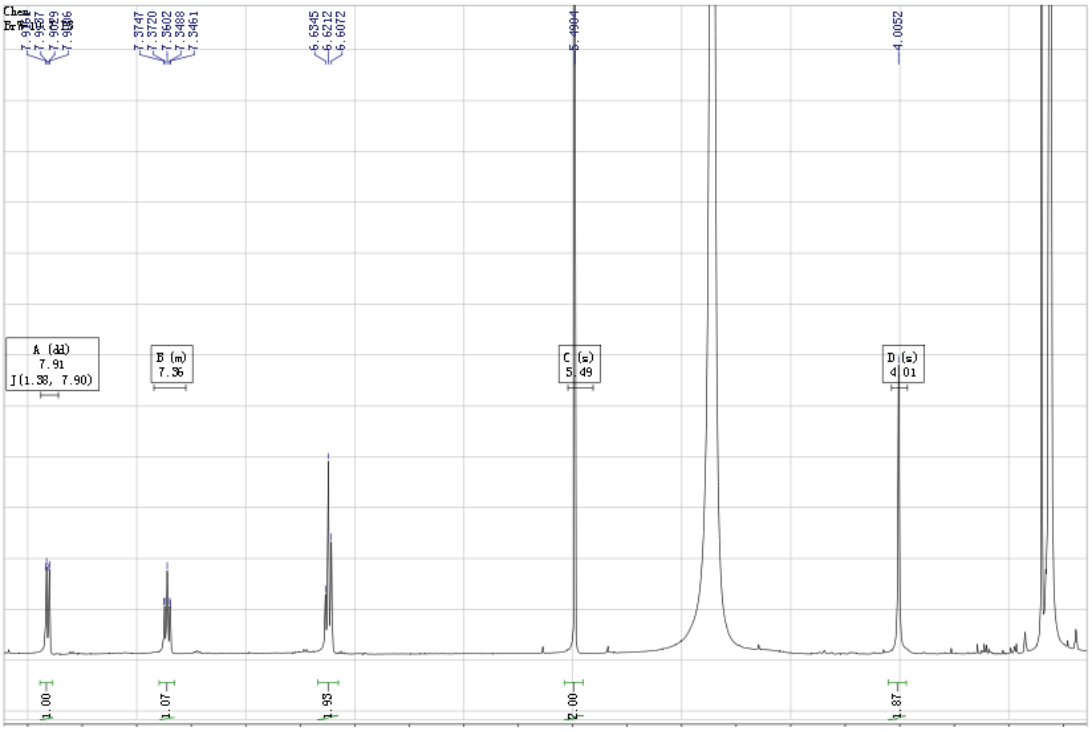

Attachment 9. The ^{1}H NMR spectrum of butyrolactone II (**10**, **known**)
(600 MHz, CD_3OD)

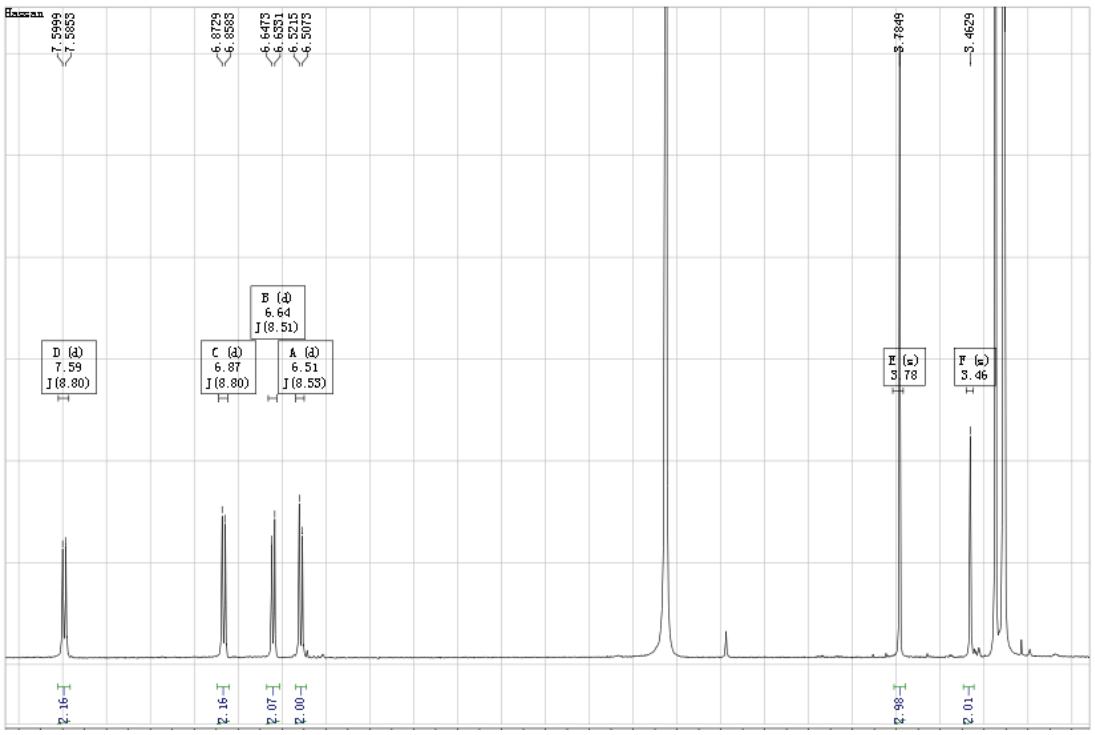

Attachment 10. The ^{1}H NMR spectrum of butyrolactone I (**11**, **known**)
(500 MHz, CD_3OD)

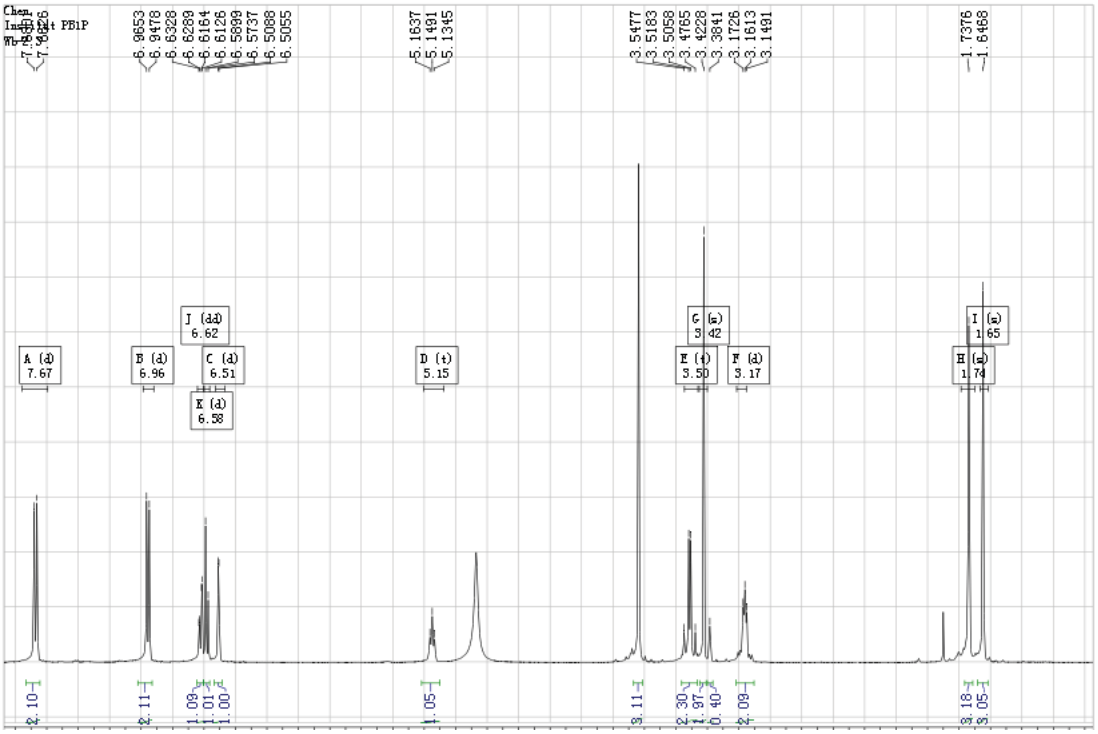

Attachment 11. The ^{1}H NMR spectrum of butyrolactone III (**12**, **known**) (500 MHz, CD_3OD)

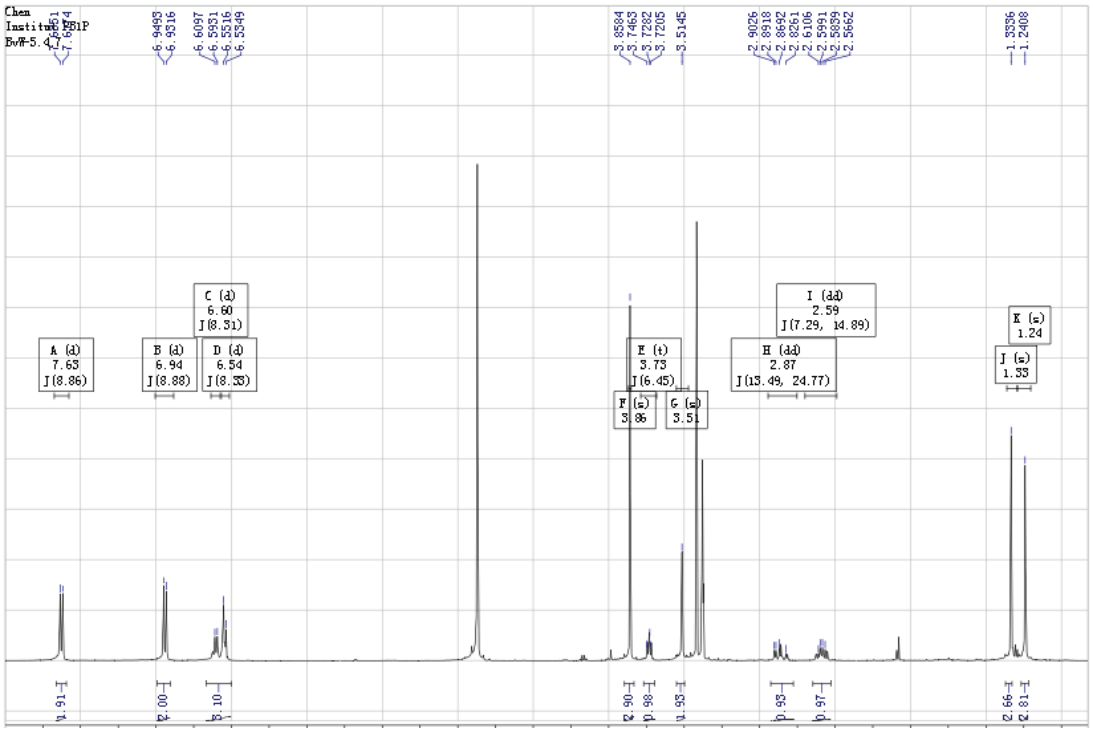

Attachment 12. The ^{1}H NMR spectrum of butyrolactone VI (**13**, **known**) (600 MHz, CD_3OD)

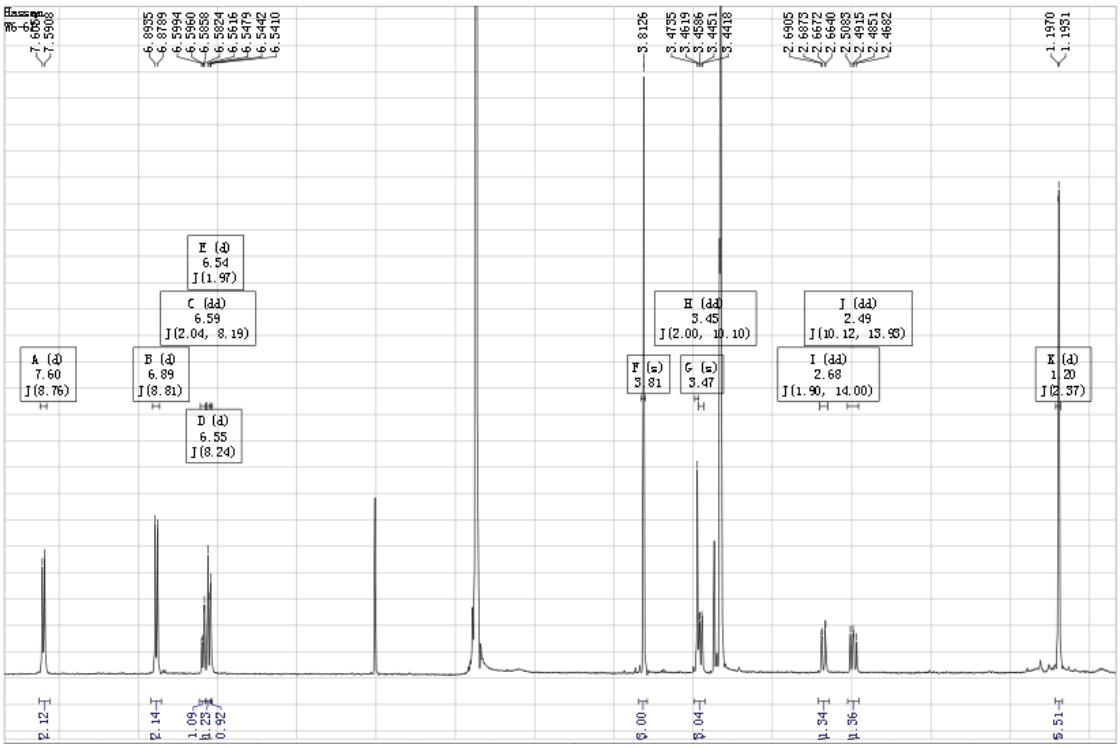

Attachment 13. The ^{1}H NMR spectrum of terrein (**14**, **known**)
(500 MHz, CD_3OD)

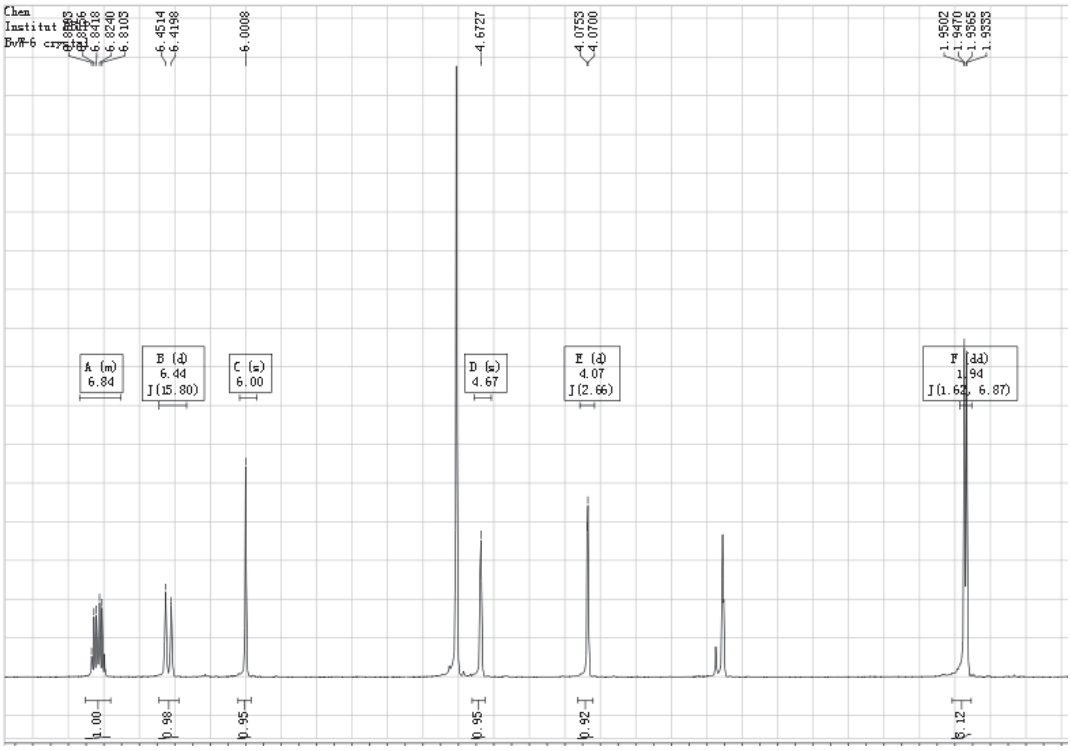

Attachment 14. The ^{1}H NMR spectrum of dihydroterrein (**15**, **known**)
(500 MHz, CD_3OD)

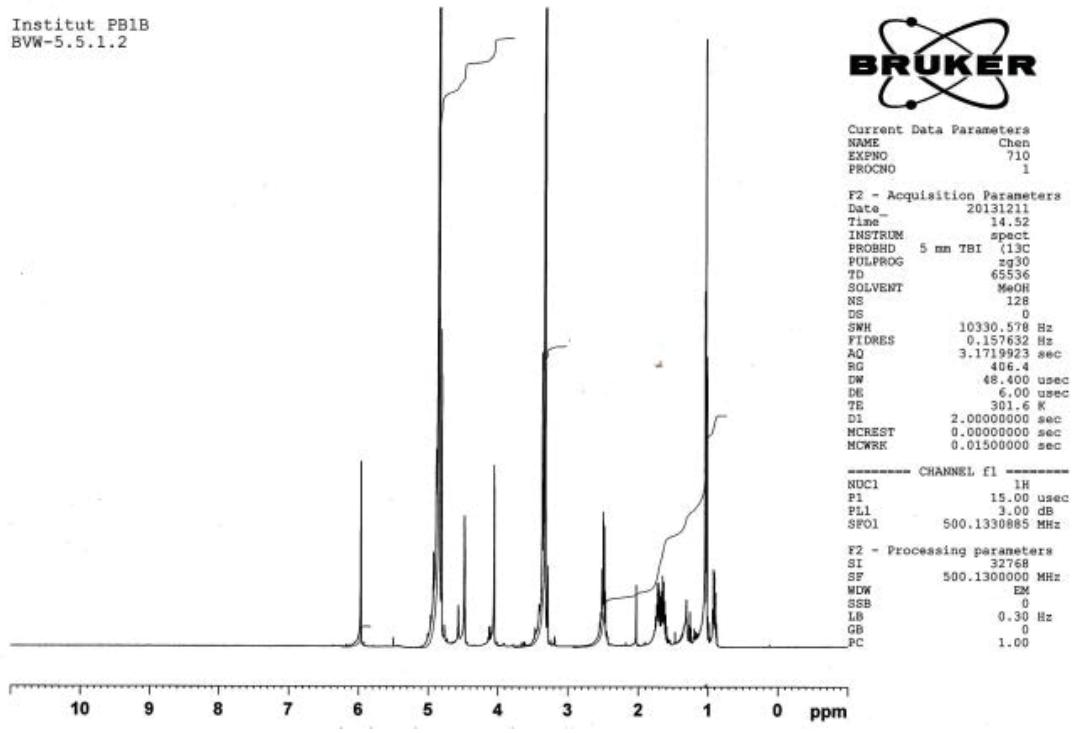

Attachment 15. The ^{1}H NMR spectrum of orsellinic acid (**16**, **known**)
(500 MHz, CD_3OD)

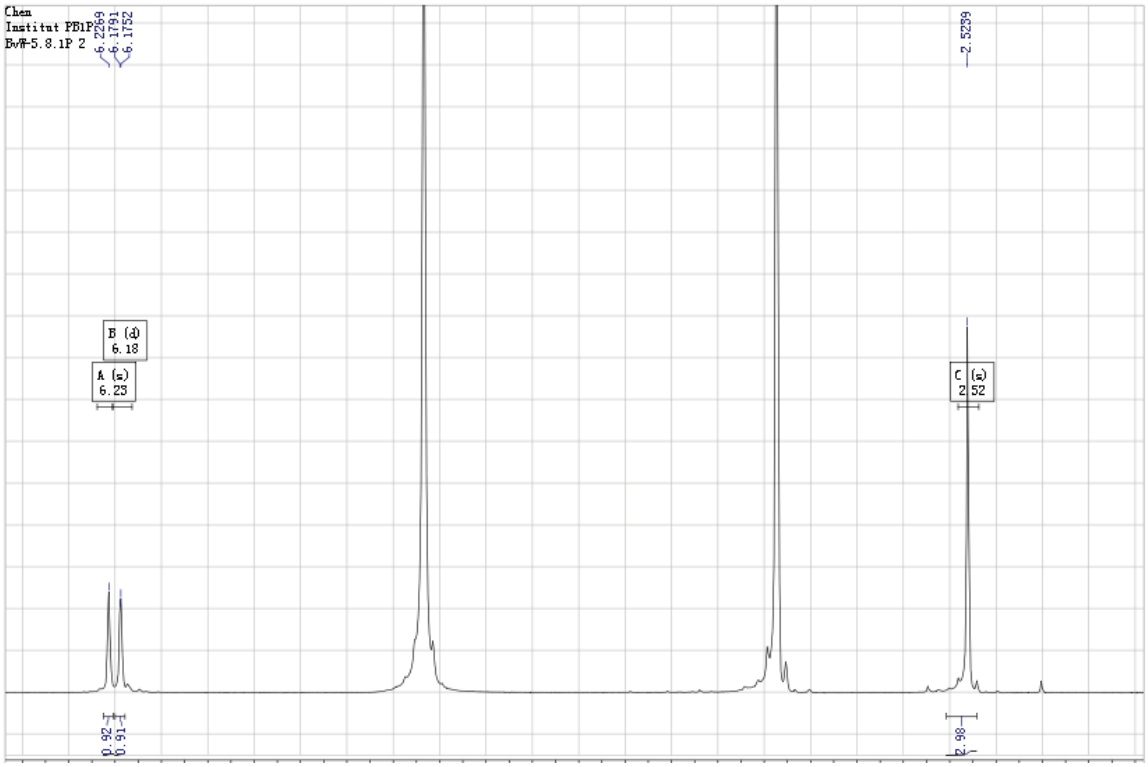

Attachment 16. The ^{1}H NMR spectrum of terreinol (**17**, **known**)
(500 MHz, CD_3OD)

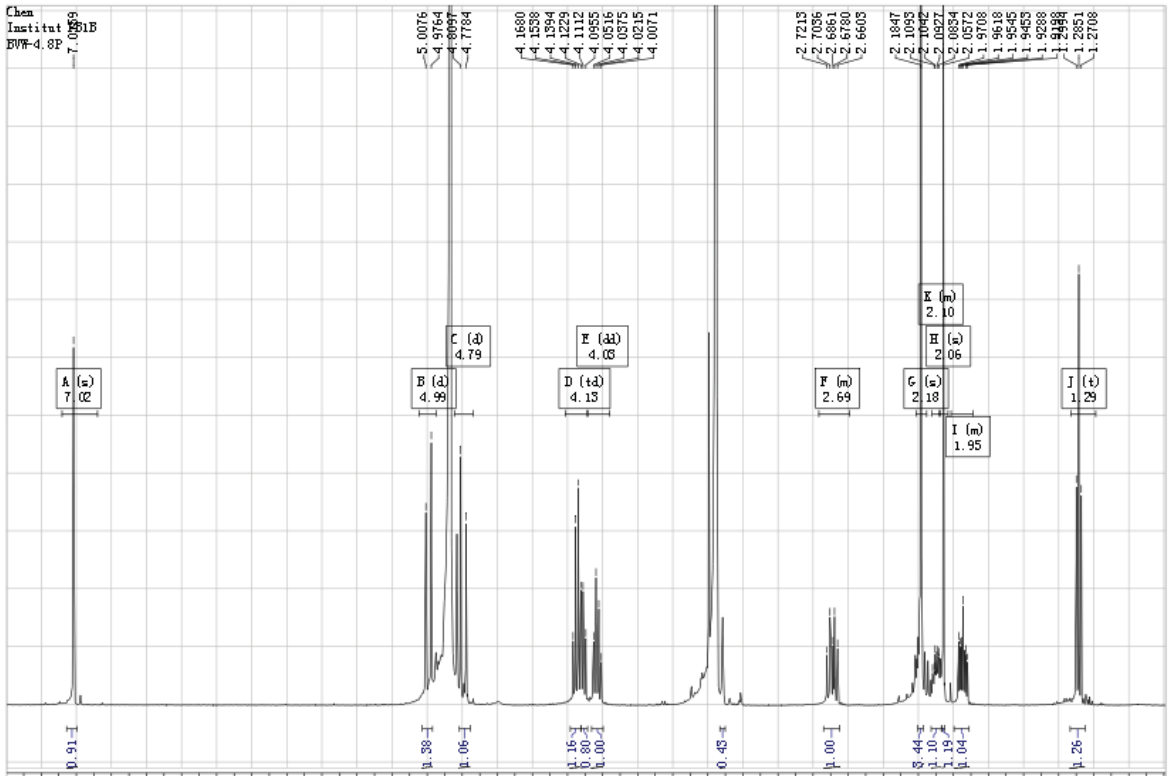

Attachment 17. The ^{1}H NMR spectrum of terretonin A (**18**, **known**) (500 MHz, CD_3Cl)

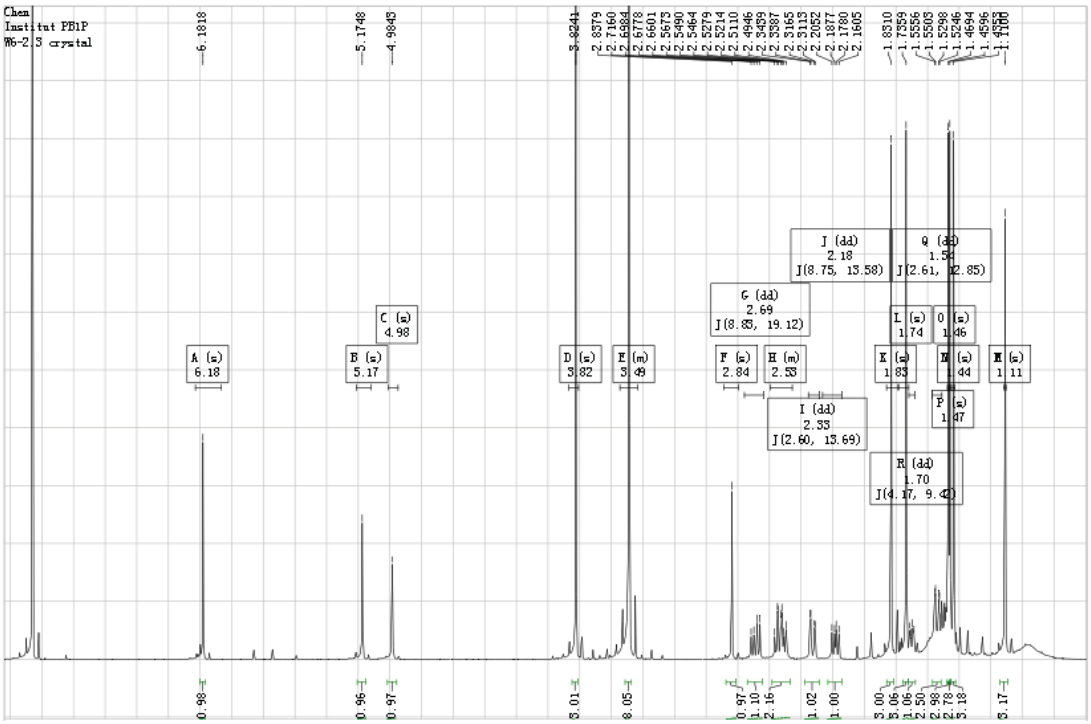

Attachment 18. The ^{1}H NMR spectrum of terretonin (**19**, **known**) (500 MHz, CD_3Cl)

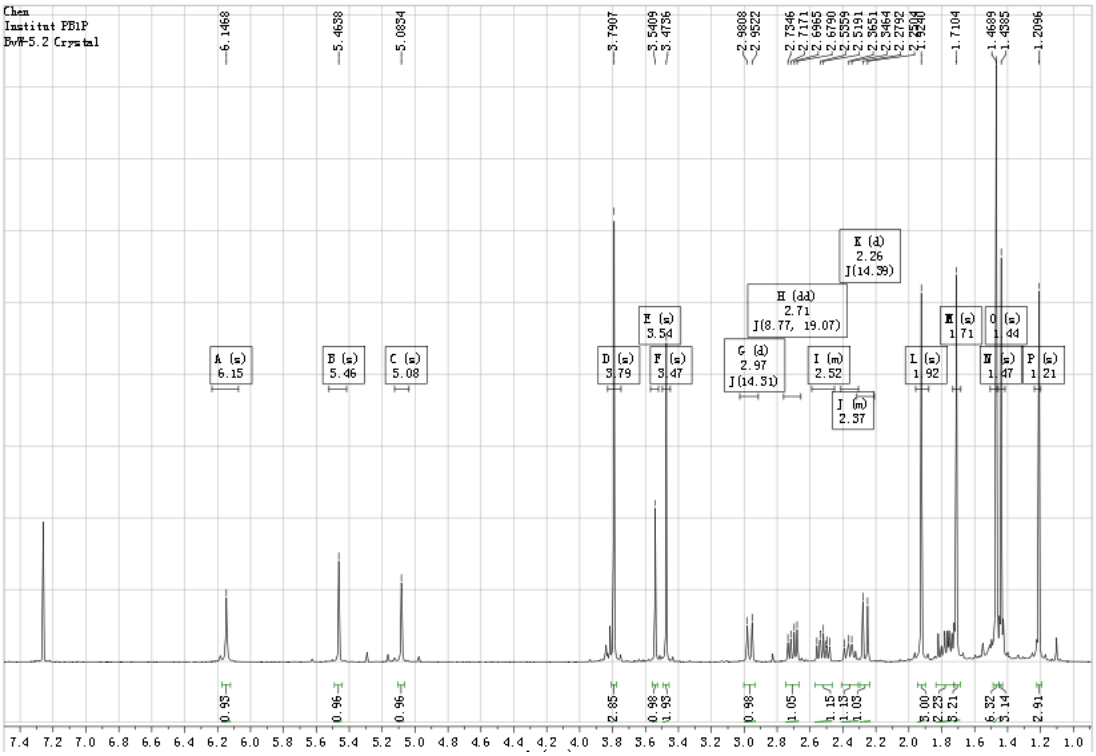

Attachment 19. The ^{1}H NMR spectrum of aspulvinone E (**20**, **known**) (500 MHz, CD_3OD)

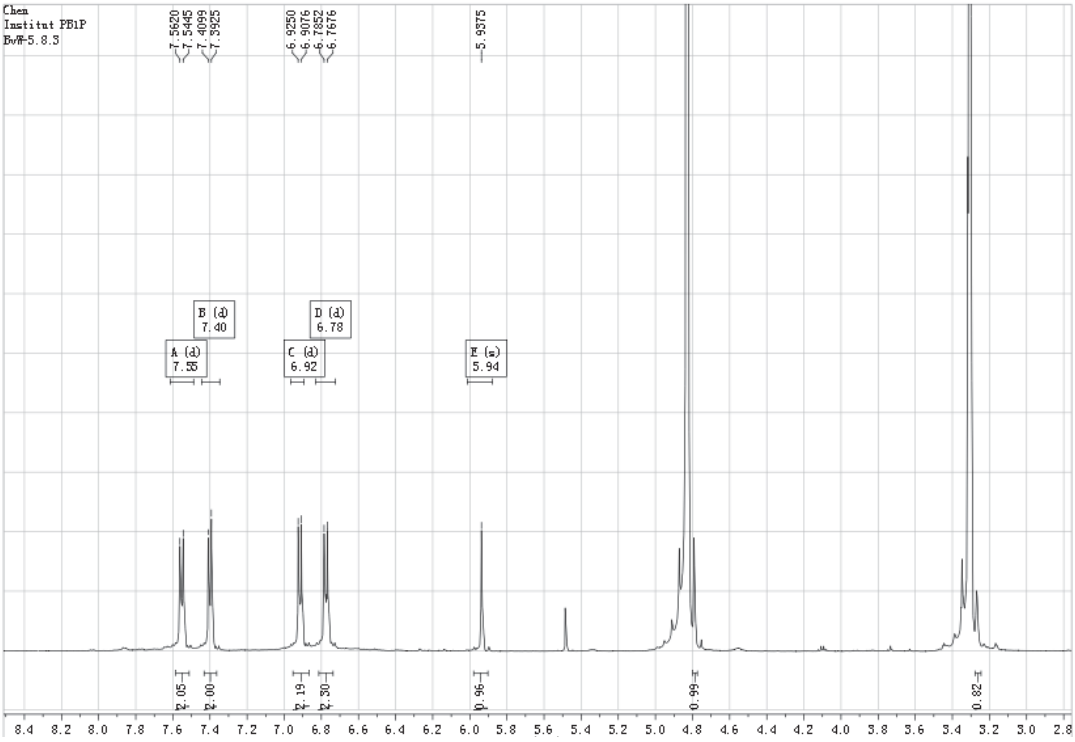

Attachment 20. 3-hydroxy-5-(4-hydroxybenzyl)-4-(4-hydroxyphenyl)furan-2(5*H*)-one (**21**, known) (500 MHz, CD_3OD)

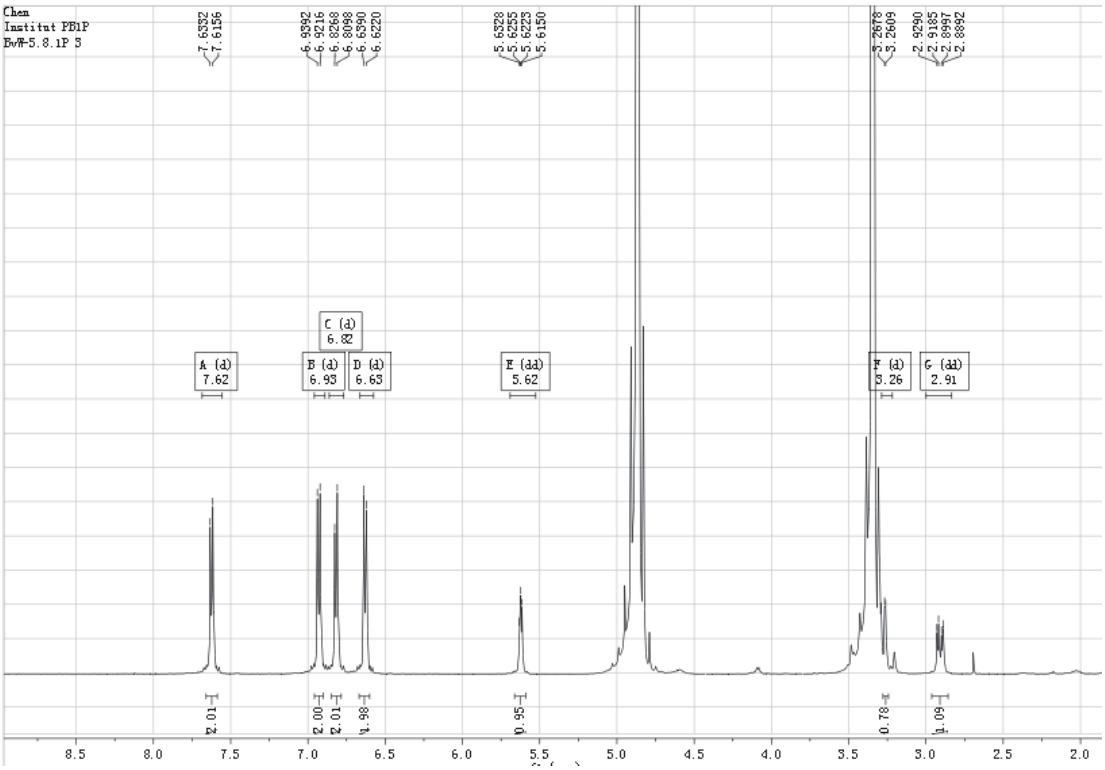

Attachment 21. The ^{1}H NMR spectrum of (2*R*, 1'*S*)-dihydroisoflavipucine (**22**, **known**) (600 MHz, CD_3OD)

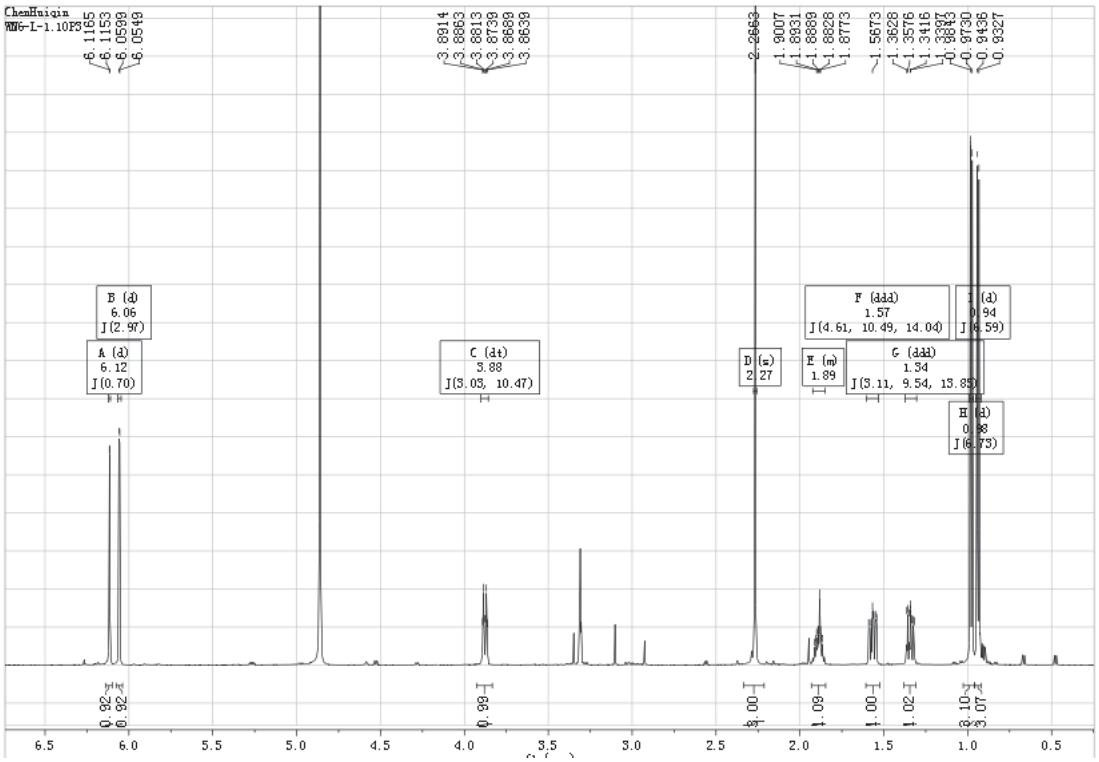

Attachment 22. The ^{1}H NMR spectrum of (2*S*, 1'*S*)-Dihydroisoflavipucine (**23**, **new**) (600 MHz, CD_3OD)

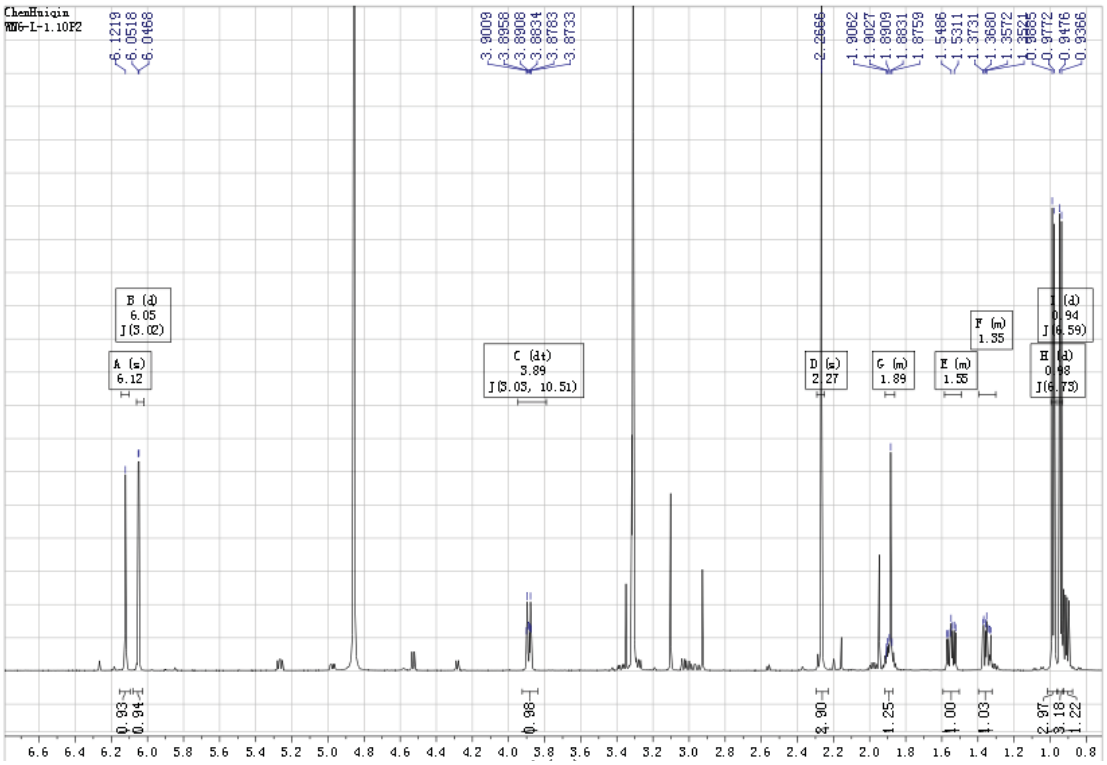

Attachment 23. The ^{1}H NMR spectrum of (**24**, **known**) (300 MHz, CD_3OD)

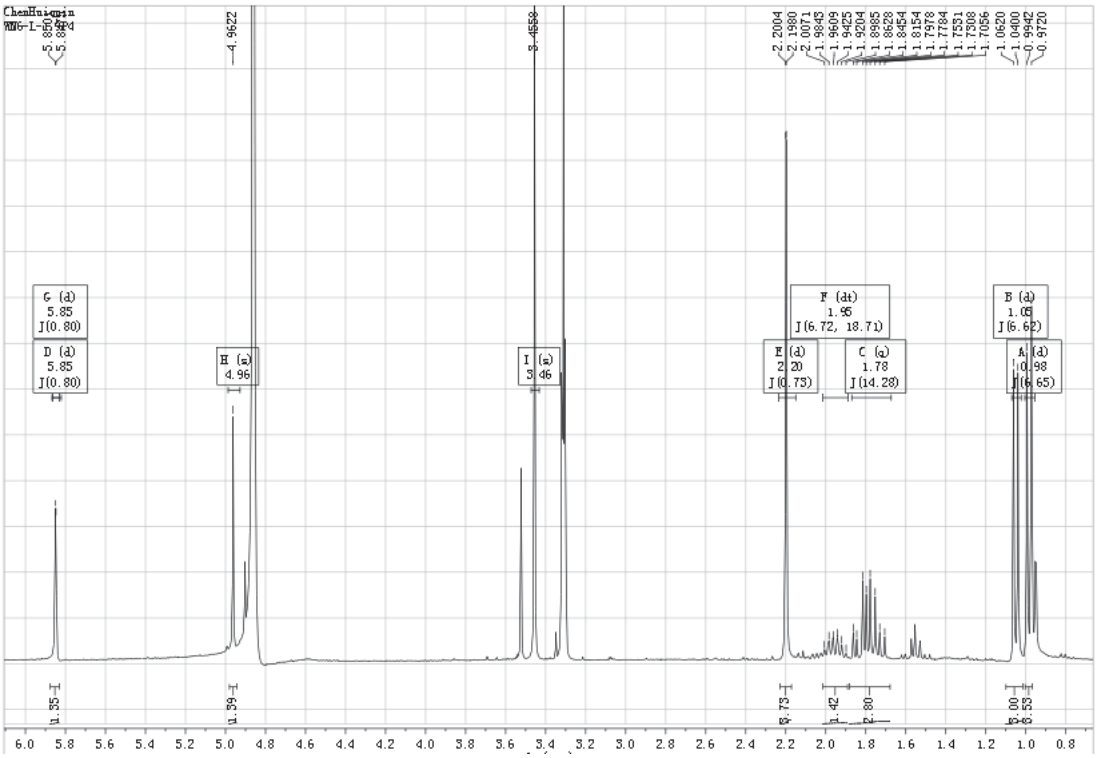

Attachment 24. The ^{1}H NMR spectrum of *cis*-4,6-dihydroxymellein (**25**, **known**) (500 MHz, CD_3OD)

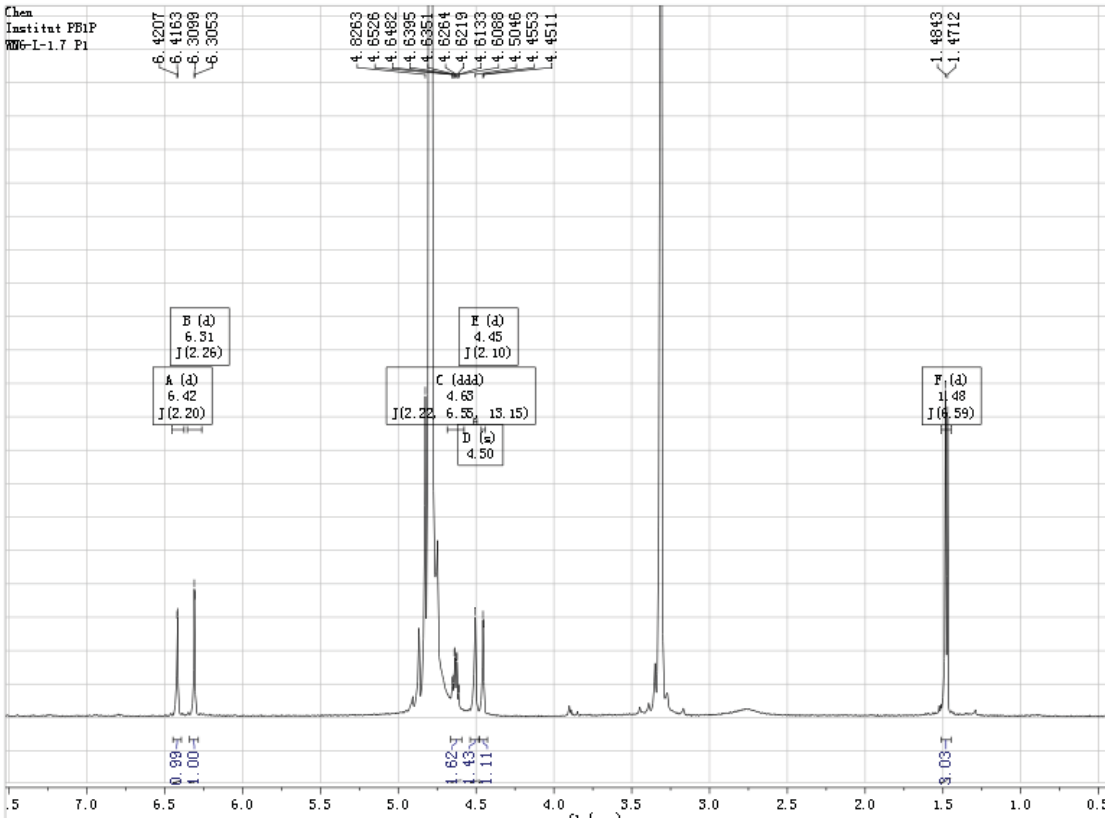

Attachment 25. The ^{1}H NMR spectrum of (3*R*,4*R*)-3,4-dihydro-4,8-dihydroxy-6,7-dimethoxy-3-methlisocoumarin (**27**, **known**) (500 MHz, CD_3OD)

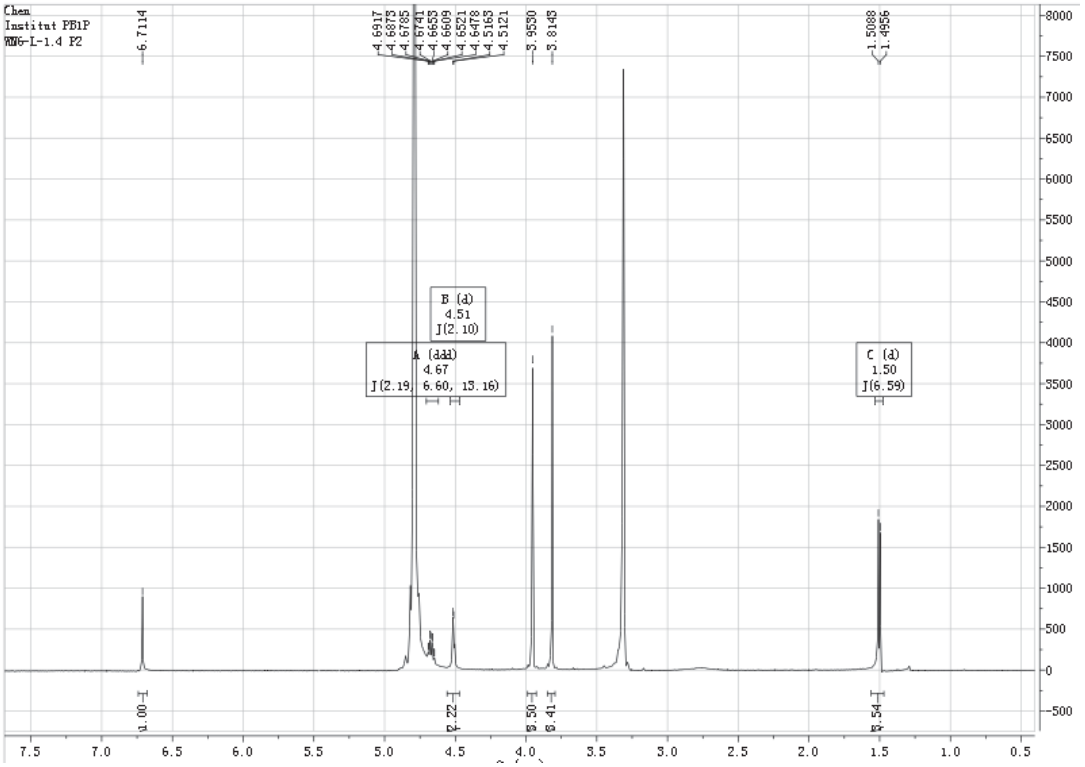

Attachment 26. The ^{1}H NMR spectrum of 1-(2',3'-dihydroxyphenyl)ethanone (**28**, **known**) (300 MHz, CD_3OD)

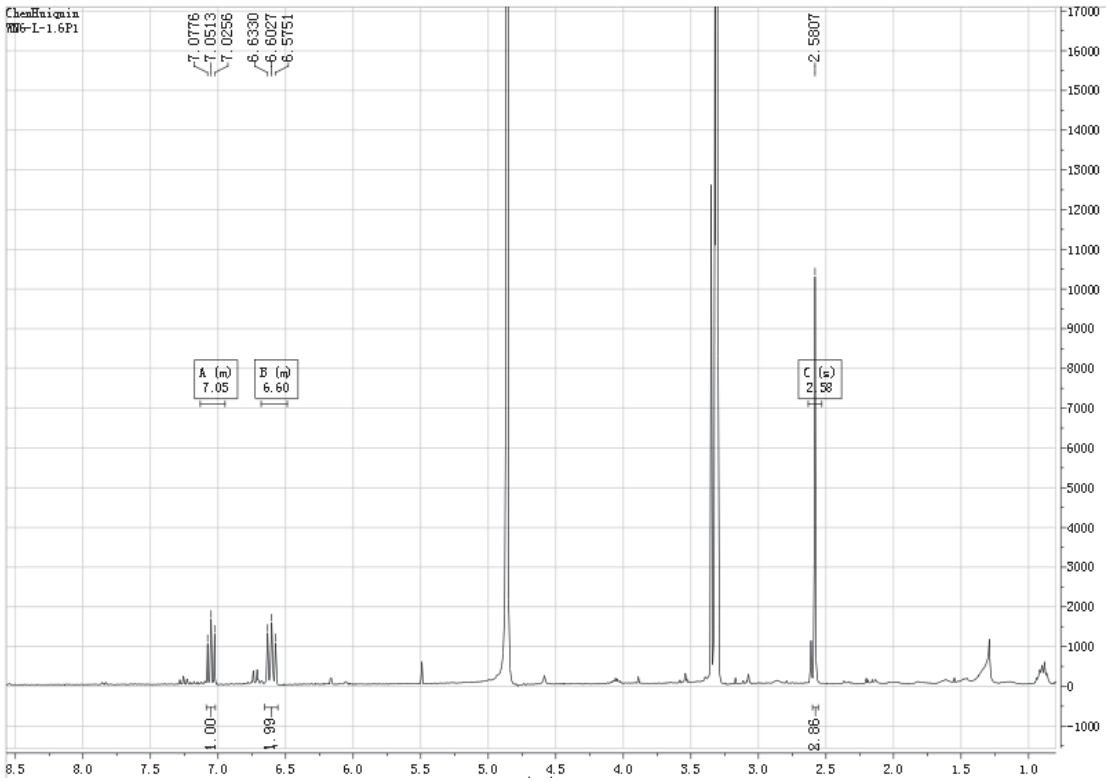

Attachment 27. The ^{1}H NMR spectrum of asterrelenin (**29**, known)
(600 MHz, CD_3OD)

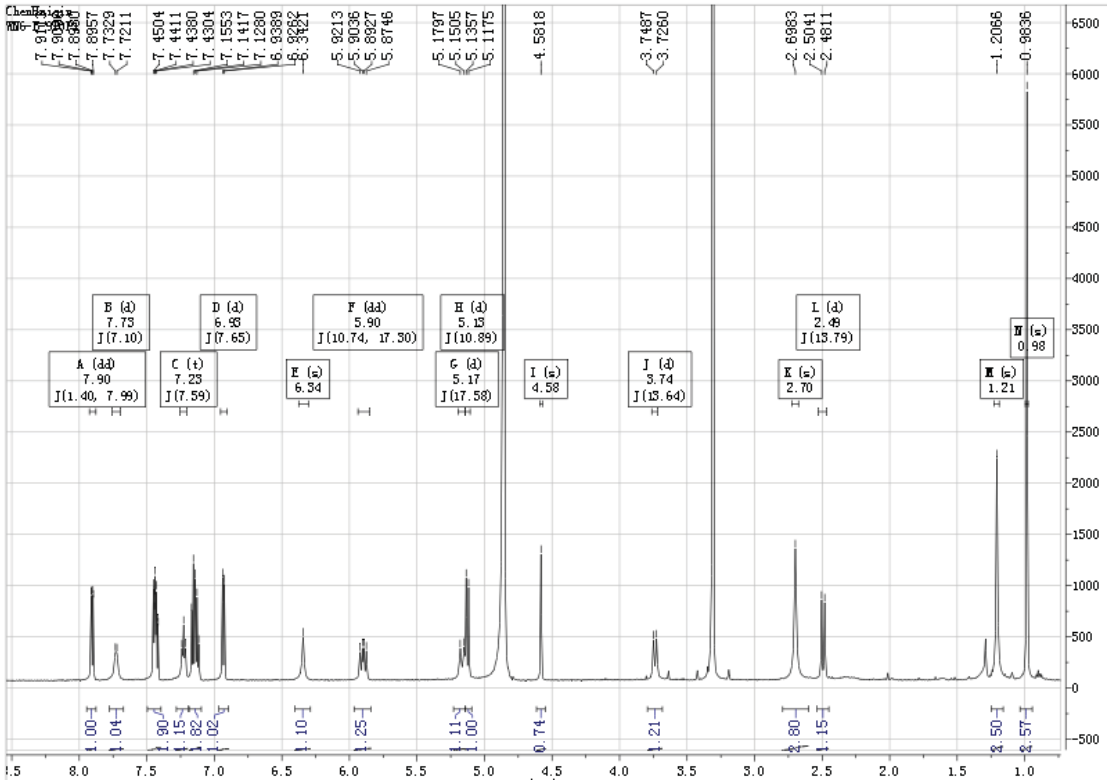

Attachment 28. The ^{1}H NMR spectrum of acetylaszonalenin (**30**, **known**)
(300 MHz, CD_3OD)

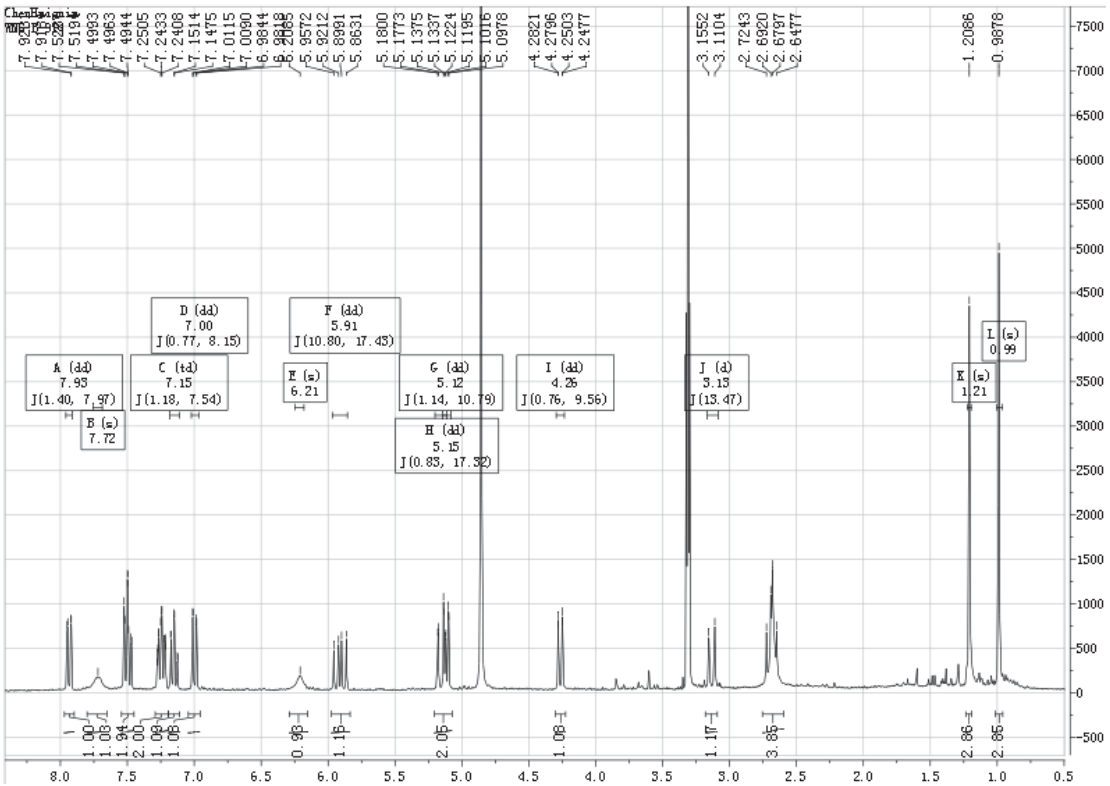

Attachment 29. The ^{1}H NMR spectrum of fusarielin I (**31**, **new**)
(600 MHz, CD_3OD)

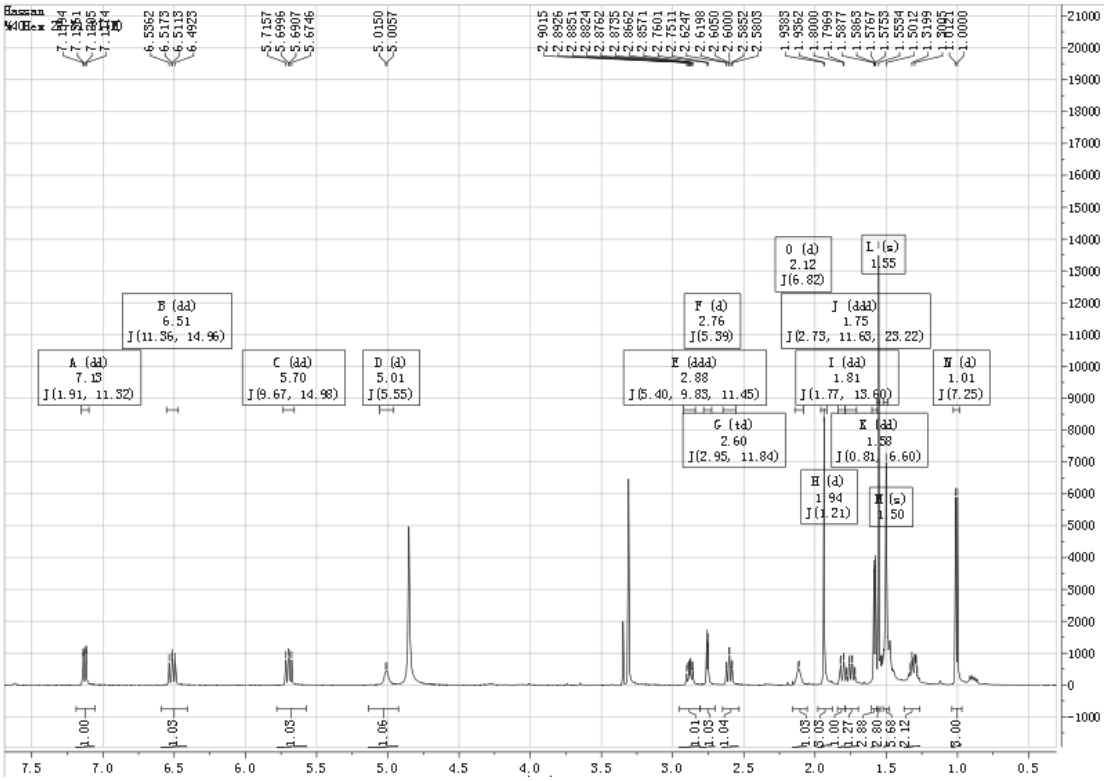

Attachment 30. The ^{1}H NMR spectrum of griseofulvin (**32**, **known**)
(500 MHz, CD_3OD)

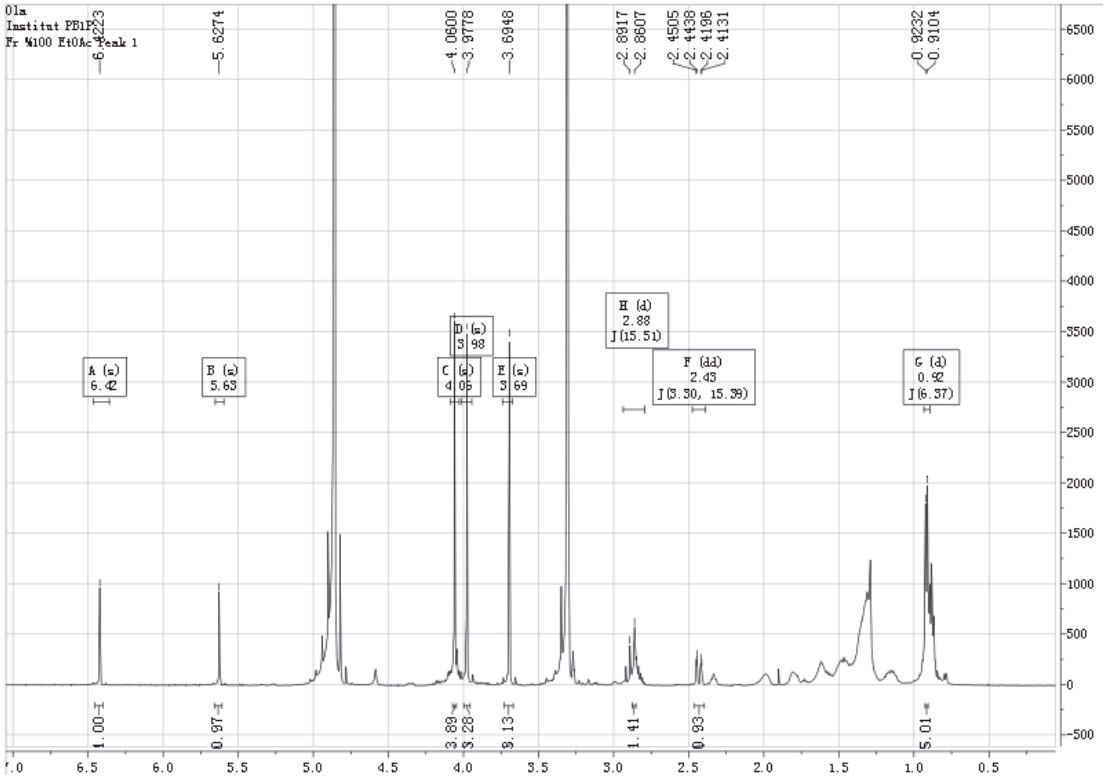

Attachment 31. The ^{1}H NMR spectrum of dechlorogriseofulvin (**33**, **known**) (500 MHz, CD_3OD)

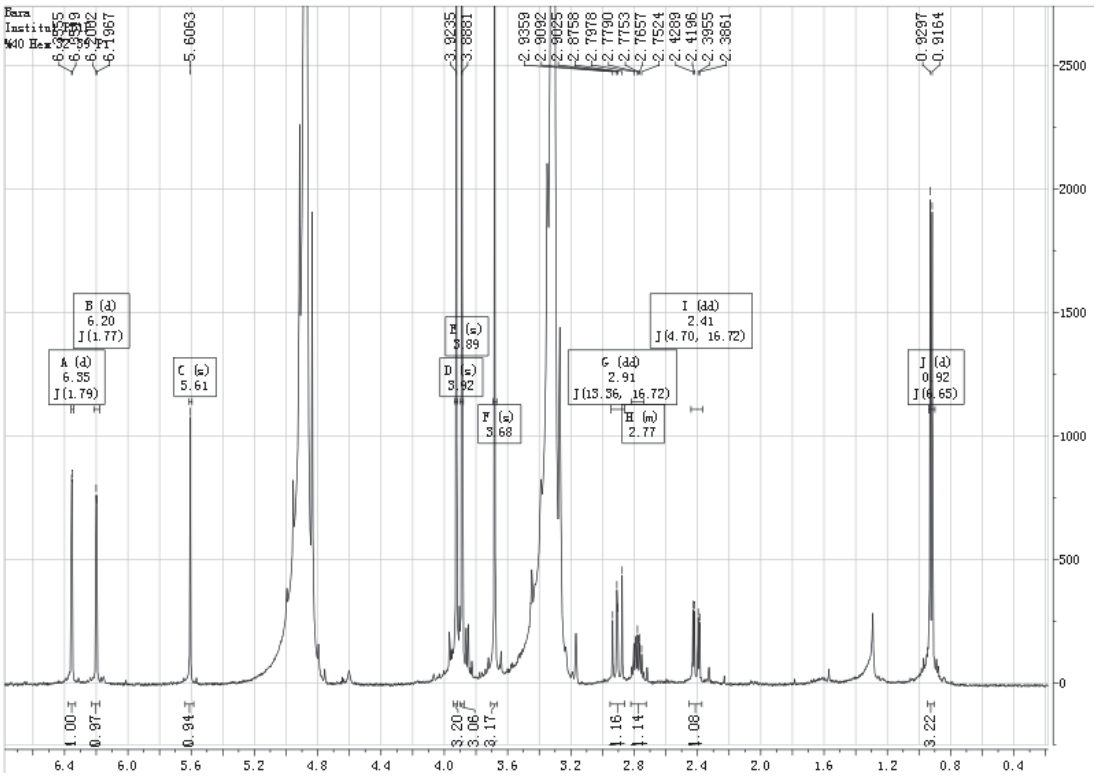

Attachment 32. The ^{1}H NMR spectrum of dehydrocurvularin (**34**, **known**) (500 MHz, CD_3OD)

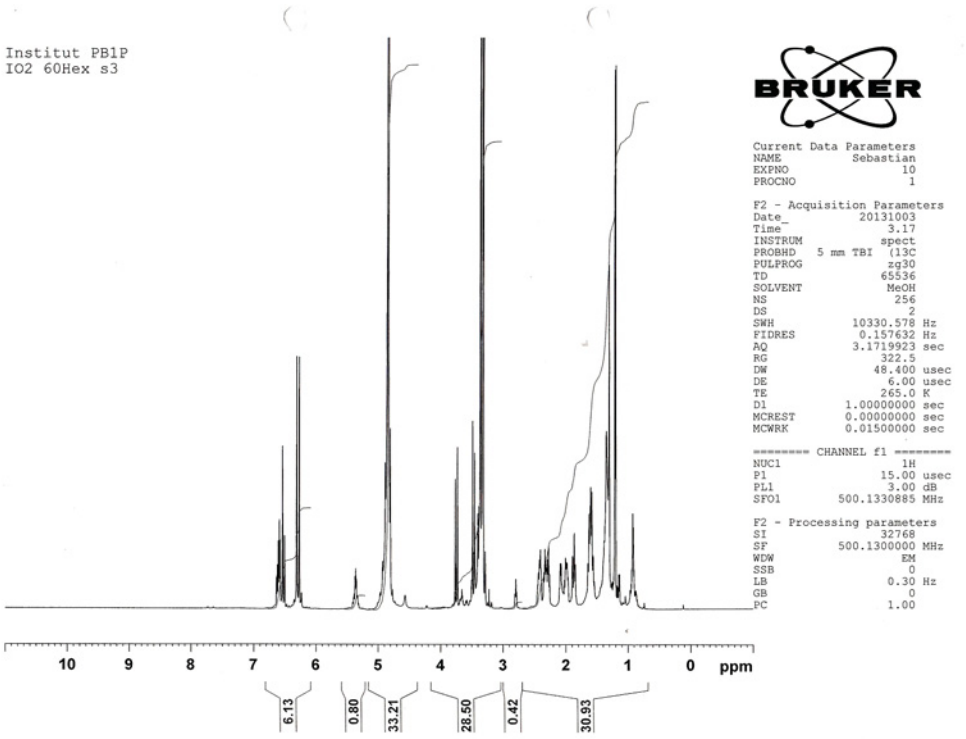

Attachment 33. The ^{1}H NMR spectrum of curvularin (**35**, **known**)

(500 MHz, CD_3OD)

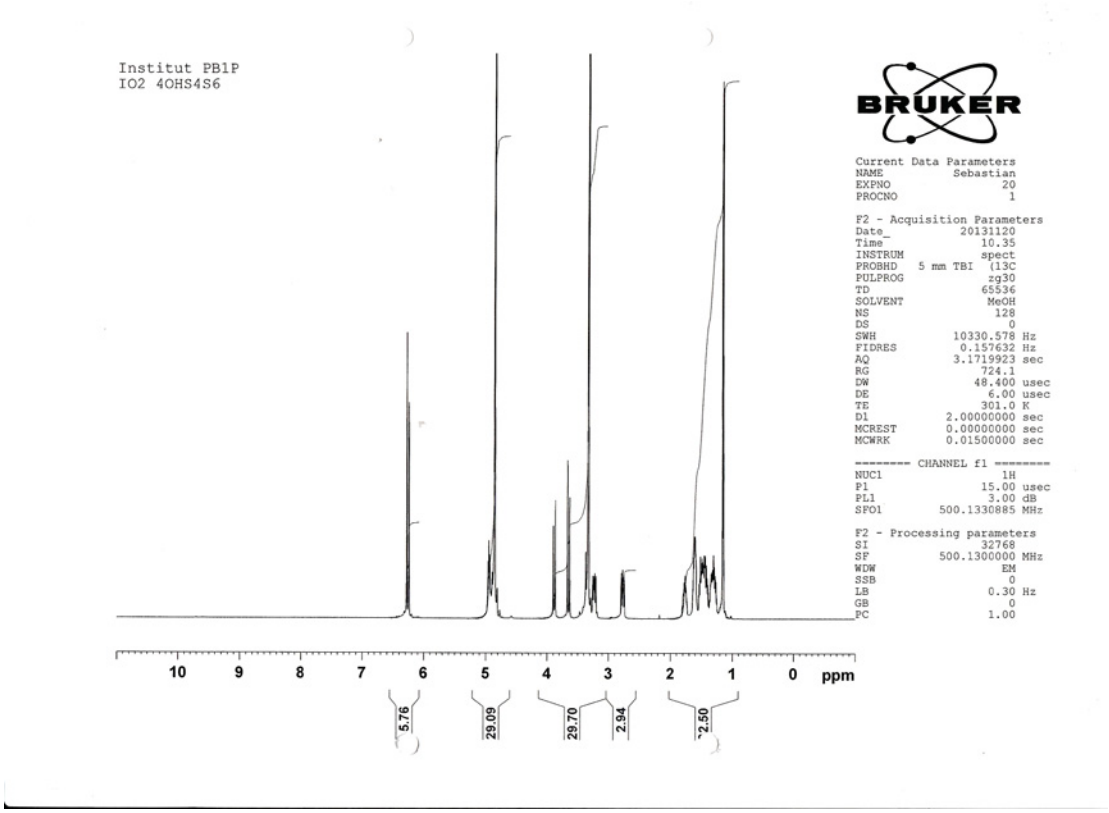

Attachment 34. The ^{1}H NMR spectrum of trichodimerol (**36**, **known**)
(600 MHz, DMSO)

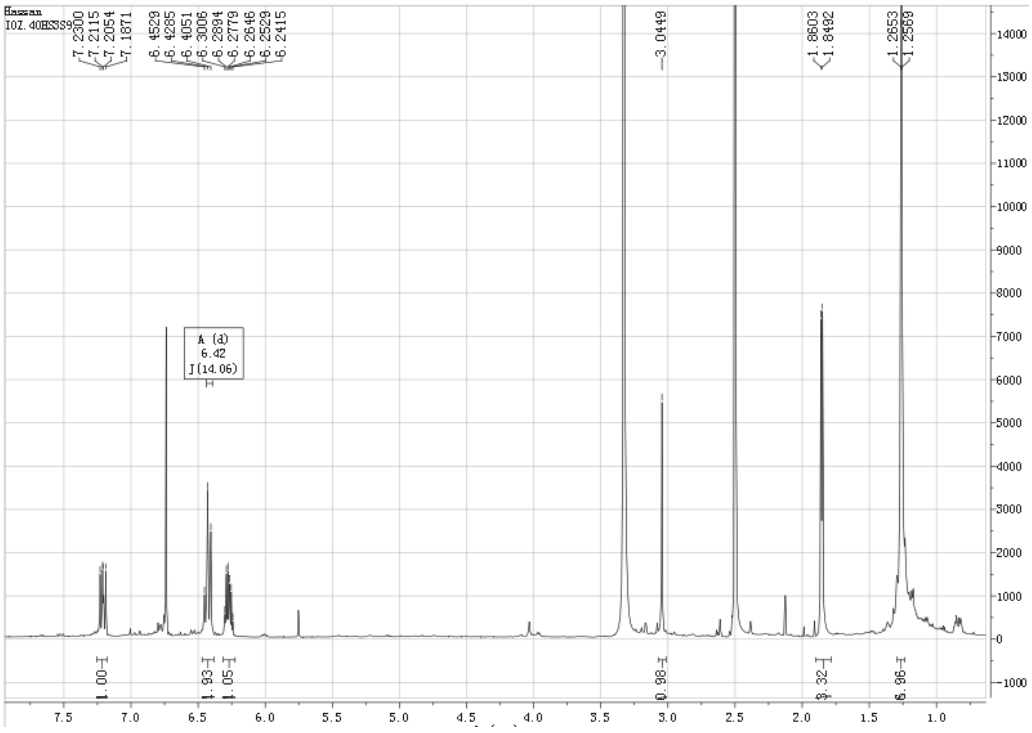

Attachment 35. The ^{1}H NMR spectrum of norlichexanthone (**37**, **known**) (500 MHz, DMSO)

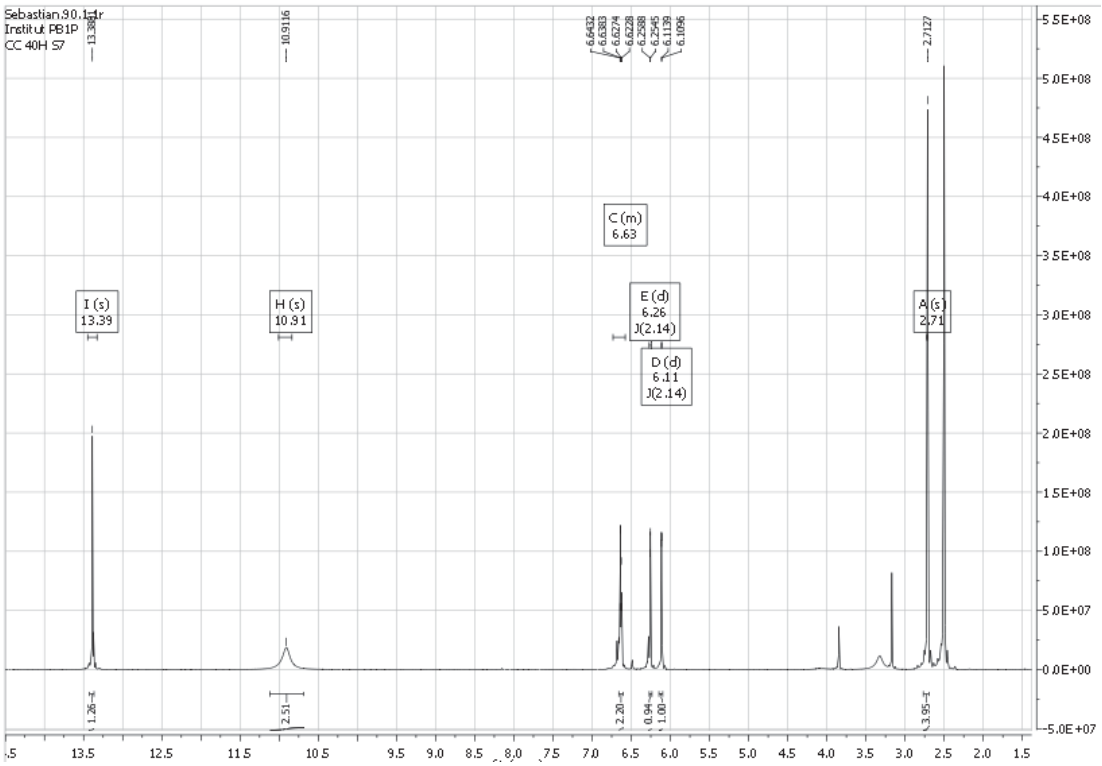

Attachment 36. The ^{1}H NMR spectrum of monocerin (**38**, **known**) (500 MHz, CD_3OD)

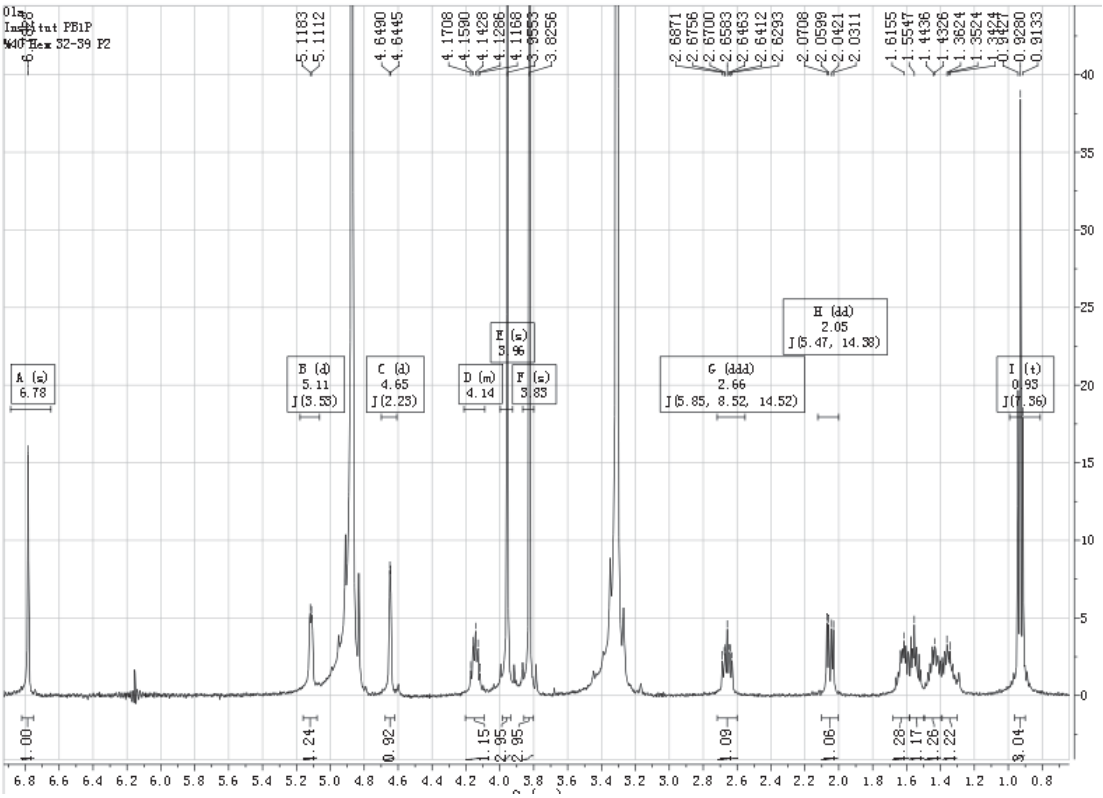

Attachment 37. The ^{1}H NMR spectrum of griseophenone B (**39**, **known**) (500 MHz, CD_3OD)

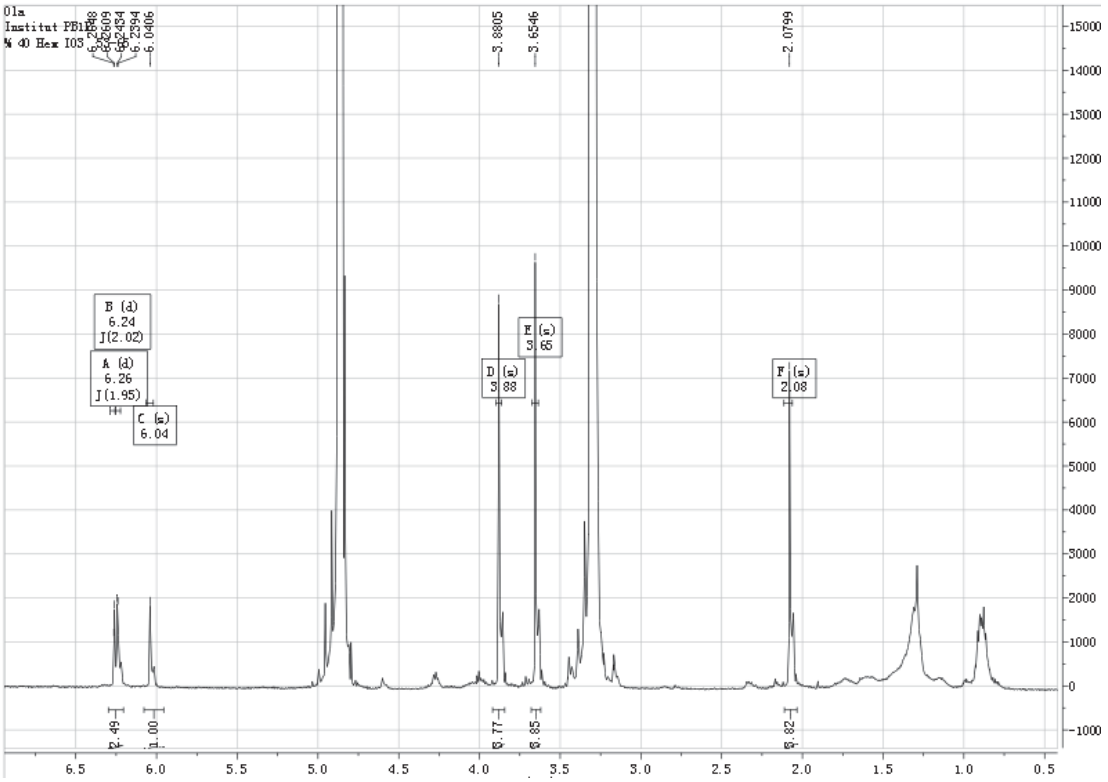

Attachment 38. The ^{1}H NMR spectrum of echinulin (**40**, **known**) (600 MHz, $CDCl_3$)

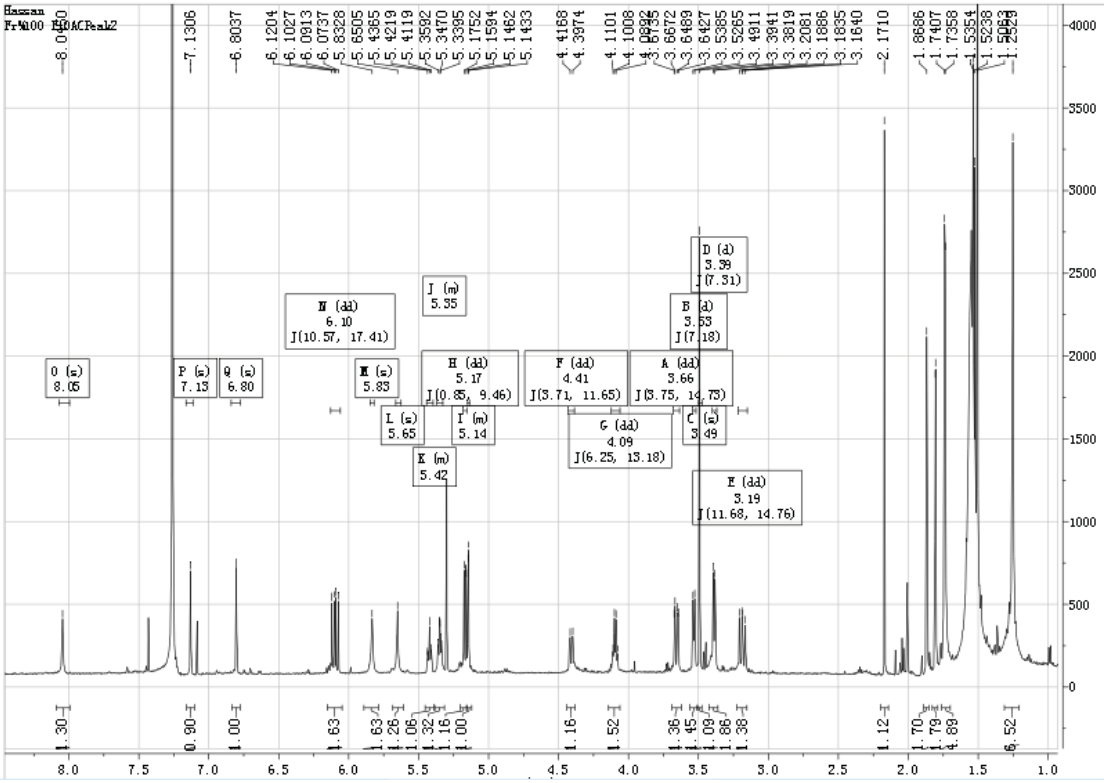

Attachment 39. The ^{1}H NMR spectrum of (5*S*)-altersetin (**41**, **known**) (600 MHz, DMSO)

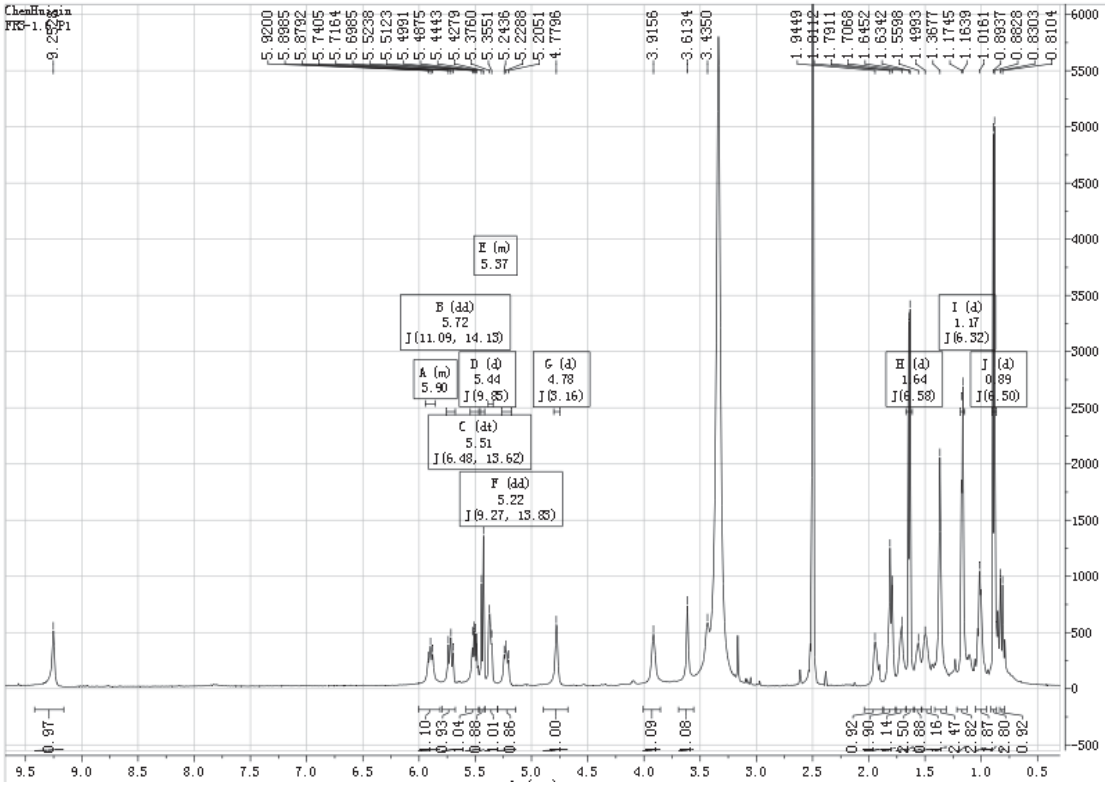

Attachment 40. The ^{1}H NMR spectrum of altersetin-2 (**42**, **known**) (600 MHz, DMSO)

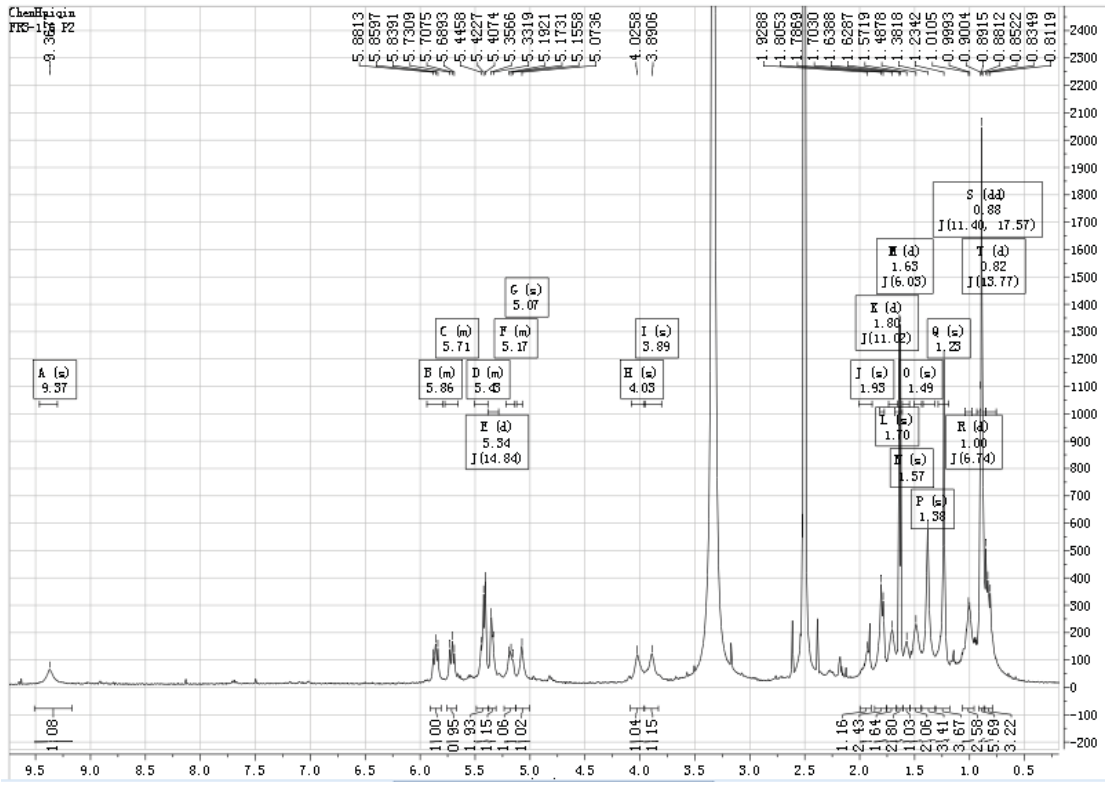

Attachment 41. The ^{1}H NMR spectrum of altertoxin II (**43**, **known**)
(600 MHz, DMSO)

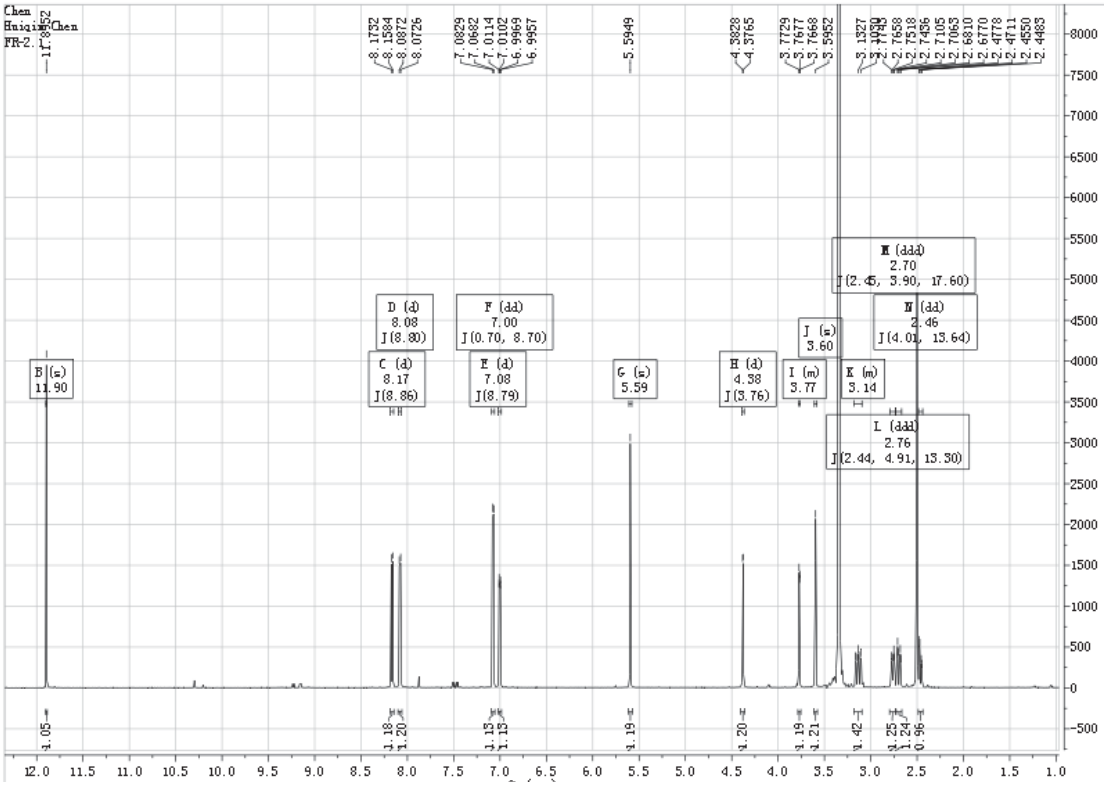

Attachment 42. The ^{1}H NMR spectrum of altertoxin I (**44**, known)
(600 MHz, DMSO)

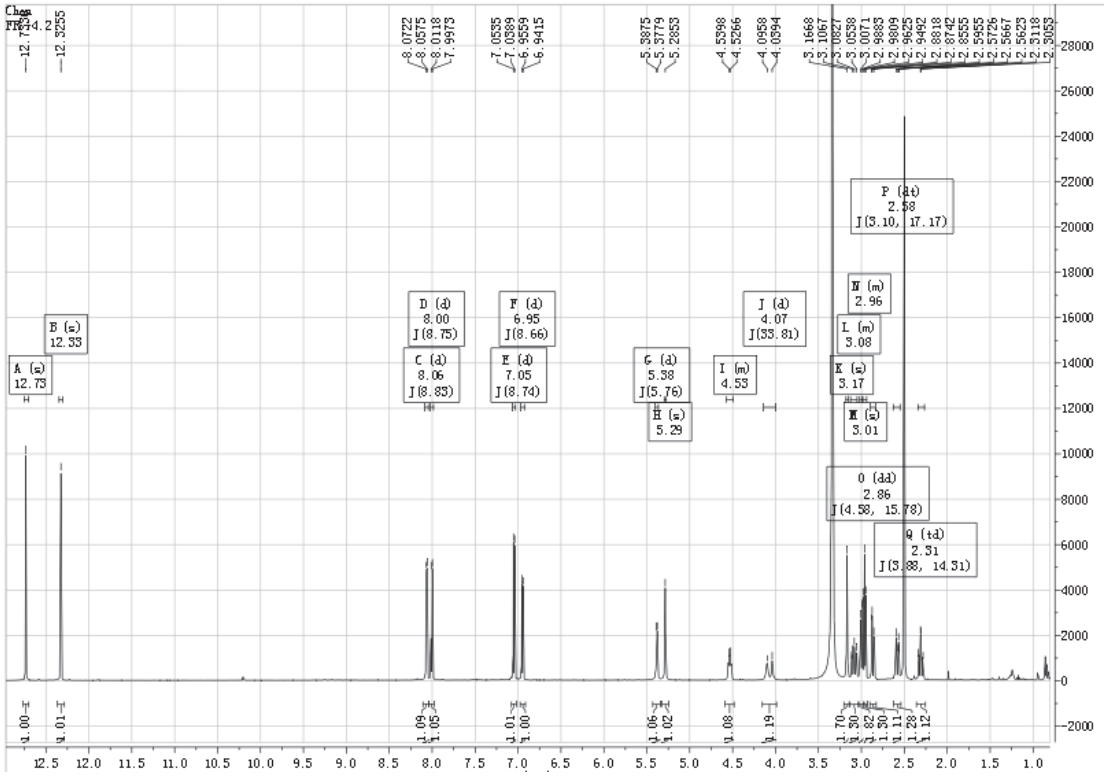

Attachment 43. The ^{1}H NMR spectrum of tenuazonic acid (**45**, known) (600 MHz, CD_3OD)

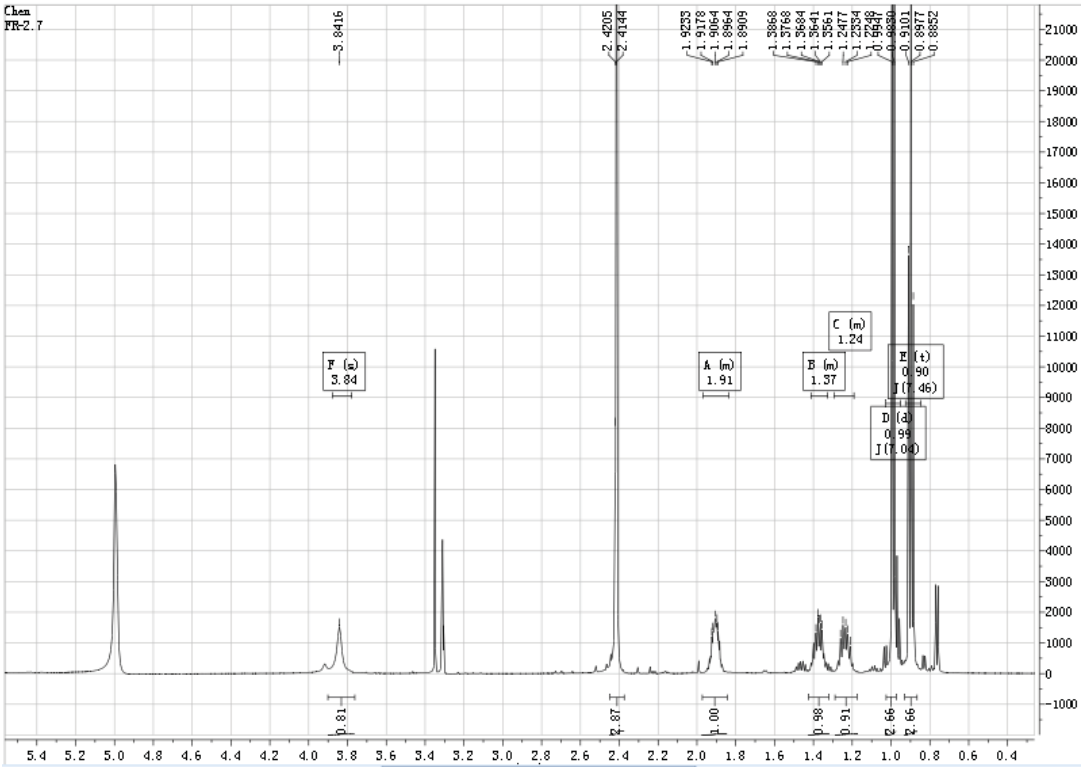

Attachment 44. The ^{1}H NMR spectrum of paxilline (**48**, **known**) (500 MHz, CD_3OD)

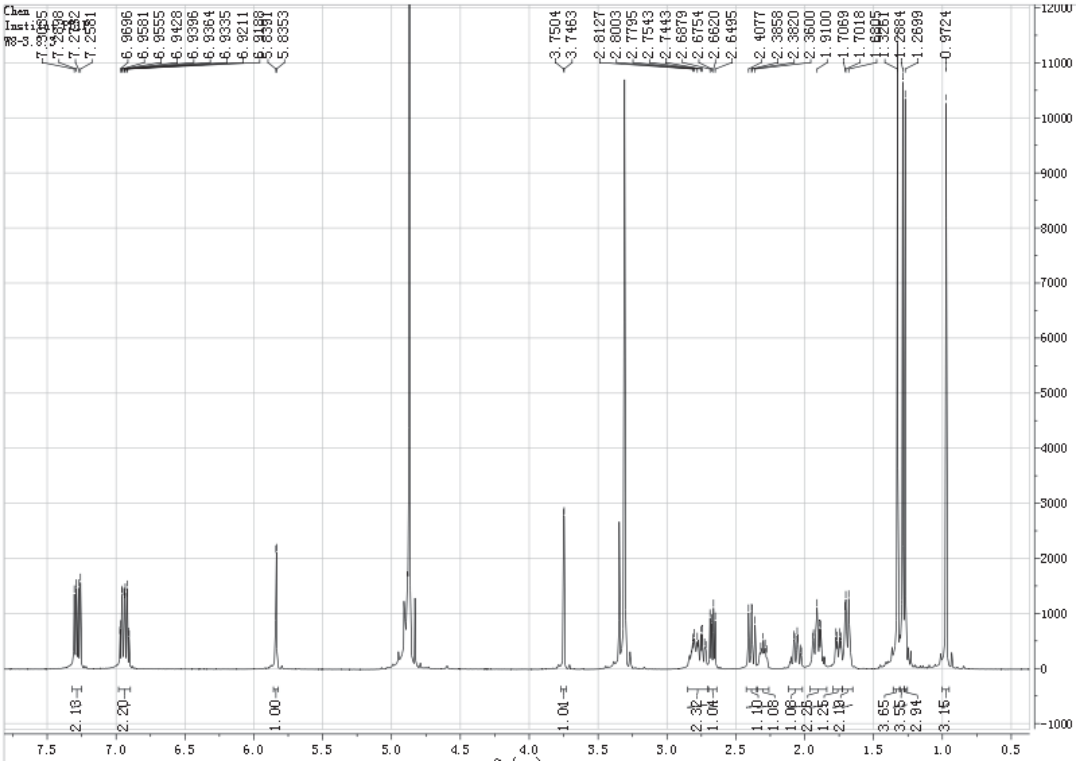

Attachment 45. The ^{1}H NMR spectrum of dehydroxy paxilline (**49**, **known**) (500 MHz, CD_3OD)

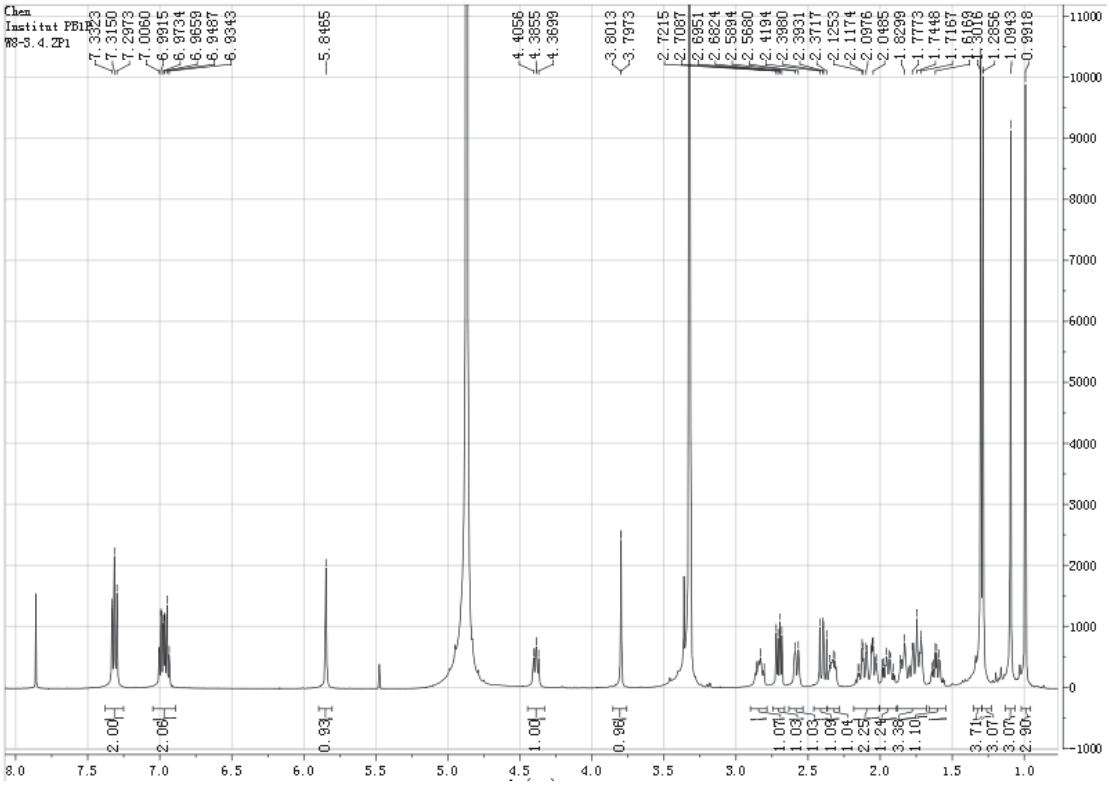

Attachment 46. The ^{1}H NMR spectrum of 21-isopentenylpaxilline (**50**, **known**) (500 MHz, CD_3OD)

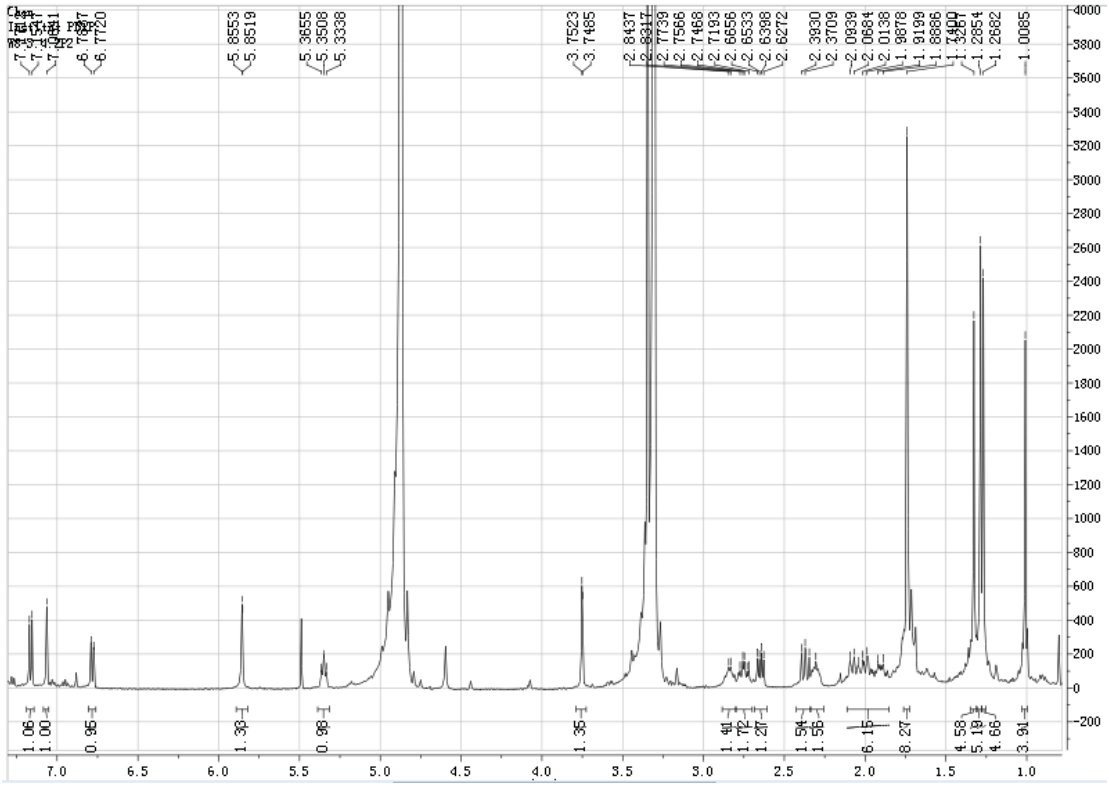

Attachment 47. The ^{1}H NMR spectrum of 10β-hydroxy-13-desoxy paxilline (**51**, **known**) (500 MHz, CD_3OD)

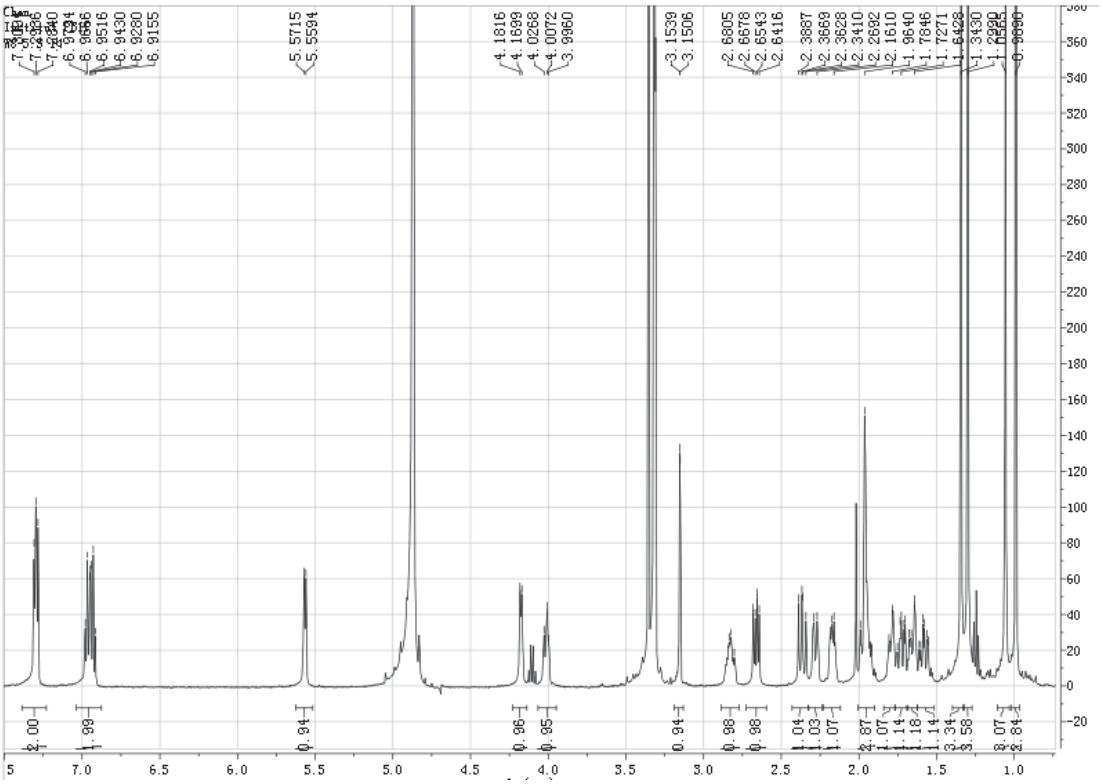

Attachment 48. The ^{1}H NMR spectrum of paspaline (**52**, known) (500 MHz, $CDCl_3$)

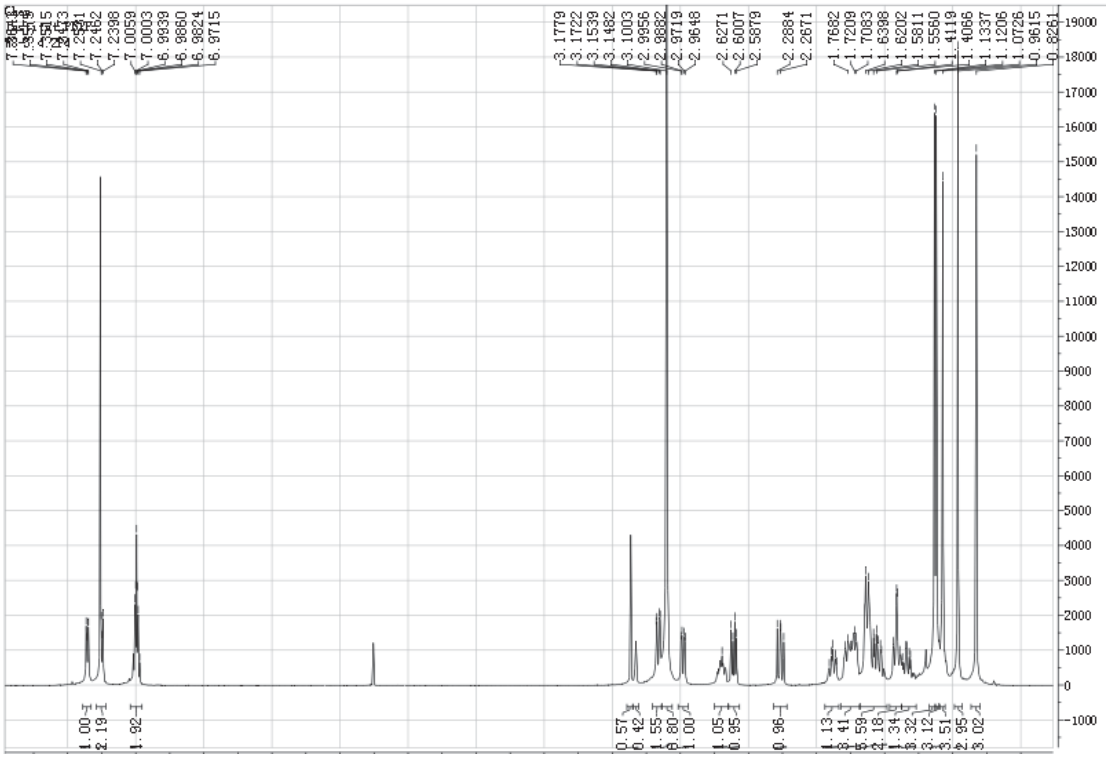

Attachment 49. The ^{1}H NMR spectrum of emindole SB (**53**, known)
(500 MHz, CD_3OD)

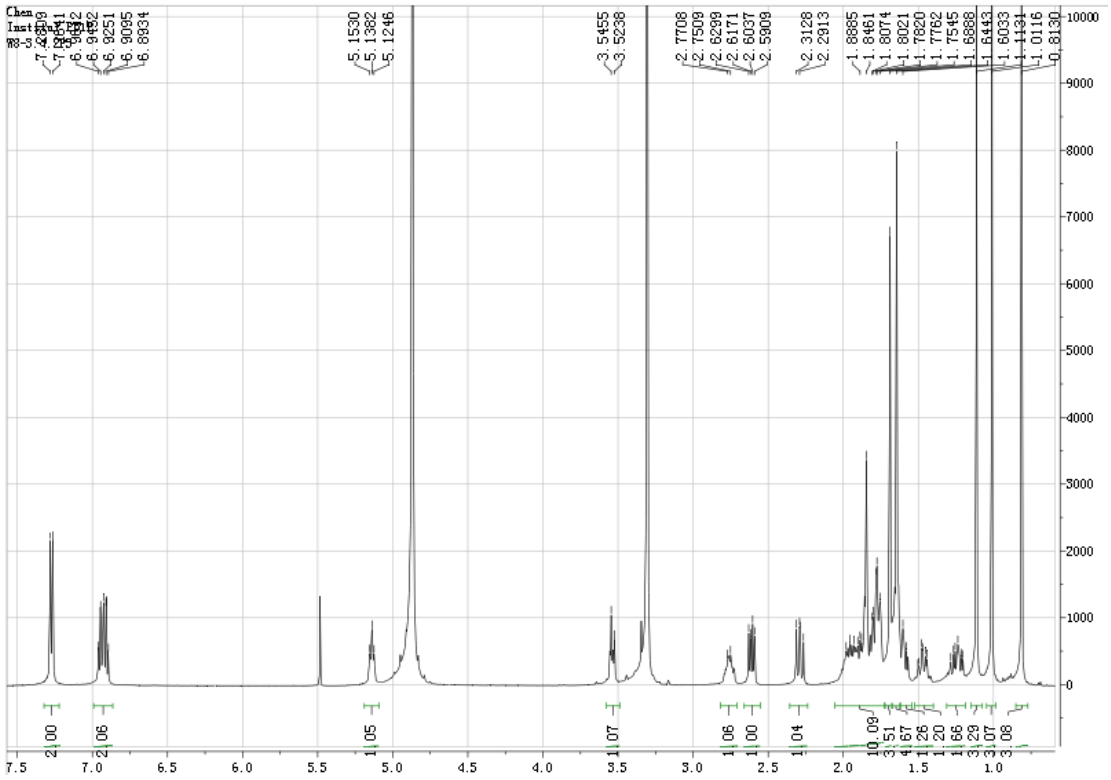

Attachment 50. The ^{1}H NMR spectrum of 12-carboxyl-paspaline (**54**, **known**)
(600MHz, CD_3OD)

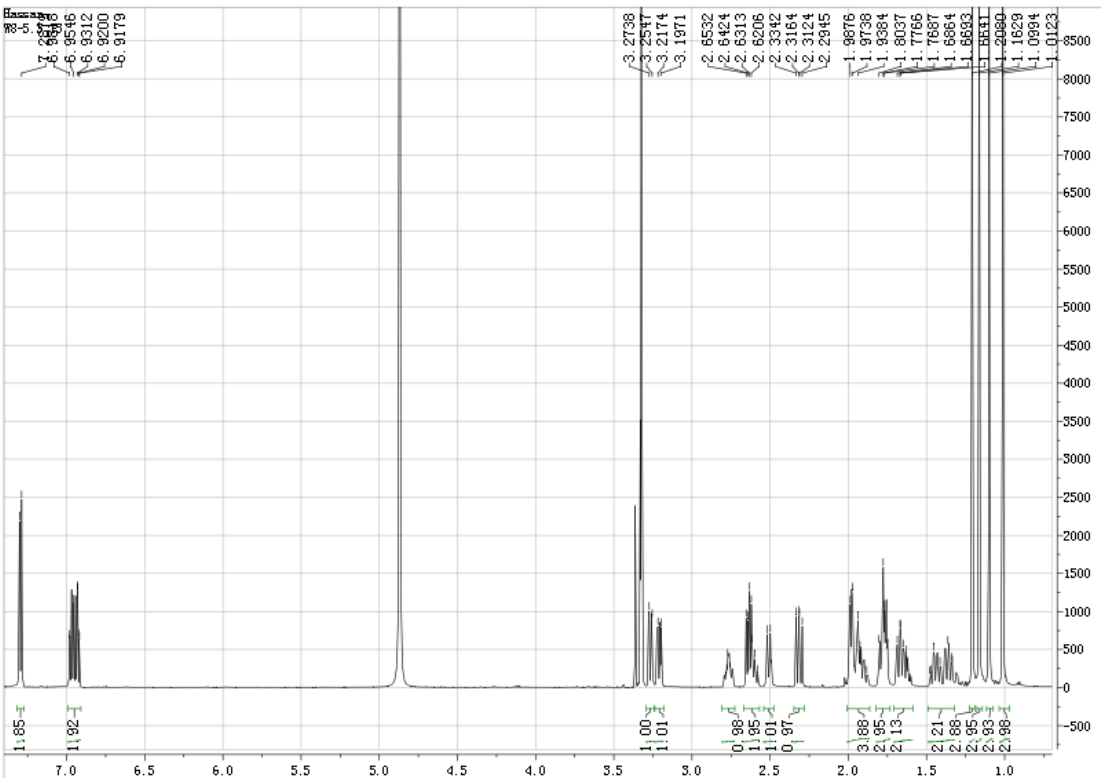

Attachment 51. The ^{1}H NMR spectrum of 3-deoxo-4b-deoxypaxilline (**55**, **known**) (500 MHz, CD_3OD)

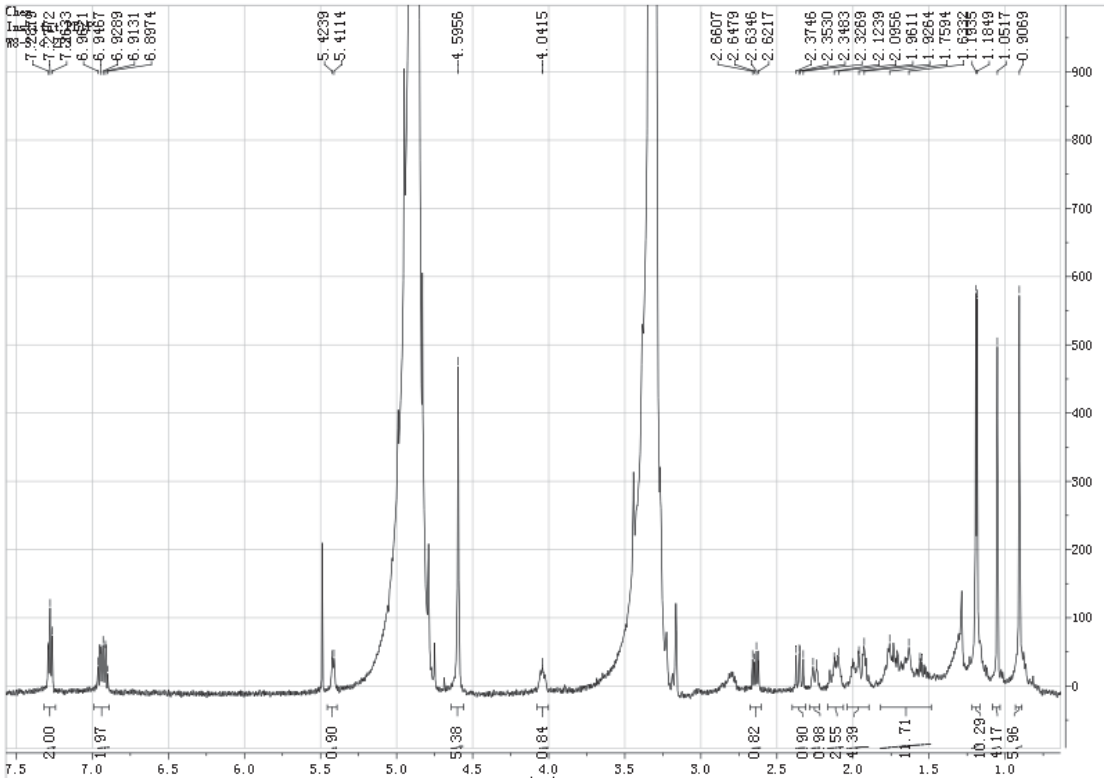

Attachment 52. The ^{1}H NMR spectrum of pyrenocine B (**56**, known) (500 MHz, CD_3OD)

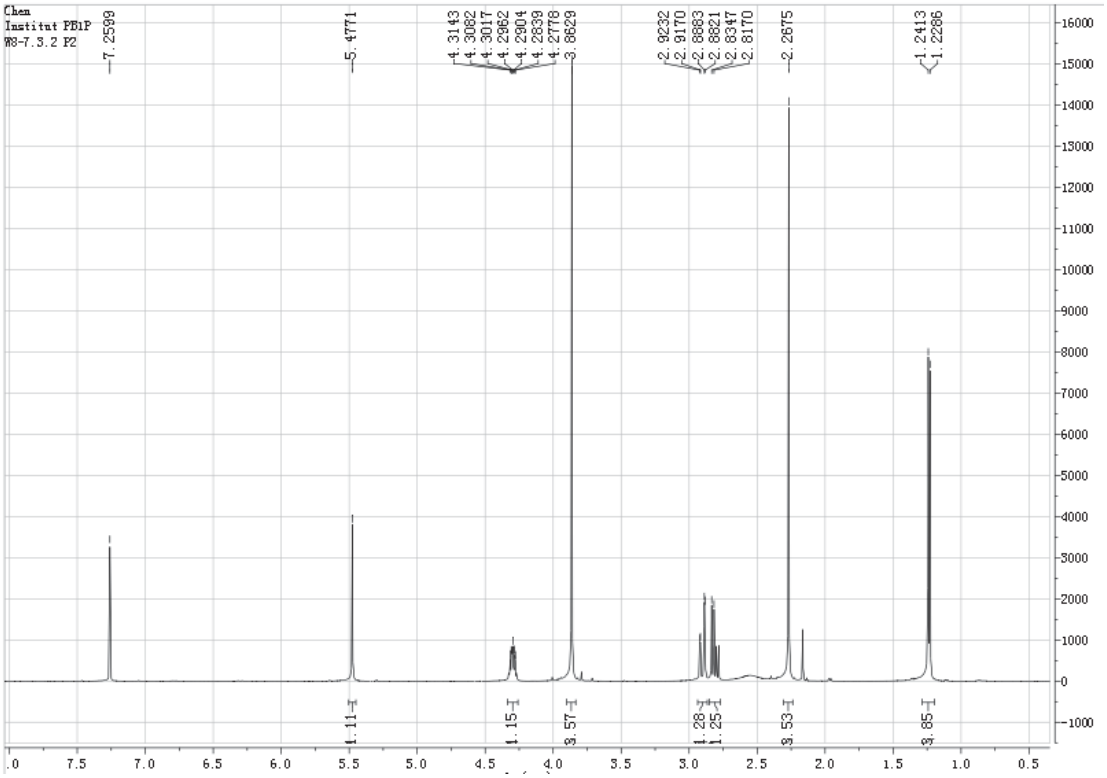

Attachment 53. The ^{1}H NMR spectrum of pyrenocine A (**57**, **known**) (500 MHz, CD_3OD)

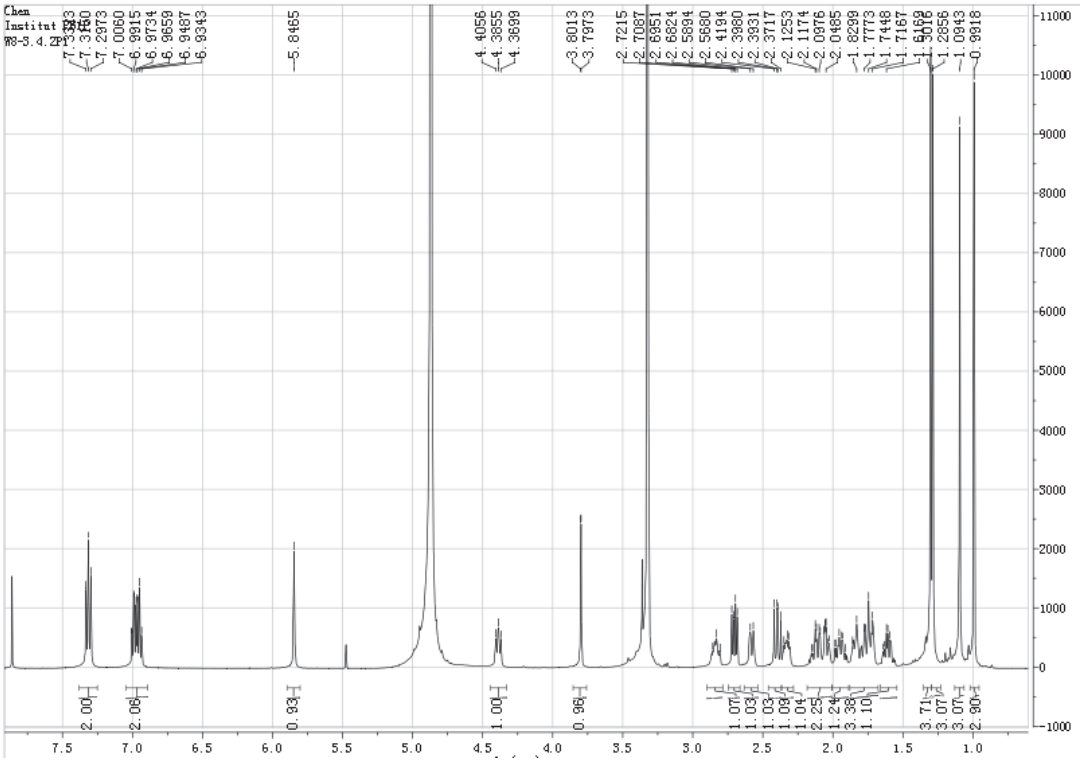

Attachment 54. The ^{1}H NMR spectrum of (+)-isorotiorin (**60**, **known**) (600 MHz, CD_3OD)

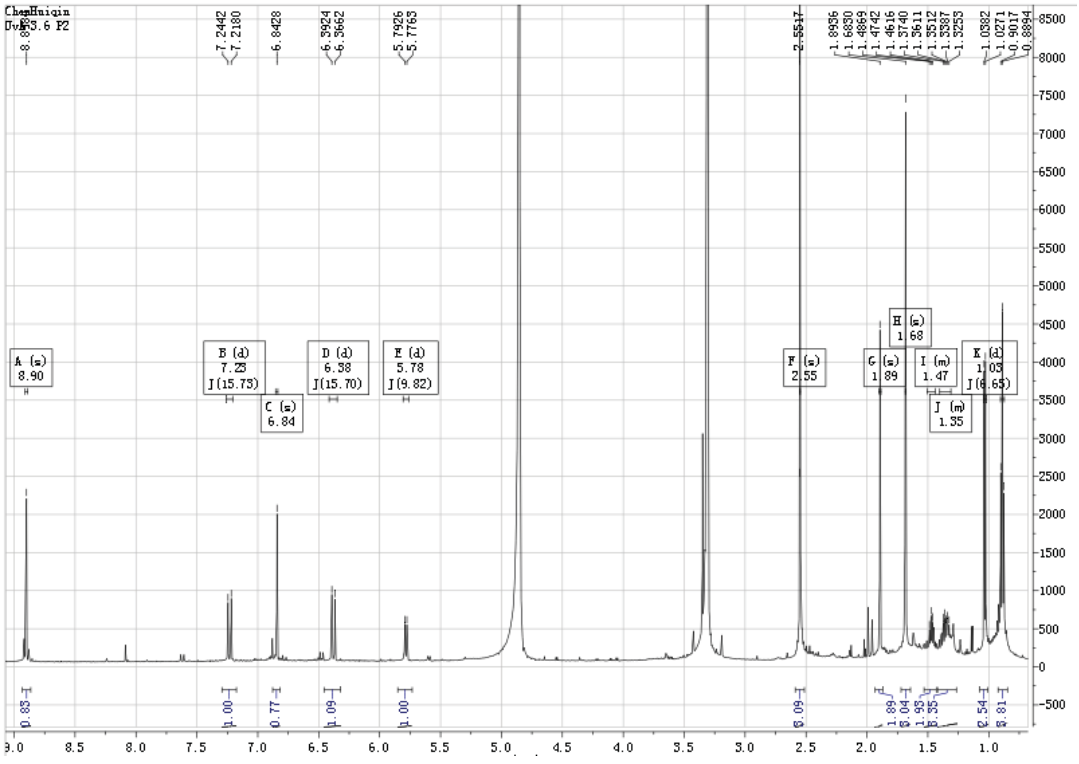

Attachment 55. The ^{1}H NMR spectrum of (+)-isochromophilone VI (**62**, **known**) (600 MHz, CD_3OD)

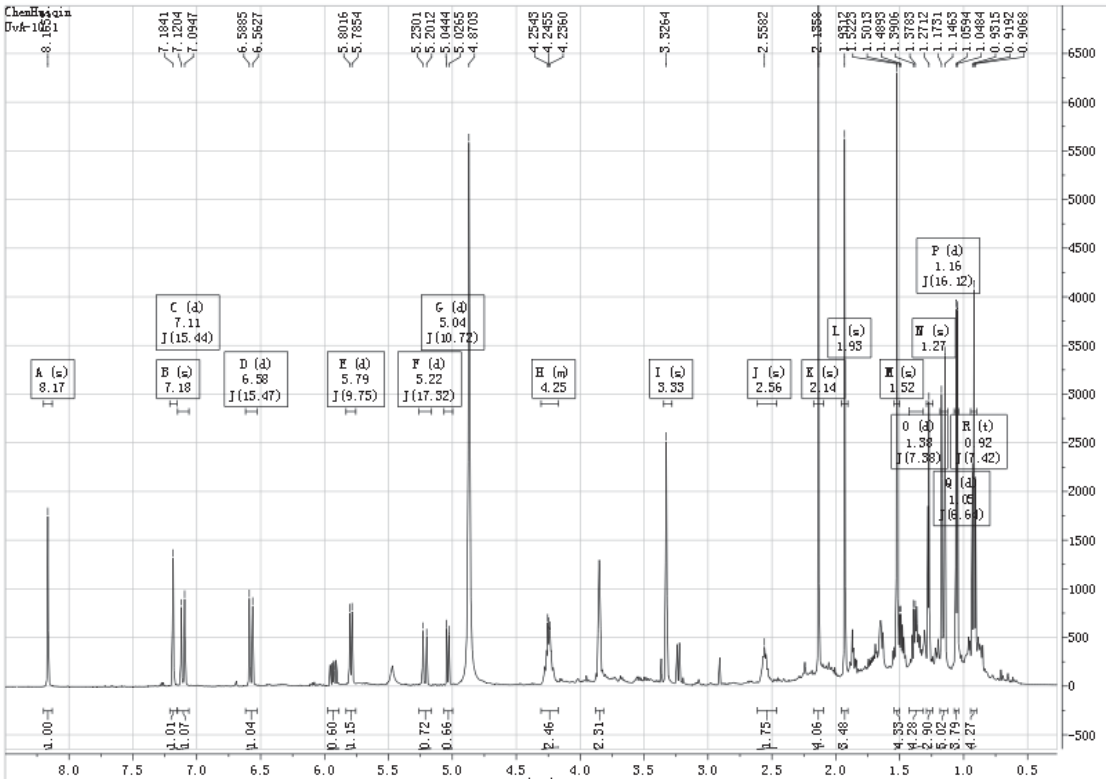

Attachment 56. The ^{1}H NMR spectrum of isoharzianic acid (**63**, **known**) (300 MHz, CD_3OD)

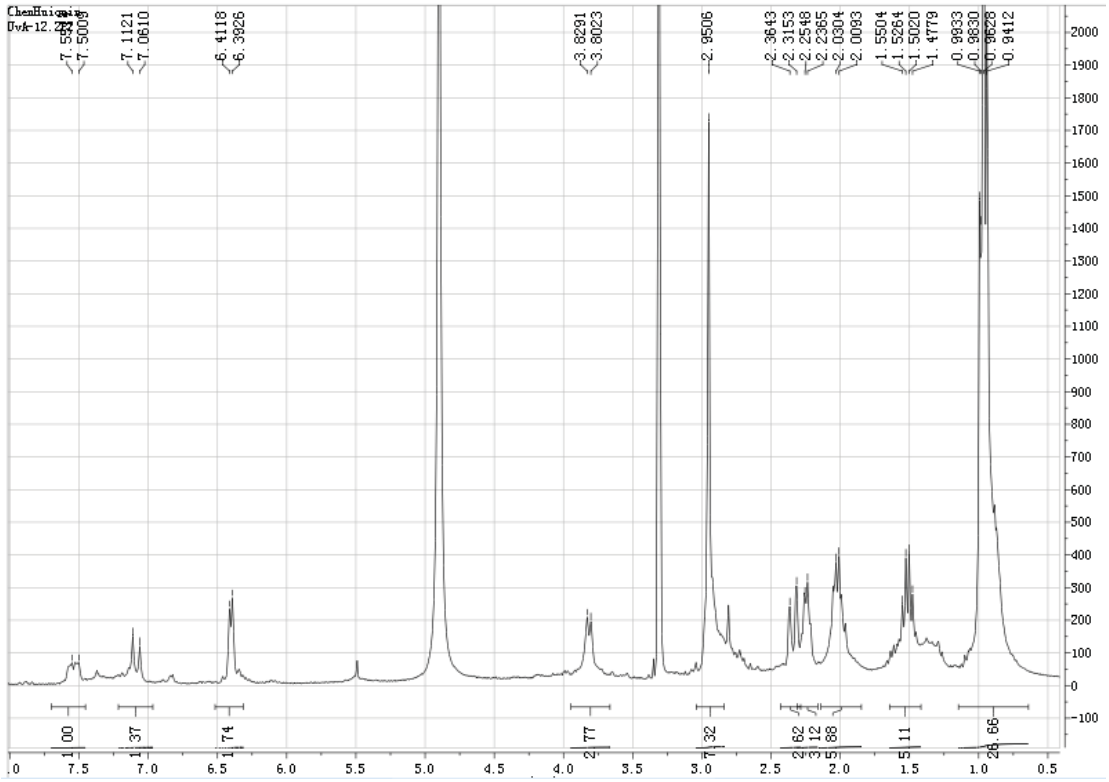

Attachment 57. The ^{1}H NMR spectrum of harzianic acid (**64**, known) (600 MHz, CD_3OD)

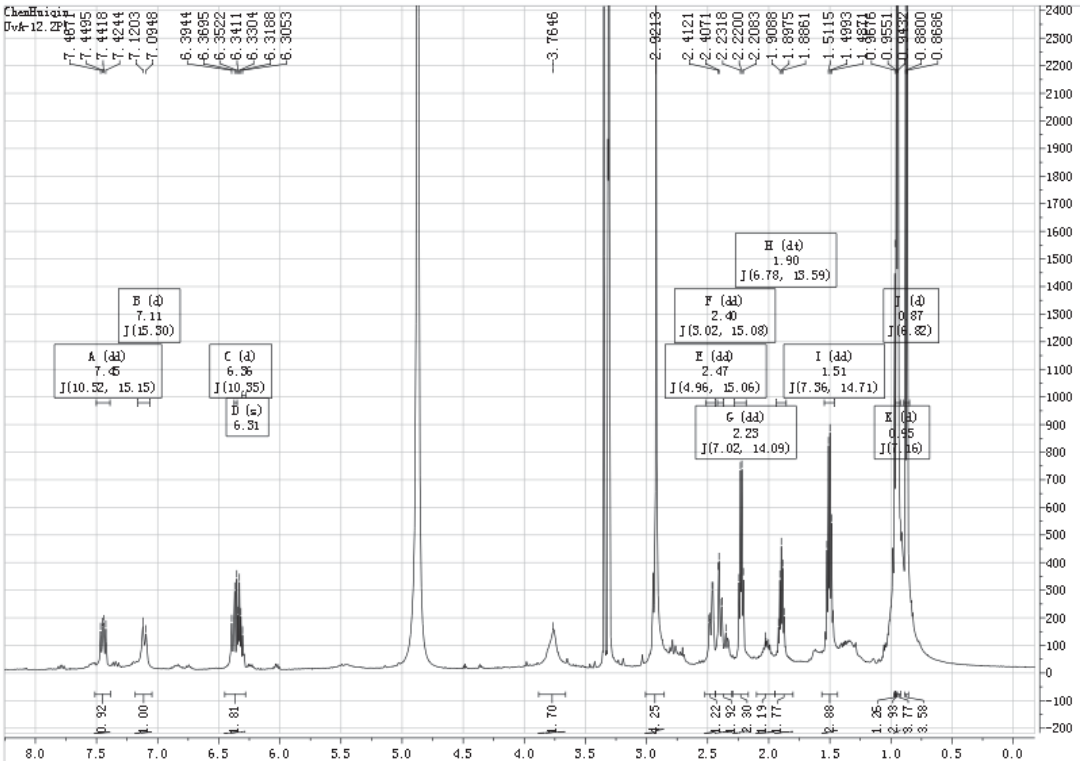

8. List of abbreviations

$[\alpha]^{20}$	Specific rotation at the sodium D-line
B	Magnetic sectors
BC	Before christ
br	Broad
Br	Bromine
ca.	Circa
CC	Column chromatography
DCM, CH_2Cl_2	Dichloromethane
CD	Circular Dichroism
$CDCl_3$	Deuterated chloroform
CD_3OD	Deuterated methanol
DEP	Direct exposure probe
CI	Chemical ionization
Cl	Chlorine
DIP	Direct insertion probe
cm	Centimeter
COSY	Correlation spectroscopy
d	Doublet
dd	Doublet of doublet signal
DEPT	Distortionless enhancement by polarization transfer
DMSO	Dimethyl sulfoxide
DNA	Deoxyribonucleic acid
DNMT	DNA methyltransferase
EI	Electron impact ionization
ESI	Electron spray ionization
et al.	et altera (and others)
EtOAc	Ethyl acetate
eV	Electronvolt
FAB	Fast atom bomhardment
FD/FI	Field Desorption/ Field Ionization
g	Gram
GC	Gas chromatograph
GGPP	Geranylgeranyl diphosphate
h	Hour
HCl	Hydrochloric acid
HMBC	Heteronuclear multiple bond connectivity
HMQC	Heteronuclear multiple quantum coherence
H_2O	Water
HPLC	High performance liquid chromatography
HRESIMS	High-resolution electrospray ionisation mass spectrometry
Hz	Hertz
IC_{50}	Half maximal inhibitory concentration

kJ	Kilojoule
L	Liter
LC	Liquid chromatography
LC-MS	Liquid chromatography-mass spectromethy
m	Multiplet signal
MALDI	Matrix assisted laser desorption ionization
MeOH	Methanol
mg	Milligram
MHz	Mega Hertz
min	Minute
mL	Milliliter
mm	millimeter
MS	Mass spectrometry
MTT	3-(4,5-Dimethylthiazol-2-yl)-2,5-diphenyltetrazolium bromide
m/z	Mass per charge
μg	Microgram
μL	Microliter
μM	Micromolar
NaOH	Sodium hydroxide
nm	Nanometer
n-BuOH	n-Butanol
NMR	Nuclear magnetic resonance
PCR	Polymerase chain reaction
ppm	Part per million
q	Quartet signal
Q	Quadrupoles
QIT	Quadrupole ion trap
ROESY	Rotating frame Overhauser enhancement spectroscopy
s	Singlet signal
SAHA	Suberoylanilide hydroxamic acid
SAM	S-adenosyl methionine
sec.	Second
Si	Silica
sp.	species
t	Triplet signal
TFA	Trifluoroacetic acid
TLC	Thin layer chromatography
TMS	Tetramethylsilane
TOF	Time-of-flight
UV	Ultra-violet
VLC	Vaccum liquid chromatography

9. Curriculum Vitae

Name: Huiqin Chen

Address: Institute of Pharmaceutical Biology and Biotechnology,
Heinrich-Heine-University,
40225, Duesseldorf

E-mail: huiqin_chen@hotmail.com

Educational background:

10. 2012 – present: Ph.D student in Pharmacy, Institute of Pharmaceutical Biology and Biotechnology, Heinrich-Heine-University, Duesseldorf, Germany

09. 2008 – 06. 2011: Master of Science of Natural Medicinal Chemistry, School of Traditional Chinese Materia Medica, Shenyang Pharmaceutical University

09. 2004 – 07. 2008: Bachelor of Traditional Chinese Medicine, School of Traditional Chinese Materia Medica, Shenyang Pharmaceutical University

Employment records:

07. 2011 – 06. 2012: Institute of Tropical Bioscience and Biotechnology, Chinese Academy of Tropical Agricultural Sciences, Haikou, China

Publications:

1. Huiqin Chen, Nihal Aktas, Belma Konuklugil, Attila Mándi, Georgios Daletos, Wenhan Lin, Haofu Dai, Tibor Kurtán, and Peter Proksch. A new fusarielin analogue from *Penicillium* sp. isolated from the mediterranean sponge *Ircinia oros*. *Tetrahedron Letters*. 2015, 56, 5317-5320.

2. Huiqin Chen, Georgios Daletos, Mohamed S. Abdel-Aziz, Dhana Thomy, Haofu Dai, Heike Brötz-Oesterhelt, WenHan Lin, and Peter Proksch. Inducing secondary metabolite production by the soil-dwelling fungus *Aspergillus terreus* through bacterial co-culture. *Phytochemistry Letters*, 2015, 12: 35-41.

3. Huiqin Chen, Georgios Daletos, Festus Okoye, Daowan Laic, Haofu Dai, and Peter Proksch. A new cytotoxic cytochalasin from the endophytic fungus *Trichoderma harzianum*, *Natural product communications*, 2015, 10(4): 585-587.

4. **Hui-Qin Chen**, Wen-Jian Zuo, Hui Wang, Hai-Yan Shen, Ying Luo, Hao-Fu Dai, and Wen-Li Mei. Two new antimicrobial flavanes from dragon's blood of *Dracaena cambodiana*. *Journal of Asian Natural Products Research*., 2012, 14(5): 436-440.

5. **Hui-qin Chen**, Wen-li Mei, Wen-jian Zuo, Hui Wang, You-xing Zhao, Hao-fu Dai, and Jin-hui Wang. Chemical constituents from Dragon' s blood of *Dracaena cambodiana*. (in Chinese) *Chinese Journal of Medicinal Chemistry*, 2011, 4: 308-311.

6. Wen-jian Zuo, Hao-Fu Dai, Jing Chen, **Hui-Qin Chen**, You-xing Zhao, Wen-li Mei, Xian Li, and Jin-Hui Wang. Triterpenes and triterpenoidsaponins from the leaves of *Ilex kudincha*. *Planta Medica*, 2011, 77(16): 1835-1840.

7. Wen-Jian Zuo, Hao-Fu Dai, Yan-Bo Zeng, Hui Wang, **Hui-Qin Chen**, and Jin-Hui Wang. Two new triterpenoid saponins from the leaves of Ilex Kudingcha. *Journal of Asian Natural Products Research*, 2012, 14 (4): 308-313.

8. Wen-jian Zuo, **Hui-qin Chen**, Xiao-dong Li, Zhen-hui Wang, Hao-fu Dai, and Jin-hui Wang. Chemical constituents of *Ilex kudingcha* leaves. (in Chinese) *Chinese Traditional and Herbal Drugs*, 2011, 42(1): 18-20.

Patent:

Jinhui Wang, Wenjian Zuo, Guoyu Li, and **Huiqin Chen**. Ilex latifolia thunb saponin compound (CN 101775061A). Patent number: CN 200910176449. 2010, 07.

Honors:

Granted a full scholarship from Program of Governmental Graduate students Scholarship launched by China Scholarship Council (2012).